Assembly and biochemical properties of a human chaperone/co-chaperone protein complex.

Anupama Vydyanath

School of Life Sciences

Assembly and biochemical properties of a human chaperone/co-chaperone protein complex

A thesis submitted in partial fulfilment of the requirements for the degree of Doctor of Philosophy
University of Westminster

Anupama Vydyanath

August 2010

Abstract

The 70kDa members of the heat shock protein family (eg. Hsp70) function as molecular chaperones by binding to exposed hydrophobic patches on nascent polypeptides forming non-covalent interactions, thereby preventing their aggregation and facilitating their proper folding. The folding reaction comprises of cyclic binding and release of the unfolded substrate powered by ATP hydrolysis. Hsp70 requires the assistance of a co-chaperone, generally provided by the Hsp40 group of proteins, for the cycle of protein folding. Biochemical analyses have mapped the possible sites of interaction between the Hsp70 and Hsp40 proteins and predicted a bipartite mode of interaction between Hsp70 and Hsp40. However, structural investigations into the mechanistic features of the folding cycle have been hampered by the transient nature of interaction. The underlying theme for this work was to therefore structurally understand the assembly of Hsp70 proteins with the Hsp40 co-chaperones as a complex during the Hsp70-assisted folding cycle. This study was carried out using human Hsc70 and HSJ1b as representatives of the Hsp70 and Hsp40 families respectively. The first step to understand this co-operation was to develop a strategy to isolate a complex of Hsc70 and HSJ1b suitable for structural studies. Previous studies have reconstituted the Hsp70/Hsp40 complex *in vitro* by combining the two proteins in molar ratios in the presence of ATP. In this work a co-expression system was developed and a recombinant form of the human Hsc70/HSJ1b complex was successfully purified using a bacterial expression system. Biochemical characterisation revealed that this chaperone complex can protect ~85% of substrate protein from thermal aggregation. Gel filtration analysis revealed that the complex was composed of a heterogenous mix of ~220 kDa and hetero-oligomeric co-polymer species. Analytical ultracentrifugation confirmed that these hetero-oligomeric co-polymer species were not aggregates, and molecular weight for this species was estimated to be 1.1 MDa. These two species represent potentially two different states of association between Hsc70 and HSJ1b. ATP and heat treatment at 42^{o}C with luciferase were identified as factors which promote the conversion of the oligomeric Hsc70/HSJ1b species to the ~220 kDa Hsc70/HSJ1b species. Domain variants of Hsc70 were then generated and their ability to complex with HSJ1b was investigated. Using these Hsc70 domain variants, the region on Hsc70 paramount for polymerisation was identified. The C-

terminal 10 kDa lid region was found to be essential for the chaperone/co-chaperone interaction, since the removal of this zone alters binding, function and conformational properties of the Hsc70 and HSJ1b interaction. X-ray crystallography studies on the full length and the domain complexes were carried out, leading to the structure of the apo form of the nucleotide binding domain of Hsc70. Preliminary electron microscopy (EM) analysis was undertaken of the recombinant Hsc70/HSJ1b complex. The preliminary results from negative staining revealed mostly circular particles and were extremely encouraging. Currently work is being carried out to improve sample homogeneity, which will facilitate further EM studies. Thus the recombinant complex generated in this study is an attractive tool to further our understanding of the functional and structural features of the interactions of Hsp70 with Hsp40.

Acknowledgments

Firstly, I would like to thank my Director of studies, Dr. Mark Odell and my second supervisor, Dr. Steve Smerdon (National Institute of Medical Research) for giving me the opportunity to work on this challenging project and for helping me throughout this study. I am also grateful to the University of Westminster for awarding me the Cavendish Research Scholarship to undertake my doctoral studies at Westminster.

Besides my supervisors, I would also thank Dr. Peter Moody from the University of Leicester for helping me with the X-ray crystallography work, Dr. Dave Scott from the University of Nottingham for carrying out the analytical ultracentrifugation analysis and Dr. Corrine Smith from the University of Warwick for helping me with the electron microscopy study.

Special thanks to Dr. Pradeep Luther for being extremely understanding and allowing me to complete my thesis writing while at work. I would also like to thank Prof. Tajalli Keshavarz, Dr. Ipsita Roy and Dr. Joanne Murray for their encouragement and support while I was writing my thesis. Many Thanks to the technical staff in the School of Biosciences for all their help, in particular I thank Mr. Thakor Tandel and Ms. Vanita Amin for their generosity and their ever willingness to help.

At this point I would also like to acknowledge with gratitude Prof. M.R.N Murthy, Prof. H.S Savitri and Dr. H.S. Subramanya for inspiring me and encouraging me to pursue research as a career. All my lab mates from IISC and Aurigene occupy a special place in my heart for all the fun times we had in the lab, especially Gayathri for patiently listening to my endless questions and finding an answer to them all.

My 5 years in Westminster would have felt longer but for the joyful company of my friends - Anatoily, Julien, Loveleen, Sheryl, Diluka, Ranjana, Hannah, and Sheetal. Thank you for being there for me every time I wanted a coffee or a shoulder to cry on!!!

The last five years would have been impossible but for the support, patience and understanding of my dear family. The encouragement I received from my parents, Amma, Anna, Ajji, Raghu, Arpana, Anant, Sindhu and all my near and dear ones kept me motivated till the end.

Words cannot describe the support I have received from my dear husband, who has stood by me through all my ups and downs and has patiently waited for me to finish. To him I dedicate this work.

Table of Contents

List of Abbreviations

°C	Degrees centigrade
ΔG	Solvation energy
2DE	Two dimensional electrophoresis
A	Absorbance
ADP	Adenosine -5'-diphosphate
AMPPNP	5'-adenylyl-beta,gamma-imidodiphosphate
ANP	Phosphoaminophosphonic acid-adenylate ester
ATP	Adenosine-5'-triphosphate
BAG	Bcl-2-associated athanogene
bp	Base pair(s)
BSA	Bovine serum albumin
$CaCl_2$	Calcium chloride
cDNA	Complementary DNA
CFTR	cystic fibrosis transmembrane conductance regulator
CHIP	carboxyl terminus of Hsc70-interacting protein
CIP	Calf Intestinal Phosphatase
CSP	Cysteine string protein
CTR	C-terminal region
CuV	Culture volume
CV	Column volume
DNA	Deoxyribonucleic acid
DTT	Dithiothreitol
E. coli	*Escherichia coli*
EDTA	Ethylendiamintetraacetic acid
ER	Endoplasmic reticulum
GAK	G-associated kinase
G/F region	Glycine-phenylalanine rich region
Hdj	Human DnaJ-like protein 1
HPD motif	Histidine, proline and aspartic acid motif
HRP	Horse radish peroxidase
His	Histidine

Hsp	Heat shock proteins
Hsp70	Heat shock 70 kDa protein
Hsc70	Heat shock cognate 70 kDa protein
Hsp40	Heat shock 40 kDa protein
HSJ1	Homo sapiens DnaJ protein 1
HspBP1	Hsp70 binding protein 1
HSE	Heat shock promoter element
HSF	Heat shock factor
Hip	Hsc70-interacting protein
Hop	Hsc70-Hsp90-organizing protein
IEF	Isoelectric focussing
IPG	Immobilised pH gradient
IPTG	iso-Propyl-β-D-thiogalactopyranoside
kav	Partition coefficient
KCl	Potassium chloride
kDa	Kilodalton
LB	Luria Bertani
LA	LB agar
mRNA	Messenger RNA
MR	Molecular replacement
MW	Molecular weight
$MgCl_2$	Magnesium chloride
N60	N-terminal 60 kDa fragment
NBD	Nucleotide binding domain
NaCl	Sodium chloride
NaOH	Sodium hydroxide
NEF	Nucleotide Exchange Factors
Ni-NTA	Nickel-nitrilotriacetic acid
NMR	Nuclear magnetic resonance
PAGE	Polyacrylamide gel electrophoresis
PBS	Phosphate buffer saline
PBD	Peptide binding domain
PCR	Polymerase chain reaction

PDB	Protein Databank
pI	Isoelectric point
PISA	Protein Interfaces, Surfaces and Assemblies
PMSF	Phenylmethanesulfonyl fluoride
RESA	Ring infected erythrocyte surface antigen
rHH	Recombinant Hsc70/HSJ1b complex
RMSD	Root mean square deviation
rpm	Revolutions per minute
RNA	Ribonucleic acid
S.cerevisiae	Saccharomyces cerevisiae
SDS	Sodium dodecyl sulphate
SEC	Size exclusion chromatography
SelMet	Seleno-l-methionine
SSM	Structure comparison service
TAE	Tris Acetate-EDTA buffer
TBS-T	Tris buffer saline Tween20
TEMED	N,N,N'N'-tetramethylethylenediamin
TMB	3,3',5,5'-Tetramethylbenzidine
TPR	Tetratricopeptide repeat
Tris	Tris-(hydroxymethyl)-aminomethane
UPS	Ubiquitin-proteosome system
UV	Ultra Violet
v/v	Volume per volume
w/v	Weight per volume

List of Figures

List of Tables

Chapter 1

Introduction

CHAPTER 1: Introduction

1.1. Proteins

Proteins form the basis of existence for living cells. They characterise the properties of living organisms because of their involvement in virtually every function of the cell. From storage and transport, to catalysing biological functions as enzymes; proteins are important macromolecules for living organisms (Creighton, 1993; Stryer *et al*., 2002). The conversion of genetic information on the DNA into a more functionally and structurally significant macromolecule - protein, is a central tenet of Biology. Figure 1.1 is a schematic representation of this ideology, where genetic information on the DNA is transcribed to form mRNA which upon translation gives rise to the nascent polypeptide (Stryer *et al*., 2002).

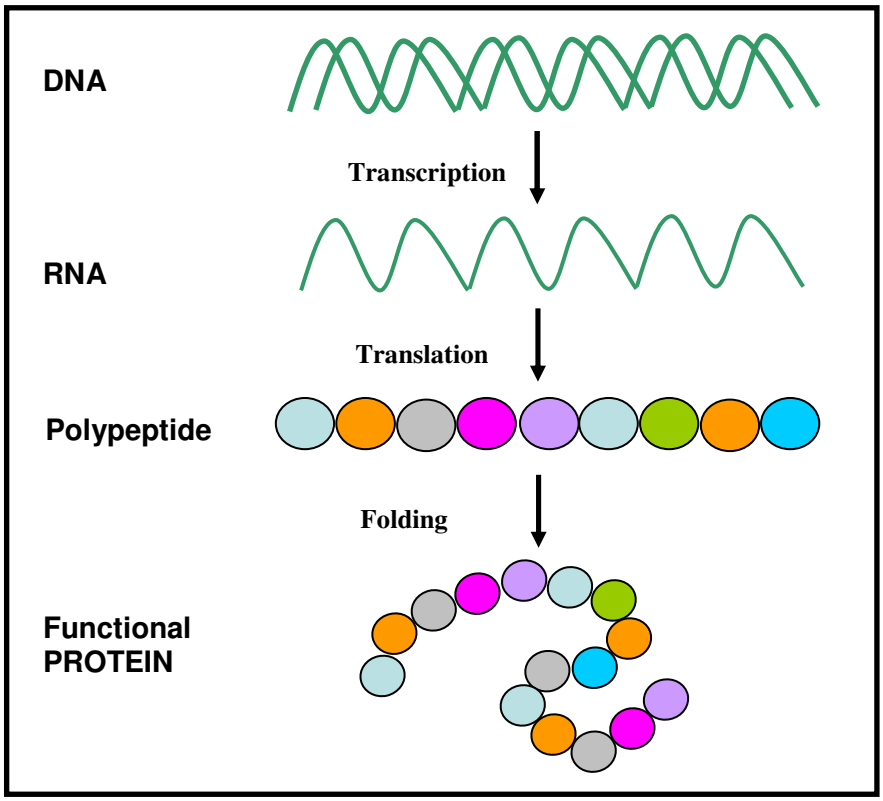

Figure 1.1: Schematic pathway of the translation of genetic material into functional proteins

One of the central dogmas of Biology explains simplistically the conversion of genetic information on the DNA into a more functionally and structurally significant form – proteins. DNA transcribes to form RNA which is translated by ribosomes to form the polypeptide. The string of amino acids emerging (polypeptide) from the ribosome needs to attain its native tertiary structure to become a fully functional protein.

Proteins are linear chains made up from a combination of the 20 essential amino acids, which differ only in the order of occurrence of the amino acids on the polypeptide chains and their post-translational modifications (Stryer *et al*., 2002). Protein structure can be considered at five different levels, the primary, secondary, super secondary, tertiary and quaternary structures (Venkatraman *et al*., 2001). The linear sequence of amino acids – the primary structure, can only partly explain the functional diversity seen in proteins. This function is dependent on the nascent polypeptide folding into its native 3-dimensional structure which is essential in allowing it to fulfil its functional fate (Branden and Tooze, 1999).

Failure to attain this native structure or misfolding of the polypeptide results in proteins unfit to carry out their biological activities (Radford and Dobson, 1999). The problem of misfolding is compounded when the misfolded proteins make unwanted interactions with other cellular proteins leading to a potentially toxic situation in the cells – protein aggregation. Alterations to protein folding have been implicated in several disease conditions. Cystic fibrosis has been attributed to mutations in the cystic fibrosis transmembrane conductance regulator (CFTR) gene which renders the protein incapable of folding, while deposition of insoluble protein material (referred to as amyloids) on degenerating nerve cells have been implicated in the development of Alzheimer's disease (Thomas *et al*., 1995; Qu *et al*., 1996; Barral *et al*., 2004). Some of the other conditions caused by problems in protein folding are Bovine spongiform encephalopathy (also known as Mad Cow disease) and Marfan's syndrome (Thomas *et al*., 1995). Table 1.1 lists some of the disease conditions caused by protein misfolding resulting in altered or in some cases total loss of function (Thomas *et al*., 1995).

Disease	Protein involved	Molecular phenotype
α-Antitrypsin deficiency	α-Antitrypsin	Mislocalisation
Amyotrophic lateral sclerosis	Superoxide Dismutase	Misfolding
Bardet-Biedel Syndrome	MKKS	Loss of chaperone activity
Cancer	p53	Misfolding
Alzheimer's disease	β-Amyloid	Aggregation
Huntington's disease	HD	Aggregation
Parkinson's disease	α-synuclein	Aggregation
Retinosa Pigmentosa	Rhodopsin	Mislocalisation

Table 1.1: Diseases that result from loss of function, mislocalisation or aggregation of proteins (data taken from Boshoff *et al*., 2004).

1.1.1. Spontaneous folding pathway

Modern theories on protein folding have evolved from Anfinsen's seminal work on the spontaneous refolding of ribonuclease for which he was awarded the Nobel Prize in 1973. He demonstrated that ribonuclease in a denatured and reduced state could refold into its active form 'spontaneously' (Anfinsen, 1973). He concluded that spontaneous refolding was possible because the information needed for a protein to attain its active conformation is all contained in its amino acid sequence. Thermodynamically, the conformation adopted would be the one favoured by the lowest Gibbs free energy for the system (Anfinsen, 1973; Yon, 2001). Under optimal *in vitro* folding conditions, Goldberger and colleagues observed that ribonuclease could take up to 20 minutes to refold (Goldberger *et al*., 1963). This time span is extremely 'slow' in the cellular context. If this was true, then even a small 100 amino acid long protein would take over a billion years to attain its correct conformation, which would be unrealistic under *in vivo* conditions (Levinthal, 1968). To counter this, Levinthal suggested that the folding process of a nascent polypeptide, therefore, could not be a random event and proposed the existence of specific folding pathways for proteins which allowed them to fold within seconds or minutes as required in the biological context.

Several folding models have emerged since then, and commonly, all try to address what is now famously called Levinthal's paradox. The classical nucleation-propagation model, the diffusion-collision model, the Jigsaw model and the hydrophobic collapse model are examples of some of the proposed models to decipher protein folding

pathways (Radford, 2000; Yon, 2001). The folding funnel hypothesis is a new approach based on the energy landscape theory, and proposes the existence of multiple micropathways, rather than a single pathway (Tsai *et al*., 1999). Figure 1.2 is a schematic representation of the possible course of events occurring during the folding cycle of a protein. Folding is triggered by hydrophobic collapse of the polypeptide chain, leading to the formation of secondary structure. The progression of unfolded protein to its native fold is often challenged kinetically by the formation of misfolded and energetically unfavourable intermediate forms resulting in protein aggregates (Yon, 2001). The occurrence of transient intermediate forms has been identified in studies conducted with lysozyme (Wetlaufer and Ristow, 1973) and bovine pancreatic trypsin inhibitor (Creighton, 1974). The rich molten globule state, on rearrangement gives rise to the native folded protein.

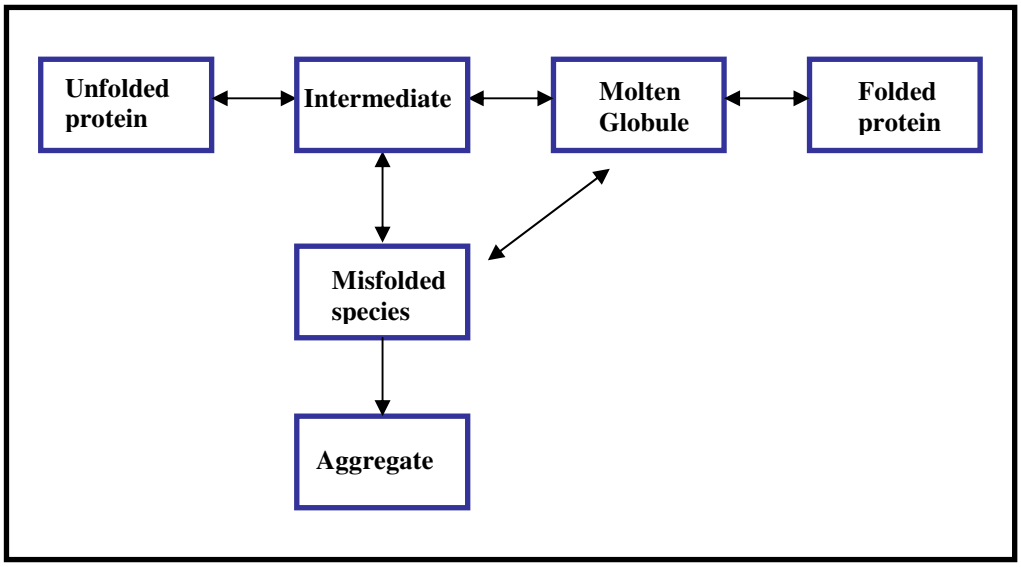

Figure 1.2: Proposed folding pathway for an unfolded protein adapted from Yon J.M (2001).

During the very fast event of protein folding, the unfolded protein sifts through various folding intermediates to attain the native folded state. Side reactions could push the intermediates into the 'off pathway' ultimately leading to aggregation and accumulation of the unfolded protein species.

The principles of protein folding established by *in vitro* studies generally hold true under *in vivo* conditions for small, single domain proteins (Hartl, 1996). However, the same principles do not extend satisfactorily to explain folding of complex multidomain proteins. It is now recognised that under *in vivo* cellular conditions not all proteins fold spontaneously and require additional assistance to reach their native fold (Ruddon and Bedows, 1997).

1.1.2. Chaperone assisted folding

One of the main factors which cannot be replicated during *in vitro* folding studies is the complex cellular environment. Nascent polypeptides emerging from the ribosome are exposed to a complex medium in the cytoplasm where macromolecules such as cellular proteins and RNA are crowded together at concentrations as high as 300 g of protein per litre (Minton, 1999). This environment promotes the formation of unwanted intermolecular interactions which pose a threat to the proper folding and can lead to aggregation. Also, during protein synthesis the emerging polypeptide can begin to fold before the entire chain has been synthesised. It therefore exists in an energetically favourable but a partially folded or unfolded intermediate state, which could potentially expose normally buried hydrophobic regions (Radford, 2000; Nicoll *et al*., 2005). This is a scenario that could potentially promote aggregation. Intervention and assistance in the folding process comes in the form of a class of proteins called the molecular chaperones (Slepenkov & Witt, 2002).

Molecular chaperones represent a family of proteins which have been extensively studied over the past 40 years. Their importance is highlighted by the gathering body of evidence on the cell and tissue pathology caused by defective chaperones (Macario and Conway de Macario, 2005; Nardai *et al*., 2006). Historically, the term molecular chaperone was first used by Laskey and co-workers to describe the behaviour of nucleoplasmins in promoting histone-histone interactions (Laskey *et al*., 1978). Ellis and Hemmingsen, applied this term to include families of bacterial and eukaryotic proteins involved in protein folding and translocation on the basis of their observations that chaperones were also essential for the folding of the plant protein ribulose bisphosphate carboxylase (Ellis, 1987).

Chaperones are an essential part of the cellular machinery and are required for the proper maintenance of the protein structure, protein translocation and oligomerization. They assist folding of the nascent polypeptide by binding to the exposed hydrophobic patches of the folding intermediates. They play a key role in leading the nascent polypeptide to its cellular destiny during protein folding in the cell (Figure 1.3) by forming non-covalent interactions with the polypeptides emerging from the ribosome, thereby preventing their aggregation and facilitating in their folding (Bukau *et al*., 2006). Polypeptides with aberrant folding are assigned to the degradation pathway

(Bukau *et al*., 2006). The structure assumed by the polypeptide is still dictated by its amino acid sequence. Chaperones cannot direct a protein to assume a different fold. Importantly, they are not part of the final folded structure (Ellis and Hartl, 1996; Hartl, 1996).

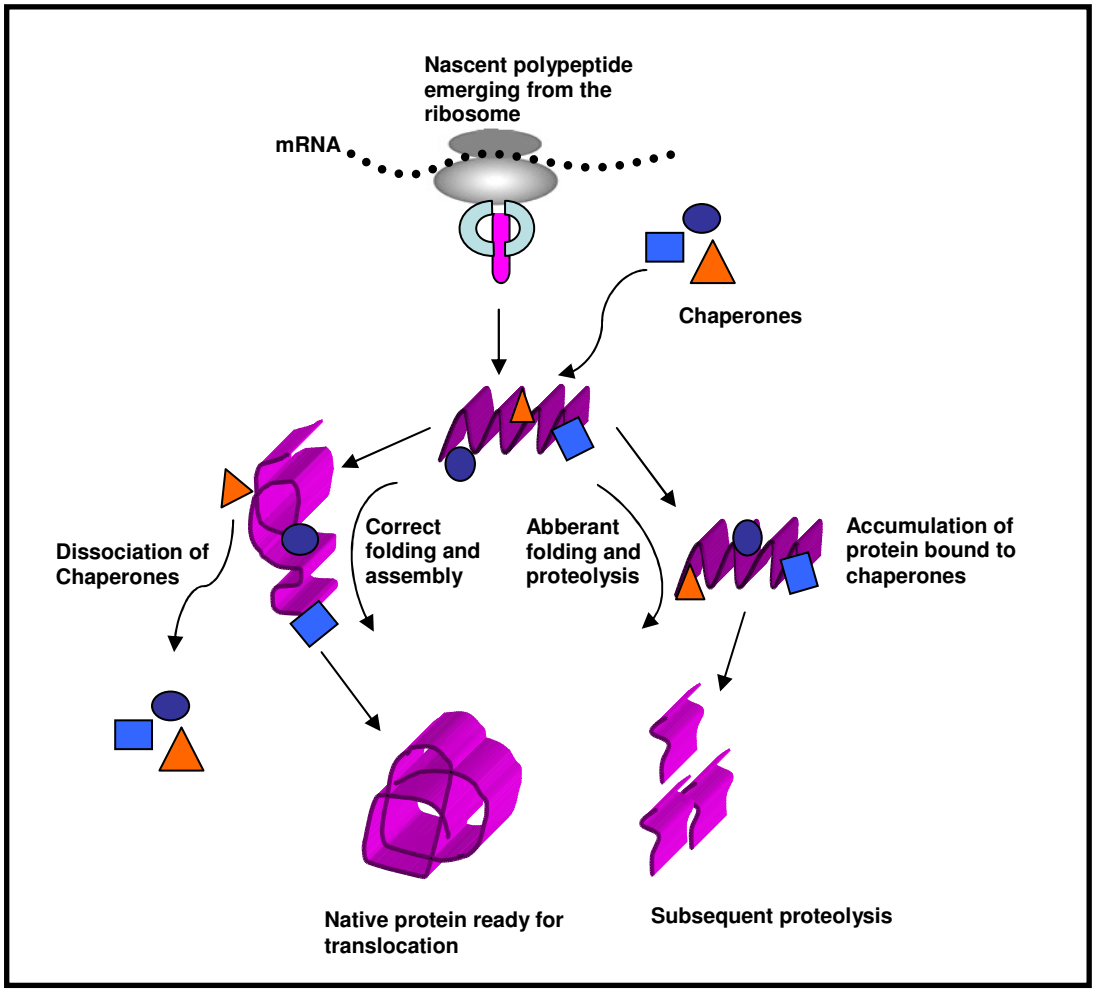

Figure 1.3: Schematic pathway for protein folding (adapted from Perlmutter DH, 1999).

Nascent polypeptide emerging from the ribosome faces a crowded intracellular environment, which promotes the formation of unwanted interactions. Polypeptides are assisted by the chaperone proteins which allow them to attain their native fold or in extreme cases direct them to the proteolysis pathway.

Currently, the term chaperone encompasses approximately 20 protein families. These families have varied functions, locations and structures. Different classes of proteins tackle specific state(s) of unfolding. The majority of proteins characterised as chaperones belong to the heat shock protein (HSP) family (Bukau and Horwich, 1998; Radford, 2000).

1.2. Heat shock proteins

The heat shock response was first reported by Feruccio Ritossa in the fruit fly (*Drosophila melanogaster*) in 1963. He observed that an elevation in temperature (heat shock) produced chromosomal puffs in the *Drosophila* salivary gland (Ritossa, 1963; Welch 1993). In 1973, Tissieres and co-workers demonstrated that chromosomal puffing was accompanied by increased expression of both a 70 and a 26 kDa protein species (Tissieres *et al*., 1974). Initially this phenomenon was believed to be unique for *Drosophila*; however, it became clear that a similar response could be observed in a wide variety of species including bacteria, yeast, complex plants such as soybean and even mammalian cells (Marx, 1983). Li and Werb correlated the expression of heat shock proteins with conferment of thermotolerance in their studies with Chinese hamster fibroblasts (Li and Werb, 1982). Cells respond to thermal shock by switching off the synthesis of most cellular proteins, however, elevated expression of one particular class of proteins called the heat shock proteins (HSP) was observed (Lindquist and Craig, 1988). Accumulation of the heat shock proteins appears to shield cells from temperature induced damage and also promotes cell survival (Li and Werb, 1982). Cells pre-exposed to non-lethal temperatures prior to exposure to lethal temperatures are found to acquire thermotolerance. They survive the heat shock while untreated cells cannot (Hanh and Li, 1982; Marx, 1983). Figure 1.4 illustrates the effect of heat treatment on cell viability.

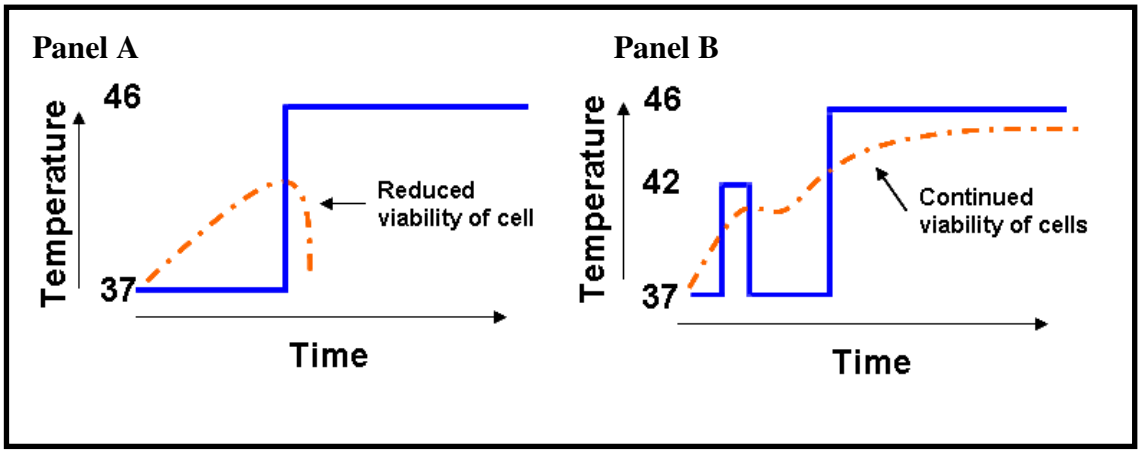

Figure 1.4: Acquired thermotolerance in *E.coli* cells subjected to elevated temperatures. (redrawn from http://www.tulane.edu/~biochem/med/hsp.htm)
Panel A depicts occurrence of cell death when cells are directly exposed to lethal temperatures of 46^{o}C.
Panel B shows increased cell viability when cells are exposed to sub-lethal temperature of 42^{o}C prior to heat shock at 46^{o}C.

It has now been established that factors other than heat also promote the over expression of heat shock proteins. For example, exposure to amino acid analogues (Li and Lazlo, 1985), heavy metals (Levinson *et al*., 1980) and depleted ATP levels (Welch 1993) are some of the conditions that have been shown to induce this response. Other physiological, pathological and environmental agents for induction of heat shock proteins are listed in Table 1.2.

Physiological	**Pathological**	**Environmental**
Cycle of cell division	Viral, bacterial and	Heat shock
Growth factors	Parasitic infections	Heavy metals
Cell differentiation	Fever	Metabolic inhibitors
Tissue development	Inflammation	Amino acid analogues
Hormonal stimulation	Ischemia	Ethanol
	Hypertrophy	Antibiotics
	Oxidant injury	Radiation
	Malignancy	
	Autoimmunity	

Table 1.2: Physiological, pathological and environmental conditions that induce the heat shock response (Schlesinger, 1990).

1.2.1. Types of heat shock proteins

The heat shock protein family are highly conserved in both eukaryotes and prokaryotes (Gupta & Singh, 1992). They are classified into six subfamilies based on their molecular weights. These proteins can be constitutively present or exhibit induced expression and can be distributed in different cellular compartments such as the cytosol, mitochondria, endoplasmic reticulum (ER) and nucleus (Bukau and Horwich, 1998). While, members of the mammalian HSP70 family are distributed in the aforementioned compartments, the HSP60 and HSP10 families are localised in the organelles and HSP100, HSP90 and HSP20 family members have been mainly detected in the cytosol. Table 1.3 tabulates the major heat shock families identified, their eukaryotic and prokaryotic counterparts of each family and their cellular distributions.

Family	Organism	Chaperone	Localisation
HSP100	*E.coli*	C1pA,B,C	Cytosol
	S.cerevisiae	Hsp104	Cytosol
HSP90	*E.coli*	HtpG	Cytosol
	S.cerevisiae	Hsp83	Cytosol
	Mammals	Hsp90	Cytosol
		Grp94	ER
HSP70	*E.coli*	DnaK	Cytosol
	S.cerevisiae	Ssa 1-4	Cytosol
		Ssb 1,2	Cytosol
		Kar2	ER
		Ssc1	Mitochondria
	Mammals	Hsc70	Cytosol/Nucleus
		Hsp70	Cytosol/Nucleus
		BiP(Grp 78)	ER
		mHsp70	Mitochondria
HSP60 (Group I and II)	*E.coli*	GroEL(GroupI)	Cytosol
	S.cerevisiae	Hsp60 (GroupI)	Mitochondria
	Plants	Cpn60 (GroupI)	Chloroplasts
	Mammals	Hsp60 (GroupI)	Mitochondria
		TCP1(GroupII)	Cytosol
	Archaebacteria	Thermosome (GroupII)	Soluble
HSP40	*E.coli*	DnaJ	Cytosol
	S.cerevisiae	YdJ1	Cytosol/Nucleus
	Mammals	Hsp40 members such as HDJ1, HDJ2,	Cytosol
Small HSP's	*E.coli*	1bp a and B	Cytosol
	S.cerevisiae	Hsp27	Cytosol
	Mammals	αA and αB crystalline	Cytosol
		Hsp27	Cytosol

Table 1.3: Classification of the heat shock protein family, distribution in different organisms and also their subcellular localization (adapted from Bukau and Horwich, 1998).

The family is represented by 'HSP'. Protein members are suffixed by 'Hsp' and a numerical designation that represents the characteristic molecular weight of family members in kDa

1.2.2. Regulation of the hsp gene expression

Expression of the *hsp* genes is regulated at the transcriptional level. Studies on cellular response to stress carried out in *Saccharomyces cerevisiae* by Finkelstein *et al*., concluded that transcriptional activity is remarkably altered after heat shock. The observed accumulation of heat shock proteins is directly correlated with an increased rate of transcription of the corresponding genes (Finkelstein *et al*., 1982). Such regulation is observed in both eukaryotic and prokaryotic systems (Bukau, 1993; Morimoto, 1993). In *E.coli* the heat shock genes are arranged in a regulon of 20 genes (Bukau, 1993). It is regulated by the σ^{32} subunit of RNA polymerase (RNAP). The σ^{32} subunit is a product of the *rpoH* gene and confers specificity to the core RNAP for transcription of the *hsp* genes (Grossman *et al*., 1984; Landick *et al*., 1984; Cowing *et al*., 1985).

In eukaryotes, heat shock transcriptional activation is mediated by heat shock transcription factor called the heat shock factor (HSF, Morimoto, 1993). The promoter regions of *hsp* genes hosts multiple adjacent and inverse iterations of the motif 5′-nGAAn-3′ called heat shock promoter elements (HSE) (Morimoto, 1998). In mammalian unstressed cells HSF exists in an inactive monomeric state, bound to HSP (Schlesinger, 1990). The stress response triggered by an increasing accumulation of unfolded/aggregated protein (Morimoto *et al*., 1993) induces binding of heat shock factor (HSF) to the HSE (illustrated in Figure 1.5). First, HSF bound to HSP separates from the HSP. The free HSF in turn is phosphorylated by a serine/threonine kinase resulting in a homotrimer structure which then enters the nucleus (Hensold *et al*., 1990; Sarge *et al*., 1993; Cotto *et al*., 1996). The trimeric HSF binds to the HSE and undergoes further phosphorylation by HSF kinase. This results in transcriptional activation of *hsp* genes and their subsequent translation. Interestingly, Hsp70's play a regulatory role in the activation of HSF during the heat shock response. Upon attenuation of the heat shock response, unengaged Hsp70 binds to HSF, which converts HSF to its inactive form, thus auto-regulating the heat shock response (Kiang and Tsokos, 1998; Morimoto, 1993).

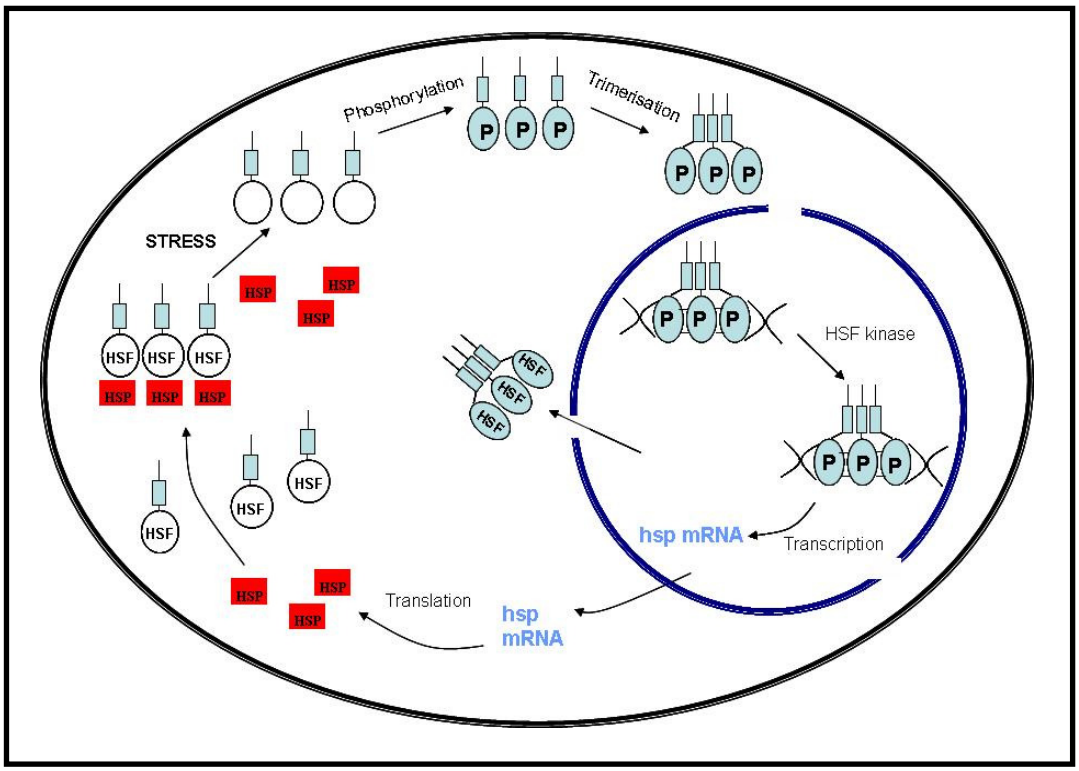

Figure 1.5: Transcriptional regulation of *hsp* gene expression (adapted from Kiang and Tsokos, 1998).

Transcription factor, (HSF), during the unstressed state is bound to HSP and is inactive. Accumulation of non-native proteins induces the heat shock response. Activated HSF separates from the HSP, undergoes phosphorylation and enters the nucleus. There it binds to the HSE on the promoter region and activates transcription of the *hsp*.

1.2.3. Functional roles

The diverse roles fulfilled by the different HSP families are summarised in Table 1.4. Proteins from the 60, 70 and 90 kDa families exhibit chaperone functions and bind to unfolded proteins. The HSP70 and HSP60 families, although structurally unrelated, bind to unfolded polypeptides in an adenosine tri-phosphate (ATP) dependent manner (Becker and Craig, 1994; Fink 1999). HSP60's also known as chaperonins, allow misfolded polypeptides to unfold and refold in their central cavity (Bukau and Horwich, 1998). HSP90 on the other hand, binds to and regulates the function of folded proteins such as tyrpsin kinase, steroid hormone receptors, actin and tubulin in an ATP dependent manner (Becker and Craig, 1994; Csermely *et al*., 1998; Lindquist and Craig 1988).

Family	Function
HSP100	Stress tolerance; helps resolubilisation of heat inactivated proteins from insoluble aggregates
HSP90	Signal transduction (e.g., interaction with hormone receptors and kinases); autoregulation of the heat shock response; role in cell cycle and proliferation
HSP70	Acts as molecular chaperones; provides cytoprotection; anti-apoptotic activity; in *E.coli* essential for lambda phage replication
HSP60	Acts as molecular chaperones; may facilitate protein degradation as cofactor of proteolytic systems.
HSP40	Co chaperone activity with Hsp70 proteins
Small HSP's	Regulates actin cytoskeleton; acts as molecular chaperone; provides cytoprotection

Table 1.4: Functional roles fulfilled by the different HSP families

For the purpose of this thesis, the rest of this chapter will concentrate on the 70 kDa heat shock protein family, its function, structure and co-chaperone partner proteins due to their relevance to the work described in this thesis.

1.3. The HSP70 chaperone family

The HSP70 class of proteins are a ubiquitous family expressed under various physiological stress conditions (Morishima, 2005). They have been identified in all eukaryotes and prokaryotes and in some but not all of archaea (Boorstein *et al*., 1994; Conway De Macario and Macario, 1994; Macario *et al*., 1999). Certain members of the archaeal kingdom such as some methanogens, extreme thermophile and halophiles have been shown to not produce the protein (Macario *et al*., 1999). The number of members of the HSP70 family expressed varies from organism to organism. Thirteen Hsp70 proteins have been identified in humans, whilst only 3 have been detected in *E.coli* (Vos *et al*., 2008). All identified *hsp70* genes are highly conserved and show at least 50% identity (Boorstein *et al*., 1993). Some of the well characterised members of the HSP70 family are DnaK from *E.coli*, SSA and SSB proteins from *S.cerevisiae*, the mammalian cystolic Hsp70 and BiP from the mammalian ER (Bukau and Horwich, 1998). In the mammalian cytosol there are two forms of Hsp70 protein, one is the inducible Hsp70, also referred to as Hsp72 while the other is the constitutive form also know as heat shock cognate (Hsc70) or Hsp73 (Brown *et al*., 1993; Welch, 1993; Jolly and Morimoto *et al*., 2000). The amino acid sequence of Hsc70 shows 90% identity with the inducible Hsp70 (O'Malley *et al*., 1985; Moon et al., 2001). Multiple sequence alignment performed using ClustalW (Figure 1.6) highlights the high degree of conservation between the Hsp70 proteins from evolutionarily divergent organisms, bacterial and bovine and also between the human inducible and constitutive forms.

Figure 1.6: Multiple sequence alignment of selected HSP70 family members

Multiple sequence alignment of HSP70 protein sequences of *E.coli*, human and bovine origin was performed using ClustalW (Thompson *et al.*, 1994). Thier UniProt ids are indicated in brackets. Asterisks indicate an identical match, colons indicate conserved substitutions and full stops indicate semi- conserved substitutions.Small and hydrophobic amino acid are coloured red, acidic coloured blue, basic residues in magenta, hydroxyl in green.

The Hsp70's perform a number of important cellular functions. The role of Hsp70 in assisting unfolded protein was first identified by Haas and Wabl while working on Bip, the Hsp70 of the ER. They showed that Bip was capable of binding incompletely assembled immunoglobulin heavy chains (Haas and Wabl, 1983). Some Hsp70's have also demonstrated the ability to solubilise protein aggregates with the aid of the Hsp100 family (Glover and Lindquist, 1998). DnaK on its own can effectively solubilise and refold small aggregates of glucose-6-phosphate dehydrogenase, however larger aggregates of up to 10 monomers required the assistance of the bacterial Hsp100 homologue, ClpB (Diamant *et al*., 2000).

Mammalian cytosolic Hsp70's have also been shown to be involved in protein translocation. Proteins carrying a pentapeptide motif (KFERQ) have been reported to be targeted to the lysosome for degradation by Hsp70 (Chiang and Dice, 1988). The *E.coli* counterpart, DnaK, also assists in protein translocation and is essential for the export of alkaline phosphatase (Wild *et al*., 1992). Studies with Ssa1p (Hsp70 from *S.cerevisiae*) highlighted the importance of cytosolic Hsp70's in the post-translational import of proteins to the mitochondria and the outer membrane of ER. Depletion of Ssa1p led to the accumulation of a mitochondrial precursor protein in the cytosol (Deshaies *et al*., 1988). Additionally, Hsc70 has also been implicated in binding and stabilizing locally unfolded nuclear localization signals and therefore is involved in nuclear protein import (Dingwall and Laskey, 1992).

Hsp70 proteins have been found to play a role in cell survival. Deletion of the *dnaK* gene is lethal to bacteria, whilst mutations in the gene disrupts several basic cellular mechanisms such as host RNA and DNA synthesis (Zylicz *et al*., 1993), initiation of bacteriophage λ and P1 DNA (Zylicz *et al*., 1988), plasmid DNA replication (Sakakibara, 1988) and expression of other heat shock proteins (Tilly, 1983). Mammalian Hsp70s promote cell survival by blocking caspase activation and suppress mitochondrial damage and nuclear fragmentation, mediated through the binding of Hsp70 with pro-apoptotic proteins such as c-myc and p53 (Mosser, 1997). This has serious implication in oncogenesis and over expression of Hsp70 has been observed in malignant human tumors. Selective deletion of the protein induces cell death in the cancer cell lines (Gyrd-Hansen *et al*., 2004). Their involvement in signal transduction, cell cycle regulation, differentiation and cell death assumes relevance also in other

pathological conditions such as neurodegenerative diseases, auto-immune diseases and viral infections (Jolly and Morimoto, 2000).

Distinct functional specificity exists between the different Hsp70's despite their high degree of conservation (Suppini, 2004). Experiments conducted with the *E.coli* DnaK and yeast mitochondrial Hsp70 (mtHsp70) show that the two Hsp70's are not interchangeable. Moro *et al*., reported that *E.coli* DnaK was incapable of promoting the import of mitochondrial precursors when introduced in place of the yeast mtHsp70 (Moro *et al*., 2002). Similarly, human Hsc70 is unable to complement an *E.coli* DnaK mutant and restore growth at high temperatures and λ phage propagation.

1.3.1. Domain architecture

All Hsp70 homologues are composed of three conserved regions. Figure 1.7 is a schematic representation of the conserved domain architecture as reported for the human Hsp70.

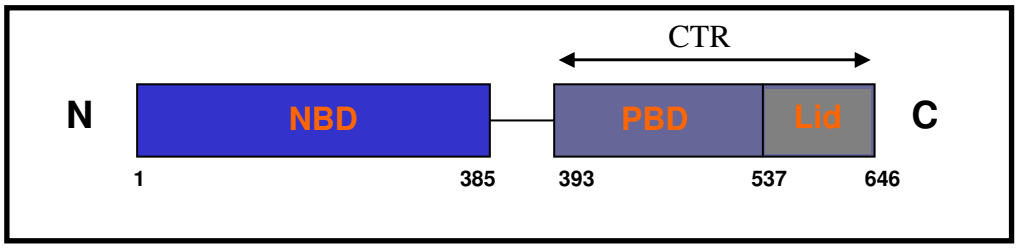

Figure 1.7: Domain architecture of Hsp70 proteins.

A diagrammatic representation of the domains present in Human Hsc70 which are conserved in the Hsp70 family. NBD represents the nucleotide binding domain. The C-terminal region (CTR) comprises of the PBD which is the peptide binding domain and the distal 10 kDa lid region.

They N-terminal region is characterised by a highly conserved 44-kDa nucleotide binding domain (NBD) followed by a 28-kDa C-terminal region (CTR) which can be subdivided into a conserved 18-kDa peptide binding domain (PBD) and a less conserved 10-kDa C-terminal lid region. The structures of the domains have been determined in isolation by X-ray crystallography.

1.3.1.1. Nucleotide binding domain

The chaperone activity of Hsp70 proteins is driven by ATP hydrolysis. X-ray structures of the bovine apo-NBD, native and various mutants of the bovine Hsc70 NBD complexed with ATP, ADP, AMP-PNP are available in the Protein data bank (PDB) (Flaherty *et al*., 1990; Flaherty *et al*., 1994; Wilbanks *et al*., 1994; Jiang *et al*., 2007). Figure 1.8 is the ribbon representation of the bovine NBD with a bound ADP molecule (Pdb id: 3HSC). The NBD is a bi-lobed structure (I and II) and each lobe is further divided into two sub-domains (A and B). Lobes I and II are separated by a deep cleft. The bottom of the cleft forms the binding site for the nucleotide in complex with Mg^{2+} ion and two Na^{+} ions (Flaherty *et al*., 1990). The opening frequency of the nucleotide binding cleft appears to be regulated by the nature of the nucleotide bound in the order of nucleotide free>ADP>ADP+Pi>ATP (Gassler *et al*.,2001)

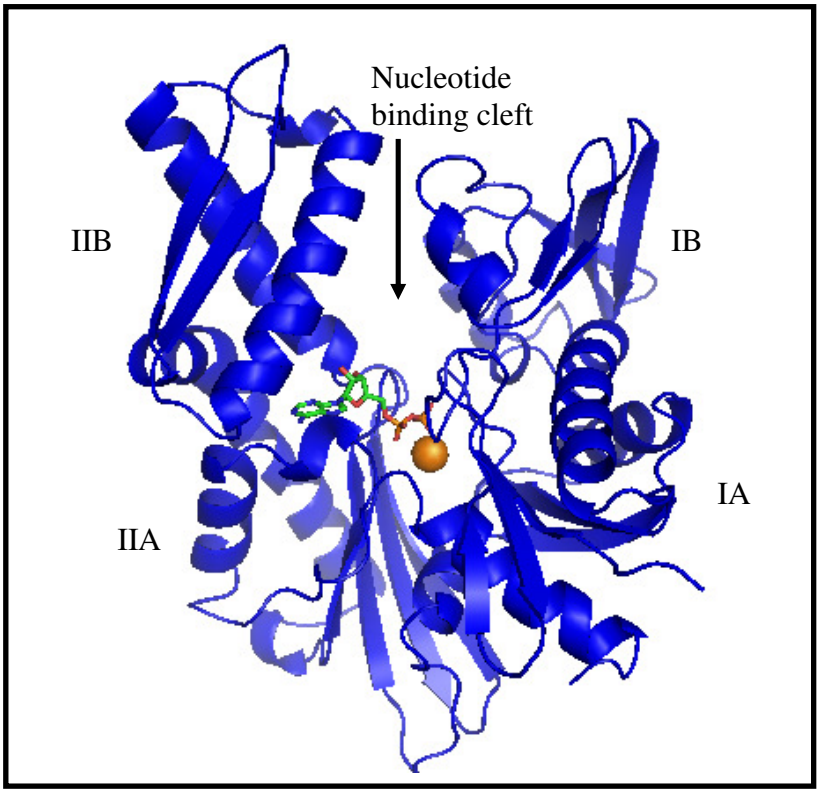

Figure 1.8: Nucleotide binding domain of bovine Hsc70 determined by X-ray crystallography

Ribbon representation of the NBD of bovine Hsc70 generated by Pymol (Pdb id: 3HSC; Flaherty *et al*., 1990). The structure is in complex with ADP, magnesium, 2 sodium ions and phosphate. In this figure ADP is represented by sticks and magnesium represented by an orange sphere. Sub-domains of lobes I and II are represented as IA, IB and IIA, IIB respectively.

However, subtle differences have been shown to exist in the NBD between members of the HSP70 family. This includes variations in an exposed loop in sub-domain IIB near the nucleotide binding cleft, the occurence of a hydrophobic patch at the top of the cleft and two putative salt bridges which could alter the polarity of the interface. Based on these differences, the HSP70 protein family can be grouped into three subfamilies. *E.coli* DnaK, *E.coli* HscA and human Hsc70 exemplify these sub-groups (Brehmer *et al.*, 2001). The three families also differ in the ADP disassociation rates with DnaK having values of 0.004-0.035 s^{-1} in presence of inorganic phosphate. Hsc70 has been reported to be 20-fold faster and HscA almost 700 fold faster (Brehemer *et al*., 2001). These differences influence the role played by nucleotide exchange factors (NEF) in the regulation of Hsp70's ATPase activity. NEFs are further discussed in Section 1.5.1.

1.3.1.2. C-terminal region

The C-terminal region is characterised by two sub-domains. The first sub-domain corresponds to the 18 kDa peptide binding domain (PBD) involved in binding to the unfolded regions of the substrate and the second sub-domain corresponds to the distal C-terminal 10 kDa lid region. The structure of the entire C-terminal domain from *E.coli* (Zhu *et al*., 1996) and also that of the sub domains in isolation has been determined (Zhu *et al*., 1996; Wang *et al*., 1998; Pellechia *et al*., 2000).

Peptide binding domain

The tertiary fold of the 18-kDa PBD comprises of a β domain followed by a single helix. The β domain is a sandwich comprising of two stacks of four anti-parallel β-sheets. The loops in between the β-strands 1, 2(L1, 2) and 3, 4(L3, 4) hosts the peptide binding site (Morshauser *et al*., 1999).

10-kDa distal C-terminal module

The 10-kDa distal fragment is an α-helical domain comprising of five antiparallel helices. It is believed to function as a lid which folds over the beta sandwich of the PBD. But there has been no evidence of it making any contact with the bound peptide (Zhu *et al*., 1996).

Figure 1.9 shows the structure of the entire C-terminal region of DnaK determined by X-ray crystallography (Pdb id: 1dkx). The two sub-domains and the loops hosting the peptide binding site are indicated on the figure.

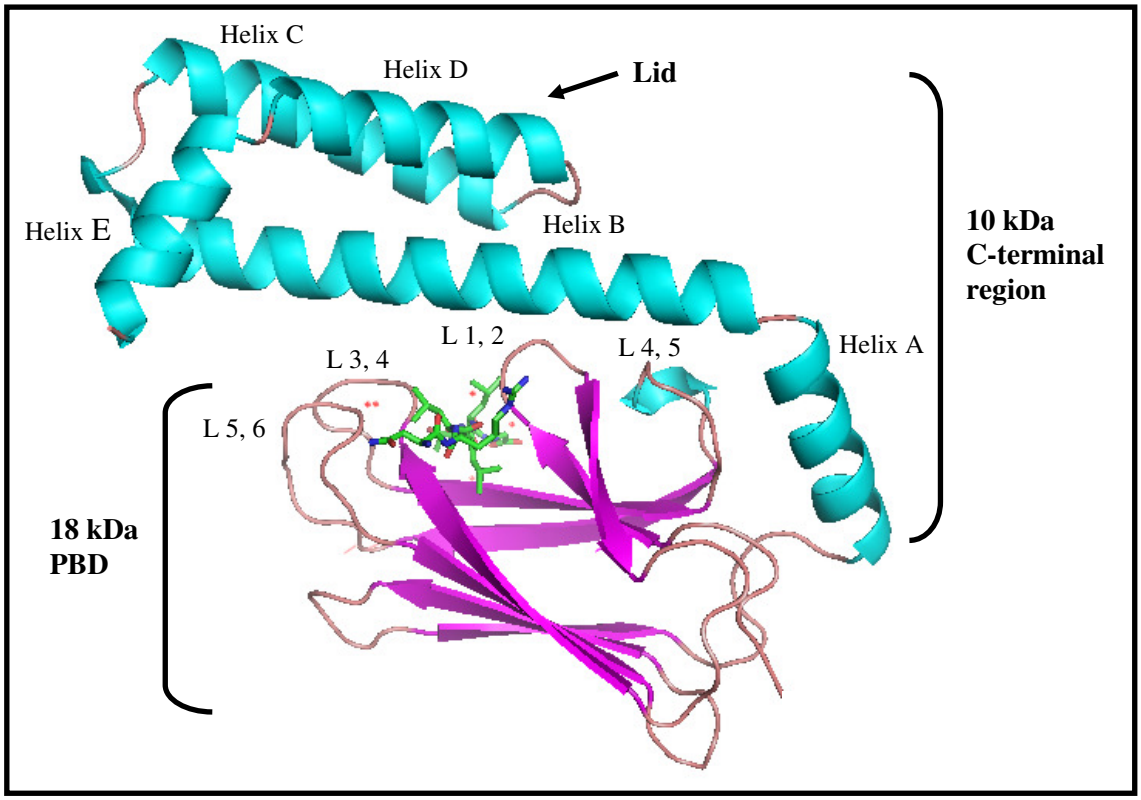

Figure 1.9: Structure of the 28-kDa C-terminal region (CTR) of *E.coli* DnaK (Pdb id: 1DKX)

Ribbon representation of the CTR of *E.coli* DnaK generated by Pymol (Pdb id: 1DKX; Zhu *et al*., 1996).The structure is in complex with bound peptide substrate (NRLLLTG) in stick representation. The 18-kDa PBD comprises of β sheets and is coloured purple. Loops 1, 2 and 3, 4 form part of the substrate binding cavity. The 10 kDa lid region is depicted in teal. The five helices making up this region are labelled A-E.

Peptide specificities

The substrate binding mechanism and specificity of the Hsp70 group of proteins have been studied using short peptides. Peptides mimic the unfolded regions of polypeptide chains which actually serve as substrates for the Hsp70's (Landry *et al*., 1992). Studies with DnaK indicate that Hsp70's bind hydrophobic segments in an extended conformation through the peptide binding domain (Zhu *et al*., 1996). Using phage display studies and cellulose bound peptide scans; DnaK has been shown to prefer peptide motifs which contain a core of 4-6 hydrophobic residues flanked by basic residues (Gragerov *et al.,* 1994; Rüdiger *et al*., 1997). An example of a high affinity peptide sequence for DnaK is NRLLLTG (Gragerov *et al.,* 1994*)*. Interestingly Hsc70

can bind with high affinity to two different peptide motifs. One is a basic peptide (NIVRKKK) while the other is a hydrophobic motif (FYQLALT) (Takenaka *et al*., 1995). The binding motif of Bip was determined to be Hy(W/*X*)Hy*X*Hy*X*Hy where Hy is a large hydrophobic residue, W is tryptophan, and *X* is any amino acid except charged residues (Blond-Elguindi *et al*., 1993). This amino acid selectivity confers substrate specificity and thereby functional diversity to the different Hsp70's. This would explain the observed inability of the different Hsp70's to function interchangeably (Terlecky *et al*., 1992; Brodsky *et al*., 1993). Suppini *et al*., reported that while a chimera of Hsc70 and DnaK constructed with the NBD of Hsc70 and C-terminal domains of DnaK could complement an *E. coli dnaK* mutant strain at 43^{o}C and support λ phage propagation, the same was not possible with either the full length Hsc70 or with an Hsc70-DnaK chimera constructed with the NBD of DnaK and the C-terminal domains of Hsc70 (Suppini *et al.*, 2004). This experiment highlights the role of the CTR in conferring functional diversity to the Hsp70 family members.

1.3.1.3. Interdomain communication

Although the two domains of Hsp70s are functional in isolation, Hsp70 chaperone activity requires the two domains to be physically linked. The linker region is a highly hydrophobic segment containing a conserved leucine triplet and the linker has been implicated for its role in the interdomain communication between the NBD and PBD (Vogel *et al*., 2006; Sousa and Lafer, 2006). Mutations to this region resulted in coupling defects in DnaK, for example, mutating two of the LL residues to DD abolished interdomain communication (Han and Christen, 2001). Residues R151, D388, D393, K155 and R167 in DnaK have been identified as multiple interaction points between the two domains (Vogel *et al*., 2006). Point mutations, T204E in the NBD (O'Brien and McKay, 1993) and K414I on the beta sheet sandwich of the PBD (Montgomery *et al*., 1999) have also been identified to disrupt the communication between the two domains. Vogel *et al*., reported the existence of a conserved proline in the NBD which acts as a 'molecular switch' to stabilize the conformations (Vogel *et al*., 2006).

A structure of the full length Hsp70, protein which could help understand the interdomain allostery, is not available. A crystal structure of a bovine Hsc70 two domain construct lacking the C-terminal 10-kDa region has been reported. However

the protein carries two mutations (D213A/E214A) on the interdomain interface (Jiang *et al*., 2005). Figure 1.10 is a cartoon representation of the 2-domain structure of the bovine Hsc70 with the NBD, PBD and the short linker region connecting them indicated (Jiang *et al*., 2005). The structure, which does not have any bound nucleotide, reveals that interdomain contact is promoted by one side of helix A of the PBD which rests in a groove between sub-domain IA and IIA of the NBD. Also the interdomain linker is solvent exposed (Jiang *et al*., 2005). An NMR model of a 54-kDa fragment of DnaK from *Thermus thermophilus* in the ADP bound state has also been reported, however, the packing arrangement of the domains reported differs from the crystal structure bovine Hsc70 (Revington *et al*., 2005). In this model, it is the region of the β sub-domain near the entry point of the interdomain linker and not the helix A of the PBD which interacts with the cleft in the ATPase domain (Revington *et al*., 2005). However since both constructs carry mutations and deletions, Swain *et al*., contemplate that these structures might not represent a physiological interdomain crystal packing interaction. Using NMR and other biophysical studies on a two-domain *E.coli* DnaK construct, they instead propose that the NBD and PBD interact only upon ATP binding, and not in the ADP or nucleotide free state (Swain *et al*., 2007). However in the absence of a full length structure, it will be difficult to decipher the exact mechanism of the interdomain interactions.

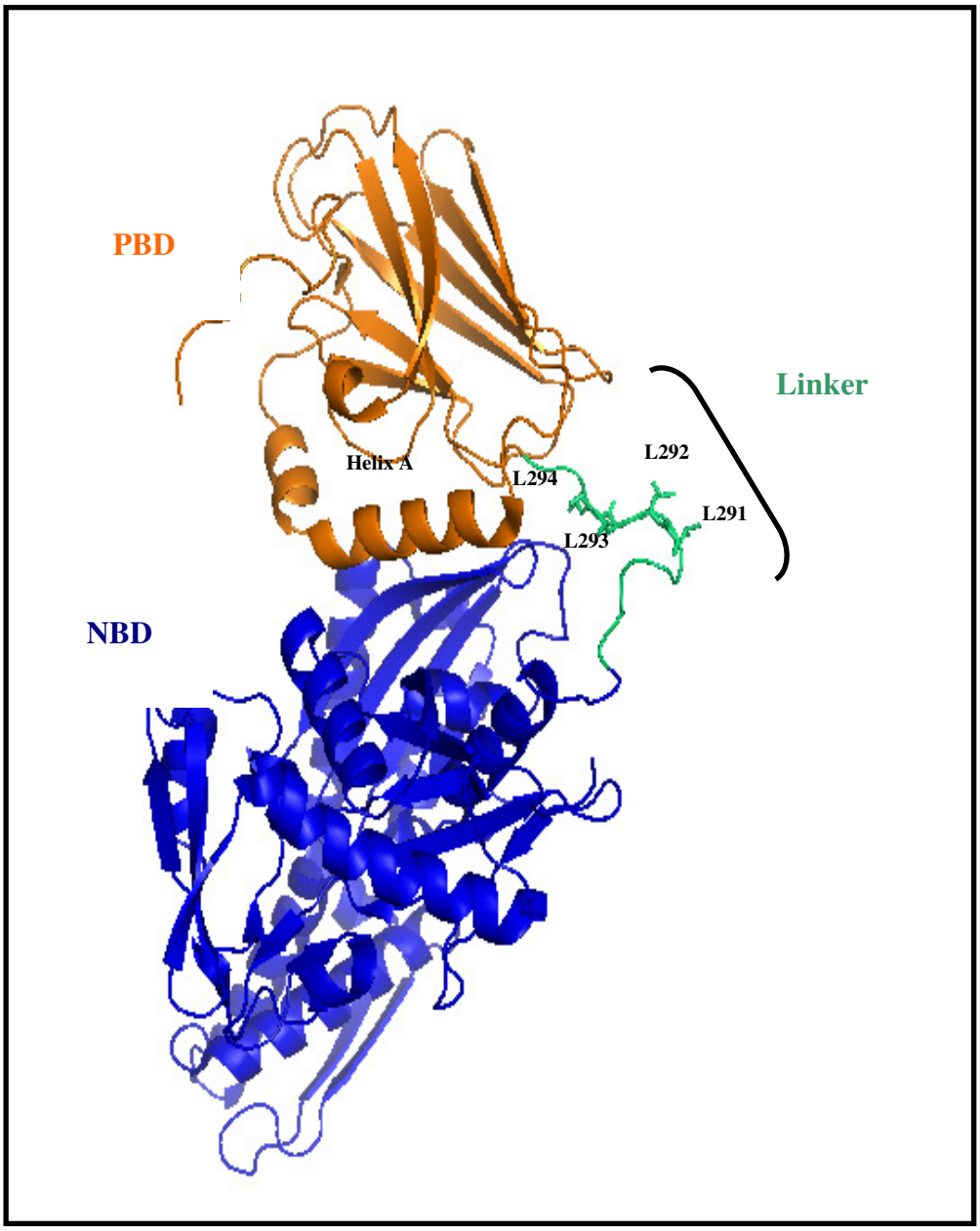

Figure 1.10: Interdomain interaction of the NBD and PBD in bovine Hsc70

Ribbon representation of the crystal structure of a two domain construct of bovine hsc70 (Pdb id: 1YUW; Jiang *et al*., 2005). The NBD is indicated in blue and the PBD in orange. The linker region involved in the interdomain communication is indicated in green, and the conserved LLLL linker sequence is rendered in green with the side-chain orientations shown. Helix A of the PBD rests in a groove between sub-domain IA and IIA of the NBD.

1.3.2. Hsp70 reaction cycle

The ATP hydrolysis activity of the NBD is allosterically coupled with the substrate binding of the PBD (Buchberger *et al*., 1995; Gassler *et al*., 1998; Suh *et al*., 1999). ATP binding induces conformational change in the PBD and opens the substrate binding cavity (Suh *et al*., 1999). In this state, the substrates have high k_{on} and k_{off} values i.e. protein has low affinity for substrate. This state is often referred to as the 'open' conformation. Substrate binding accelerates the ATP hydrolysis rate which causes a conformational change in the PBD resulting in the closure of the substrate binding cavity. This creates high affinity for substrate and represents the 'closed' state of the protein (Bukau and Horwich, 1998; Mayer *et al*., 2000).

The reaction cycle of the *E.coli* DnaK works in co-ordination with its co-chaperone partners, DnaJ and GrpE. The co-chaperone requirement for the Hsp70 reaction cycle is discussed in detail in the section 1.6. The cycle begins with the detection of the unfolded protein. Two schools of thought exist relating to the binding of unfolded protein to DnaK. One suggests that DnaK in the ATP bound form directly binds to the substrate and undergoes ATP hydrolysis upon interaction with the *E.coli* DnaJ, a representative of the HSP40 family (McCarty *et al*., 1995). The other asserts that it is the DnaJ co-chaperone protein which binds to the substrate and subsequently targets the substrate to DnaK (Hartl, 1996). Figure 1.11 illustrates the stages determined for the *E.coli* Hsp70, DnaK from the perspective that the DnaJ recruits the unfolded protein. The cycle described for the *E.coli* DnaK chaperone is generally accepted to represent the reaction cycle of other Hsp70 members, although certain differences do exist on the basis of co-chaperone requirement. The various steps of the DnaK cycle are as follows:

Step 1: Association of Hsp40 with substrate

Step 2: Transfer of the substrate to the ATP-bound form of Hsp70. First, DnaJ interacts transiently with DnaK to form an intermediate DnaK.DnaJ.S.ATP complex (referred to as Step 2a in Figure 1.11). Binding of both substrate and DnaJ results in the stimulation of ATP hydrolysis thereby converting DnaK to its ADP bound form. This in turn stabilises the DnaK.DnaJ.S.ADP complex (referred to as Step 2b in Figure 1.11).

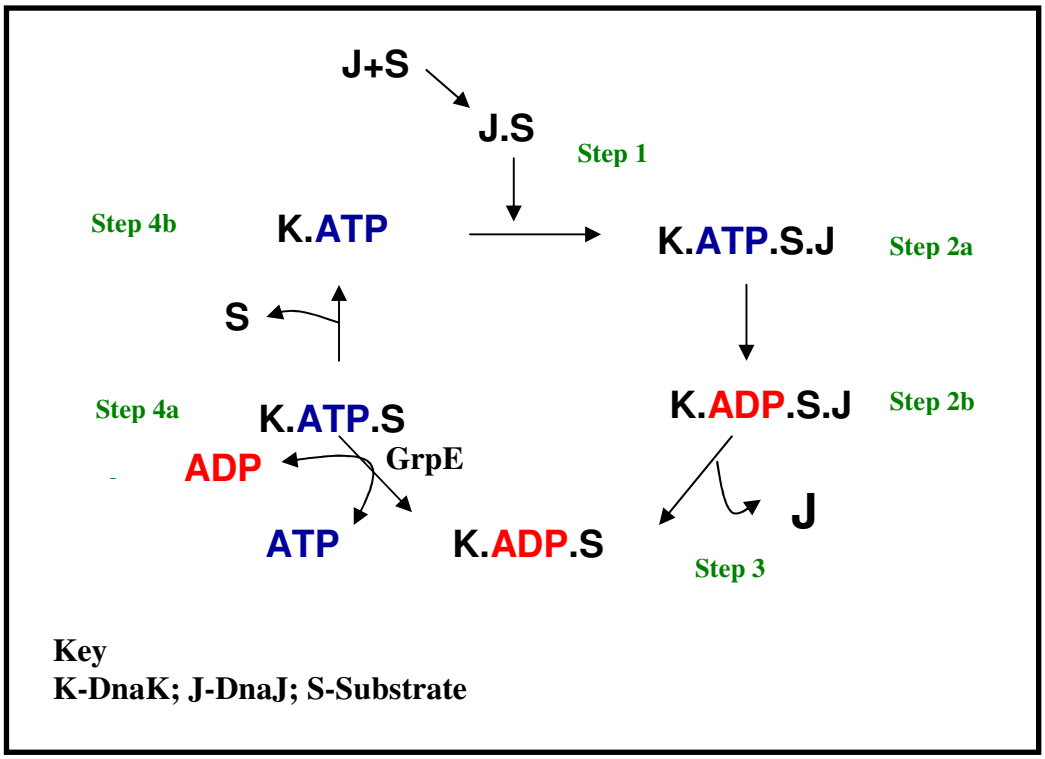

Figure 1.11: The DnaK/DnaJ/GrpE reaction cycle (adapted from Fink, 1999).

DnaJ binds to unfolded polypeptide and presents it to the ATP bound DnaK. Simultaneously DnaJ stimulates ATP hydrolysis by DnaK, to convert it from its low affinity ATP bound state to its high affinity ADP bound state. This results in the formation of a ternary complex between DnaK, DnaJ and the substrate. Subsequently, nucleotide exchange is facilitated by GrpE resulting in the release of the substrate.

Step 3: DnaJ disassociates from the complex to yield DnaK**.**ADP.S complex

Step 4: Exchange of ADP to ATP is carried out by another co-chaperone GrpE, a nucleotide exchange factor found in bacteria and mitochondria. Binding of ATP releases the substrate, and reverts DnaK to its low substrate affinity, ATP bound state (Bukau and Horwich, 1998 and Fink, 1999).

1.3.3. Hsp70 co-chaperones

The switch between the high and low substrate affinity Hsp70 states is mediated with the assistance of various co-chaperones proteins (Bukau and Horwich, 1998), that interact with Hsp70s to regulate and direct their chaperone activity (Caplan, 2003; Mayer and Bukau, 2005). Three major families of co-chaperones have been documented. They are the:

- The J-domain containing Hsp40 protein family

- Nucleotide Exchange Factors (NEF)

- Tetratricopeptide repeat (TPR) motifs containing co-chaperones

Table 1.5 summarises some of co-chaperones identified in the eukaryotic and prokaryotic systems from the above mentioned co-chaperone families. Also tabulated is the role played by them in regulating the function of the Hsp70 proteins.

Co-chaperone	Role played with Hsp70
HSP40 family	Catalyses ATP hydrolysis by Hsp70
GrpE	Nucleotide exchange factor in prokaryotes
BAG-1	Nucleotide exchange factor in eukaryotes
Hsp110	Nucleotide exchange factor in eukaryotes
Hip	TPR containing, stabilises Hsp70-ADP state
Hop	TPR containing, connects Hsp70 and Hsp90
Chip	TPR, Ubox, ubiquitin ligase

Table 1.5: Hsp70 regulation by the various co-chaperone proteins

The time span of the Hsp70**.**substrate complex is defined by NEFs which accelerate disassociation of ADP from Hsp70. In *E.coli*, GrpE is the only family of NEF identified (Harrison *et al*, 1997), while three types of human NEFs have been identified. They are BAG-1, HspBP1 and Hsp110 (Hohfeld and Jentsch, 1997; Sondermann *et al*, 2001; Shomura *et al*, 2005). BAG-1 belongs to the Bcl-2-associated athanogene (BAG)-family of proteins. They are characterised by a conserved C-terminal domain termed the BAG domain (Takayama *et al*., 1999). The BAG domain has been implicated in interacting with the NBD of the eukaryotic cytosolic Hsc70 and trigger nucleotide exchange (Hohfeld, 1997; Alberti *et al*., 2003). Although the molecular mechanism of BAG-1 differs from that of GrpE, the conformational switch induced in the NBD by the both NEF's are similar. Both proteins induce a 14^{o} rotation in the lobe II of the NBD of Hsp70 (Sondermann *et al* 2001; Mayer and Bukau, 2005). Human HspBP1 (Hsp70 binding protein 1) was identified as a eukaryotic NEF and homologues have been identified in several eukaryotic domains and in *S.cerevisiae* (Raynes and Guerriero 1998; Chung *et al*. 2002; Kabani *et al*. 2002a). In contrast no such homologue of the BAG-1 protein has been identified. HspBP1 not only functions as a NEF but it can also stimulate the ATPase activity of Hsc70 along with Hsp40

(Shomura *et al.*, 2005). X-ray crystallographic studies have revealed that the structural mechanism of nucleotide exchange mediated by HspBP1 is different from that reported for GrpE and Bag-1 (Shomura *et al*., 2005). HspBP1 promotes nucleotide release by wrapping around lobe II of the ATPase domain, which causes a subsequent displacement of lobe I (Shomura *et al*., 2005). In contrast, BAG-1 and GrpE triggers nucleotide release through a conformational change in lobe II of the ATPase domain (Harrison *et al*., 1997; Sondermann *et al*., 2001). Another structurally unrelated eukaryotic NEF recently identified is HSP110, a subclass of the Hsp70 superfamily, was identified in yeast (Andréasson *et al*., 2008). Thier domain architecture is similar to that of Hsp70, only differing by an extended C-terminal domain and the insertion of an acidic region between in the β-sheet sub-domain of the PBD (Easton *et al*., 2000; Liu and Hendrickson, 2007). No other NEF possess a PBD, and in the Hsp110, this domain makes contact with the lobe II of the Hsp70 NBD (Schuermann *et al*., 2008).

The co-chaperone protein family containing Tetratricopeptide repeat (TPR) motifs possess a 34-amino-acid motif with a loose consensus that functions as a protein-protein interaction module (Blatch, 1999). Hsc70-interacting protein (Hip; also known as p48), Hsc70-Hsp90-organizing protein (Hop; also known as p60 or Sti1) and the carboxyl terminus of Hsc70-interacting protein (CHIP) are three eukaryotic TPR-containing proteins that have been identified as interacting with the Hsc70. Hip has been found to stabilize the ADP bound form of Hsc70 (Höhfeld *et al*., 1995), while Hop connects the Hsc70 to Hsp90 (Smith *et al*., 1993) and CHIP negatively regulates the ATPase activity of Hsc70 (Ballinger *et al*., 1999).

The Hsp40 class of co-chaperones plays a key regulatory role by stimulating the rate of ATP hydrolysis of Hsp70 proteins (Laufen *et al*., 1999) and is dealt in detail in the following section.

1.3.4. Hsp40 co-chaperone family

Forty-two known Hsp40 homologues have been identified in humans, six in *E.coli* and around twenty in *S.cerevisiae*. Their cellular distribution is widespread having been identified in the cytosol, ER, nucleus, endosome, mitochondria and ribosome (Qiu *et al*., 2006) and their localisation dictates the function of the Hsp40 proteins. The HSP40 family, unlike the other the heat shock protein families is highly diverged and only shares a conserved region of seventy amino acids called the J-Domain (Cheetham

& Caplan, 1998). Members of the the HSP40 family can be classified as type I, type II and type III depending upon the additional domains that are coupled to the conserved J-domain (Bukau *et al*., 1998; Walsh *et al*., 2004; Westhoff *et al*., 2005). The domain architecture of the subtypes of Hsp40 family is illustrated in Figure 1.12. Members of the type I subgroup are similar to *E.coli* DnaJ and are characterised by the presence of a J-domain, a Gly/Phe rich region and cysteine repeat region. The type II subgroup only possess the Gly/Phe rich region in addition to the J domain, while the type III members do not have any conserved features other than the J domain (Qiu *et al*.,2006).

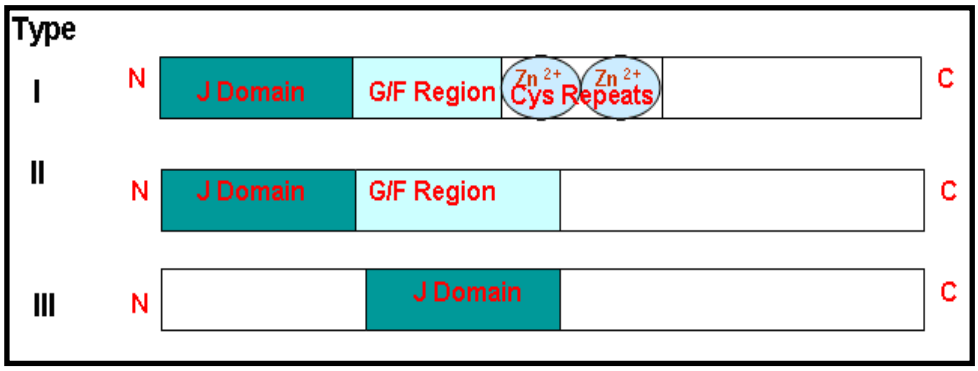

Figure 1.12: Classification and domain architecture of the Hsp40 family of proteins (adapted from Cheetham & Caplan, 1998).

A diagrammatic representation of the domains present in the three types of Hsp40's. They are composed of the conserved J domain, G/F stands for the glycine-phenylalanine rich region and cysteine repeats represents the zinc finger-like motifs.

The J-domain is usually located at the N-terminus; although in some proteins such has auxillin the J-domain is located at the C-terminus. In fact, in type III Hsp40 members the J-domain can occur anywhere along the length of the protein (Cyr *et al*., 1994; Cheetham and Caplan, 1998). The J-domain of DnaJ alone is not sufficient to stimulate ATP hydrolysis in DnaK, however when coupled with the G/F region it can stimulate hydrolysis, albeit to a lesser extent than the full length protein (Wall *et al*., 1994; Karzai *et al*., 1996). It is important to note that maximal stimulation of ATPase activity can be achieved by the J-domain only in the presence of a peptide substrate (Karzai *et al*., 1996). The three dimensional structure of the J Domain of human Hsp40 (HDJ1) (see figure 1.13, Qian *et al*., 1996) and the J domain of *E.coli* DnaJ have been solved by NMR (Hill *et al*., 1995; Pellechia *et al*., 1996). The different structures confirm that the tertiary fold for the J-domain is conserved.

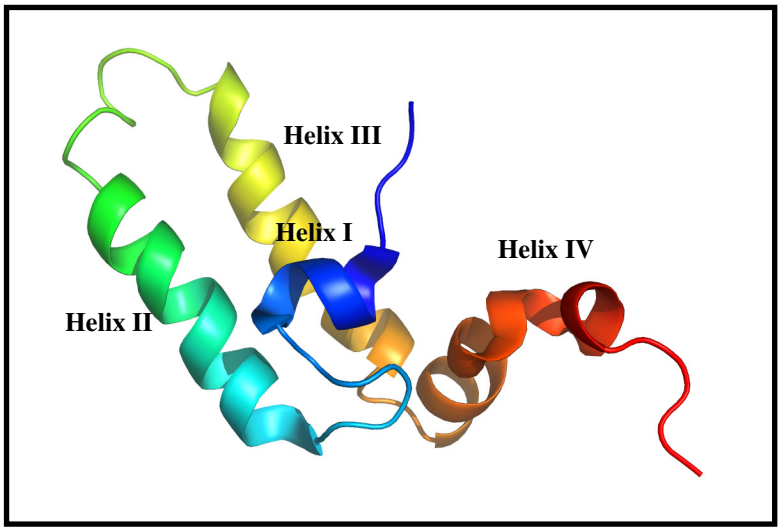

Figure 1.13: NMR structure of the J Domain of human hsp40 (1HDJ, Qian *et al.*, 1996).

A ribbon representation of the J domain of human HDJ1 (Pdb id: 1HDJ) determined by NMR. The figure was generated in Pymol. The four helices making up the J-domain are labeled 1 to 4 on the figure. The conserved HPD motif is located on the loop region between helix II and III.

The domain is made up of 4 helices (Figure 1.13). Helices II and III are anti-parallel and are stabilized by a hydrophobic core. Helices I and IV serve to stabilise the interactions of helix II and III. The conserved HPD motif characteristic of all J-domains is positioned in the loop region between Helix II and III (Burkholder *et al.*, 1996; Qian *et al.*, 1996). An exception to this are the ring infected erythrocyte surface antigen (RESA) proteins of *Plasmodium falciparum* (Bork *et al.* 1992), the *E. coli* DjlB/DjlC family of proteins (Kluck *et al.* 2002) and the *S.cerevisiae* protein Tim16/Pam16 (Truscott *et al.*, 2003; Walsh *et al.* 2004).

Although type I and type II proteins differ in their domain composition, it has been reported that they are functionally similar. Both sub-groups can bind to non-native substrates and target them to the Hsp70 chaperone (Johnson and Craig, 2001). A peptide binding region has been identified in the C-terminus of both the type I and II proteins (Li and Sha, 2005). Rűdiger *et al.*, deduced the substrate binding specificity of DnaJ using a cellulose-bound peptide scan. DnaJ was observed to prefer peptides enriched in aromatic and large hydrophobic aliphatic residues (Rűdiger *et al.*, 2001).

For the type I DnaJ-like proteins, the zinc finger-like motif has been implicated in peptide binding (Szabo *et al.*, 1996). The NMR structure of the motif reveals it as a V-shape with two zinc atoms bound, with the conserved hydrophobic pocket in the

middle of the motif proposed as the peptide binding site (Martinez-Yamout *et al*., 2000). The type II proteins bind substrate through the C-terminal region (Sha *et al*., 2000), while the type III proteins show no evidence of binding to non-native polypeptides and appear to have specialized functions. The type III proteins are functionally and structurally diverse. Additional motifs such as transmembrane helices have been observed for the *E.coli* DjlA, *S.cerevisiae* Sec63 and human DjC9/hSec63 (Cheetham and Caplan, 1998; Mayer and Bukau, 2005).

1.3.5. Mechanism of interaction between Hsp70 and Hsp40 proteins

Hsp40 proteins cooperate with their Hsp70 partner to fulfill various cellular functions. In *E.coli,* DnaJ has been reported to behave independently as a chaperone, although refolding activity requires the presence of DnaK (Mayer *et al*., 2000). The role of Auxillin and G-associated kinase (GAK) in Hsc70 mediated clathrin disassociation is well documented (Greener *et al*., 2000). TRP2 mediates transfer of substrate from Hsp90 to Hsp70 and Csp mediated involvement of Hsc70 in exocytosis has been reported (Caplan *et al*., 1993). The interaction of Hsp70 with Hsp40 as a bipartite mechanism has been proposed for DnaK/DnaJ system (Figure 1.14, Hennessy *et al*., 2005). It has been proposed that helix II and possibly helix III on the J-domain of DnaJ are suggested to interact with the negatively charged underside cleft of the DnaK ATPase domain while helix I and II can bind to DnaK's peptide-binding domain (PBD). By behaving as a peptide mimic, these helices could act to keep the PBD open for client substrate (Hennessy *et al*., 2005).

The loop between helix II and helix III holds the highly conserved His-Pro-Asp (HPD) motif and is essential for the interaction of human Hsp40 with the Hsp70 (Qian *et al*., 1996). Substitution mutations in the tripeptide such as H33Q and D35N have been shown to abolish the binding of Hsp40 to Hsp70 (Burkholder *et al*., 1996; Hartl *et al*., 1996). Apart from the H33Q and D35N mutations, alterations in residues Y25, K26 and F47 in *E.coli* DnaJ abolish J-domain functions *in vivo* (Genevaux *et al*., 2002). Genevaux *et al*. observed that most of these mutations are confined to a small solvent exposed face of the J-domain. These appear to define a conserved interaction surface, as similar mutations on the human Hsp40; HDj1 resulted in similar loss of function (Genevaux *et al*., 2002).

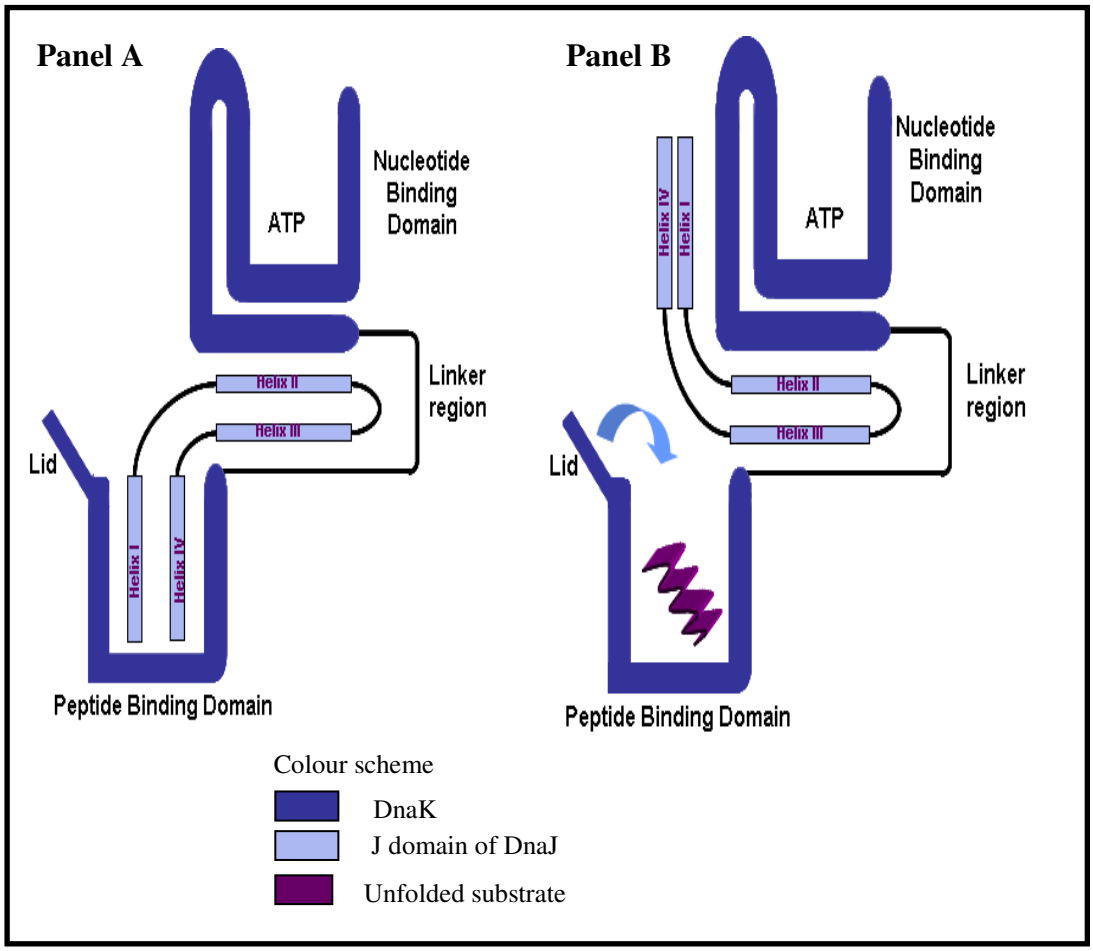

Figure 1.14: Mechanism of binding of DnaJ to DnaK (redrawn from Hennessy *et al*., 2005).

Panel A: Helix II and III of the DnaJ's J-domain interact with the underside of the DnaK NBD. Helix I and IV of the J-domain of DnaJ are suggested to act as a client protein mimic and interact with the PBD of DnaK
Panel B: When an appropriate client peptide is presented, helix I and IV are displaced by the client substrate coupled with ATP hydrolysis. This results in closure of the lid (indicated by arrow).

The interaction and activity of DnaJ with DnaK has been demonstrated to require a linked NBD and PBD (Gassler *et al*., 1998). Using surface plasmon resonance (BIAcore) Gassler and colleagues showed that DnaJ failed to interact with DnaK fragments containing either just the NBD (amino acids 1-385) or the C terminus spanning from residues 386-638. Successful interaction of DnaJ was observed only in experiments performed with full length DnaK and DnaK 1-538 (Gassler *et al*., 1998). BIAcore assays have also revealed that only the ATP bound form of DnaK could bind to DnaJ immobilized on the sensor chip.

Experiments conducted by Suh *et al*., have also demonstrated that the interaction of DnaJ with DnaK is dependent on ATP binding and that the formation of the DnaK-DnaJ complex required ATP hydrolysis (Suh *et al*., 1999). Previous experiments have shown that DnaK undergoes conformational changes upon ATP binding (Liberek *et al*., 1991b). From these data and the results from BIAcore assays, Su *et al*., concluded that the two domain requirement demonstrated by DnaJ is because the formation of the DnaK-DnaJ complex requires ATP induced conformational change of DnaK (Suh *et al*., 1999).

Reports that the J-domain alone is not sufficient to stimulate ATP hydrolysis, but requires the presence of either the G/F region or a substrate peptide raised the possibility that interaction of DnaJ with DnaK is bimodal (Karzai and McMacken 1996; Mayer *et al*. 1999; Suh *et al*. 1999). NMR perturbation mapping has shown that helix II and the adjacent loop host a DnaK binding site (Greene *et al*., 1998). Using a biochemical and genetic approach, Suh *et al*., confirmed the presence of two binding sites for DnaJ on DnaK, one on the underside of the NBD in the cleft between the two NBD sub-domains and the other binding site at or near the PBD (Suh *et al*., 1998).

Recently Jiang *et al*., reported the structure of auxillin's J-domain in complex with the NBD+linker region of bovine Hsc70 (Jiang *et al*., 2007). The protein complex was stabilized by creating a disulphide bond through the substitution of the D876 of the J-domain and R171 of the Hsc70 NBD with cysteines. These residues have been previously shown to interact in the DnaJ-DnaK complex (Jiang *et al*., 2007). The authors report that the interdomain linker is critical to propagate the J-domain activation of Hsc70 (Jiang *et al*., 2007). Structural studies have shown that a mutation in either the Hsc70 or DnaK interdomain linker reduces or abolishes the stimulatory effect of the J-domain (Jiang *et al*., 2005). In the cross linked structure, the J-domain binding deflects the linker towards a hydrophobic patch on the NBD and requires the displacement of the interaction between PBD and NBD, leaving the PBD free to bind to appropriate substrates (Jiang *et al*., 2007). The structure of the J-domain and Hsc70 NBD provides interesting information about the structural mechanism of interaction between the HSP70 and HSP40 families. However this structural information is incomplete because the structural data has been obtained using crosslinked protein and may not be representative of the native state of the complex.

1.4. Aims

A structure of the full length, unmodified Hsp70/Hsp40 complex is necessary to understand the full extent of domain rearrangements induced by the binding of Hsp40 co-chaperone. A major constraint so far has been the inability to isolate a stable form of a complex of Hsp70 and Hsp40, which will allow meaningful structural and biochemical analysis of their interaction. The broad objective of this thesis was to therefore isolate a stable form of the Hsp70/Hsp40 protein complex and undertake structural studies on such a purified complex.

This study aimed to achieve the following:

- ✓ **To develop a recombinant methodology for the expression and purification of the chaperone/co-chaperone complex using a bacterial system.**

- ✓ **To characterise the behaviour of the recombinant complex on the basis of ATP-hydrolysis, substrate protection and polymerisation.**

- ✓ **Structural investigation of isolated complex using x-ray crystallography and electron microscopy and biophysical investigation such as analytical ultracentrifugation.**

Chapter 2

General Materials and Methods

CHAPTER 2: Materials and Methods

2.1 Materials

2.1.1 General chemicals and reagents

General chemicals such as magnesium chloride ($MgCl_2$), sodium chloride (NaCl), potassium chloride (KCl) were purchased from Fisher, Acros or Sigma and were of reagent grade or higher. Isopropyl-β-D-thiogalactopyranoside (IPTG) and Dithiothreitol (DTT) was obtained from Melford Laboratories Ltd. All restriction enzymes and T4 DNA ligase were obtained from New England Biolabs (NEB), UK. Oligonucleotide primers for amplification were synthesized by Invitrogen, UK. Taq master mix used for Polymerase chain reaction (PCR) amplification was obtained from Promega, UK. The Ni-NTA resin was obtained from Qiagen, UK. ATP-agarose, Superdex-200 and Mono-Q resins were obtained from Sigma. All other common reagents used during the course of cloning, protein expression and purification experiments were purchased either from Sigma or Acros and were of reagent grade.

2.1.2 Media

2.1.2.1 Luria Bertani (LB)

The composition of the medium (per litre) is as follows:

Tryptone	10 g
Yeast Extract	5 g
Sodium Chloride	5 g

The pH was adjusted to 7.4 before sterilisation by autoclaving.

For LB agar (LA) plates, bacteriological agar was added to the media to a final concentration of 1.5% (w/v) before autoclaving.

2.1.3 Kits

2.1.3.1 Molecular biology kits

The following kits were used obtained from Qiagen, UK. The kits provide spin columns containing DNA affinity resin, buffers, and collection tubes for silica-membrane-based purification of DNA fragments.

QIAquick PCR Purification Kits – for purification of DNA from PCR reaction mixes. The purification procedure removes primers, unused nucleotides, enzymes, mineral oil, salts, etc from the samples. PCR products purified using the kit can then be directly used for restriction digestion reactions.

QIAquick Gel Extraction Kits – for the extraction and purification of DNA from agarose gels after enzymatic reactions. It is a silica-membrane-based purification of DNA fragments from gel slices (up to 400 mg slices).

2.1.4 Bacterial strains

The following *E. coli* strains were used during the course of this thesis:

STRAIN	GENOTYPE	SOURCE
DH5α T1 phage resistant cells	F-, ϕ 80d*lacZ*ΔM15,Δ (*lacZY- argF*)U169, *deoR*, *recA*1, *endA*1, *hsdR*17(rk-, mk+), *phoA*, *supE*44, λ -*thi*-1, *gyrA*96, *relA*1*tonA*	Invitrogen, UK
One Shot BL21(DE3) cells	*F– ompT gal dcm lon hsdS$_B$ (r_{B-} m_{B-}) λ (DE3 [lacI lacUV5-T7 gene 1 ind1sam7 nin5])*	Novagen, UK

Table 2.1: The strains used in this study and their respective genotypes

2.1.4.1 Maintenance of bacterial strains

Bacterial strains were maintained in glycerol solution for long-term storage at -80°C (Morrison, 1977). Using a wire loop, the desired bacterial cultures were streaked out onto LB agar plates and allowed to grow overnight at 37°C. A single colony from such plates were grown overnight in 10 ml LB broth. Glycerol stocks were prepared the following morning by adding 15% (v/v) sterile glycerol to the cell culture. One ml aliquots were prepared and stored at -80°C.

2.1.5 Vectors

2.1.5.1 pGEM®-T Easy Vector

The pGEM®-T Easy Vector System (Figure 2.1), purchased from Promega, is 3015 bp in size. It is prepared by cutting with *EcoR*V and with the addition of 3' terminal thymidine to both ends provides a compatible overhang for PCR products generated by Taq polymerases.

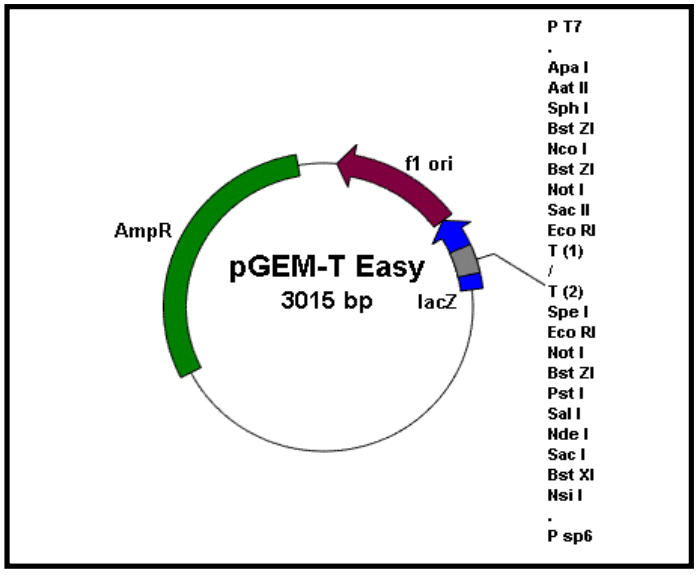

Figure 2.1: pGEM®-T Easy Vector map (adapted from the pGEM®-T Easy Vector technical manual, Promega)

This vector contains T7 and SP6 RNA polymerase regions for sequencing of PCR insertion regions. These flanking multiple cloning sites and α-peptide region labelled LacZ of β-galactosidase enzyme for blue and white colony screening. It also has an ampicillin resistance gene shown as (AmpR),) and f1 origin of replication shown as (f1 ori).

2.1.5.2 pET-16b

The pET-16b plasmid (Figure 2.2) is 5711 base pairs in size and is used for the cloning and expression of recombinant proteins in *E. coli*. The target genes are under the control of the strong bacteriophage T7 promoter and expression can be induced by isopropyl-β-D-thiogalactopyranoside (IPTG), provided a source of T7 RNA polymerase under similar IPTG inducible control is in the host cell. The presence of an N-terminal His•Tag® sequence that is fused in frame with the cloned gene allows purification of the expressed protein by affinity chromatography. The pET-16b plasmid was purchased from Novagen.

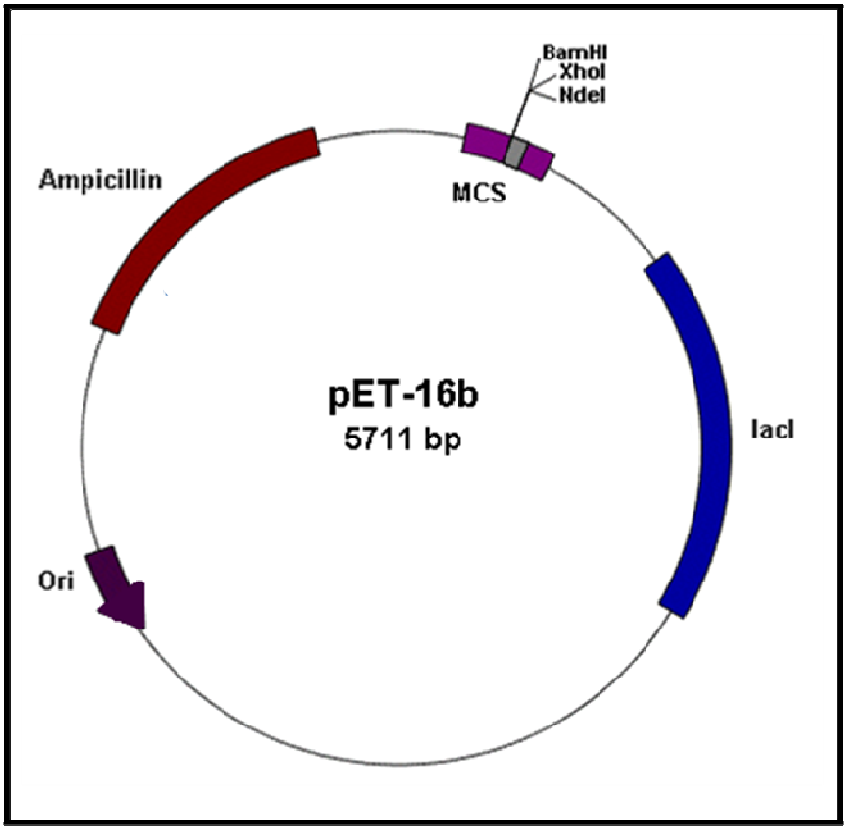

Figure 2.2: pET-16b vector map (adapted from the Novagen technical manual)

The pET-16b vector carries an ampicillin resistance gene (brown). The multiple cloning site (MCS) is shown in purple and carries three cloning sites (*Bam*HI, *Nde*I and *Xho*I). The origin of replication (ori) and lac repressor gene (lacI) are shown on the vector.

2.1.5.3 pET-24a

The pET-24a plasmid (Figure 2.3) is 5310 base pairs in size and has a kanamycin resistance gene as selectable marker. The pET-24a plasmid was obtained from Novagen.

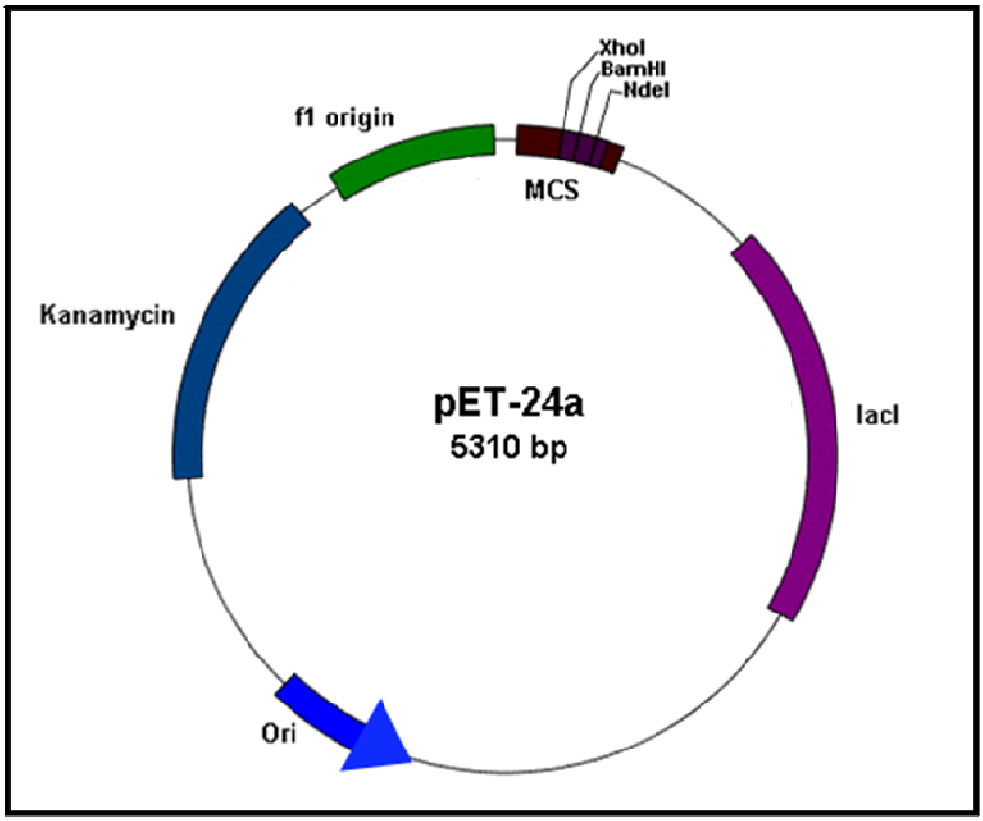

Figure 2.3: pET-24a vector map (adapted from the Novagen technical manual.

This vector has a kanamycin resistance gene as selectable marker. The multiple cloning site carries *BamH*I, *Nde*I and *Xho*I restriction sites. The origin of replication (ori), f1 origin of replication (f1 ori) and lac repressor gene (lacI) are shown on the vector.

2.1.6 Antibodies

Primary antibody

Anti-Hsc70: Biotin conjugate monoclonal antibody (SPA-815B) was obtained from Stressgen, UK. The antibody was supplied at a concentration of 1 mg/ml. It was used at a 1:500 dilution in Western Blotting experiments.

DnaK mouse monoclonal antibody (SPA 880D) was also obtained from Stressgen, UK. The antibody was supplied at a concentration of 1 mg/ml and used at a 1:1000 dilutions.

Secondary probes

Horse radish peroxiase (HRP) conjugated streptavidin (Pierce) was used as secondary probe with Hsc70 primary antibody and used at a 1:10000 dilution.
Anti-Mouse IgG (whole molecule)–peroxidase antibody produced in goat (Sigma) was used as secondary with the DnaK primary antibody at a 1:10000 dilution.

2.2 Preparation of chemically competent cells

Using a wire loop, bacteria from glycerol stocks of commercial competent cells were streaked out onto LB agar plates and allowed to grow overnight at 37^{o}C. A single colony from this plate was grown overnight in 10 ml LB broth. The overnight culture was diluted 1 in 100 into fresh LB media and grown at 37^{o}C with shaking until it reached an absorbance, OD_{595} of 0.4 for *E.coli* DH5α cells and 0.5 for *E.coli* BL21(DE3) cells respectively. The cultures were then chilled on ice for 30 minutes. All subsequent procedures were carried out at 4^{o}C. All buffers and materials used were sterilized by autoclaving and pre-chilled prior to use.

The cells were centrifuged at 3,500 rpm for 7 min using a Sorvall SuperT100 centrifuge (Thermo Scientific, UK) SL250T rotor at 4^{o}C. The pellets were gently re-suspended in 100 mM ice-cold magnesium chloride ($MgCl_2$). The volume of $MgCl_2$ used was 25% of the culture volume (CuV). The cell suspensions were centrifuged at 3,500 rpm for 7 min and the cell pellet was again gently re-suspended in 50% CuV equivalent with 100 mM calcium chloride ($CaCl_2$). The cell suspensions were incubated on ice for 30 min and pelleted as before. Finally, the cell pellets were re-suspended in 2% CuV of 100 mM $CaCl_2$ plus 15% glycerol v/v. 50 µl aliquots were transferred into chilled, sterile 1.5 ml Eppendorf tubes and flash frozen in liquid nitrogen or on dry ice before being transferred to -80^{o}C.

2.3 Small-scale preparation of plasmid DNA

Plasmid DNA extraction was performed according to the standard alkaline lysis mini prep protocol of Sambrook *et al.*, (1989). A single colony of transformed *E. coli* cells was picked and grown in 10 ml of LB broth with appropriate antibiotic selection at 37^{o}C

overnight in a shaking incubator. The cells were centrifuged for 10 minutes at 4,000 rpm in a Sorvall SuperT100 centrifuge using an SL250T rotor. The resulting pellet was resuspended in 250 µl of ice-cold Solution I (50 mM glucose, 25 mM Tris-HCl (pH 8), 10 mM EDTA). The suspension was mixed well by vortexing and transferred to a sterile Eppendorf tube. In the next step, 250 µl of freshly prepared solution II (0.2 M sodium hydroxide (NaOH) and 1% w/v sodium dodecyl sulphate (SDS)) was added to the tube and mixed by inverting gently. Finally, 300 µL of ice-cold Solution III (3 M potassium acetate set to pH 5 with glacial acetic acid) was added to the tube and mixed well by inversion. The tubes were stored on ice for 3-5 minutes and then centrifuged at 13,000 rpm for 12 minutes in a microfuge. To the supernatant an equal volume of phenol:chloroform (1:1) was added and then spun at 13,000 rpm for 10 minutes to achieve segregation of DNA from free proteins and cell debris. The top aqueous layer was transferred to a sterile fresh tube and DNA was precipitated by the addition of an equal volume of Isopropanol. The tube was then centrifuged at 13000 rpm for 20 minutes in a microfuge. The resultant DNA pellet was spun with ice cold 75% (v/v) ethanol for 5 minutes at 13000 rpm. The supernatant was discarded and spun again for 1 minute to remove all traces of ethanol. The DNA pellet was either air dried at room temperature or dried at 37^{o}C. The final pellet containing DNA was dissolved in 35 µl autoclaved distilled water and stored at -20^{o}C until required.

2.4 Separation of DNA by agarose gel electrophoresis

DNA was routinely analysed on a 0.8% (w/v) agarose gel prepared by melting agarose in 1X TAE Buffer (40 mM Tris-HCl, 1 mM EDTA and 20 mM acetic acid, and pH 8.2). Ethidium bromide (10 mg/ml stock) was added to the gel mix at a final concentration of 0.5 µg/ml and the agarose was allowed to set in a sealed gel platform. DNA was mixed with 6X sample buffer (0.4% (w/v) orange G, 0.03% (w/v) bromophenol blue, 0.03% (w/v) xylene cyanol FF, 15% (w/v) Ficoll 400 in 1X TAE buffer) and loaded into the wells of the gel submerged in 1X TAE buffer. The samples were resolved for at least 40 minutes at 100 V. The DNA fragments were detected using a UV Transilluminator (Ultra-Violet Products Ltd, UK). Long wavelength UV light (315-400 nm) was used to analyse

the gel when the DNA was to be used for cloning purposes, and short wavelength UV light (200-280 nm) was used when photographic images of gel were taken.

2.5 PCR amplification

PCR reactions were usually set up using the Promega Taq Master Mix unless otherwise stated. The master mix contained: 50 U/ml Taq DNA polymerase (in Promega proprietary reaction buffer), 400 μM dATP, 400 μM dGTP, 400 μM dCTP, 400 μM dTTP and 3 mM $MgCl_2$.

Component	Final concentration
PCR Master Mix (2X)	1X
Primers (Forward and reverse primers)	10 μM each
Template	3 ng

Table 2.2: Components of the PCR reaction

The components of the PCR reaction and their concentrations are listed in Table 2.2. The PCR reaction was overlaid with 50 μl of mineral oil (Sigma, UK) and the amplification was carried out in a DNA Thermal Cycler 480 (Perkin Elmer, UK). The amplification quality and size was confirmed by agarose gel electrophoresis of the product on a 0.8% agarose gel along with Promega's 1 Kb DNA ladder. Amplified PCR products were purified using the Qiagen PCR purification kit according to the QIAquick DNA purification protocol (Qiagen).

Briefly, five volumes of Buffer PBI (the composition of the buffer is proprietary of Qiagen; contains guanidine hydrochloride and propan-2-ol) was added, the sample was mixed and applied to the QIAquick column and centrifuged at 16000 x g for 60 seconds. The flow through was discarded and the column washed with 750 μl of Buffer PE before centrifugation at 16000 x g for 60 seconds. The DNA sample was eluted from the column with 50 μl sterile distilled water.

2.6 Restriction digestion

2.6.1 Restriction digestion of PCR products and their purification

Restriction digests were set up using the conditions recommended by the New England BioLab's (NEB) technical manual. Typically the template was incubated with the appropriate restriction buffer (to a final concentration of 1X) and 10 U of each restriction enzyme and incubated at 37^{o}C for 3-4 hrs. At the end of the incubation period, the digested PCR product was re-purified using the Qiagen PCR purification kit (as described in section 2.5) and finally eluted in 12-15 µl of water. The purified PCR product was used for the ligation reaction (see section 2.7).

2.6.2 Restriction digestion and purification of vector DNA

Vector DNA was extracted from a 10 ml overnight culture grown with the appropriate antibiotic. The plasmid extraction was performed by the alkaline lysis protocol as described in the section 2.4. Restriction digestion of the vector was carried out following the same protocol as that for the PCR product (section 2.6.1). At the end of the incubation period 1 U of Calf Intestinal Phosphatase (CIP, NEB) was added to remove the terminal phosphate residues of the linear DNA and the reaction mixture was further incubated for 30 minutes at 37^{o}C. The digested vector was analysed on a 0.8% agarose gel and the fragment corresponding to size of vector was excised from the gel under a long wavelength UV transillumination and purified from the gel using the Qiagen Gel extraction kit according to manufacturer's protocol.

Briefly, to the DNA fragment excised from the gel, three volumes of Buffer QG (the composition of the buffer is proprietary of Qiagen; contains guanidine thiocyanate) was added and incubated at 50^{o}C until the gel slice had dissolved. One gel volume of isopropanol was added and the sample was mixed. 800 µl of the sample was applied to the QIAquick column and centrifuged at 16000 x g for 60 seconds. The flow through was discarded and the column washed with 750 µl of Buffer PE before centrifugation at 16000 x g for 60 seconds. The flow through was again discarded and the column centrifuged at 16000 x g for 60 seconds to remove any residual buffer. The column was placed in a clean

1.5 ml eppendorf tube and the digested vector was eluted in 15-20 µl of sterile water and was used in subsequent ligation reactions.

2.7 Ligation

Usually a 10 µl ligation reaction was set up. The vector and insert were mixed at a ratio of 1:3 along with T4 DNA ligase (NEB) and 1X ligase buffer and incubated either at room temperature for 4 hrs or overnight at 4^{o}C. The reaction mixture was transformed into *E. coli* DH5α cells.

2.8 Transformation protocol

Chemically competent cells were transformed using the heat-shock methodology (Mandel and Higa, 1970). Briefly, 50 µl aliquots were gently thawed on ice for 5 min. 10 µl of ligation mixture or 1 µl of purified plasmid was added to the tubes which were incubated on ice for a further 30 minutes. The cells were heat-shocked at 42^{o}C in a water bath for 60 seconds and returned to ice for 5 minutes. LB media was added (0.5-1 ml) and the cells were incubated at 37^{o}C for one hour and subsequently plated onto LB Agar plates containing the appropriate antibiotic.

2.9 Confirmation of clones

Plasmid DNA was isolated from transformed bacterial colonies (as described in section 2.4) and positive clones were identified by restriction digest analysis of the isolated plasmid DNA (as described in section 2.6). The digestion reactions were analysed on a 0.8% agarose gel along with Promega's 1 Kb DNA ladder. Positive clones were identified by digestion products which yielded DNA fragments of the correct insert and vector size (compared with the DNA ladder). Clones were sequenced to confirm the lack of any undesirable mutations through a commercial arrangement with the Advanced Biotechnology Centre (ABC), Imperial College, UK.

2.10 Protein expression and purification

2.10.1 Expression of recombinant proteins

To study protein expression, the appropriate recombinant plasmids were transformed into *E. coli* BL21(DE3) cells and selected for, using drugs to which the *E. coli* host was now resistant. A single colony was grown overnight in LB broth plus antibiotics at 37°C in a shaking incubator at 250 rpm. The overnight culture was used as an inoculum into fresh LB medium (plus antibiotics) which was then grown at 37°C until an OD_{595} of 0.6-0.8. Protein expression was induced by the addition of IPTG to a final concentration of 0.4 mM and growth was continued for a further 3 hrs at 37°C. The induced cells were harvested via centrifugation with a Sorvall Super T21 centrifuge and SL250T rotor at 6,000 rpm for 15 minutes at 4°C. The supernatant was discarded and the pellet was re-suspended in lysis buffer and stored at -80°C until required. The lysis buffer composition specific for each protein, depending on the chromatography being employed, is described in the subsequent chapters.

2.10.2 Purification of poly-histidine tagged proteins

All purification procedures were performed at 4°C. Lysozyme and phenylmethylsulphonyl fluoride (PMSF) were added to the thawed cell pellet to a final concentration of 2.0 µg/ml and 100 mM respectively in lysis buffer. The lysis buffer composition specific for each protein has been described in the subsequent chapters. The cell lysate was disrupted by sonication (6 x 30 seconds ON cycles, Status 200, MS73 probe set to 40% maximum power output). The cell debris was removed by centrifugation at 18,000 rpm for 45 minutes at 4°C with a Sorvall Super T21 centrifuge and SL50T rotor. The soluble, supernatant fraction was applied to a 4 ml nickel-nitrilotriacetic acid (Ni-NTA) agarose column pre-equilibrated with the lysis buffer. The column was washed with 5 column volumes of lysis buffer and again with 5 column volumes of lysis buffer containing 30 mM imidazole. The protein was eluted with 3 column volumes of lysis buffer containing 200 mM imidazole. The elution profiles of the recombinant proteins were analysed by 12% sodium dodecyl sulphate-polyacrylamide gel electrophoresis (SDS-PAGE).

2.10.3 Ion exchange chromatography

The protein fractions eluting from the Ni-NTA column with 200 mM imidazole were diluted to 25 mM NaCl using dilution buffer (50 mM Tris-HCl, pH 8.0) and were applied to a 20 ml Q sepharose column (Sigma). The column was pre-equilibrated with equilibration buffer (50 mM Tris-HCl pH 8.0, 25 mM NaCl and 5% (v/v) glycerol). The resin was next washed with 2 column volumes of equilibration buffer. The protein was step eluted with equilibration buffer containing 100, 250, 500 and 1000 mM NaCl. The elution profile was monitored by SDS-PAGE.

2.10.4 Size exclusion chromatography

The recombinant proteins were evaluated by gel filtration chromatography. A 90 ml Superdex 200 column (exclusion limit of 600 kDA, purchased from Sigma, UK) was packed in house. The chromatography was performed at 4^{o}C with 20 mM Tris-HCl pH 8.0 plus 100 mM potassium chloride. The molecular weight standards (obtained from Sigma) used for calibrating the column are tabulated in Table 2.3

The void volume was determined using blue dextran and was found to be 36 ml. The protein sample was applied to the column pre-equilibrated with two column volumes of gel filtration buffer. The gel filtration buffer composition specific for each protein is described in the subsequent chapters. The sample volume was usually concentrated down to less than 2% of the column volume using 30 kDa molecular weight cut off centricon (YM-30, Millipore). One ml fractions were collected from after the void volume. The fractions were analysed for protein content using a Bradford assay (described in section 2.10.6) and a graphical plot of the absorbance on the y-axis versus the elution volume on the x-axis was used as a representation of the chromatogram. The protein peak fractions (determined by Bradford assay) were analysed by SDS-PAGE electrophoresis.

Standard protein	Molecular weight in kDa
Porcine thyroglobulin	660
β-amylase	200
Alcohol dehydrogenase	150
Bovine serum albumin	66, 132

Table 2.3: Standard proteins used for calibrating the gel filtration chromatography

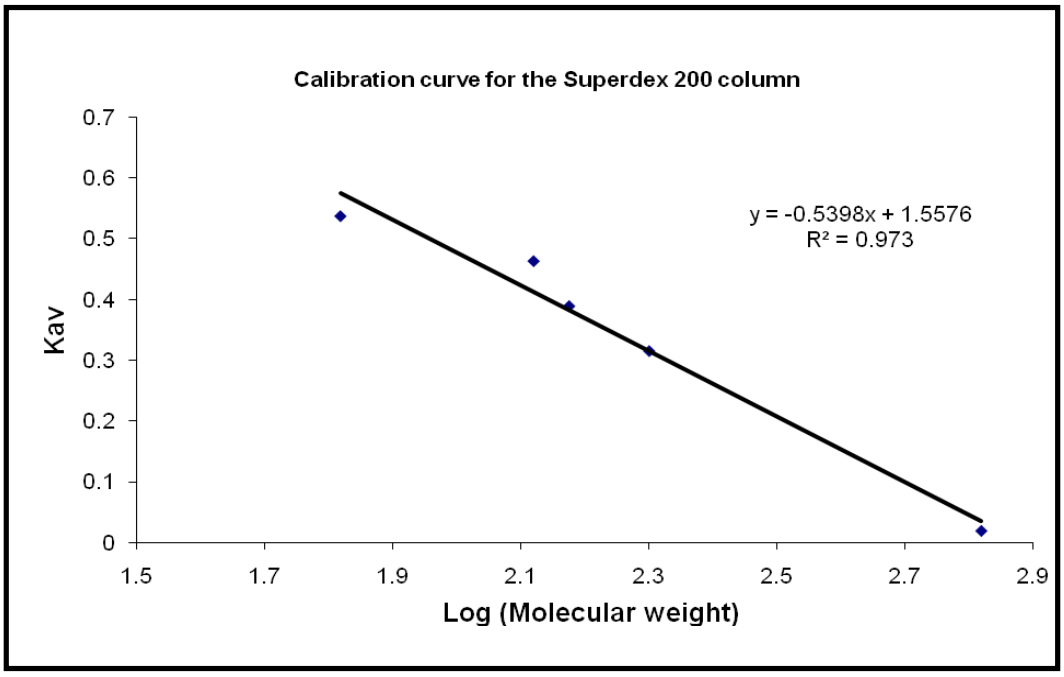

Figure 2.4: Calibration curve of the Superdex 200 size exclusion column.

The chromatography was performed as described using the standard proteins listed in table 2.4. A calibration curve using partition coefficient (kav) versus the logarithm of the protein molecular weight was prepared. The partition coefficient was calculated using the formula Kav = Ve-Vo/ Vt-Vo where Ve = elution volume of the protein, Vo = void volume of the column and Vt is the total bed volume.

2.10.5 SDS polyacrylamide gel electrophoresis

Protein samples were resolved using a modification of the standard method (Laemmli, 1970). The Mini-Protean® 3 Cell electrophoresis unit (Bio-Rad, UK) was used for running the gels. Generally a 12% separating gel and a 4% stacking gel were used. The

reagent compositions of the 12% separating gel and 4% stacking gel are tabulated in Tables 2.4 and Table 2.5 respectively.

Reagent	**Volume (ml)**
Sterile distilled water	4.3
1.5 M Tris-HCl (pH 8.8)	2.5
10% sodium dodecyl sulphate	0.1
40% acrylamide/bisacrylamide (29:1)	3
10% ammonium persulphate	0.1
TEMED	0.01
Total volume = ~10 ml	

Table 2.4: Composition of 12% separating gel

Reagent	**Volume (ml)**
Sterile distilled water	3.1
0.5 M Tris-HCl (pH 6.8)	1.25
10% sodium dodecyl sulphate	0.05
40% acrylamide/bisacrylamide (29:1)	0.5
10% ammonium persulphate	0.05
TEMED	0.005
Total volume = ~5.0 ml	

Table 2.5: Composition of 4.0% stacking gel

Samples were prepared in 4X SDS-PAGE sample buffer (0.0625 M Tris-HCl, pH 6.8, 10% glycerol (v/v), 2% SDS (w/v), 5% β-mercaptoethanol (v/v), 0.05% bromophenol blue (w/v)) and boiled for 5 minutes in a heating block set to 95^{o}C. The gel was run in 1X SDS-PAGE gel running buffer (10X SDS-PAGE gel running buffer 0.25 M Tris base, 1.92 M glycine and 1% SDS (w/v)). The samples were resolved at 200V until the blue dye front had reached the end of the gel plates. The gel was then stained with Coomassie

staining solution (90% water, 10% glacial acetic acid (v/v) and 0.25% Coomassie Brilliant Blue R350 (w/v)) and then destained with (40% methanol (v/v), 50% water and 10% glacial acetic acid (v/v)).

2.10.6 Determination of protein concentration

Protein concentrations were determined using a Bradford assay (Bradford, 1976). Bradford reagent was commercially purchased from Bio-Rad, UK. The assay was performed in 1 ml reactions as follows. 200 µl of Bradford reagent was added to the sample (usually 5 µl) and the volume was made up to 1 ml with water or appropriate sample buffer. The reaction was incubated for 5 min at room temperature and the absorbance was read at 595 nm using a NovaSpec II Spectrophotometer, (GE Healthcare, UK). The protein concentration was estimated from a standard curve plotted using the absorbance values obtained for 1-5 µg of BSA.

2.10.7 Dot blot protocol

First, the nitrocellulose membrane was soaked in TBS-T buffer (10 mM Tris-HCl, 150 mM NaCl, 0.05% Tween-20 (v/v), pH 8.0) for 1 min. Then 2 µl of the protein sample was spotted onto the membrane. To minimise the area that the solution penetrated the protein spot was allowed to dry and if necessary more sample was applied. The membrane was allowed to dry and then stained with 0.2% (w/v) Ponceau S in 10% (v/v) acetic acid for 1 min to visualise the protein samples. Non-specific sites were blocked in 5% (w/v) BSA in TBS-T for 2 hrs at room temperature. The membrane was next incubated with primary antibody (either anti-DnaK or anti-Hsc70) diluted in TBS-T (dilution factor mentioned in section 2.1.6) for 2 hours at room temperature. At the end of the incubation the membrane was given three, five minute washes with TBS-T and then probed with the secondary antibody conjugated with HRP by incubating at room temperature for 30 min with shaking. The membrane was then washed three times with TBS-T (15 min once and 5 min twice). The bands were visualised using 3 ml of 3,3′,5,5′-Tetramethylbenzidine (TMB) Liquid Substrate System (Sigma-Aldrich, UK).

Chapter 3

Isolation of the Hsc70/HSJ1b complex

CHAPTER 3: Isolation of the Hsc70/HSJ1b complex

3.1 Introduction

Extensive biochemical analyses have been carried out to understand the interactions of the chaperone and co-chaperone proteins using various Hsp70/Hsp40 model systems, such as the *E. coli* DnaK/DnaJ proteins (Laufen *et al*., 1999), the human Hsc70/HDJ1 proteins (Minami *et al*., 1996) and the *S. cerevisiae* Ssa1p/YDJ1p proteins (Cyr *et al*., 1992). In this study, we have worked with the human Hsc70 - the constitutively expressed member of the Hsp70 family and the human Hsp40 homologue-HSJ1b protein. Hsc70 has been reported to facilitate protein folding and is also involved in normal cellular process such as protein assembly and translocation (Kiang and Tsokos, 1998; Meimaridou *et al*., 2009). Hsc70 also ensures that damaged proteins are subjected to degradation, either by the ubiquitin-proteosome system (UPS) or via the lysosomal degradation machinery (Majeski & Dice, 2004). The Hsc70 protein along with the HSJ1b co-chaperone protein has been directly implicated in the sorting of ubiquitylated client proteins into the proteosomal degradation pathway (Chapple *et al*., 2004). HSJ1b is the larger isoform of the neuronally enriched HSJ1 family of proteins. HSJ1 proteins have been reported to regulate the ATPase and substrate binding activities of the Hsc70 protein (Chapple & Cheetham, 2003). It is a type II Hsp40 protein, and is targeted to the cytoplasmic face of the ER and also undergoes prenylation (Chapple & Cheetham, 2003). Other than the conserved J-domain, the protein is also characterised by the presence of ubiquitin-interacting motifs (UIM) (Westhoff *et al*., 2005). The interaction of the Hsc70 and HSJ1b co-chaperone is thought to exemplify the co-operation between the chaperone and the UPS, a crucial aspect for protein quality control (Gao and Hu, 2008). The Hsc70/HSJ1b protein complex was therefore an interesting chaperone/co-chaperone model system to use in our study.

Most often Hsp70/Hsp40 complexes have been studied by combining the two individually purified proteins in molar ratios and in the presence of ATP. Using the above approach, Minami *et al*., (1996) have successfully shown the formation of a ternary complex between Hsc70, Hsp40 and denatured substrate. Therefore, our initial plan was to purify the individual full length Hsc70 and HSJ1b proteins separately and

then mix the two homogenous proteins in appropriate molar ratios in the presence and absence of various substrates and ATP analogues for crystallisation trials. However this presented us with enormous permutations and combinations, and hitting upon the correct molar proportions required for crystallisation was not guaranteed. This problem was highlighted by Jiang *et al*., who reported the structure of auxillin's J-domain in complex with the NBD+linker region of bovine Hsc70 (Jiang *et al*., 2007). Preliminary crystallisation trials set up by mixing the purified Hsc70 NBD+linker region and auxillin's J-domain in the presence of various co-factors only yielded crystals of the individual proteins. Crystals of the complex were obtained only after mutating the residues D876 of the J-domain and R171 of the Hsc70 NBD into cysteines, thereby cross linking the complex via disulphide bond formation (Jiang *et al*., 2007). Thus a primary hurdle towards better structural understanding of chaperone/ co-chaperone interaction lies in the isolation of a stable Hsp70/Hsp40 protein complex, and this is the focus of the study described in Chapter 3.

In this chapter we describe the work carried out towards developing and executing an alternative strategy for the isolation of an intact Hsp70/Hsp40 protein complex. A dual plasmid co-expression system was used, wherein, two plasmids differing in their antibiotic resistance were expressed simultaneously by the bacterial cells, instead of a single plasmid used in conventional expression systems. For this purpose the individual *Hsc70* and *HSJ1b* genes were cloned into appropriate expression vectors, protein expression was induced using IPTG in a bacterial system and the Hsc70/HSJ1b complex successfully isolated by Ni-NTA chromatography. The relevant experimental work carried out to achieve these results is presented in the following sections.

.

3.2 Materials and Method

3.2.1 PCR amplification of Human Hsc70 and HSJ1b genes

Hsc70 gene was amplified using cDNA prepared from HB4a cells (Normal breast epithelial cell line) as template (cDNA kindly provided by, Dr. Anatoily Markiv from University of Westminster, UK). Full length human *HSJ1b* was amplified using a pET-14b_*HSJ1b* plasmid template obtained from Dr. Blatch from Rhodes University, SA. Primers were designed complimentary to the coding sequence of the respective genes. The primers for amplification of the *Hsc70* and *HSJ1b* genes were obtained from Invitrogen and were diluted to the required concentration (10 µM, Table 3.1). Restriction sites were also designed into the primers as shown in Table 3.1.

Gene	Primers (5'-3')	Restriction enzyme	Product size
Hsc70Fwd	GGATTCCATATGTCCAAGGGACTGCAGTTGG	*Nde*I	1.941 Kbps
Hsc70Rev	GATCGGATCCTTAATCAACCTCTTCAATGGTGG	*Bam*HI	
HSJ1bFwd	GATCGGATCCCATGGCATCCTACTACGAGATCCTAGACG	*Bam*HI	975 bp
HSJ1bRev	GATCAAGCTTTCAGAGGATGAGGCAGCGAGAGG	*Hind*III	

Table 3.1: Primer design, restriction sites and PCR product size for *Hsc70* and *HSJ1b* genes.

Base pairs underlined and highlighted in red indicate the restriction endonuclease recognition sequence introduced into the primers to enable directional cloning of the PCR products.

PCR conditions

The parameters used for the PCR amplification reactions for the human *Hsc70* and *HSJ1b* genes are listed in Table 3.2

Segment	Number of cycles	Temperature (^{o}C)	Time
Initial Denaturation	1	95	1 minute
Denaturation, primer annealing and extension	30	95 60 72	1 minute 1 minute 2 minutes for *Hsc70* 1 minute for *HSJ1b*
Final extension	1	72	7 minutes
Final Hold	1	4	Indefinite

Table 3.2: PCR conditions for the amplification of the Human *Hsc70* and *HSJ1b* genes

3.2.2 Insertion of Hsc70 into pGEM-T vector

The *Hsc70* gene was initially cloned into the TA cloning vector, pGEM-T. The PCR product, purified using the QIAquick PCR purification kit, was ligated directly into the pGEM-T vector. The ligation reaction was incubated for 4 hours at room temperature and transformed into *E. coli* DH5α cells using the protocol described in Chapter 2. The transformed cells were plated onto LB agar plates containing 100 µg/ml ampicillin, 0.5 mM isopropyl-β-D-thiogalactopyranoside (IPTG) and 80 µg/ml X-Gal to allow for blue/white colony selection. White colonies were screened for positive clones. Cells were grown overnight and plasmids extracted using alkaline lysis (described in Section 2.3, Chapter 2). Clones were confirmed by restriction digestion of the extracted plasmid. The plasmid generated in the pGEM-T vector will be henceforth referred as pGEMt-*Hsc70*.

3.2.3 Generation of pET-16b-Hsc70 and pET-16b-HSJ1b constructs

The *Hsc70* and *HSJ1b* genes were cloned into the pET-16b bacterial expression vector. The pET-16b DNA was extracted from a 10 ml overnight culture grown with 100 µg/ml of ampicillin using alkaline lysis (Sambrook *et al*., 1989). The vector was prepared for ligation as described in Chapter 2. First, the purified plasmid DNA was

digested with restriction endonucleases compatible with the sites present on the corresponding PCR product and incubated for 3-4 hrs at 37^{o}C. At the end of the incubation period 1U of CIP was added for the removal of the terminal phosphate residues and the reaction mixture was further incubated for 30 minutes. The digested vector was analysed on a 0.8% agarose gel and the 5.7 Kb fragment (corresponding to size of digested pET-16b vector) was extracted from the gel and purified using Qiagen's Gel purification kit. The digested and CIP treated vector was finally eluted in 15-20 µl of water.

The *HSJ1b* PCR product was prepared for ligation as described in Chapter 2. Briefly, the PCR product was purified using Qiagen's PCR purification kit, digested with *Bam*HI and *Hin*dIII enzymes and re-purified using the same PCR purification kit prior to ligation. Similarly the *Hsc70* insert was obtained by restriction digestion of the confirmed pGEMt-*Hsc70* plasmid with *Bam*HI and *Nde*I enzymes and then gel purified from a 0.8% agarose gel purified using Qiagen's Gel purification kit.

The vector and insert were ligated together at a ratio of 1:3 and transformed into *E.coli* DH5α cells using protocols previously described in Chapter 2. Clones were confirmed by restriction digest analysis of plasmid DNA isolated by alkaline lysis from transformed colonies (protocol described in Chapter 2). The sequence of the obtained pET-16b-*Hsc70* and pET-16b-*HSJ1b* plasmids were confirmed by sequencing the plasmids at the Advanced Biotechnology Centre (ABC), Imperial College, UK.

3.2.4 Generation of pET-24a-HSJ1b construct

To generate the pET-24a-*HSJ1b* construct, the *HSJ1b* insert was obtained by restriction digestion of the pET-16b-*HSJ1b* clone with *Bam*HI and *Hin*dIII restriction enzymes. The pET-24a DNA was purified by the alkaline lysis method and was prepared for ligation by digestion with *Bam*HI and *Hin*dIII (refer to Chapter 2). The insert and vector were ligated as previously described (3.2.3) and transformed into *E.coli* DH5α cells. The identities of the constructs were confirmed by sequencing the plasmid at the Advanced Biotechnology Centre (ABC; Imperial College, London).

3.2.5 Co-transformation of Hsc70/HSJ1b plasmids

Plasmids pET-16b-*Hsc70* and pET-24a-*HSJ1b* vector were co-transformed into the *E. coli* expression strain BL21(DE3). The transformation protocol described in Chapter 2, section 2.8 was followed. Both plasmids were added in equal amounts to the competent cells. The transformed cells were plated onto LB agar containing 50 µg/ml of ampicillin and 25 µg/ml kanamycin and incubated overnight at 37°C.

3.2.6 Confirmation of plasmid stability by colony PCR

Individual BL21(DE3) colonies transformed with pET-16b-*Hsc70* and pET-24a-*HSJ1b* plasmids were picked using sterile 10 µl pipette tips and suspended in 10 µl sterilised distilled water. 1 µl of the bacterial suspension was used as a template and two amplification reactions were set up for each colony; one with *Hsc70* specific primers and other with *HSJ1b* specific primers. PCR reactions were set up as described in section 2.5 and the amplification conditions were the same as those described in Table 3.2. The results of the amplification was analysed on a 0.8% agarose gel.

3.2.7 Expression studies

Over-expression of Hsc70 and HSJ1b

Small-scale expression studies were carried out with 10 ml of LB broth. Individual Hsc70 and HSJ1b proteins were expressed using the pET-16b-*Hsc70* and pET-24a-*HSJ1b* plasmids. The individual plasmids were transformed into BL21(DE3) cells. A single colony was used for overnight inoculation into LB broth containing 100 µg/ml of ampicillin or 50 µg/ml kanamycin and grown at 37°C. 10 ml LB was inoculated with a 1 in 100 dilution of the overnight culture. Cells were grown at 37°C to an OD_{595} of 0.6-0.8. Protein expression was induced by the addition of IPTG to a final concentration of 0.4 mM. After induction, cells were grown for a further 3 hrs. The cells were harvested via centrifugation as described Chapter 2, section 2.10.1. The supernatant was discarded and the cell pellet was re-suspended in 200 µl of 1X SDS-PAGE sample buffer. The expression profile of the recombinant proteins was analysed on a 12% SDS-PAGE gel. The samples were boiled at 95°C for 15 minutes and 10 µl of each sample was loaded on the gel.

Co-expression of Hsc70/HSJ1b

Growth and induction for the Human Hsc70/HSJ1b complex was carried out using the protocol described in Chapter 2, section 2.10.1. Plasmids, pET-16b-*Hsc70* and pET-24a-*HSJ1b* were co-transformed into BL21(DE3) cells and grown in the presence of ampicillin at a concentration of 50 µg/ml and kanamycin at 25 µg/ml concentrations. Small-scale expression studies were carried out with 10 ml cultures and the expression profile analysed as described in previously for Hsc70 and HSJ1b. For large scale production, the culture volume was scaled up to 2 l. The cells were harvested via centrifugation as described in Chapter 2, section 2.10.1, using a Sorvall Super T21 centrifuge and SL250T rotor at 6,000 rpm for 15 minutes at 4^{o}C. The supernatant was discarded and cell pellet was re-suspended in the lysis buffer (50 mM Tris-HCl pH 8.0, 100 mM NaCl and 5 mM imidazole) and stored at -80^{o}C until required for purification.

3.2.8 Ni-NTA purification

All purification procedures were performed at 4^{o}C. Purification of the recombinant was performed following the protocol for the purification of poly histidine tagged proteins described in Section 2.10.2 in Chapter 2. Briefly, the re-suspended cell pellet was lysed by sonication (6 x 30 seconds ON cycles, Status 200, MS73 probe set to 40% maximum power output), followed by centrifugation at 18,000 rpm for 45 min at 4^{o}C. The lysate was applied to pre-equilibrated Ni-NTA resin and the protein was eluted with lysis buffer containing 200 mM imidazole (Chapter 2; 2.10.2). The elution profiles of the recombinant proteins were analysed on a 12% SDS-PAGE gel.

3.2.9 Ion Exchange chromatography

Ion exchange chromatography was performed as described in chapter 2, section 2.10.3. The Hsc70/HSJ1b complex fractions from the Ni-NTA column containing 200 mM imidazole were diluted to 25 mM NaCl using dilution buffer (50 mM Tris-HCl, pH 8.0) and were applied to a pre-equilibrated 20 ml Q sepharose column (Sigma). The resin was washed with 2 column volumes (CV) of equilibration buffer and the protein step eluted with 100, 250, 500 and 1000 mM NaCl. The elution profile was monitored by SDS-PAGE.

3.2.10 ATP-agarose chromatography

ATP-agarose chromatography was performed by following a protocol modified from Ménoret (2003). The ATP-agarose slurry (Sigma) was prepared according to the manufacturer's protocol. A 5 ml column was packed and washed with 10 CV of equilibration buffer (20 mM Tris-HCl pH 8.0, 20 mM NaCl, 15 mM β-Mercaptoethanol and 3 mM $MgCl_2$). The Hsc70/HSJ1b elution fraction from Ni-NTA chromatography was diluted in 20 mM Tris-HCl pH 8.0, 15 mM β-Mercaptoethanol and 3 mM $MgCl_2$ to bring down the final concentration of NaCl in the sample to 25 mM. The protein was loaded onto the column and washed with 5 CV of equilibration buffer. The agarose was incubated in elution buffer (20 mM Tris-HCl pH 8.0, 20 mM NaCl, 15 mM β-Mercaptoethanol, 3 mM $MgCl_2$ plus 3 mM ATP) for 30 minutes before the fractions were collected. The elution profile was monitored by SDS-PAGE analysis.

3.2.11 2-Dimensional analysis

3.2.11.1 IEF/SDS-PAGE analysis

First dimension: Isoelectric focusing

Protein samples were dialysed against water at 4°C overnight. A 10 µg aliquot of the protein was then mixed with rehydration buffer (6 M urea, 2M thiourea, 0.5% (w/v) CHAPS, 0.4% (w/v) DTT, 0.5% Pharmalyte 3-10) to give a final volume of 120 µl. The mixture was loaded on a 7cm IPG strip pH 3-10 (Bio-Rad) using a re-swelling tray (Amersham Biosciences). The strip was rehydrated overnight at room temperature according to the method described by Görg *et al*. (2004). Isoelectric focusing was carried out on the following day using the Multiphor II apparatus (Pharmacia BIOTECH.) as described in the handbook of 2-D electrophoresis (GE Healthcare, 2004). Briefly, focussing was performed at 20°C under the following conditions: 300V for 30 min; 600V for 45 min; 3500V for 2 hours and 45 minutes using an Amersham EPS 3501 power pack. After focussing the IPG strip was stored at -80°C until analysed by SDS-PAGE.

Second dimension: SDS-PAGE

In the second dimension, the focussed strips were equilibrated for 15min in 50 mM Tris-HCl, pH 8.8, 6 M urea, 30% (v/v) glycerol, 2% (w/v) SDS, 1% (w/v) DTT for 15 min in 50 mM Tris-HCl, pH 8.8, 6 M urea, 30% (v/v) glycerol, 2% (w/v) SDS, 2.5% (w/v) iodoacetamide. Equilibrated strips were loaded onto a 12% acrylamide gel, covered with sealing buffer (0.5% (w/v) agarose, 25 mM Tris-Base, 192 mM glycine, 0.1% (w/v) SDS, trace of bromophenol blue) and run at 150 V in running buffer (25 mM Tris, 192 mM Glycine, 0.1% (w/v) SDS).

3.2.11.2 Native/SDS-PAGE analysis

First dimension: Native PAGE

In the first dimension, protein samples were separated on an 8% native gel. The composition for an 8% native gel is shown in Table 3.3. The gel comprised solely of the separating layer and did not have a stacking layer. The gels were resolved using a Mini-Protean® 3 Cell electrophoresis unit (Bio-Rad, UK).

Reagent	**Volume (ml)**
Sterile distilled water	5.3
1.5 M Tris-HCl (pH 8.8)	2.6
40% Acrylamide/Bis acrylamide (29:1)	2
10% ammonium persulphate	0.1
TEMED	0.01
Total volume = 10.0 ml	

Table 3.3: Composition of 8% native gel

Protein samples were prepared in 4X Native-PAGE sample buffer (0.0625 M Tris-HCl, pH 6.8, 10% (v/v) glycerol and 0.05% (w/v) bromophenol blue) and were loaded without boiling at 95^{o}C to avoid denaturation. The gel was run in 1X Native-PAGE gel running buffer (25 mM Tris base and 192 mM glycine). The samples were resolved at 100V at 4^{o}C until the blue dye front had reached the end of the gel plates.

Second dimension: SDS-PAGE

For the second dimension, the lanes carrying the protein sample was cut from the native gel. It was equilibrated in 1X SDS-PAGE sample buffer for 15 minutes at room temperature. The equilibrated strip was loaded onto a 12% acrylamide gel and run at 150 V in running buffer (25 mM Tris, 192 mM Glycine, 0.1% (w/v) SDS).

3.3 Results

A co-expression system was used for the isolation of recombinant Hsc70/HSJ1b proteins expressed and purified from *E. coli*. The experimental strategy involved in this chapter has been outlined in Figure 3.1. The work described in this chapter was divided into two stages. In stage 1, the *Hsc70* and *HSJ1b* genes are both individually cloned into the pET-16b vectors. Since the proteins will be expressed with a histidine tag, these clones were used to purify the individual Hsc70 and HSJ1b proteins using Ni-NTA chromatography, and, this will be discussed in Chapter 5. We then proceeded to use these clones in stage 2 of the experiment, which was the development of the co-expression system. In this system, two plasmids differing in their antibiotic resistance are expressed simultaneously by the bacterial cells, instead of a single plasmid used in conventional expression systems. For this purpose, the *HSJ1b* gene was sub-cloned into the pET-24a vector and used in conjunction with Hsc70 cloned into the pET-16b vector. Though the two carry incompatible origins, they carry different antibiotic resistance genes – ampicillin in pET-16b and kanamycin in pET-24a. Purification of the complex was performed by affinity chromatography over Ni-NTA resin. The individual steps are described in detail in the following sections.

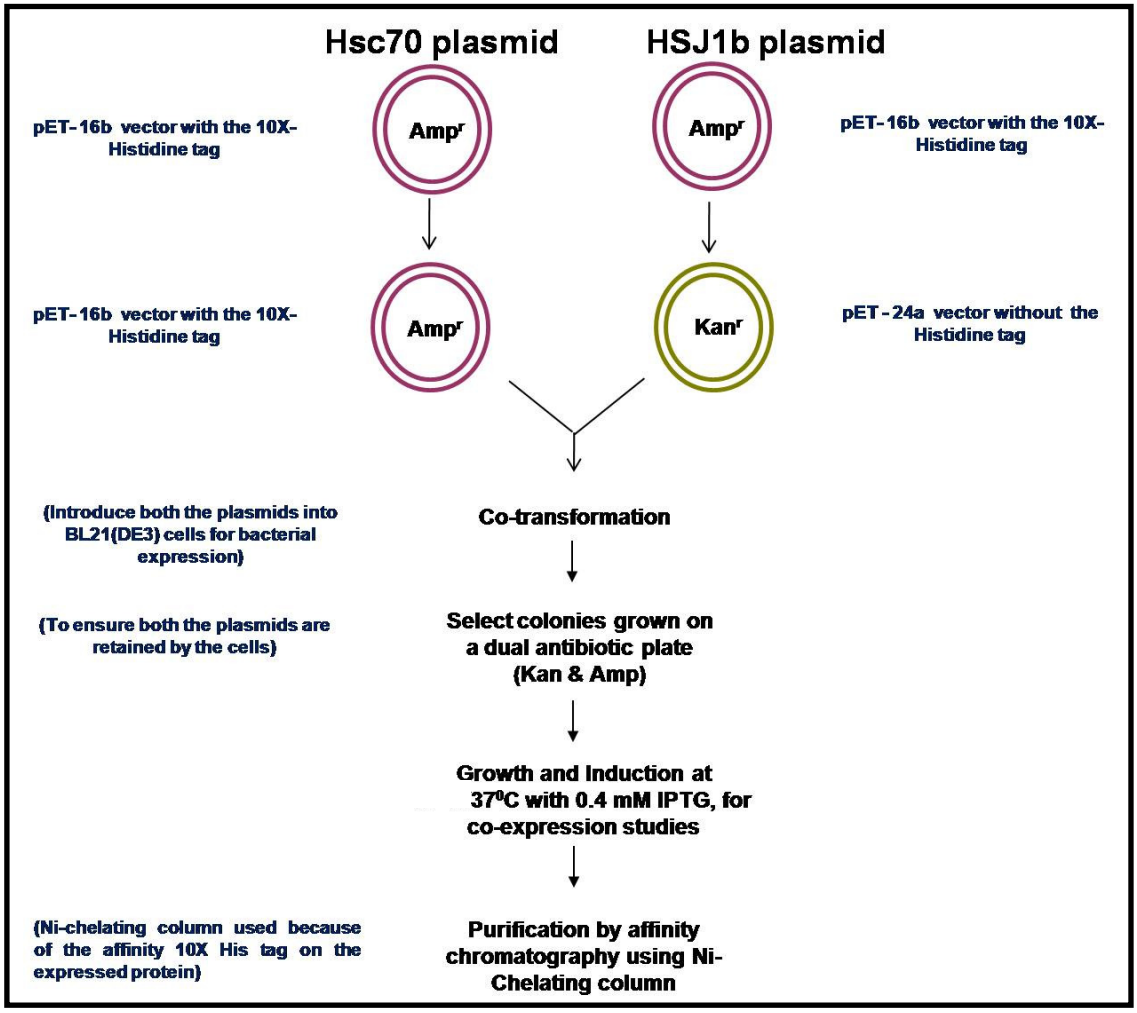

Figure 3.1: Experimental design for the co-expression studies.

A flow chart listing step-by-step the methodologies followed to establish co-expression system for the expression and purification of the Hsc70/HSJ1b complex from *E. coli.*

3.3.1 Cloning of the Hsc70 gene

3.3.1.1 PCR amplification of Hsc70

The nucleotide sequence of the *Homo sapiens Hsc70* ORF (1-1941 bp) was obtained from the NCBI database (accession number NM_006597). Primers complementary to the 5' and 3' ends of the nucleotide sequence of the polypeptide were designed (sequences given in section 3.2.1). cDNA prepared from HB4a cells was used as a template for amplification of the *Hsc70* gene by PCR. The amplification reaction was successful and the product was consistent with the expected size for the *Hsc70* gene of 1941 bp when analysed by electrophoresis (Figure 3.2). The *Hsc70* PCR product was subjected to a confirmative restriction digest. *Hin*dIII cleavage occurs at positions 337 and 1043 in the coding sequence and releases fragments sized 337 bp, 706 bp and 897 bp respectively. Figure 3.2 shows the results of this *Hin*dIII restriction digestion reaction. Lane 1 is the undigested PCR product and lane 3 clearly shows the expected 706 bp and 897 bp products however the 337 bp band is much fainter and cannot be clearly identified.

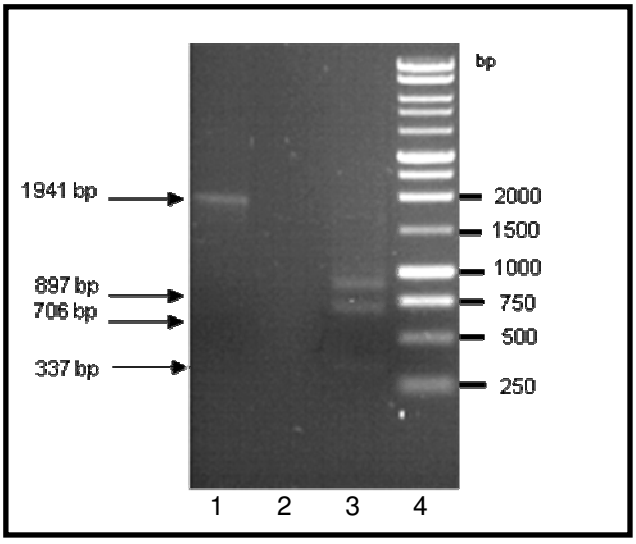

Figure 3.2: Diagnostic restriction analysis of *Hsc70* PCR product

10 µl of the PCR product was subjected to restriction digestion by *Hin*dIII. The digestion products were analysed on a 0.8% agarose gel along with 10 µl of undigested PCR product for comparison. . The DNA was visualised by staining with ethidium bromide at 0.5 ug/ml and photographed under UV illumination. Lane 1 contains 10 µl of the undigested PCR product, lane 2 is a blank lane, lane 3 contains *Hind*III digested PCR product and lane 4 contains 6 µl of Promega 1Kb DNA Ladder (molecular weight marker).

3.3.1.2 Insertion of the Hsc70 gene into pGEM-T vector

Despite repeated attempts, ligation of *Hsc70* gene directly into the pET-16b vector was unsuccessful. Therefore cloning of the gene into pGEM-T vector was undertaken. The pGEM-T vector is a TA-cloning vector system and the vector (from Promega) is supplied with a 5' 'T' (thymine) overhang. This complements with the 'A' (adenine) overhang introduced into the PCR product by the *Taq* polymerase. The 'TA' complementation increases the ligation efficiency allowing the purified PCR product of *Hsc70* to be directly ligated into the pGEM-T vector. Screening of colonies in pGEM-T was based on blue-white colony selection. The vector carries the *lac-Z* gene for the production of beta-galactosidase which converts the chemical substrate X-gal into a blue coloured product. The presence of the foreign gene insert disrupts the activity and function of the enzyme which is observed as a white bacterial colony. Plasmid DNA extracted from overnight *E. coli* cultures grown by inoculating selected white colonies was digested with the enzymes *Nde*I and *Bam*HI. Digestion of the pGEM-T clones that contain the human *Hsc70* gene yield yielded two fragments; a 3000 bp product which is the size of the pGEM-T vector and a 1941 bp product which is the expected size of the *Hsc70* gene (see lane 2, Figure 3.3).

1

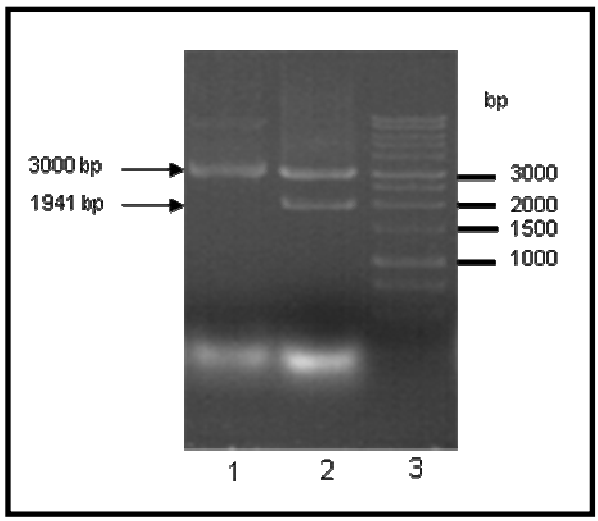

Figure 3.3: Restriction digest analysis of an *Hsc70* clone in pGEM-T vector.

Single white colonies were inoculated into LB broth and grown overnight with ampicillin. Plasmid DNA was extracted by alkaline lysis, 15 µl of which was used for restriction digestion by *Nde*I and *Bam*HI enzymes and visualized on a 0.8% agarose gel. The DNA was visualised by staining with ethidium bromide at 0.5 ug/ml and photographed under UV illumination. Lane 1 is the undigested plasmid, lane 2 contains *Nde*I and *Bam*HI digested plasmid DNA and lane 3 contains 6 µl of Promega 1Kb DNA Ladder (molecular weight marker).

3.3.1.3 Insertion of Hsc70 into pET-16b

In order to over-express the Hsc70 protein in *E. coli*, the gene was sub-cloned from the pGEM-T vector into the pET-16b bacterial expression vector. Panel A in Figure 3.4 shows the cloning region on the pET-16b vector. The 10X His Tag (pink box in Figure 3.4) allows for the affinity purification of the expressed protein and the downstream Factor Xa protease cleavage site allows for the removal of the tag and release of the protein in its native form, if required.

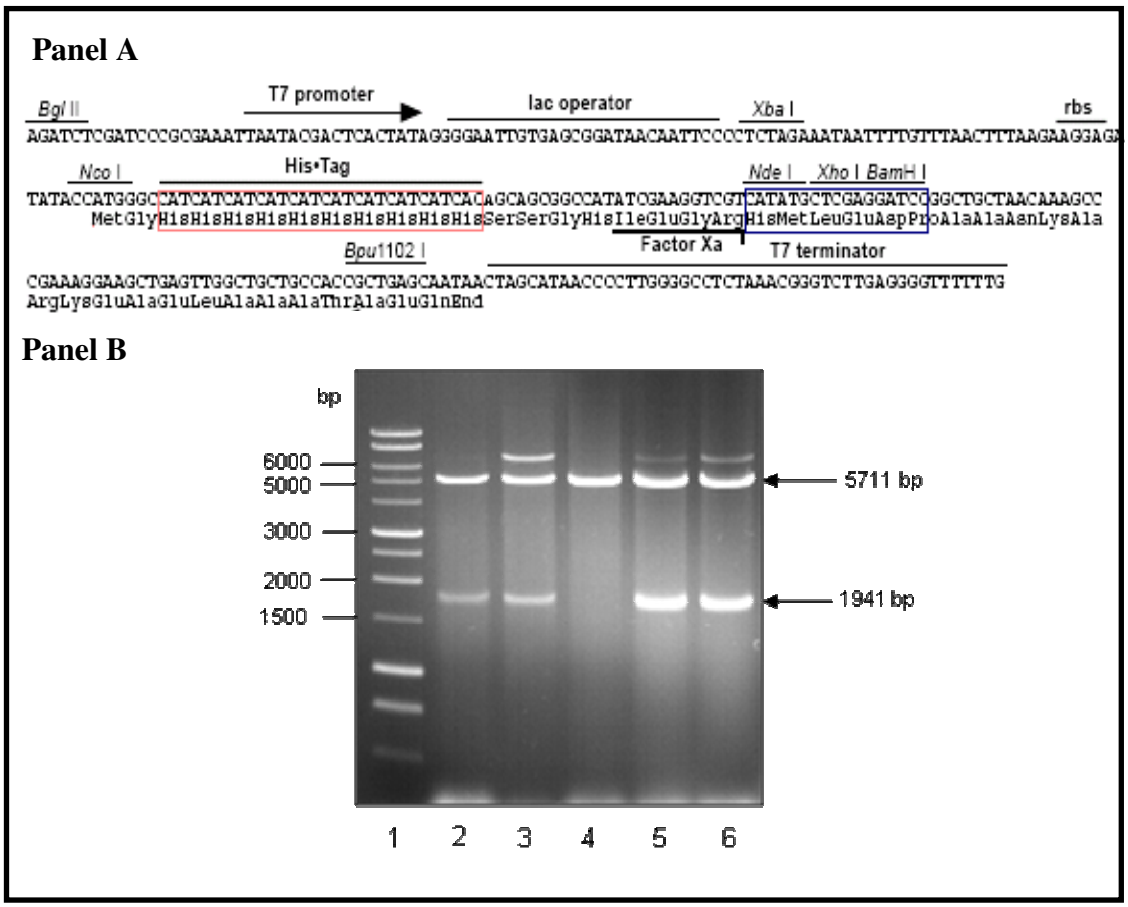

Figure 3.4: Insertion of *Hsc70* into pET-16b.

Panel A) The pET-16b vector cloning region. This figure illustrates the region on the pET-16b vector which codes for the Histidine tag (pink box), the Factor Xa protease cleavage site and also the multiple cloning sites (MCS) (blue box) of the vector.
Panel B) Confirmation of *Hsc70* gene into the pET-16b vector. Plasmid DNA from a number of representative clones was digested with *Nde*I and *Bam*HI enzymes and electrophoresed through a 0.8% agarose gel. The DNA was visualised by staining with ethidium bromide at 0.5 ug/ml and photographed under UV illumination. Lane 1, 6 µl Promega 1Kb DNA ladder molecular weight marker, lanes 2-6 shows *Nde*I/*Bam*HI digested plasmid DNA.

The gene was inserted between the *Nde*I and *Bam*HI restriction sites of the pET-16b vector to generate the pET-16b-*Hsc70* plasmid. The total size of the pET-16b plasmid containing the vector and *Hsc70* insert was 7652 bp, with the vector accounting for 5711 bp and the gene 1941 bp. Plasmid DNA from a number clones was subjected to restriction digestion and analysed on an agarose gel to confirm the presence of the *Hsc70* gene (see Panel B, Figure 3.4). Lane 2, 3, 5 and 6 in Figure 3.4 shows the successful release of the expected 1941 bp insert. Also, an additional band running higher than 5600 bp in lanes 3, 5 and 6 can be observed. This is probably due to incomplete digestion of the plasmid and is therefore running slower than the remaining fragments. The variable digestion observed could be due to inequality in the amounts of plasmid used for restriction digestion. Lane 4 shows no insert release and appears to run at the same position as digested pET-16b vector at 5711bp (compared with the other lanes of the gel) suggesting that this is a wild type plasmid that has probably arisen from the re-ligation of the vector.

3.3.2 Cloning of the HSJ1b gene

A plasmid carrying the *HSJ1b* gene was kindly provided by Professor Greg Blatch (Rhodes University, Republic of South Africa). Since the gene was already in a bacterial expression vector, pET-14b, expression studies were undertaken directly with the provided plasmid using *E. coli* BL21(DE3) cells. However no expression was observed (data not shown) and when the plasmid was subjected to a diagnostic restriction digest no insert release was obtained (data not shown). Due to the ambiguous nature of the plasmid map provided, it was decided to PCR amplify the *HSJ1b* gene using the pET-14b *_HSJ1b* plasmid as template, and clone it into the pET-16b expression vector.

3.3.2.1 Insertion of HSJ1b into pET-16b

The nucleotide sequence of the *Homo sapiens HSJ1b* ORF (1-975 bp) was obtained from the NCBI database (accession number NM_006736.5). Primers complementary to the 5' and 3' ends of the nucleotide sequence of the polypeptide were designed (sequences given in section 3.2.1) and *Bam*HI and *Hin*dIII cleavage sites were introduced at the 5' and 3'end's respectively. The forward primer also carried an extra nucleotide after the *Bam*H1 restriction site to ensure that the translation product of the gene was in frame with that of the vector. The *HSJ1b* gene was successfully amplified and the PCR product obtained was of the expected size of 975 bp (as seen in 3.5, panel A, lane 2). The PCR product was subjected to a diagnostic restriction digest using the enzyme *Eco*RI which cuts at position 313 in the *HSJ1b* sequence. Figure 3.5, Panel A, lane 3 shows the results of the restriction digest and the expected 313 bp and 662 bp digest fragments obtained. Insertion of the *HSJ1b* into the pET-16b vector was confirmed by *Bam*HI/*Hin*dIII digestion. Analysis by agarose gel electrophoresis revealed two bands - one at 975 bp corresponding to the *HSJ1b* gene size and the other at 5711 bp tallied with the size of the pET-16b vector (as shown in Figure 3.5, panel B, lane 3).

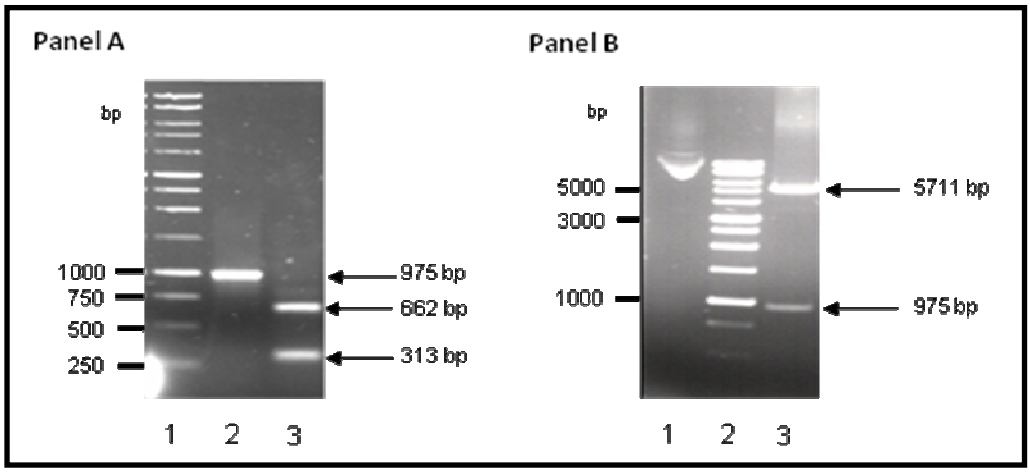

Figure 3.5: Analysis of the *HSJ1b* PCR product and its cloning into the pET-16b vector

Panel A) Full length human *HSJ1b* was amplified from the pET-14b_HSJ1b plasmid DNA using gene specific primers. 10 µl of PCR product was taken and subjected to restriction digestion by *Eco*RI. The digestion products were analysed on a 0.8% agarose gel along with 10 µl of undigested PCR product for comparison. Lane 1 is 6 µl of Promega 1Kb DNA Ladder (molecular weight marker), lane 2 is the undigested PCR product and lane 3 shows *Eco*RI digested PCR product.

Panel B) Cloning of *HSJ1b* into pET-16b vector. Lane 1 is the plasmid prior to digestion, lane 2 is 6 µl Promega's 1 Kb DNA molecular weight markers, lane 3 is *Bam*HI/*Hin*dIII digested plasmid.

3.3.2.2 Sub-cloning of HSJ1b into pET-24a for co-expression studies

For the successful implementation of the co-expression strategy, *HSJ1b* gene was sub-cloned into the pET-24a vector. The pET-16b-*HSJ1b* plasmid was digested using the restriction enzymes *Bam*HI and *Hind*III and the released insert was purified and ligated into pET-24a vector between the same restriction sites. Clones were confirmed by restriction analysis for the presence of the 975 bp *HSJ1b* insert (Figure 3.6). The total size of the pET-24a-*HSJ1b* plasmid was 6285 bp, with the vector accounting for 5310 bp and the gene 975 bp (lane 2, Figure 3.6).

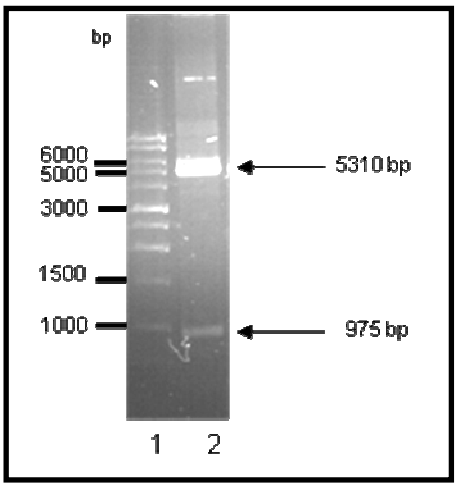

Figure 3.6: Cloning of the *HSJ1b* gene into the pET-24a vector

To generate the pET-24a-*HSJ1b* construct, the *HSJ1b* insert was obtained by restriction digestion of the pET-16b-*HSJ1b* clone with *Bam*HI and *Hin*dIII restriction enzymes. The pET-24a DNA was purified by alkaline lysis and was prepared for ligation by digestion using the same enzymes. The insert and vector were ligated as previously described in section 3.2.4 and transformed into *E.coli* DH5α cells. Overnight cultures of the transformants were used for plasmid extraction by alkaline lysis. 15 µl of the extracted plasmid DNA was used for restriction digestion by *Bam*HI and *Hin*dIII enzymes and visualized on a 0.8% agarose gel by staining with ethidium bromide at 0.5 ug/ml and photographing under UV illumination. Lane 1 is 6 µl Promega 1Kb DNA Ladder (molecular weight marker), lane 2 shows *Bam*HI/*Hin*dIII digested pET-24a-*HSJ1b* plasmid.

3.3.3 Small scale expression studies

Preliminary expression studies were carried out with the pET-16b-*Hsc70* or pET-24a-*HSJ1b* constructs to confirm expression of the individual Hsc70 and HSJ1b polypeptides in *E.coli* BL21(DE3). Growth and induction was carried out with 10 ml cultures of *E. coli* BL21(DE3) cells carrying either the pET-16b-*Hsc70* or pET-24a-*HSJ1b* plasmid, as described in the materials and methods. Expression of both the genes were under the control of the T7 promoter and protein production was initiated by the addition of the inducer, IPTG, to a final concentration of 0.4 mM. 1ml culture samples were collected before and after induction and centrifuged at 13,000 rpm. The pellet was re-suspended in 1X SDS-PAGE sample buffer and lysed by boiling. The soluble protein fraction was analysed by gel electrophoresis (Figure 3.7). Comparing the uninduced and the induced samples by SDS-PAGE gel electrophoresis, it was possible for us to identify induced expression of a ~70 kDa polypeptide corresponding to the estimated molecular weight of Hsc70 (lane 2 in panel A of Figure 3.7). This polypeptide is not observed in the uninduced sample (lane 1 in panel A of figure 3.7). Similarly, a ~38-40 kDa polypeptide was over-expressed in the BL21(DE3) cells carrying the pET-24a-*HSJ1b* plasmid (lane 2 in panel B of figure 3.7). A low level of basal expression was detected in the uninduced samples also (lane 1 in panel B of Figure 3.7).

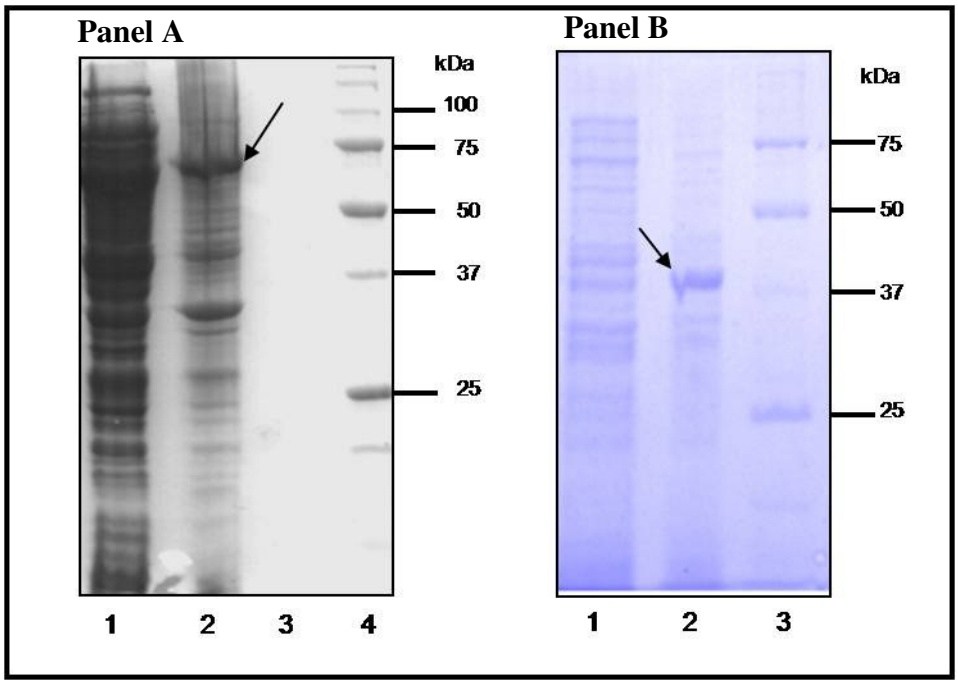

Figure 3.7: Expression profile for Hsc70 and HSJ1b proteins

The individual plasmids (pET-16b-*Hsc70* and pET-24a-*HSJ1b*) were transformed into *E.coli* BL21(DE3) cells. Single colony was used for overnight inoculation into 10 ml LB broth containing 100 µg/ml of ampicillin and grown at 37°C. 10 ml LB was inoculated with a 1 in 100 dilution of the overnight culture. Cells were grown at 37°C to an OD_{595} of 0.6-0.8. Protein expression was induced by the addition of IPTG to a final concentration of 0.4 mM. 1 ml cultures were collected before and after induction and spun down at 13,000 rpm. The supernatant was discarded and the pellet was re-suspended in 120 µl of 1X SDS -PAGE buffer and analysed on a 12% gel. Panel A) Lanes 1 and 2, Samples before (lane 1) and after (lane 2) induction for cells carrying Hsc70 plasmid, lane 4 Bio-Rad precision plus molecular weight marker proteins (broad range) Panel B) Samples before (lane 1) and after (lane 2) induction for *E.coli* BL21(DE3) cells carrying HSJ1b plasmid lane 3 Bio-Rad precision plus molecular weight marker proteins (broad range). Putative Hsc70 and HSJ1b protein species are highlighted by black arrows.

Once expression of the individual genes were confirmed, small scale co-expression studies were carried out as described in section 3.3.4 using 10 ml cultures of *E. coli* BL21(DE3) cells carrying both the pET-16b-*Hsc70* and pET-24a-*HSJ1b* plasmids. The co-transformed *E.coli* BL21(DE3) cells were selected with two antibiotics – ampicillin and kanamycin to ensure that both the plasmids were retained. One ml culture samples were collected before and after induction with IPTG and spun down. The pellet was re-suspended in 1X SDS-PAGE sample buffer and lysed by boiling. The sample was analysed by gel electrophoresis (Figure 3.8).

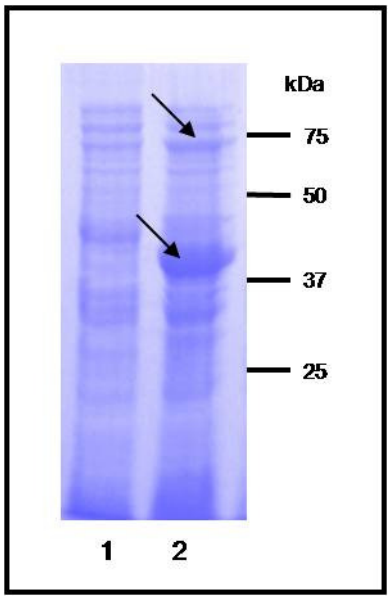

Figure 3.8: Expression of both Hsc70 and HSJ1b polypeptides under co-expression conditions

Plasmids pET-16b-*Hsc70* and pET-24a-*HSJ1b* were co-transformed into the *E. coli* expression strain BL21(DE3). Single colony was used for overnight inoculation into 10 ml LB broth containing 50 µg/ml of ampicillin and 25 µg/ml kanamycin and grown at 37°C. 10 ml LB was inoculated with a 1 in 100 dilution of the overnight culture. Cells were grown at 37°C to an OD_{595} of 0.6-0.8. Protein expression was induced by the addition of IPTG to a final concentration of 0.4 mM. 1ml cultures were collected before and after induction and spun down at 13,000 rpm. The supernatant was discarded and the pellet was re-suspended in 120 µl of 1X SDS -PAGE buffer and analysed on a 12% gel. Lanes 1 and 2, Samples before (lane 1) and after (lane 2) induction for *E.coli* BL21(DE3) cells co-transformed with pET-16b-*Hsc70* and pET-24a-*HSJ1b* plasmids. Putative Hsc70 and HSJ1b protein species are highlighted by black arrows. Moleuclar weightd (kDa) are indicated to the right of the gel.

Under the co-expression conditions, the production of both the 70 kDa and 40 kDa polypeptides were observed (indicated by arrows in lane 2 of Figure 3.8), after the addition of IPTG. The relative amounts of the two proteins suggested that the HSJ1b was better expressed than the larger Hsc70 protein. Also a 70 kDa species was observed in the uninduced sample. This could be attributed either due to leaky expression of the Hsc70 or the 70 kDa polypeptide could correspond to *E. coli*'s endogenous Hsp70- DnaK.

3.3.4 Confirmation of plasmid stability during co-transformation

To confirm definitively that the *E.coli* BL21(DE3) colonies grown with dual antibiotic selection actually maintained both the Hsc70 and HSJ1b plasmids, individual colonies were selected, re-suspended in distilled water and subjected to PCR. Two PCR reactions were carried out for each colony, using two different set of primers. One set of primers was specific for the *Hsc70* gene and the second specific for the *HSJ1b* gene.

The reactions were performed on two different BL21(DE3) colonies. The results of the amplification reactions were analysed on a 0.8% agarose gel (Figure 3.9). Panel A of Figure 3.9 showing amplification of a product at 1941 bp (lanes 2 and 3) confirms the presence of the *Hsc70* gene, while panel B of Figure 3.9 showing amplification of a 975 bp fragment (lanes 2 and 3) confirms the presence of the *HSJ1b* gene in the same BL21(DE3) colony. The expected amplification size was calculated using the gene sequence.

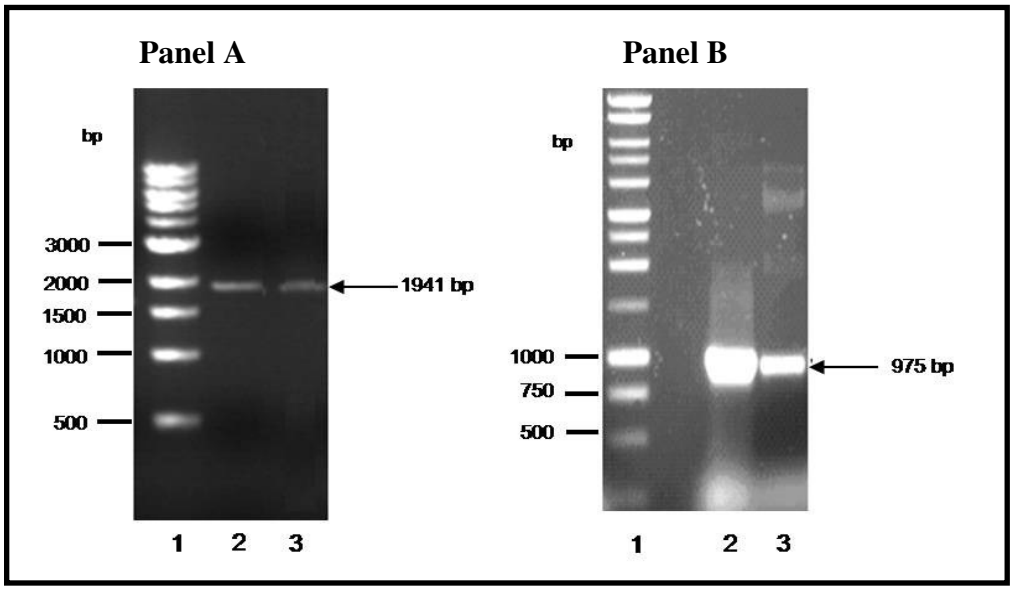

Figure 3.9: Confirmation of co-transformation into BL21 (DE3).

Single BL21(DE3) colonies transformed with both the *Hsc70* and *HSJ1b* plasmids were picked and re-suspended in 10 µl of water. 1 µl was then used as a template for PCR under the conditions previously described for both the genes (see materials and methods) using the gene respective primers detailed in table 3.1. The results were analysed on a 0.8% agarose gel with the DNA being visualised by staining with ethidium bromide at 0.5 ug/ml and photographing under UV illumination. Colonies carrying the gene show an amplification corresponding to the respective gene size which is indicated to the right-hand side of each respective gel. PCR was performed on two colonies.
Panel A) Lane 1 has the NEB 1Kb DNA Ladder (molecular weight marker) lanes 2 and 3 shows positive amplification of a 1941 bp product in colony 1 and 2 respectively. **Panel B)** Lane 1 has the Promega 1Kb DNA Ladder (molecular weight marker) lanes 2 and 3 shows amplification of a 975 bp product in colony 1 and 2 respectively.

In order to confirm that neither plasmid was lost due to segregation during the course of growth and induction, a sample of the induced cells were plated onto LB agar plates containing both antibiotics. Overnight incubation at 37^{o}C gave rise to colonies, thereby confirming that both plasmids were present at the end of the 3 hour incubation period.

3.3.5 Purification of Hsc70/HSJ1b co-expressed proteins

The co-expressed Hsc70/HSJ1b proteins were isolated using a one-step, Ni-NTA affinity column. Cells co-expressing the human Hsc70 and HSJ1b proteins were lysed as described in section 2.10.2 and the soluble fraction was loaded onto a Ni-NTA column. Protein was eluted using 200 mM imidazole and analysed by SDS-PAGE (Figure 3.10). Hsc70 expressed from pET-16b has a molecular weight of 73.4 kDa while the untagged HSJ1b has a calculated molecular weight of 35.5 kDa. From the SDS-PAGE analysis of the polypeptide co-eluting from the nickel resin the HSJ1b protein displays anomalous migration, running at ~40 kDa (Figure 3.10). From the gel, it was observed that a part of the Hsc70 and HSJ1b proteins expressed remained soluble while a significant percentage was detected in the insoluble pellet (comparing lane 1 and lane 2, Figure 3.10).

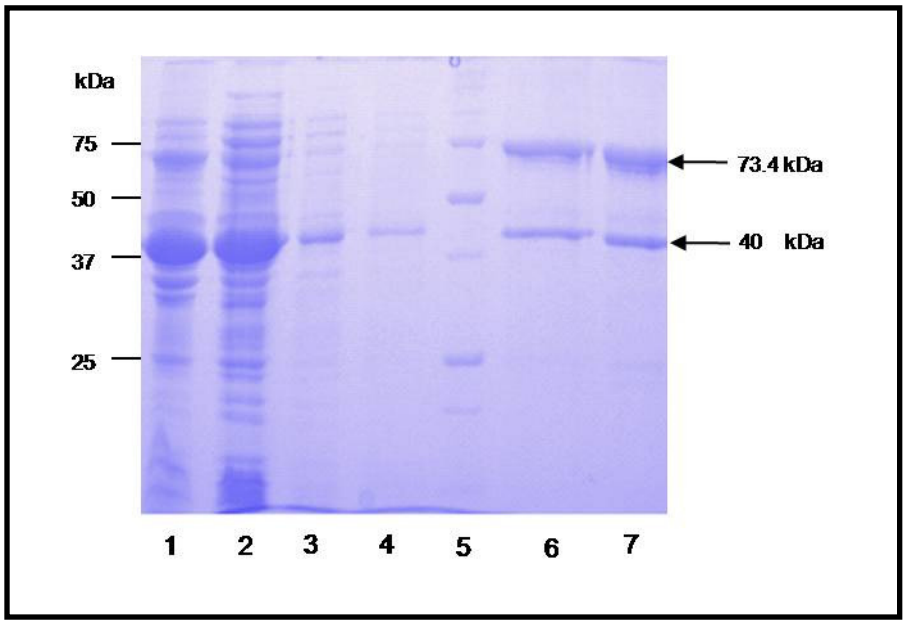

Figure 3.10: Chromatography profile of the Hsc70/HSJ1b complex on Ni-NTA resin

Recombinant Hsc70/HSJ1b proteins were co-expressed in *E. coli* BL21(DE3) cells by induction with 0.4 mM IPTG for three hours at 37°C. The lysed, soluble extract was applied to a Ni-NTA column, extensively washed with buffer A (50 mM Tris-HCl pH 8.0, 100 mM NaCl, 5 mM imidazole) containing 30 mM imidazole and eluted with buffer A containing 200 mM imidazole. The polypeptide composition was analysed by SDS-PAGE (12% resolving gel) stained with Coomassie Brilliant Blue and photographed: Lane 1 soluble extract, lane 2 insoluble pellet, lane 3 column flow through, lane 4 Wash with 30 mM imidazole, lane 5 Bio-Rad precision plus pre-stained molecular weight marker (broad range), lanes 6 & lane 7 200 mM imidazole elution

One of the reasons for the insolubility could be the inability of the cells to handle very high levels of over expression as observed for the complex. Despite only 50%

solubility observed in the expressed protein, typical yield from a 2 litre culture was up to 6-8 mg of protein, which was sufficient for our studies. Hsc70 expressed from the pET-16b vector carries a 10X Histidine tag suitable for affinity purification by nickel chelating resin, while the HSJ1b does not express any affinity tag. Thus only the Hsc70 is capable of binding to the Ni-NTA column and the tagless HSJ1b can remain on the column only if it associates with the Hsc70 moiety. HSJ1b which failed to associate with the tagged Hsc70 protein was observed in the flow through and wash fractions (lane 3 and 4, Figure 3.10). This could be either as a result of the complex dissociating during the wash or more likely as a result of excess expression of the HSJ1b. Figure 3.10 also shows that both Hsc70 and HSJ1b remain bound to the column after extensive washing and co-elute when 200 mM imidazole is applied to the column. This strongly suggests that the two proteins have formed a complex when expressed recombinantly (lane 6 and 7, Figure 3.10). A complex comprising of a 70 kDa polypeptide and a 40 kDa polypeptide (molecular weight corresponding to Hsc70 and HSJ1b) is observed in the 200 mM imidazole elution (lane 6 and 7, Figure 3.10). Whilst it is not possible to be completely accurate about the stoichiometry of the complex the relative intensities of the Coomassie staining suggest a 1:1 association. The recombinant Hsc70/HSJ1b complex isolated from bacterial cells using Ni-NTA chromatography will be referred to as rHH henceforth.

3.3.6 *Absence of non specific binding of untagged HSJ1b to Ni-NTA beads*

To confirm that the HSJ1b observed in the rHH elution fraction was not due to non-specific binding of the expressed HSJ1b protein to the Ni-NTA beads, pET-24a-*HSJ1b* plasmid was expressed individually under the same conditions as rHH and processed over Ni-NTA resins. Figure 3.11 is the analysis of the elution profile of this chromatography by SDS-PAGE. The absence of untagged HSJ1b in the 200 mM imidazole elution fraction (lane 6, Figure 3.11) confirms that the ~40 kDa band observed in the purified rHH was not due to non-specific binding of HSJ1b to the Ni-NTA agarose beads.

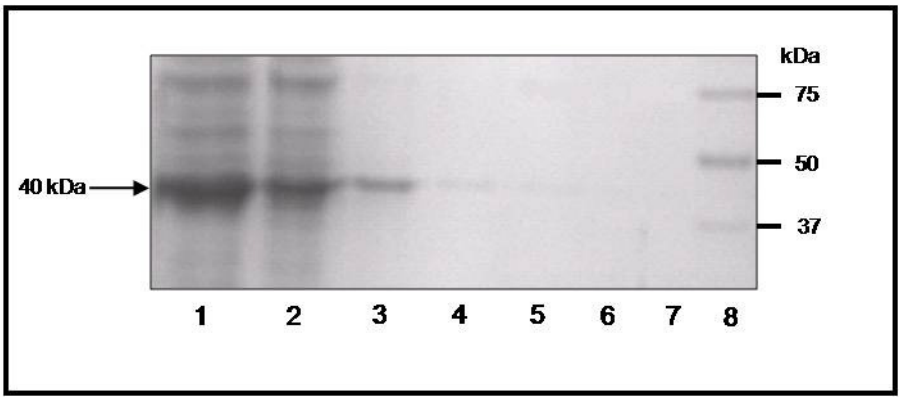

Figure 3.11: Chromatography of untagged HSJ1b protein over Ni-NTA resin.

The pET-24a-HSJ1b was expressed in *E. coli* BL21(DE3) by induction with 0.4 mM IPTG for three hours at 37°C. The soluble extract was applied to a Ni-NTA column and eluted was performed with 200 mM imidazole. The polypeptide composition was analysed by SDS-PAGE (12% resolving gel) and the gel stained with Coomassie Brilliant Blue: Lane1 soluble extract, lane 2 insoluble pellet, lane 3 column flow through, lane 4 Wash with buffer A (50 mM Tris-HCl pH 8.0, 100 mM NaCl, 5 mM imidazole), lane 5 Wash with buffer A containing 30 mM imidazole, lane 6 with buffer A containing 200 mM imidazole elution & lane 7 Bio-Rad precision plus prestained molecular weight marker (broad range).

3.3.7 Stability of the isolated complex

We next wanted to confirm that the isolated complex was stable and that the HSJ1b protein that was seen in the wash and flow-through fractions of the Nickel column was there because of the excess HSJ1b being expressed not because the complex was gradually dissociating. The integrity of the complex isolated by Ni-NTA chromatography was assessed by reloading the rHH complex onto the Ni-NTA column. Imidazole washing and elution was carried out as described earlier in the Materials and Methods. If the complex was unstable, re-chromatography over the Ni-

NTA column might destabilise the protein complex. Analysis of the rHH complex once rebound to Ni-NTA resin showed that the complex remains intact, eluting with 200 mM imidazole (Figure 3.12, lane 5) and showing no signs of HSJ1b dissociation during column washes with buffer (Figure 3.12, lanes 3 and 4).

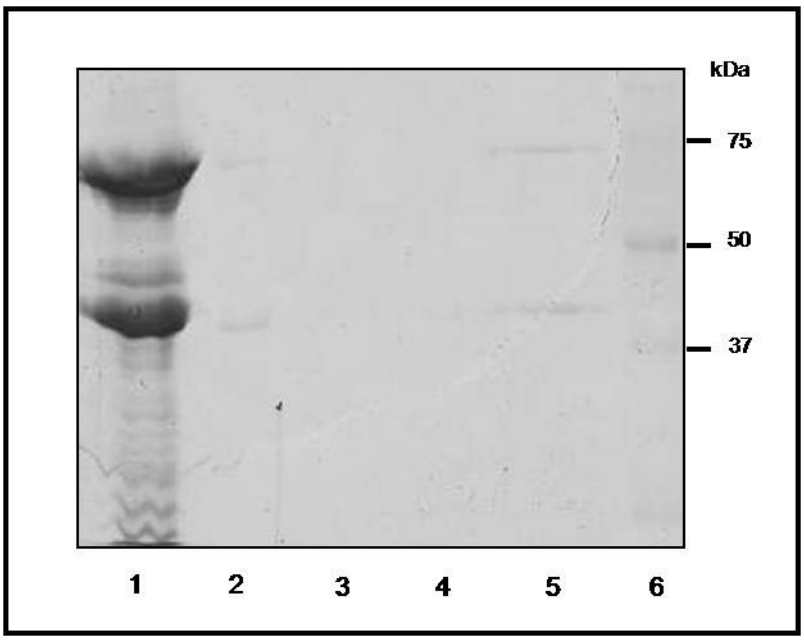

Figure 3.12: Re-chromatography of the rHH protein over the Ni-NTA column.

An aliquot of the rHH protein eluted from the Ni column, described in section 3.3.4.2, was diluted with buffer (50 mM Tris-HCl pH 8.0, 100 mM NaCl) to bring down the imidazole concentration to 20 mM and reloaded onto 200 µl of Ni-NTA agarose. The protein was eluted with buffer (50 mM Tris-HCl pH 8.0, 100 mM NaCl, 5 mM imidazole) containing 200 mM imidazole and the fractions were analysed on a 12% gel. Lane 1 is an aliquot from which the rHH protein sample was used for the chromatography, lane 2 column flow through, lane 3 Wash, lane 4 Wash with 30 mM imidazole, lane 5 200mM imidazole elution & lane 6 Bio-Rad precision plus prestained molecular weight marker (broad range).

3.3.8 Additional Purification strategies

The rHH complex purified by Ni-NTA chromatography was isolated with variable purity; compare the preparation shown in figure 3.10 with figure 3.12. Ion exchange was undertaken to further purify the rHH protein obtained after Ni-NTA chromatography for the purposes of obtaining a pure complex that could be used in crystallographic analysis. The rHH complex was predicted to have a pI point of 5.78 suggesting it would bind to the anion exchange resin, Q-sepharose. A trial analysis was undertaken by binding a sample of the rHH from the Ni-NTA resin to Q sepharose resin. The protein was eluted using a step gradient of NaCl up to 1 M concentration. At 250 mM NaCl, elution of the complex was observed (Figure 3.13), however the stoichiometry of the Hsc70/HSJ1b complex eluting from the column was not

consistent with that loaded onto the column (compare lanes 1 and 4, Figure 3.13). Furthermore, a proportion of the Hsc70 eluted independently at 500 mM NaCl and it is not clear where the rest of the HSJ1b protein has gone. The predicted pI point of HSJ1b alone, 5.6, suggests that this protein will not bind any more tightly than Hsc70 (pI point 5.9) to Q-sepharose. No polypeptide species corresponding to HSJ1b elutes with up to 1 M NaCl applied to the column. The most likely explanation was that the protein was lost in the lower NaCl wash fractions, which were unfortunately not analysed by gel electrophoresis. It was concluded that ion-exchange chromatography does not represent a useful means of further enhancing the purity of the complex.

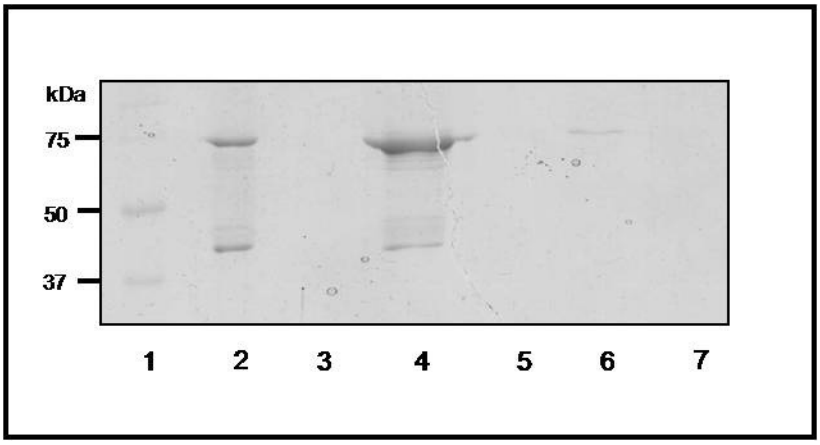

Figure 3.13: Elution profile of rHH complex separated by ion exchange chromatography

Ion Exchange chromatography was performed using Q sepharose ion exchange resin. The Hsc70/HSJ1b complex fractions from the Ni-NTA column containing 200 mM imidazole were diluted to 25 mM NaCl using dilution buffer (50 mM Tris-HCl, pH 8.0). The protein was applied to a 20 ml Q sepharose column pre-equilibrated with buffer B (50 mM Tris-HCl, pH 8.0. The resin was washed with 2 column volumes of equilibration buffer and the protein step eluted with a NaCl step gradient from 0-1 M in buffer B. 100, 250, 500 and 1000 mM NaCl. The elution profile was monitored by SDS-PAGE Lane1 Bio-Rad precision plus prestained molecular weight marker proteins, lane 2 rHH complex load, lane 3 flow through from the column, lanes 4 & 5 250 mM NaCl elution fractions, lane 6 500 mM NaCl elution, lane 7 1 M NaCl elution

An alternative purification strategy used frequently to remove contaminants from Hsc70 is the use of ATP-agarose chromatography. Schlossman and co-workers first used it to purify Hsc70 from bovine brain (Schlossman *et al.,* 1984), and since then it is used routinely in the purification of Hsp70 proteins (Ménoret, 2004, Nicoll *et al*., 2006). There were initial misgivings about the use of an ATP-agarose column with the Hsc70/HSJ1b complex, since re-binding of ATP to any Hsp70/Hsp40 complex could stimulate the release of its Hsp40 co-chaperone partner. However based on the reports of Motohashi *et al* who have used this chromatography technique to successfully

purify a native DnaK/DnaJ complex from *Thermus thermophilus*, small scale experiment was carried out by binding a sample of the rHH from the Ni-NTA resin to an ATP-agarose column (Figure 3.14).

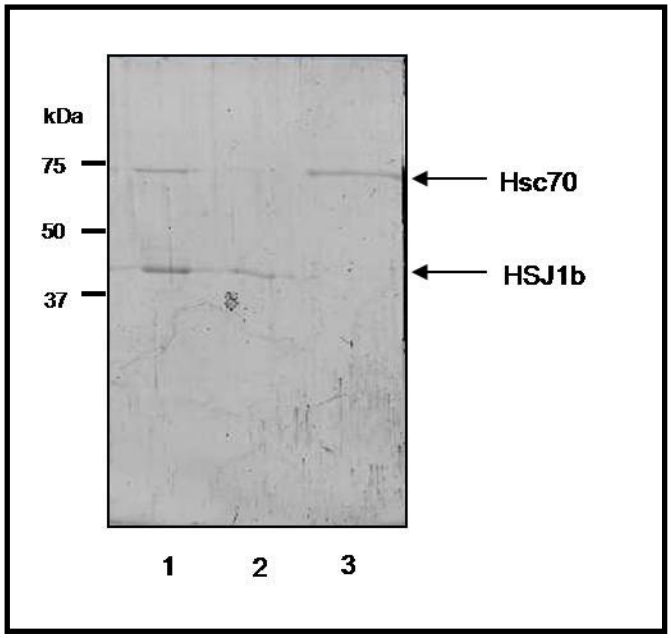

Figure 3.14: Elution profile of rHH complex separated by ATP-agarose chromatography

5 ml of the ATP-agarose slurry was packed into a column that was washed with 10 column volumes (CV) of equilibration buffer (20 mM Tris-HCl pH 8.0, 20 mM NaCl, 15 mM β-Mercaptoethanol and 3 mM $MgCl_2$). The Hsc70/HSJ1b elution fraction from Ni-NTA chromatography was diluted in 20 mM Tris-HCl pH 8.0, 15 mM β-Mercaptoethanol and 3 mM $MgCl_2$ to bring down the final concentration of NaCl in the sample to 25 mM. The protein was loaded onto the column and washed with 5 CV of equilibration buffer. The agarose was incubated in elution buffer (20 mM Tris-HCl pH 8.0, 20 mM NaCl, 15 mM β-Mercaptoethanol, 3 mM $MgCl_2$ plus 3 mM ATP) for 30 minutes before the fractions were collected. The elution profile was analysed by denaturing 12% SDS-PAGE and Coomassie brilliant blue staining. Lane 1 flow through from the column, lane 2 Wash with equilibration buffer and lane 3 Elution with 3 mM ATP

The protein was eluted using 3 mM ATP. It was observed that only a fraction of the complex was bound to the column, since a fraction of the complex was also detected in the flow through from the column (lane 1, Figure 3.14). The reason for this is not clear. Also, the stoichiometry of the Hsc70/HSJ1b complex detected in the flow through was not consistent with that loaded onto the column (compare lanes 1 in Figure 3.14 with lane 7 in Figure 3.10). Analysis of the wash and elution fraction (lanes 2 and 3, Figure 3.14) confirmed that a proportion of the complex was disassociating over the column. HSJ1b from the separated complex is observed in the flow through fraction (lane 2, Figure 3.14), while Hsc70 eluted independently with 3 mM ATP (lane 3, Figure 3.14).

It was concluded that ATP-agarose chromatography was not a suitable additional purification strategy because of its destabilising effect on the complex.

3.3.9 Assessment of DnaK contamination

Usage of a bacterial system for the isolation of recombinant Hsp70's has been reported to carry the risk of the protein preparation getting contaminated with the endogenous bacterial Hsp70, DnaK (Ménoret, 2004). In order to confirm that the 70 kDa polypeptide band observed on the SDS-PAGE corresponded solely to Hsc70 and does not have any contamination from endogenous *E. coli* DnaK, a dot blot was performed on the Ni-NTA elution fractions using anti-DnaK and anti-Hsc70 antibodies. Results from the dot blot however indicated that the rHH protein indeed had contamination from DnaK protein (panel A, Figure 3.15). Panel B in Figure 3.15 was the control reaction performed with Hsc70 antibodies. Hsc70 and DnaK have different pI values. The pI calculated for Hsc70 is 5.9 while that of DnaK is 4.8. This difference in pI values between Hsc70 and HSJ1b was exploited to determine the percentage of DnaK contamination. Protein was separated in the first dimension by isoelectric focussing followed by 2nd dimension resolution by SDS-PAGE. Panel C, Figure 3.15 shows the successful separation of the DnaK contaminant fragment from the total rHH protein. The percentage of contamination was estimated by densitometry at 3.5 % of the total and was therefore considered to be negligible. Similarly the rHH protein was probed for the presence of contaminating DnaJ protein. The pI value for HSJ1b is 5.6 while that of DnaJ is 7.98. From Figure 3.15, panel D, the level of *E. coli* DnaJ contamination in the rHH preparation can be considered negligible.

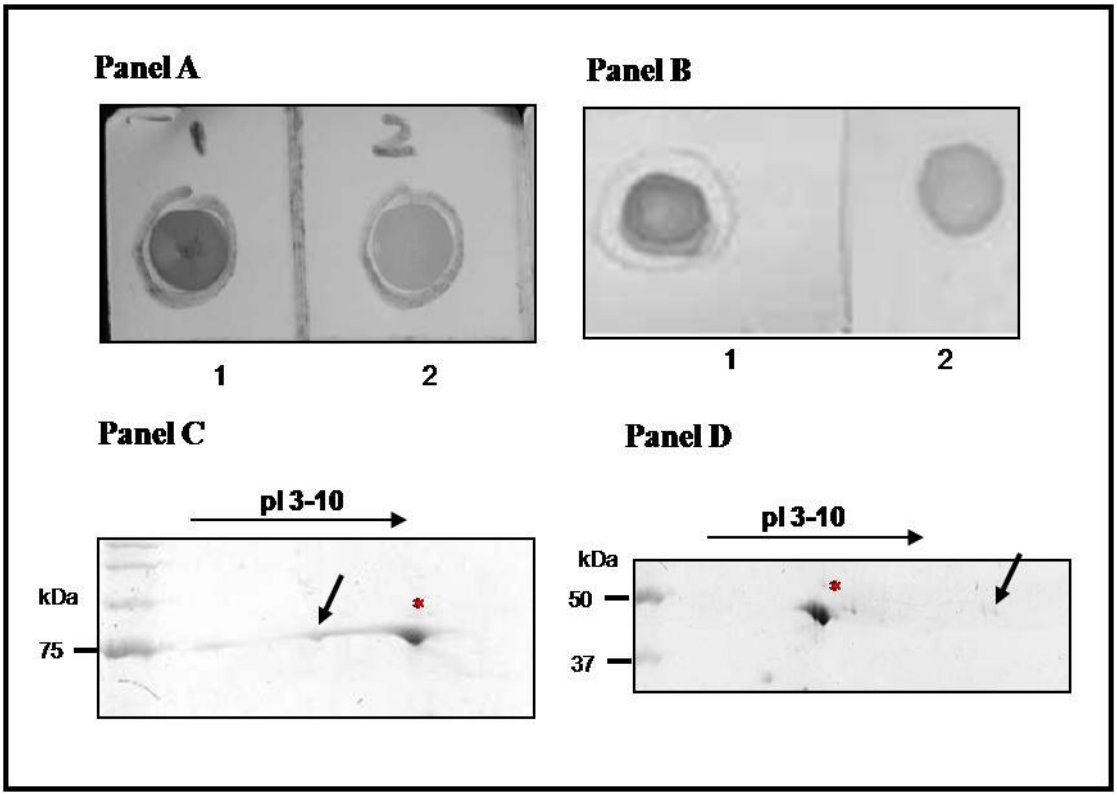

Figure 3.15: Qualitative and quantitative detection of DnaK contamination of the rHH protein fraction.

Panel A and B are the results of the dot blot analysis (described in section 2.10.7, chapter 2). The rHH protein purified by Ni-NTA chromatography was immobilised on the nitrocellulose membrane soaked in TBS-T buffer (10 mM Tris-base, 150 mM NaCl, 0.05% (v/v) Tween-20, pH 8.0) for 1 min. 2 µl of the protein sample was spotted onto the membrane; membrane dried and blocked in 5% (w/v) BSA in TBS-T for 2 hrs at room temperature. The membrane was next incubated with primary antibody (either anti-DnaK or anti-Hsc70) diluted in TBS-T (dilution factor mentioned in section 2.1.6) for 2 hours at room temperature. At the end of the incubation the membrane was given three, five minute washes with TBS-T and then probed with the appropriate secondary antibody conjugated with HRP. The bands were visualised using 3 ml of 3,3′,5,5′-Tetramethylbenzidine (TMB) Liquid Substrate System (Sigma-Aldrich, UK).

Panel A: Dot blot performed using anti-DnaK antibody. Sample 1 is the DnaK positive control and sample 2 is the rHH protein being probed for the presence of DnaK contamination.

Panel B: Dot blot performed using anti-Hsc70 antibody. Sample 1 is the Hsc70 positive control and sample 2 is the rHH protein.

Panel C and D shows the 2DE separation of rHH proteins. 15 µg of protein was loaded onto a linear 7 cm IPG strip in the pH range 3-10 overnight. Isoelectric focusing was carried out on the following day using the Multiphor II apparatus (Pharmacia BIOTECH.) as described in the handbook of 2-D electrophoresis (GE Healthcare, 2004). Briefly, focussing was performed at 20°C under the following conditions: 300V for 30 min; 600V for 45 min; 3500V for 2 hours and 45 minutes using an Amersham EPS 3501 power pack. The strip was sealed onto the top of a 12% SDS-polyacrylamide gel and separated at 150 V.

Panel C: Identification of contaminating DnaK species based on their in pI value. The black arrow indicates the putative position of the acidic DnaK and the red star marks the position of Hsc70.

Panel D: Identification of contaminating DnaJ species based on their in pI values. The black arrow indicates the putative position of the DnaJ and the red star marks the presumed position of HSJ1b.

3.3.10 Two-dimensional analysis of by native/SDS-PAGE analysis

To verify the nature of the interaction between the Hsc70 and HSJ1b components of the observed recombinant complex, two-dimensional analysis was undertaken. For the first dimension, Ni-NTA fractions containing the rHH complex were separated on an 8% native gel where separation of polypeptides is based solely on the charge-mass ratio. From the native gel, under the electrophoretic condition studied, the complex resolved into multiple bands on the gel (see Figure 3.16). The lowest molecular weight component was observed at ~140 kDa with several higher molecular weight components. The presence of several bands on the 1st dimension separation by native gel suggests that the complex assumes more than one oligomeric state and possibly the different forms could indicate different states of association or disassociation of the complex. Next, gel strips carrying the separated protein fractions were treated with 1X SDS-PAGE sample buffer before being transferred onto a second dimension SDS-PAGE gel. In the presence of SDS, protein complexes dissociate and therefore, in the resulting second dimension gel the subunits of a protein complex are ordered according to their molecular weight in vertical rows. From the 2nd dimension analyses the protein species migrating at 140 kDa on the native gel, comprised predominantly of Hsc70 (running at 70 kDa, indicated by a red circle on Figure 3.16). The higher molecular weight species from the native gel appeared to correspond to intact Hsc70/HSJ1b complex (as evidenced by the presence of both the 70 kDa and 40 kDa polypeptide in the 2nd dimension). Thus the 2D analysis by Native and SDS-PAGE successfully demonstrates that the isolated rHH protein contains a complex of Hsc70 chaperone with its co-chaperone partner -HSJ1b proteins.

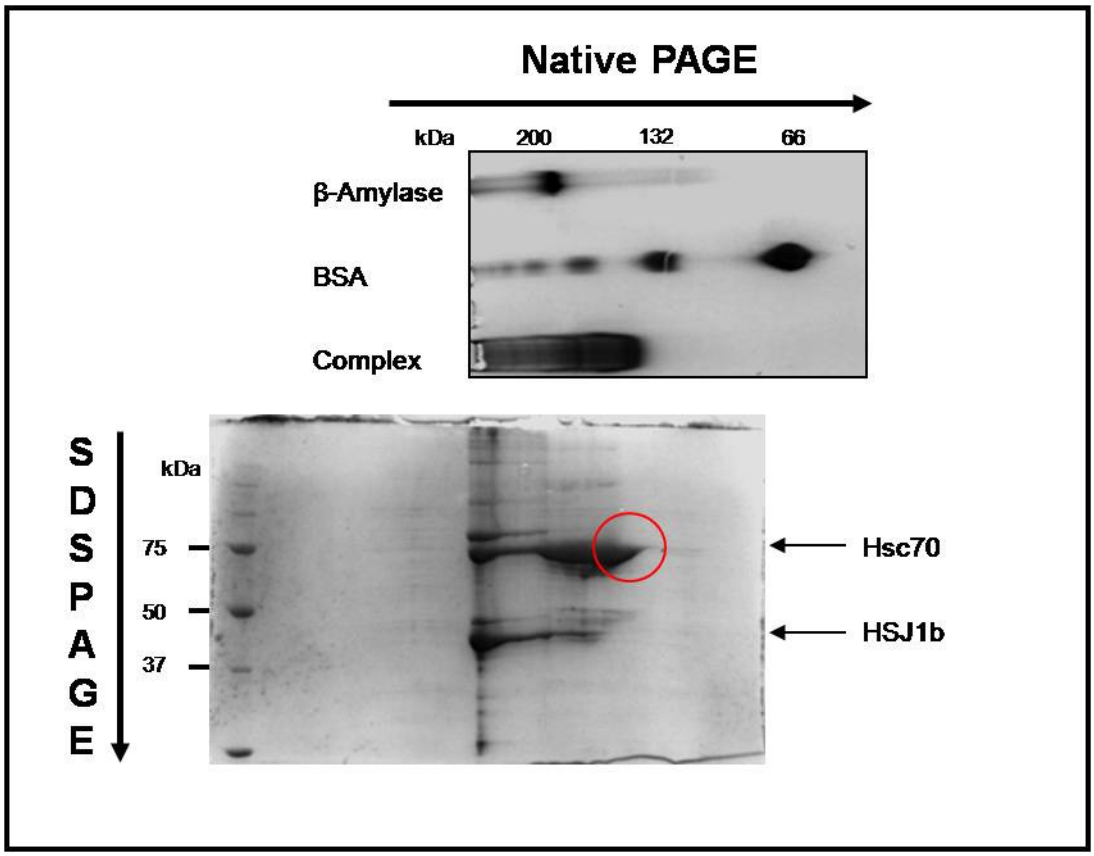

Figure 3.16: Two-dimensional analysis by native and denaturing gel electrophoresis of rHH protein

The rHH complex was resolved in the first dimension on an 8% native gel. Protein samples were prepared in 4X Native-PAGE sample buffer (0.0625 M Tris-HCl, pH 6.8, 10% (v/v) glycerol and 0.05% (w/v) bromophenol blue) and were loaded without boiling at 95°C. The gel was run in 1X Native-PAGE gel running buffer (25 mM Tris base and 192 mM glycine). The samples were resolved at 100V at 4°C until the blue dye front had reached the end of the gel plates. The native gel was run with BSA (66,132 kDa) and β-amylase (200 kDa) as markers. The lane of the native gel containing the complex was cut out, equilibrated in 1X SDS-PAGE sample buffer and transferred horizontally on a 12% SDS-PAGE in the second dimension with Bio-Rad broad range protein markers. The gel was run at 150 V in running buffer (25 mM Tris, 192 mM Glycine, 0.1% (w/v) SDS), stained with Coomassie Brilliant Blue and photographed.

3.4 Discussion

In this chapter, we sought to establish an expression system from which the Hsp70/Hsp40 complex, preferentially in a soluble form, could be produced. For this project we have used the human heat shock cognate 70 (*Hsc70*) and a type II neuronal DnaJ homologue - *HSJ1b*, as representatives of the Hsp70 and Hsp40 families respectively. Routinely, the individual Hsp70 and Hsp40 proteins are independently purified, and the Hsp70/Hsp40 system has been reconstituted by mixing the two proteins in the presence of ATP and characterised the complex thus formed (Minami *et al*., 1996). The individual proteins have been purified either from their native source, for example Hsc70 has been extracted from bovine brain (Schlossman *et al.,* 1984), or by employing recombinant methods (Minami *et al*., 1996; Chamberlain and Burgoyne, 1997). However the mechanism of assembly into a complex upon reconstitution is not well understood. Also the similarity of their assosciation to the *in vivo* system has not been well studied. Alternatively, Motohashi *et al*., (1994) reported the isolation of the native DnaK/DnaJ complex purified from *Thermus thermophilus*. The complex, isolated from the strain *T. thermophilus* HB8 (ATCC 27634), involved four purification steps through DE-52 cellulose column, ammonium sulphate precipitation, a hydroxyapatite column, a Butyl-Toyopearl column and a final polishing step using gel filtration. However due to the lengthy purification procedures only a 2% recovery of the *T. thermophilus* DnaK/DnaJ complex was obtained (Motohashi *et al*., 1994). Also, the yield of protein from a native source is dependent on the relative abundance and distribution of the target protein and might not be a feasible option if a large quantity of protein is required.

The isolation of a recombinant, co-expressed Hsc70/HSJ1b complex has been reported for the first time in this study. Two strategies are normally employed to co-express proteins in *E. coli*. One is to use a bicistronic vector, such as pETDuet-1 from Novagen, and clone two target genes into one vector. The other method is a 2-plasmid co-expression system in which the target genes are cloned into two separate vectors with compatible origins of replication and thus avoid competition in replication, segregation and ultimate loss of one plasmid (Johnston *et al*., 2000; Scheich *et al*., 2007). For example, the human cell cycle and transcriptional regulatory protein complexes have been produced in bacteria using a 2-plasmid co-expression system

(Johnston *et al*., 2000). A variant of the above methodology was described by Yang *et al*., (2001), who successfully demonstrated co-expression of proteins using incompatible plasmids with the same replicon but with different antibiotic resistance genes. They observed that under antibiotic selection pressure, it was possible to maintain both plasmids in the same cell for at least 14 hours (Yang *et al*., 2001).

In this work, *Hsc70* and *HSJ1b* genes were both cloned into the pET-16b initially. The pET-16b-*Hsc70* and pET-16b-*HSJ1b* clones were then used to isolate and purify the individual proteins. The work carried out with this regard will be discussed in detail in Chapter 5. For the sake of the co-expression studies, the *HSJ1b* gene was sub-cloned into the pET-24a vectors. The two plasmids (pET-16b and pET-24a) have the same origin of replication, but have different antibiotic selectivity and this difference is essential for successful co-expression of the two genes. The pET-24a vector has a kanamycin resistance marker, while pET-16b has an ampicillin resistance marker. Dual antibiotic selection allows bacterial cells transformed with pET-16b-*Hsc70* and pET-24a-*HSJ1b* plasmids to maintain both the plasmids simultaneously.

The genes were successfully overexpressed in *E. coli* BL21(DE3). DE3 indicates that the host is a lysogen of λDE3, and therefore carries a chromosomal copy of the T7 RNA polymerase gene, under the control of a lacUV5 promoter. Thus, this strain is suitable for production of protein from target genes cloned in pET vectors under the control of a T7 promoter, by induction with IPTG. Since the two plasmids had incompatible *ori'*s, it was necessary to ensure that both plasmids are maintained in the bacterial cell. Yang *et al*., reported that under dual antibiotic selection pressure, it was possible to maintain both plasmids in the same cell for at least 14 hours (Yang *et al*., 2001). In our case, cells were grown at 37^{o}C for only 3 hours after IPTG induction. To further confirm the effectiveness of the dual antibiotic selection in maintaining both the plasmids, colony PCR of the transformed *E. coli* BL21(DE3) cells was undertaken. Colony PCR is usually used as a quick screen to confirm the presence of the gene of interest in bacterial cells, and was successfully used in this case to confirm the coexistence of both the plasmids.

Purification of the Hsc70/HSJ1b proteins took advantage of another important difference between the two vectors. While pET-16b expresses a 10X N-terminal histidine tag , pET-24a does not carry an N-terminal tag. Instead, pET-24a has a C-

terminal histidine tag. However, since *HSJ1b* inserted into pET-24a vector has been amplified with a stop codon, expressed HSJ1b protein will not carry a histidine tag. This was an important for the successful isolation of the complex from Ni-NTA chromatography. Untagged HSJ1b protein is incapable of binding to Ni-NTA agarose. Despite this a ~40 kDa species corresponding to the molecular weight of HSJ1b was observed in the elution fractions along with the 70 kDa Hsc70 species. This is possible only if untagged HSJ1b associated with the histidine tagged Hsc70 protein and eluted as a complex from the Ni-NTA column. To rule out non-specific binding of HSJ1b to the Ni agarose, untagged HSJ1b was chromatographed over the Ni-NTA column. All of the expressed HSJ1b protein was present only in the flow through and wash fractions. No species ~40 kDa was detected in the higher imidazole elution. Also, re-chromatography of the purified rHH complex over Ni beads failed to destabilise the Hsc70-HSJ1b interaction.

The experimental design as such did not allow co-elution of the untagged HSJ1b subunit from the Ni-NTA column until and unless bound to the His-tagged Hsc70. However, it was essential to confirm that the two polypeptides detected in the Ni-NTA elution fractions (Hsc70 and HSJ1b) represented two interacting proteins and not merely an artefact of protein co-elution. 2D analysis by native and SDS-PAGE has been used extensively in the isolation of large protein complexes from chloroplast and respiratory protein complexes of mitochondria (Schagger and von Jagow, 1991, Kugler *et al*., 1997). Protein separation under native conditions in the first dimension conserves protein-protein interactions. Subsequent separation by SDS-PAGE causes disassociation of protein complexes and the subunits of distinct protein complexes are arranged based on their molecular weight. The interaction between the two subunits was further verified using 2-Dimensional electrophoresis. Analysis of the migration pattern of the recombinant Hsc70/HSJ1b complex confirmed the interactions of the Hsc70 and HSJ1b subunits of the rHH complex. Thus, a complex of Hsc70/HSJ1b proteins was successfully isolated using an *E. coli* co-expression system.

There were two major drawbacks in using an *E. coli* expression system. One, is the possible contamination of the isolated Hsc70/HSJ1b complex with the bacterial Hsp70 i.e. DnaK. Wang and Lee, (1993) have observed the co-elution of DnaK during the purification of rat Hsc70 from *E. coli* (Wang and Lee, 1993). Similarly, Ménoret haa

also observed contamination of recombinant Hsp70 with DnaK (Ménoret, 2004). Dot blot analysis of the recombinant protein compels with anti-DnaK antibody confirmed the presence of DnaK contamination in our protein preparations. The extent of contamination was determined using 2-dimensional analysis using IEF. IEF is routinely used for electrophoretic separation of protein mixtures based on their isoelectric points (Görg *et al*., 2004). Using IEF/SDS-PAGE analysis, a DnaK (pI of 4.8) species was clearly separated from Hsc70 (pI of 5.9) protein and the percentage of DnaK contamination was calculated. Since this was less than 5% of the total protein the contamination was considered to be negligible. The two dimensional analysis also confirmed that the protein preparation was free from DnaJ (pI of 7.9), the endogenous bacterial Hsp40.

The other drawback of expressing a chaperone complex in *E. coli* is the co-elution of several contaminating protein species (Nicoll *et al*., 2006). A plausible explanation for observed contamination could be the affinity of the chaperone/co-chaperone complex to bind to unfolded substrates present in the bacterial cytosol, thereby co-eluting with contaminants even after the Ni-NTA chromatography. The presence of its Hsp40 partner exaggerates this problem since it stimulates ATPase activity of Hsc70 and converts it to its high substrate affinity ADP bound form (Frydman *et al*., 1994). Routinely, ATP-agarose (Welch and Feramisco, 1985) and ion exchange chromatography (Nam and Walsh, 2002) have been used as additional Hsp70 purification procedures. Both these methods have also been used to combat DnaK contamination in recombinant HSP70 preparations. It has been observed by Ménoret that the DnaK and Hsp70 bind to the ATP agarose under different conditions and therefore this represents a useful method to isolate the rHH complex from the DnaK contaminant protein (Ménoret, 2004). Also, HSP70 proteins have low affinity for substrates when bound to ATP (Palleros et al., 1993; Bukau and Horwich, 1998), therefore chromatography using ATP-agarose has been shown to limit the extent of contamination (Welch and Feramisco, 1985). Similarly, differences in elution of Hsp70 and DnaK from the DEAE-Sephacel column have also been observed. DnaK was found to elute at a salt concentration higher than 150 mM, while 50% of Hsp70 could be recovered with a 100 mM NaCl elution from the column (Ménoret, 2004). Therefore these two chromatography techniques were used to further purify the rHH elutions from the Ni-NTA column. However both chromatography methods, when

used for the rHH complex, resulted in destabilisation of the complex leading to the separation of the protein into two subunits, Hsc70 and HSJ1b. Therefore further purification of the rHH protein was abandoned and protein eluates from the Ni-NTA column were used for the characterisation experiments. An alternative avenue to investigate in the future is the use of tandem affinity purification to achieve higher purity of the rHH protein. This can be achieved by introducing a second affinity tag such as the glutathione-S-transferase (GST) tag in addition to the 10X Histidine tag. This tag can be introduced via PCR either on the *Hsc70* or *HSJ1b* gene sequence, and will permit a simple two-step purification strategy.

In this chapter the successful purification of a recombinant form of the human chaperone/co- chaperone complex using a T7 expression system has been described. To date there have been no reports of the full length Hsp70/Hsp40 complex being produced by recombinant methods. This is also the first report of the use of a co-expression system to express and purify the complex (represented by the Hsc70/HSJ1b complex) using *E. coli* as the expression host. The success of this strategy provides an attractive method to isolate and study various other chaperone/co-chaperone complexes from different systems and organisms. The complex isolated in the above described manner has been characterised with regards to its substrate protection capabilities and polymerisation. The results from the characterisation are discussed in the next chapter.

Chapter 4

Characterisation of the recombinant Hsc70/HSJ1b complex

CHAPTER 4: Characterisation of the recombinant Hsc70/HSJ1b complex

4.1. Introduction

Hsp70's interaction with its Hsp40 co-chaperone and the subsequent stimulation of Hsp70's functional activities have been the subject of extensive studies. These studies have looked to facilitate understanding of the biochemical, structural and mechanistic features of the folding reaction. The chaperone cycle of Hsp70 is an ATP-hydrolysis driven, substrate folding reaction. The cycle in its simplest form alternates between two states: the low substrate affinity, ATP-bound state of Hsp70, when the substrate binding pocket is open and the high affinity, ADP-bound state when the binding pocket is closed, thereby resulting in cyclic peptide binding and release (Palleros *et al*., 1994; Bukau and Horwich, 1998). Hsp70 on its own is known to have low intrinsic ATPase activity (Russell *et al.*, 1999). However in the presence of its Hsp40 co-chaperone partner, the rate of ATP turnover has been shown to increase by several fold (McCarty *et al*., 1995). Stimulation of ATP hydrolysis by Hsp40's promotes substrate binding to Hsp70 and formation of a stable ternary complex (Laufen *et al*., 1999).

Minami *et al*., 1996; Chamberlain *et al*., 1997 and other groups have studied and characterised the chaperone/co-chaperone complexes by combining the two individual components of the complex at specific molar ratios. From their studies it has been established that neither the Hsp70 nor the Hsp40 protein alone was sufficient in preventing substrate denaturation; the combined action of a reconstituted Hsp70-Hsp40 complex in the presence of ATP was required (Minami *et al*., 1996). We have adopted similar protocols and used them to characterise the recombinant Hsc70/HSJ1b complex, the isolation of which was described in detail in Chapter 3. This chapter describes the biochemical characterisation of the complex and its interpretation with a preliminary structural analysis.

4.2. Materials and Methods

4.2.1. Thermal aggregation assay

The assay followed the protocol reported by Minami *et al* (1996) using luciferase as the model substrate protein (Minami *et al*., 1996). 15 µl reactions containing 0.8 µM of luciferase (Promega) and 1.27 µM of the recombinant rHH protein (calculated using molecular weight 110 kDa) were made up in assay buffer (20 mM Tris-HCl pH 8.0, 50 mM potassium chloride, 3 mM magnesium chloride and 2 mM DTT). The reaction was incubated for 5 minutes at room temperature and then transferred to a water bath set at 42^{o}C for 10 minutes. The reactions were centrifuged at 13,000 rpm for 10 minutes at 4^{o}C. The pellet and supernatant fractions were separated and dissolved in 4X SDS-PAGE buffer. The samples were boiled for 5 minutes and resolved on a 12% SDS-PAGE gel. The methodology for the running and Coomassie Blue staining of SDS-PAGE gel has been described earlier in chapter 2. Luciferase present in the soluble and pellet fraction was quantified by densitometry and plotted as a percentage of the total amount of luciferase in the reaction. For reactions containing nucleotides (ATP, ADP, AMP or AMP-PNP), a final concentration of 2 mM was used in the assay.

4.2.2. Refolding of thermally denatured luciferase

Thermal aggregation of luciferase was carried out as described in Section 4.2.1. Luciferase (0.8 µM) was thermally denatured at 42°C for 10 minutes, in the presence or absence of the chaperone complex and 2 mM ATP. Refolding was initiated by shifting the reactions to 25°C to allow refolding. Reactivation was monitored over a two hour period. At specific time intervals, 1 µl was withdrawn from the reactions, 50 µl of luciferase assay buffer (Promega) was added and luciferase activity was measured using a luminometer.

4.2.3. UV absorption spectroscopy

Absorption measurements of purified rHH complex were obtained with a Perkin Elmer spectrophotometer using a 1 cm path-length quartz cuvette. The spectrum was measured between 200-400 nm with a 15 second delay.

4.2.4. HPLC analysis of nucleotide content

Nucleotides were extracted by treating the protein samples with 0.6 M perchloric acid and then centrifuged at 10,000 rpm for 10 minutes in a microfuge. The supernatant was collected and neutralised with potassium hydroxide (KOH) and clarified by another centrifugation. Nucleotides were analysed by reverse-phase HPLC with a C18 column run at a flow rate of 1 ml/min for a total elution time of 15 minutes and samples detected at 254 nm. Samples were loaded onto the column with a 100 µ1 sample loop. The elution system was 50 mM potassium phosphate (pH 7.0). Each nucleotide was identified by its retention time compared to nucleotide standards.

4.2.5. ATPase assay

Phosphate release measurement for the rHH complex was performed using a colourimetric assay (Chamberlain and Burgoyne, 1997a; Chamberlain and Burgoyne, 1997b). 50 µl reactions containing 1.27 µM of rHH complex was incubated for 5 minutes at 37^{o}C in 20 mM Tris-HCl pH 8.0, 50 mM potassium chloride, 3 mM magnesium chloride and 2 mM DTT. The reaction was initiated by the addition of 2 mM ATP and the reactions were incubated at 37^{o}C for 1 hour. To study the effect of denatured substrate on the ATP hydrolysis, a thermal denaturation assay was carried out as described in section 4.2.1 and then incubated at 37^{o}C for 1 hour. The reaction was stopped by the addition of 50 µl of 10% (w/v) SDS. For the colour development, 50 µl of 1.25% (w/v) ammonium molybdate prepared in 6.5% (v/v) sulphuric acid was added followed by the addition of 50 µl of 9% (w/v) ascorbic acid. The reaction mix was further incubated for 1 hour at 37^{o}C and readings were measured at 620 nm. A standard curve was set up using potassium phosphate and used to calculate the phosphate release attributed to Hsc70's ATP hydrolysis activity.

4.2.6. Limited proteolysis with trypsin and chymotrypsin

Limited proteolytic studies were carried out using both trypsin and chymotrypsin. 5 mg/ml stock solutions of the protease was prepared in buffer containing 10 mM Tris-HCl pH 8.0 and 5% (v/v) glycerol and stored at -20^{o}C. The digestion was performed at a protease to protein ratio of 1:300. The protease was diluted to the required concentration in 20 mM Tris-HCl pH 8.0, 50 mM potassium chloride, 3 mM magnesium chloride and 2 mM DTT just before setting up the reaction. Digestion was

started by the addition of protease (trypsin or chymotrypsin) to the reaction mix. At specific time intervals, 15 µl aliquots were withdrawn from the reaction mix and the proteolysis was stopped by the addition of 0.5 µl of 10 mg/ml Trypsin inhibitor prepared in 10 mM Tris-HCl pH 8.0. 5 µl of 4X SDS-PAGE loading dye was added and the sample was incubated at 95^{o}C for 2 minutes and stored on ice until all reactions were completed. The proteins were resolved on a 12% SDS-PAGE gel. The methodology for the running and Coomassie Blue staining of SDS-PAGE gel has been described earlier in chapter 2. The different digest fragments were quantified by densitometry.

4.2.7. Size exclusion chromatography

Size exclusion chromatography was performed with a 90 ml Superdex-200 column. The column was equilibrated with 20 mM Tris-HCl pH 8.0 plus 100 mM potassium chloride. 1 ml fractions were collected after 25 ml of buffer had passed. The fractions were analysed for protein content using Bradford assay (refer section 2.10.6). The peak fractions were analysed by SDS-PAGE electrophoresis.

For analysis of the effects of ATP, rHH was incubated for 30 minutes with 2 mM ATP at room temperature in buffer consisting of 20 mM Tris-HCl pH 8.0, 100 mM potassium chloride, 3 mM magnesium chloride and 2 mM DTT. The chromatography was also performed in the same buffer.

For analysis of the effects of denatured luciferase, a thermal aggregation assay was set up as described in section 4.2.1 using 75 µg of rHH protein with 50 µg of luciferase. The supernatant recovered after centrifugation at 13,000 rpm for 10 minutes was loaded onto the gel filtration column. The chromatography was performed in the assay buffer (20 mM Tris-HCl pH 8.0, 50 mM potassium chloride, 3 mM magnesium chloride and 2 mM DTT).

4.2.8. Electron microscopy

Protein samples were prepared for electron microscopy by dialysing the Ni-NTA elution fractions against 20 mM Tris-HCl pH 8.0, 50 mM potassium chloride overnight at 4^{o}C and then concentrating it to 0.8 mg/ml using a YM-100 centricon (Millipore).

The protein complex was negatively stained with freshly made 2% (w/v) uranyl acetate on thin carbon-coated grids previously glow-discharged for 15 seconds.

4.2.9. Analytical ultracentrifugation (AUC)

For the AUC analysis, the Ni-NTA elution fractions were dialysed against 20 mM Tris-HCl pH 8.0, 50 mM potassium chloride overnight at 4^{o}C and concentrated to 0.8 mg/ml using a YM-100 centricon (Millipore). Experiments were performed on a Beckman-Coulter XL-A analytical ultracentrifuge using absorbance optics. The samples were loaded into 2 channel cells, and buffer was used as a blank for optical purposes. Buffer densities and viscosities were calculated using SEDNTERP. The data were processed using SEDFIT (www.analyticalultracentrifugation.com) using the c(S) method (Schuck, 2000). For molecular weight determination, data was processed using ULTRASCAN (Demeler, 2005) using the genetic algorithm implemented in the software and the analysis was performed using the supercomputing facility accessed through the LIMS software interface.

4.2.10. Protein crystallisation

Purified protein was concentrated using centricon YM-100 centrifugal Filter Devices (Millipore). The final protein concentration was determined via the Bradford protein assay. Protein at a concentration of 4 mg/ml was used for initial screening. Crystallization trials were set up at room temperature using the hanging-drop vapour-diffusion method. Preliminary trials were carried out with Crystal Screen and Crystal Screen 2 from Hampton Research (Jancarik & Kim, 1991; Cudney *et al.*, 1994).

4.3. Results

One of the fundamental properties defining a functional chaperone unit is its ability to bind unfolded protein. In this study we have evaluated the *in vitro* activity of the rHH chaperone complex in preventing aggregation of a model substrate (luciferase) and in addition studied the effect of the denatured substrate on the ATPase activity. Studies were also carried out to understand the conformational and oligomeric properties of the rHH complex. Preliminary structural studies were carried out using both X-ray crystallography and electron microscopy.

4.3.1. Protection of denatured substrate

Studies have shown that Hsp70s can bind chemically and thermally denatured protein substrates such as citrate synthase (CS), firefly luciferase, rhodanese, β-galactosidase and permanently unfolded carboxymethylated α-lactalbumin (CMLA) (Zhang and Guy, 2006). In our studies, the ability of the recombinant complex in preventing substrate aggregation was studied using luciferase as a substrate. Aggregation of luciferase was induced by elevating the temperature to 42^{o}C in the presence and absence of the co-expressed rHH chaperone complex and in the presence and absence of ATP to understand the effect of the nucleotide on the chaperone function. After 10 minutes the reactions were centrifuged to separate the soluble and aggregated fractions and then analysed by SDS-PAGE (Figure 4.1). In the control reactions, luciferase was subject to thermal denaturation in the absence of the chaperone complex (Panel A, Figure 4.1) where the majority of the luciferase in the control reactions was in the pellet fraction (Lane 2, Panel A, Figure 4.1). In the presence of the chaperones, by visual inspection of the gel, it was apparent that the majority of the ~61 kDa luciferase was present in the supernatant fraction (lanes 2 and 4, Panel B, Figure 4.1). The amount of luciferase in the soluble and pellet fraction from the SDS polyacrylamide gel was quantified by densitometry and plotted as percentage of total luciferase present in the reaction (Figure 4.2).

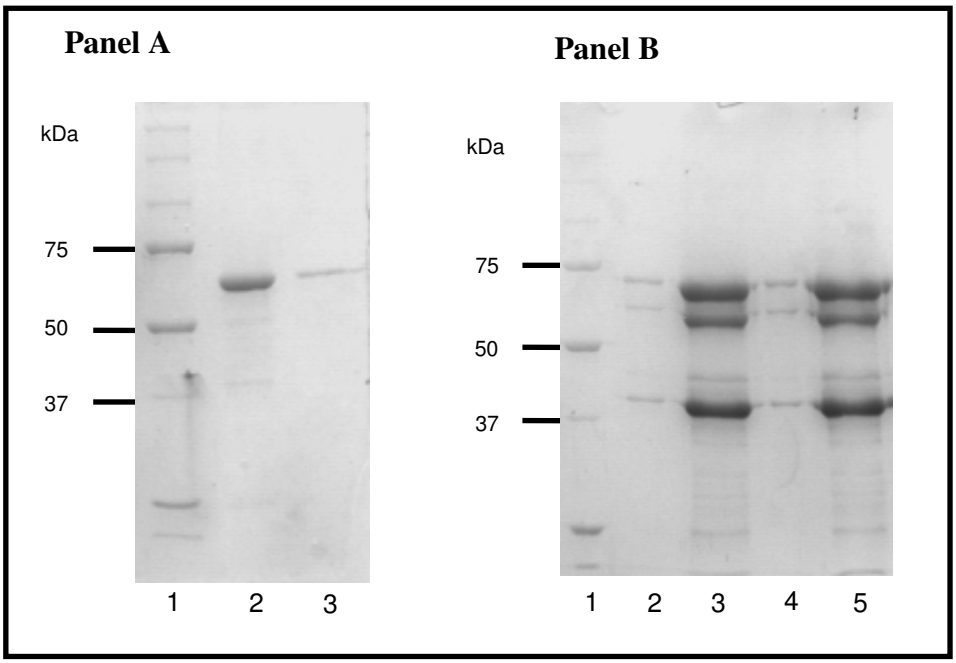

Figure 4.1: SDS-PAGE analysis of luciferase aggregation with rHH chaperone complex

0.8 µM of luciferase was thermally denatured at 42^{o}C for 10 minutes in the presence/absence of the 1.27 µm chaperones. For the reactions containing ATP, the nucleotide was added at a concentration of 2 mM. The reaction was centrifuged at 13,000 rpm to separate the soluble and aggregated fractions and analysed by SDS-PAGE.

Panel A) Control aggregation assay performed in the absence of the chaperone proteins. Lane 1 Bio-Rad broad range protein markers, lane 2 and lane 3 pellet and supernatant fractions for reactions carried out in the absence of rHH complex.

Panel B) Aggregation assay performed in the presence of the rHH complex. Lane 1 Bio-Rad broad range protein markers, lane 2 and lane 3 pellet and supernatant fractions for reactions carried out in the presence of the rHH complex, lane 4 and lane 5 pellet and supernatant fractions for reactions carried out in the presence of the rHH complex and ATP.

In the absence of the chaperone system, 81.4% of luciferase aggregated during a 10 minute incubation at 42°C (Figure 4.2, column 3). However, when the recombinant Hsc70/HSJ1b complex was present during thermal inactivation, 82.4% of the total luciferase protein remained soluble (Figure 4.2, column 1). Significantly this chaperone effect was ATP independent since addition of ATP improved the solubility of luciferase by only 5% (Figure 4.2, column 2). The rHH protein used in the assay was used directly after elution from the Ni-NTA column and contained 200 mM imidazole. In order to confirm that the imidazole did not play any role in the observed ATP independent luciferase protection, the assay was repeated with dialysed protein. However this did not affect the results of the assay (data not shown).

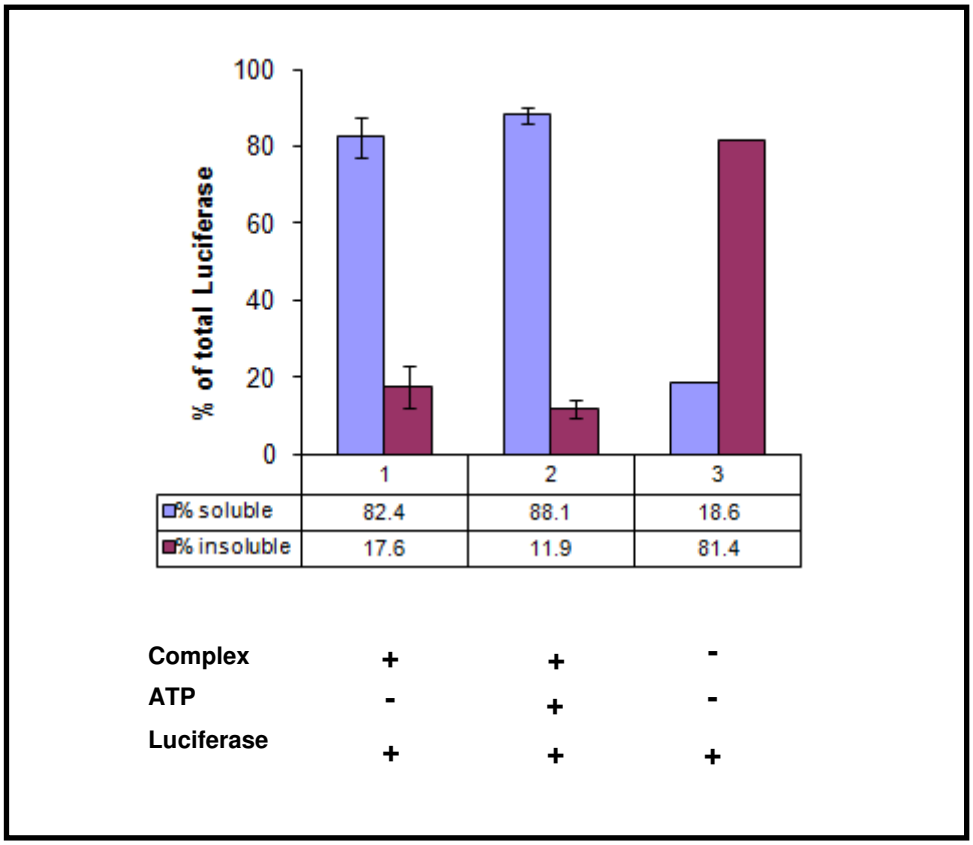

Figure 4.2: Prevention of luciferase aggregation by the rHH complex.

0.8 µM of luciferase was thermally denatured at 42°C for 10 minutes in the presence/absence of the 1.27 µM chaperones. For the reactions containing ATP, the nucleotide was added at a concentration of 2 mM. The reaction was centrifuged at 13,000 rpm to separate the soluble and aggregated fractions and analysed by SDS-PAGE. The amount of luciferase present in each fraction was quantified by densitometry and the percentage of soluble and aggregated luciferase for each reaction was calculated and plotted using MS Excel. Data for the luciferase reactions performed in the presence of rHH protein (+/- ATP) are expressed as mean values +/-S.E. (n = 4)

The nucleotide independent nature of the protection was confirmed when the assay was performed in the presence of different nucleotides such as ADP, AMP and AMP-PNP (Figure 4.3). In all cases the rHH protein showed consistent levels of luciferase protection. In the assay performed without any nucleotide the levels of soluble luciferase was observed to be 85.7% which was comparable to the percentage of luciferase protected in the presence of nucleotides. Thus, the percentage of luciferase protected by the rHH complex at 42°C appeared to be nucleotide independent.

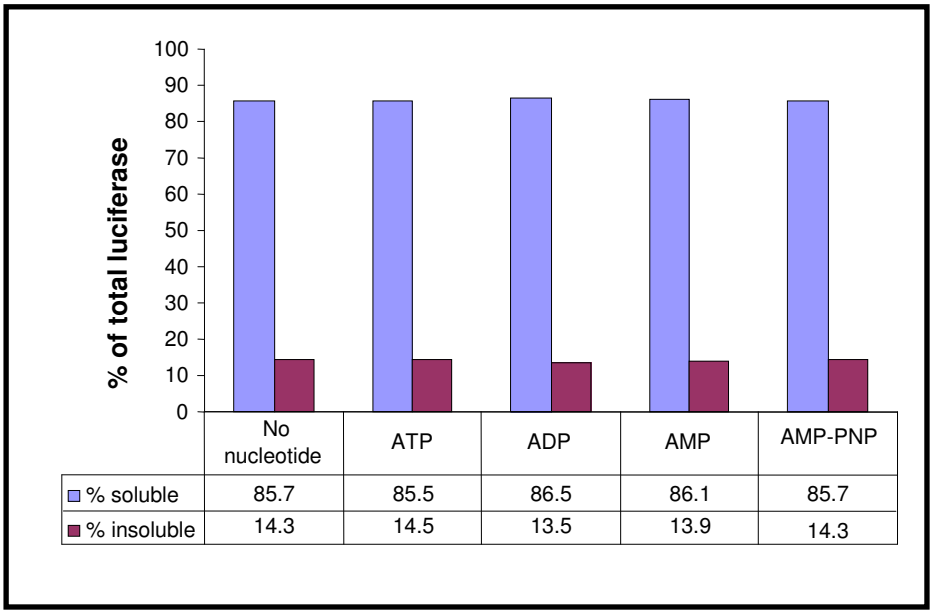

Figure 4.3: Effect of nucleotides on the solubility of thermally denatured luciferase

0.8 µM of luciferase was thermally denatured at 42°C for 10 minutes in the presence of the 1.27 µM chaperones. The different nucleotides (ATP, ADP, AMP, AMP-PNP) were added at a concentration of 2 mM. The reactions were centrifuged at 13,000 rpm to separate the soluble and aggregated fractions and analysed by SDS-PAGE. The amount of luciferase present in each fraction was quantified by densitometry and the percentage of soluble and aggregated luciferase for each reaction was calculated and plotted on MS Excel.

Using the thermal aggregation assay we also studied the response of the rHH complex to increasing concentration of denatured substrate (Figure 4.4). Thermal denaturation assays were performed as described previously, only the amount of luciferase used in the assay was varied. The assay was carried out at constant chaperone concentration (1.27 µM, calculated using MW of rHH as 110 kDa) with increasing concentrations of luciferase (0.3-1.27 µM). It was observed that the recombinant complex could maintain luciferase in a soluble state up to a ratio of 1:1 (protein: luciferase) concentration, beyond which the efficiency of protection reduced by almost 60%. As with the previous studies, addition of ATP did not alter the capacity of the chaperone complex to bind denatured substrate.

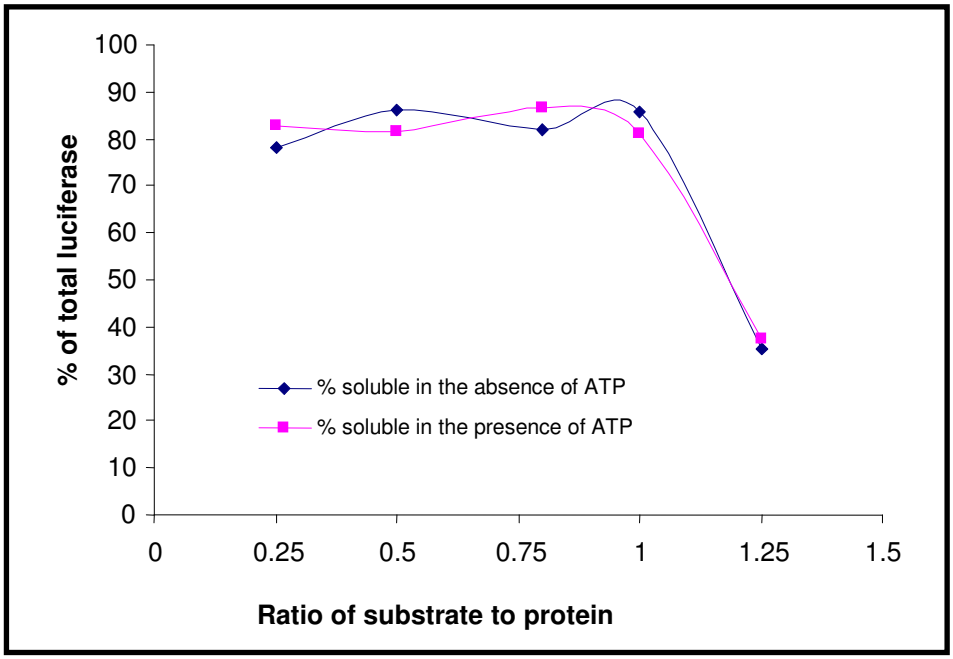

Figure 4.4: Efficiency of luciferase protection offered by the rHH complex.

The assay was carried out with varying amounts of luciferase as described in the previous section. Briefly, 0.3, 0.6, 0.8, 1 and 1.27 µM of luciferase was thermally denatured at 42°C for 10 minutes in the presence of the 1.27 µM chaperones. For the reactions containing ATP, the nucleotide was added at a concentration of 2 mM. The reaction was centrifuged at 13,000 rpm to separate the soluble and aggregated fractions and analysed by SDS-PAGE. The amount of luciferase present in the two fractions was quantified by densitometry and represented as percentage of combined luciferase in soluble and aggregated fractions for each reaction and plotted using MS Excel.

A divalent cation in the form of magnesium is routinely used in the aggregation assay. However Hsc70 has been shown to be capable of binding to both calcium and magnesium metal ions (Flaherty *et al*., 1994, Sriram *et al*., 1997). We therefore studied the effect of replacing the Mg^{2+}, normally used in the assay, with equal amounts of Ca^{2+}. Replacement of Mg^{2+} with Ca^{2+} at a concentration of 3 mM had a negligible effect on the percentage of luciferase protection (reduced by 6%). At the same time we also performed the assay with Ni^{2+} to assess if any other cation (not just Ca^{2+}) could take up the role of Mg^{2+} in the reaction (Figure 4.5). However, substitution of Mg^{2+} with Ni^{2+} completely abolished the chaperone protein's ability to bind to denatured substrate. This clearly emphasised that divalent cations in the form of Mg^{2+} or Ca^{2+} are crucial for mediating the interaction of chaperone complex and the denatured substrate.

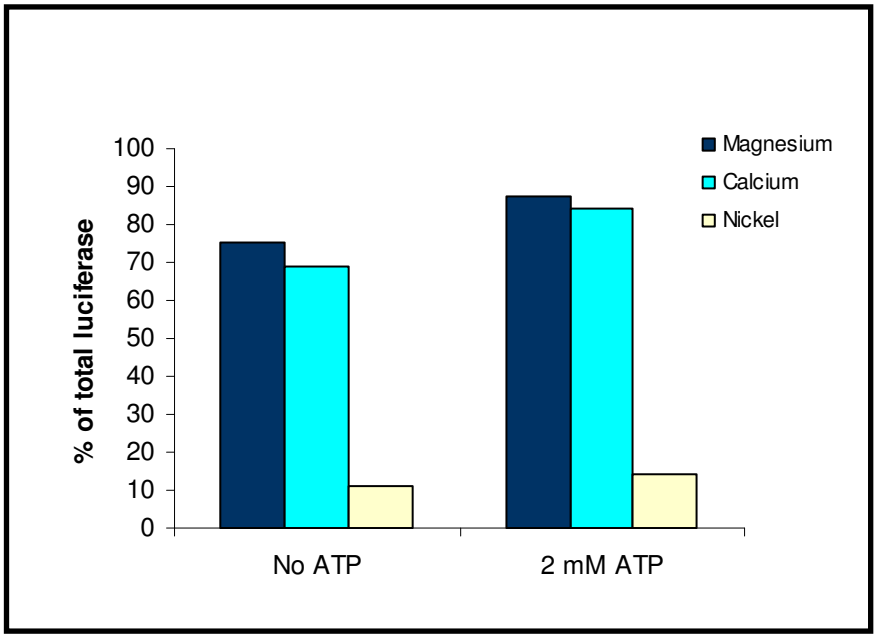

Figure 4.5: Divalent cation requirement of the rHH complex.

0.8 µM of luciferase was thermally denatured at 42°C for 10 minutes in the presence of the 1.27 µM chaperones, and presence/absence of 2 mM ATP in assay buffer (20 mM Tris-HCl pH 8.0, 50 mM potassium chloride, 3 mM magnesium chloride and 2 mM DTT). The divalent cation requirement of the complex for efficient substrate protection was established by performing the assay in the presence of 3 mM Ca^{2+} or Ni^{2+}. The reaction was centrifuged at 13,000 rpm to separate the soluble and aggregated fractions and analysed by SDS-PAGE. The amount of luciferase present in each fraction was quantified by densitometry and the percentage of soluble and aggregated luciferase for each reaction was calculated and plotted using MS Excel.

4.3.1.1. Protection of functional activity of thermally denatured luciferase

While the rHH complex could prevent aggregation in 82-88% of luciferase subjected to thermal denaturation assay, it was also necessary to assess if the rHH complex could maintain the protected luciferase in a functionally competent state. Functional activity of the soluble luciferase was quantified by measuring the luminescence readings for the reaction of luciferase with its substrate luciferin. Oxidation of luciferin by luciferase results in the production of light and so luminescence readings for the non-aggregated luciferase after thermal denaturation was measured (Figure 4.6). From the assay it was observed that the luminescence readings for the luciferase subjected to thermal aggregation in the presence of chaperone proteins, but absence of ATP, was three fold less than in the presence of ATP. However this value was less than 1% of activity measured for native luciferase which was not subjected to stress at 42°C (data not shown). Therefore it was concluded that the luciferase, although protected from thermal aggregation by the rHH complex, was not functionally active.

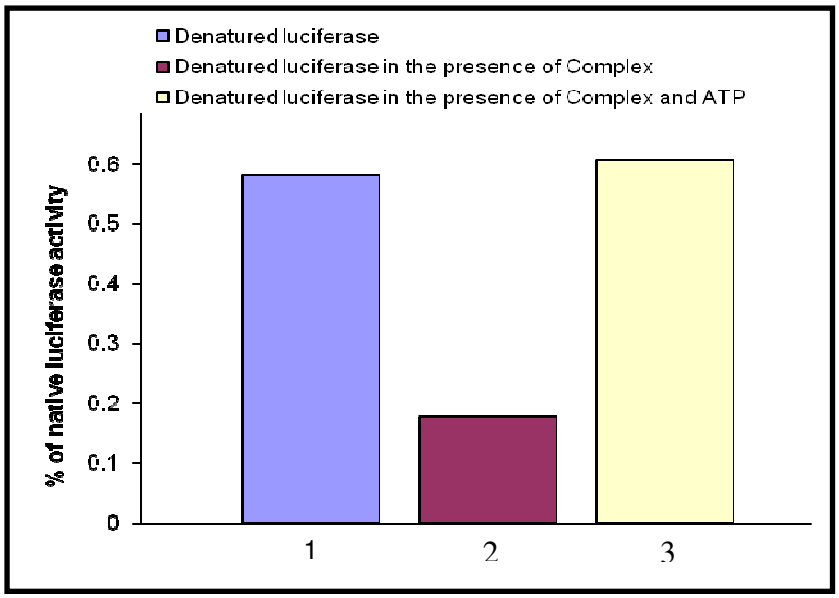

Figure 4.6: Functional activity of the soluble luciferase

0.8 µM of luciferase was thermally denatured at 42°C for 10 minutes in the presence of the 1.27 µM chaperones, and presence/absence of 2 mM ATP in assay buffer (20 mM Tris-HCl pH 8.0, 50 mM potassium chloride, 3 mM magnesium chloride and 2 mM DTT). The reaction was centrifuged at 13,000 rpm to separate the soluble and aggregated fractions. To the soluble fraction, 50 µl of luciferase assay buffer (Promega) was added. Luminescence readings were measured for using a luminometer and plotted as percentage of native luciferase activity. Reaction 1 contained luciferase on its own. Reaction 2 contained luciferase in the presence of the rHH complex and Reaction 3 contained luciferase in the presence of the rHH complex and ATP.

We next checked if reactivation of luciferase activity could be encouraged by a temperature downshift from 42°C to 25°C. Luminescence readings for denaturation reactions carried out in the presence/absence of chaperones and also in the presence/absence of ATP were measured every 20 minutes for up to 1 hour and 40 minutes (Figure 4.7). Although refolding reactions carried out for in the presence of chaperone proteins and ATP exhibited higher and continually increasing luminescence readings, the readings obtained were still < 2% of activity measured for native luciferase which was not subjected to stress at 42°C and therefore considered to be insignificant. Thus, although the rHH complex could hold denaturing luciferase in a soluble state, it was incapable of refolding it into its functional state.

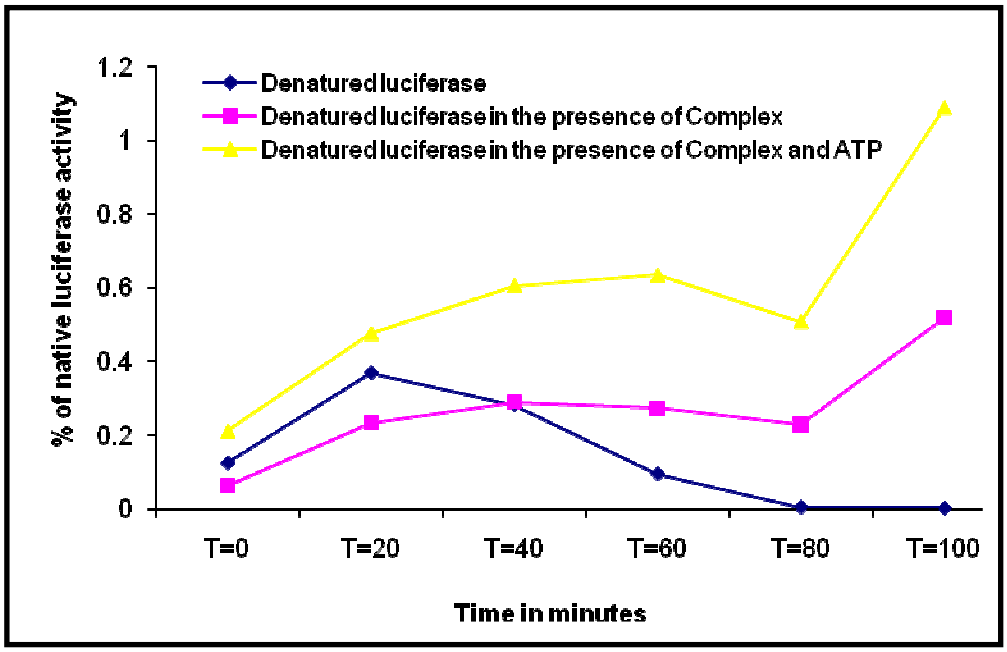

Figure 4.7: Refolding of thermally denatured luciferase by rHH complex.

Luciferase (0.8 µM) was thermally denatured at 42°C for 10 minutes in the presence or absence of the indicated concentrations of chaperones (1.27 µM) and then allowed to refold at 25°C. 2 µl was withdrawn from the reaction every twenty minutes and luciferase activity was measured after the addition of 50 µl of luciferase assay buffer (Promega). Activity was measured for various times using a luminometer and plotted as percentage of native luciferase activity.

4.3.1.2. ATP hydrolysis assay

Hsc70 displays low intrinsic ATPase activity which is stimulated by binding to denatured substrate (Flynn *et al*., 1989). The phosphate released upon the addition of 2 mM ATP was measured using a colorimetric assay. Under normal assay conditions at 37^{o}C, 50 nmol/mg/min of phosphate was released (column 1, Figure 4.8). The stimulation of ATPase activity of rHH complex by denatured luciferase was studied by measuring the phosphate released from the system after thermal aggregation (columns 2 and 3, Figure 4.8). The ATPase activity measured for the rHH protein was very similar irrespective of the absence (22.5 nmol/mg/min, column 2) or presence of unfolded substrate (25.4 nmol/mg /min, column 3). It was found that the rHH complex exhibited far greater phosphate release under non-denaturing conditions (37^{o}C) than denaturing condition (42^{o}C). At 42^{o}C phosphate release is reduced by almost 50%, possibly due to protein aggregation. At 42 ^{o}C, a combination of HSJ1b and luciferase did not produce any significant increase in Hsc70 ATP hydrolysing activity above that for HSJ1b alone at 42^{o}C. ATP hydrolysis is necessary to stabilise the ternary complex formed between the Hsc70 and unfolded substrate. However in the case of the rHH, Hsc70 has probably pre-attained this stable conformation due to its interaction with HSJ1b.

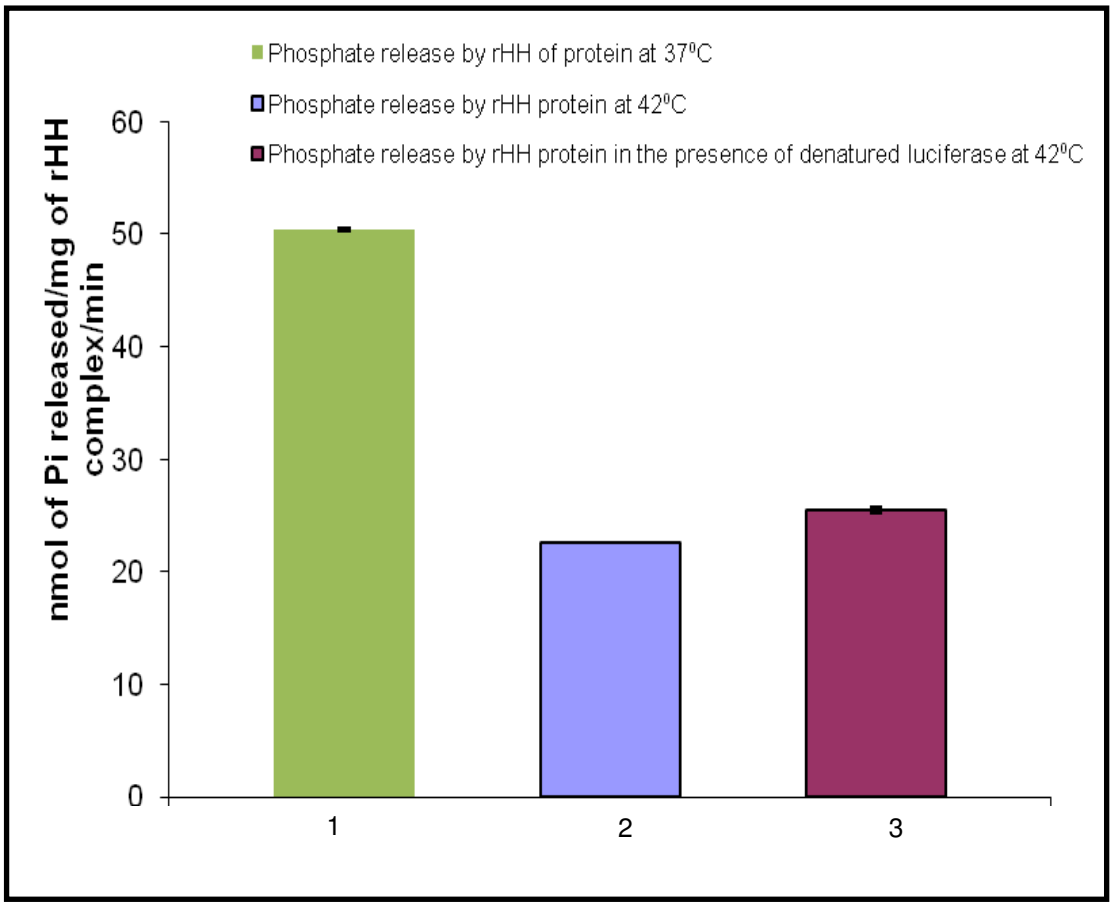

Figure 4.8: Effect of denatured luciferase on the ATPase activity of Hsc70 of the rHH complex

rHH complex (1.27 µM) was incubated in ATPase assay buffer with and without luciferase (0.8 µM) at 42°C, and release of free phosphate was measured by a spectrophotometric method (OD620). The levels of phosphate released for each condition were converted into nanomoles of free phosphate liberated by comparison with a KH_2PO_4 standard. Data are expressed as means +/-S.E. (n = 3)

4.3.2. Detection of bound nucleotide

The recombinant Hsc70/HSJ1b complex did not appear to require nucleotides for substrate protection activity (refer section 4.3.1). This was possible if the purified Hsc70/HSJ1b complex contained endogenously bound nucleotide. To determine this, a preliminary analysis was carried out by deriving the UV absorption spectrum of the purified complex between 230-400 nm (Figure 4.9). A pure protein is expected to have symmetric curve with a maximum at 280 nm. Also the absorbance at 320 nm is expected to be close to zero, since absorbance at 320nm is an indication of sample turbidity and protein aggregation (Aitken and Learmonth, 1998). In the case of the rHH protein, a symmetrical curve was not obtained and the absorbance at 260 nm and 280 nm were determined to be 0.176 and 0.119 respectively. However, the absorbance at 320 nm for the complex was observed to be only 0.03 (indicated by an arrow on Figure 4.9), indicating the absence of aggregation in the protein sample. The A260/A280 ratio for pure protein should be 0.5-0.7 (Held, 2008). The A260/A280 ratio for the rHH protein was calculated to be 1.4, suggesting the presence of additional A260 absorbing material such as ATP, other nucleotides, or nucleic acid such as DNA or RNA.

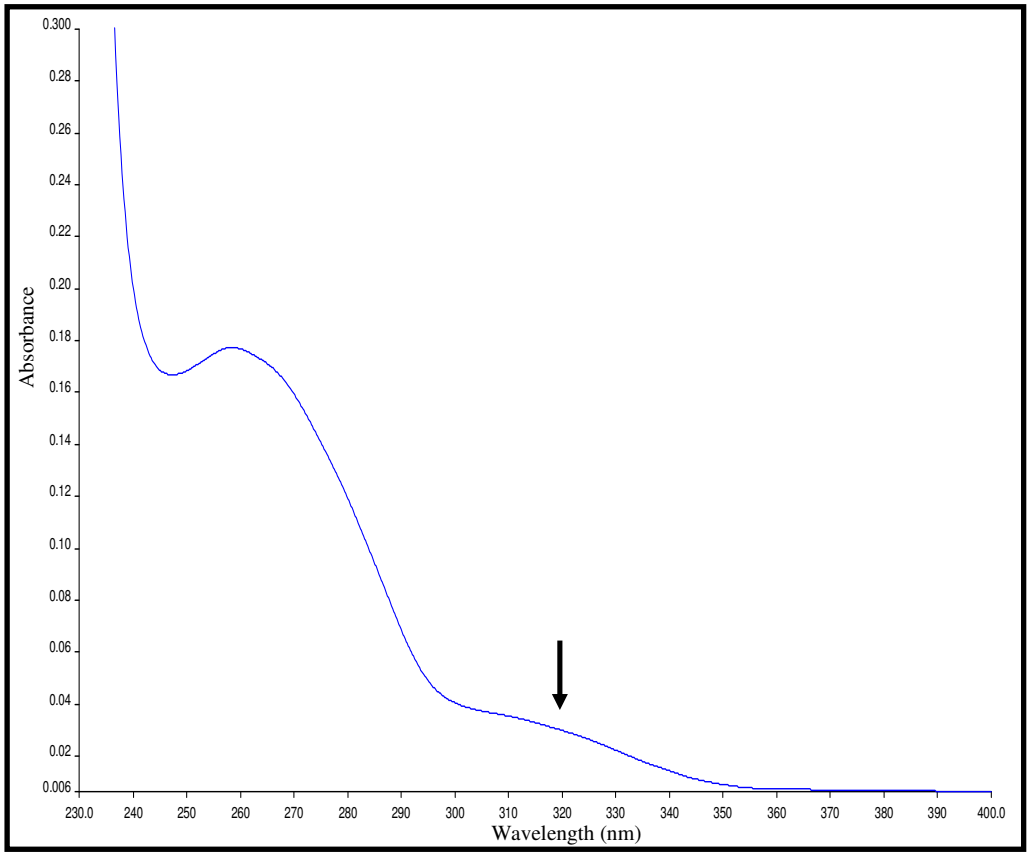

Figure 4.9: UV absorption spectroscopy of the rHH complex

Absorption measurements of purified rHH complex were obtained with a Perkin Elmer spectrophotometer using a 1 cm path-length quartz cuvette. The spectrum was measured between 200-400 nm with a 15 second delay. The UV spectrum of rHH protein) has a maximum at approximately 258 nm and the A260 /A280 ratio has a value of 1.4. The A320 position is indicated by a black arrow.

In order to confirm the identity of the co-purifying nucleotides with the purified rHH protein, extraction of any bound nucleotide was performed using perchloric acid and the samples were analysed on a C18 HPLC column (Figure 4.10). The elution profile of the extracted nucleotide (Panel C, figure 4.10) was compared with the elution peaks obtained for standard ADP (Panel A, Figure 4.10) and ATP (Panel B, Figure 4.10). Several low intensity elution peaks were observed at various retention times (indicated by an arrow in Panel C) and therefore the analysis was inconclusive. The peak observed between 1.5-3.0 ml in Panel C was attributed to the reagents used in the extraction protocol, and was observed in all samples subjected to perchloric acid based extraction.

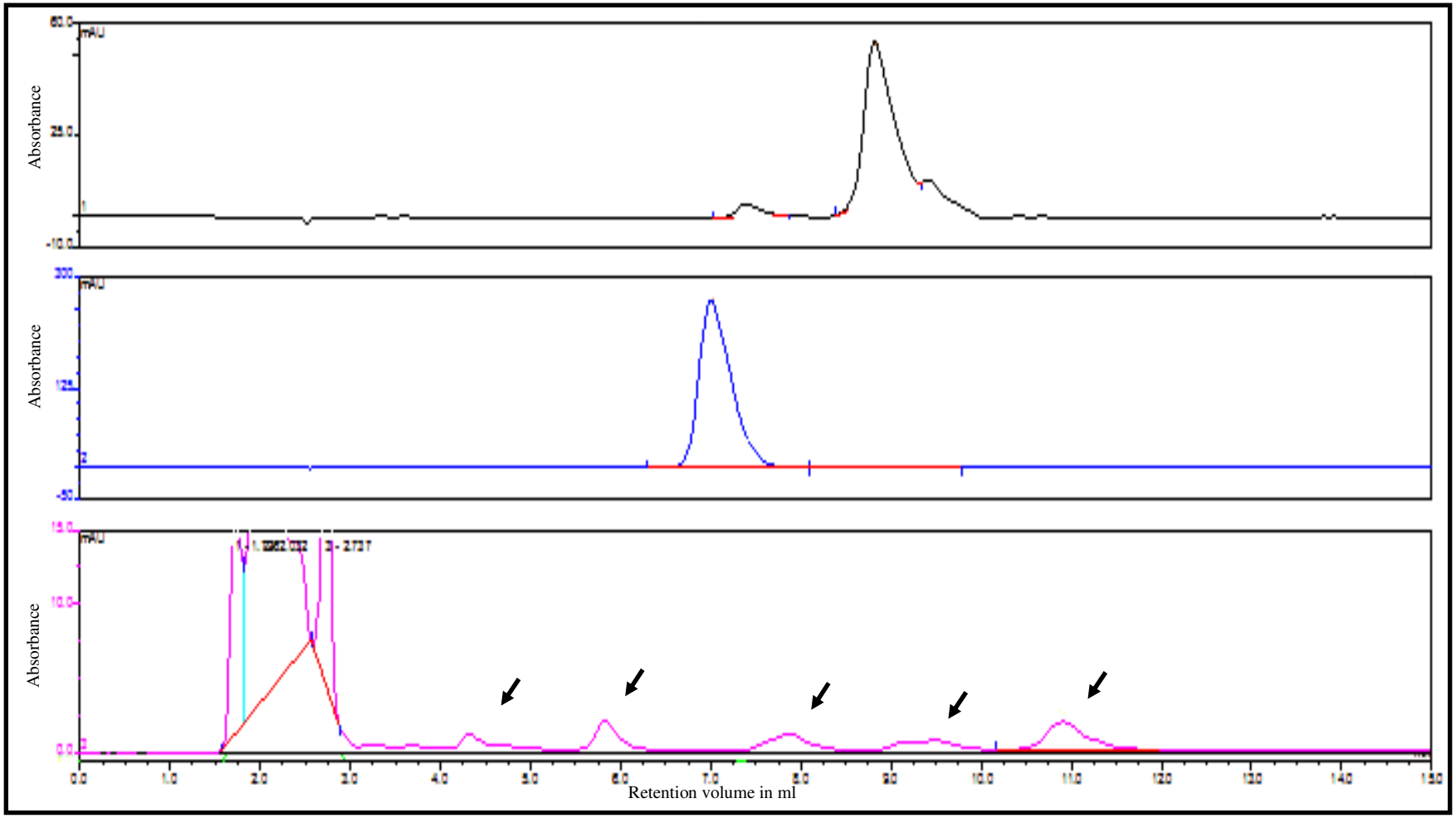

Figure 4.10: HPLC analysis of nucleotide content of the rHH complex

Nucleotides were extracted by treating the rHH protein sample with 0.6 M perchloric acid and then centrifuged at 10,000 rpm for 10 minutes in a microfuge. The supernatant was collected and neutralized with KOH and clarified by another centrifugation. Nucleotides were analysed by reverse-phase chromatography with a C18 column and detected at 254 nm. The column was run at a flow rate of 1 ml/minutes for a total elution time of 15 minutes. The elution system contained 50 mM potassium phosphate (pH 7.0). Panel A is ADP elution profile, Panel B is elution profile of ATP and Panel C is that of the nucleotide extracted from rHH protein complex. The position of the various elution peaks are indicated by arrows in Panel C.

4.3.3. Partial proteolysis studies

Limited proteolysis experiments using trypsin and chymotrypsin were undertaken to study the conformation flexibility in the arrangement of the Hsc70 and HSJ1b subunits in the rHH complex. The change in protease accessibility upon nucleotide binding was also investigated, and these results are presented in the following sections.

4.3.3.1. Determination of optimal temperature for proteolysis

The optimal temperature for the proteolysis of the rHH complex using chymotrypsin was determined by performing the assay at both 30°C and 4°C for 15 minutes using chymotrypsin. Electrophoresis of the digested and undigested fragments suggested that at 30°C the proteolysis occurred extremely quickly, resulting in total digestion of the 40 kDa HSJ1b species (lane 2, Figure 4.11, whereas at the lower temperature i.e. 4°C the proteolysis proceeds more slowly and immediate proteolysis of HSJ1b polypeptide does not occur (lane 3, Figure 4.11). A similar experiment was performed with trypsin also, and again proteolysis at 4°C was found to be a more suitable temperature to monitor the proteolysis (data not shown). Therefore all subsequent experiments were performed at 4 °C.

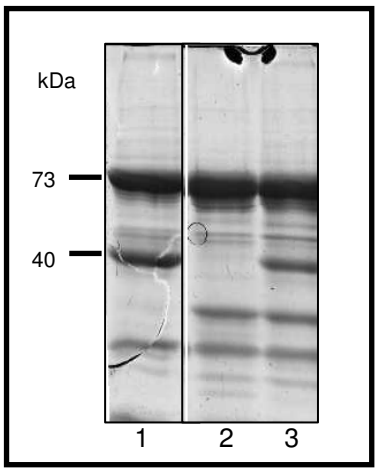

Figure 4.11: Determination of optimal temperature for the proteolysis of rHH complex

Limited proteolysis of the recombinant complex was carried out using chymotrypsin at 30°C and 4°C. 5 µg of the protein was incubated with 0.016 µg of chymotrypsin. The digestions were performed in buffer containing 20 mM Tris-HCl pH 8.0, 50 mM potassium chloride, 3 mM magnesium chloride and 2 mM DTT for 15 minutes and the products were analysed on a 12% polyacrylamide gel stained with Coomassie Blue. Lane 1 is the control protein in the absence of chymotrypsin, lane 2 is the proteolysis performed at 30°C and lane 3 is the reaction performed at 4°C.

4.3.3.2. Time course for chymotrypsin proteolysis

The Hsc70/HSJ1b complex was digested with chymotrypsin in the absence of nucleotides or in the presence of ATP at 4^{o}C. The reaction was stopped at various time points by the addition of protease inhibitor and the digestion products were visualised by SDS-PAGE (Figure 4.12). Lanes 4-8 represent the proteolysis pattern obtained in the absence of nucleotide and lanes 9-14 were the reactions carried out in the presence of ATP. The HSJ1b was more sensitive to proteolysis than Hsc70. Proteolysis of HSJ1b (40 kDa) and the subsequent appearance of a ~30 kDa proteolysis product (indicated by a red arrow, Lane 4) could be observed within 10 minutes of commencement of the proteolysis reaction. The majority of the full length HSJ1b protein was proteolysed within 60 minutes. Hsc70 protein showed limited signs of proteolysis and no major proteolysis product arising from this subunit could be detected. However two minor products observed at ~49 kDa and 52 kDa are indications of possible Hsc70 proteolysis.

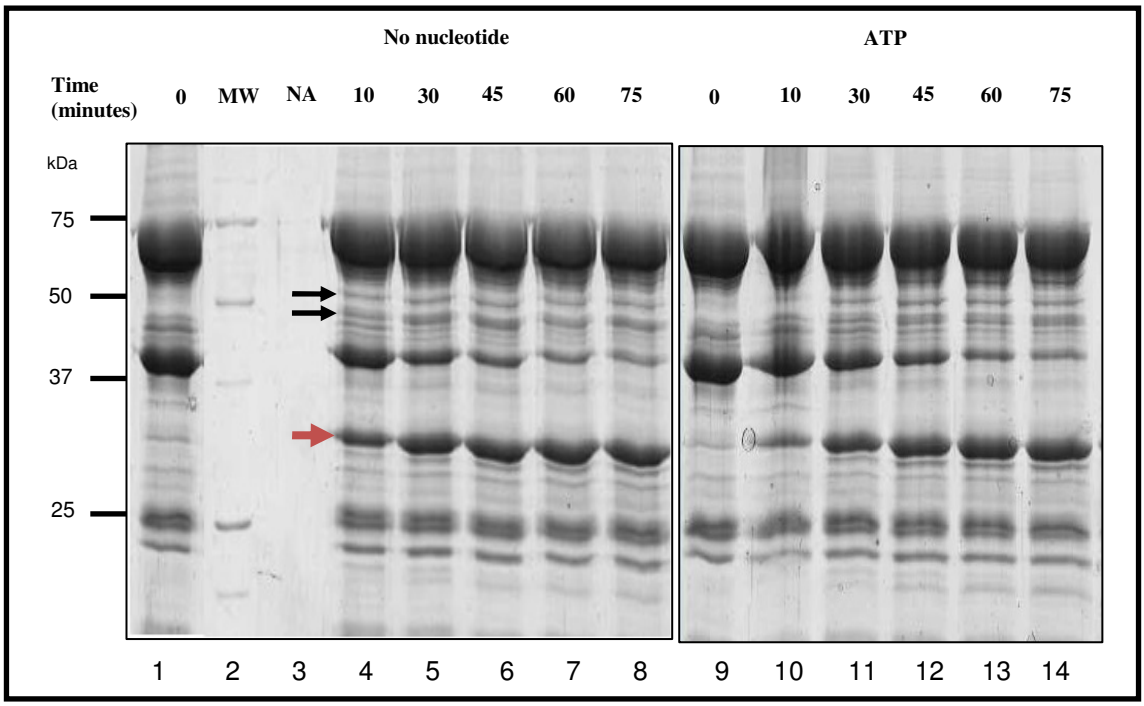

Figure 4.12: Time course for chymotrypsin proteolysis of the rHH complex.

Limited proteolysis of the recombinant complex was carried out using chymotrypsin at 4°C. Digestion was started by the addition of chymotrypsin to the reaction mix. 30 µg of the protein was incubated with 0.1 µg of chymotrypsin. At specific time intervals, 15 µl aliquots were withdrawn from the reaction mix and the proteolysis was stopped by the addition of 0.5 µl of 10 mg/ml trypsin inhibitor prepared in 10 mM Tris-HCl pH 8.0. 5 µl of 4X SDS-PAGE loading dye was added and the sample was incubated at 95°C for 2 minutes and stored on ice until all reactions were completed. The proteins were resolved on a 12% polyacrylamide gel stained with Coomassie Blue. Lanes 1 and 9 is the control protein in the absence of chymotrypsin, lane 2 is the Bio-Rad molecular weight markers, lanes 4-8 are the proteolysis products observed at t=10, 30, 45, 60 and 75 minutes respectively and lanes 10-14 are the proteolysis products formed in the presence of ATP at t=10, 30, 45, 60 and 75 minutes respectively. The red arrow indicates the position of the potential HSJ1b cleavage product, while the black arrow marks the position of possible Hsc70 cleavage products.

The rate of proteolysis of both the subunits was monitored and quantified using densitometry (Panel A and B in Figure 4.13). In the absence of ATP, 86.7% of Hsc70 remained undigested at the end of the 75 minutes. This was only 8% more than the undigested Hsc70 quantified in the reactions carried out in the presence of ATP (Panel A in Figure 4.13). Therefore the presence or absence of ATP in the proteolysis reaction does not appear to overtly alter the rate of Hsc70 proteolysis. Similarly, the presence/absence of nucleotides did not appear to alter the rate of HSJ1b proteolysis. Again an 8% increase in the digestion of HSJ1b was observed in the presence of ATP (Panel B, Figure 4.13). Thus, both the Hsc70 and HSJ1b components of the recombinant complex display only a very slight increase in sensitivity to proteolysis in the presence ATP, and almost 60% of HSJ1b is digested within 75 minutes.

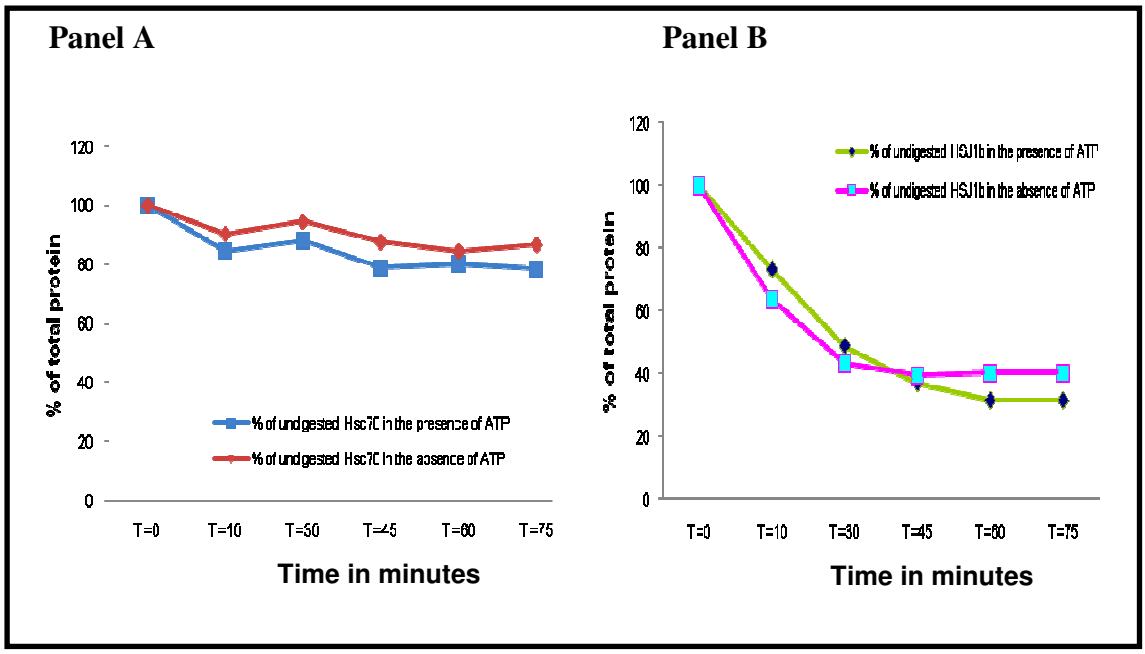

Figure 4.13: Densitometric analysis of undigested Hsc70 and HSJ1b

Limited proteolysis was performed as described in the previous section and the digestion products were analysed on a 12% polyacrylamide gel stained with Coomassie Blue. The gel used in this analysis has been presented in figure 4.12. From the gel, Hsc70 (Panel A) and HSJ1b (Panel B) were quantified by densitometry for the entire duration of proteolysis (75 minutes).

4.3.3.3. Time course for trypsin proteolysis

We next subjected the rHH protein to limited proteolysis by trypsin. Chymotrypsin and trypsin have different amino acid cleavage specificity, and therefore this could extend the scope of our proteolysis studies. Trypsin predominantly cleaves peptide chains at the carboxyl side of the amino acids lysine and arginine, while chymotrypsin targets the carboxyl side of tyrosine, tryptophan, and phenylalanine (amino acids containing an aromatic ring) (Stryer *et al*., 2002). Trypsin proteolysis was carried out following the same protocol used for chymotrysin. Panel A Figure 4.14 is the trypsin digest pattern obtained in the absence (Lanes 1-7, Panel A, Figure 4.14) and presence of ATP (Lanes 8-14, Panel A, Figure 4.14) respectively.

Two prominent features were noticed. Firstly, HSJ1b appears to undergo very rapid proteolysis. No evidence of the polypeptide is observed as early as 10 minutes into the reaction. This is consistent both in the presence and absence of ATP. A possible proteolysis product is observed at ~32-35 kDa (indicated by arrow on Figure 4.14) at t=10 minutes, which subsequently disappears. Also proteolysis of Hsc70 can be observed. The site of proteolysis appears to be at the extreme C or N-terminal region of the protein since the size of the resulting proteolysis product differs from the undigested product (73 kDa) by only 1 or 2 kDa (~70-71 kDa). An analysis of the protein sequence by the Generunner software established that the only potential cleavage site which can give rise to a 71 kDa product occurs in the Factor Xa site which follows the N-terminal His•Tag® sequence on the pET-16b expression vector. The resulting 71 kDa product could be therefore the native Hsc70 without the histidine tag. The percentage of undigested Hsc70 was calculated by densitometry. From Panel B in Figure 4.14 it can be observed that within 30 minutes more that 70% of the protein has undergone proteolysis to form the ~70-71 kDa product. The proteolysis proceeds in a similar fashion both in the presence and absence of ATP. No other proteolysis product formed by the subsequent proteolysis of 70 kDa fragment is apparent, suggesting that the rest of the protein is protected from trypsin proteolysis.

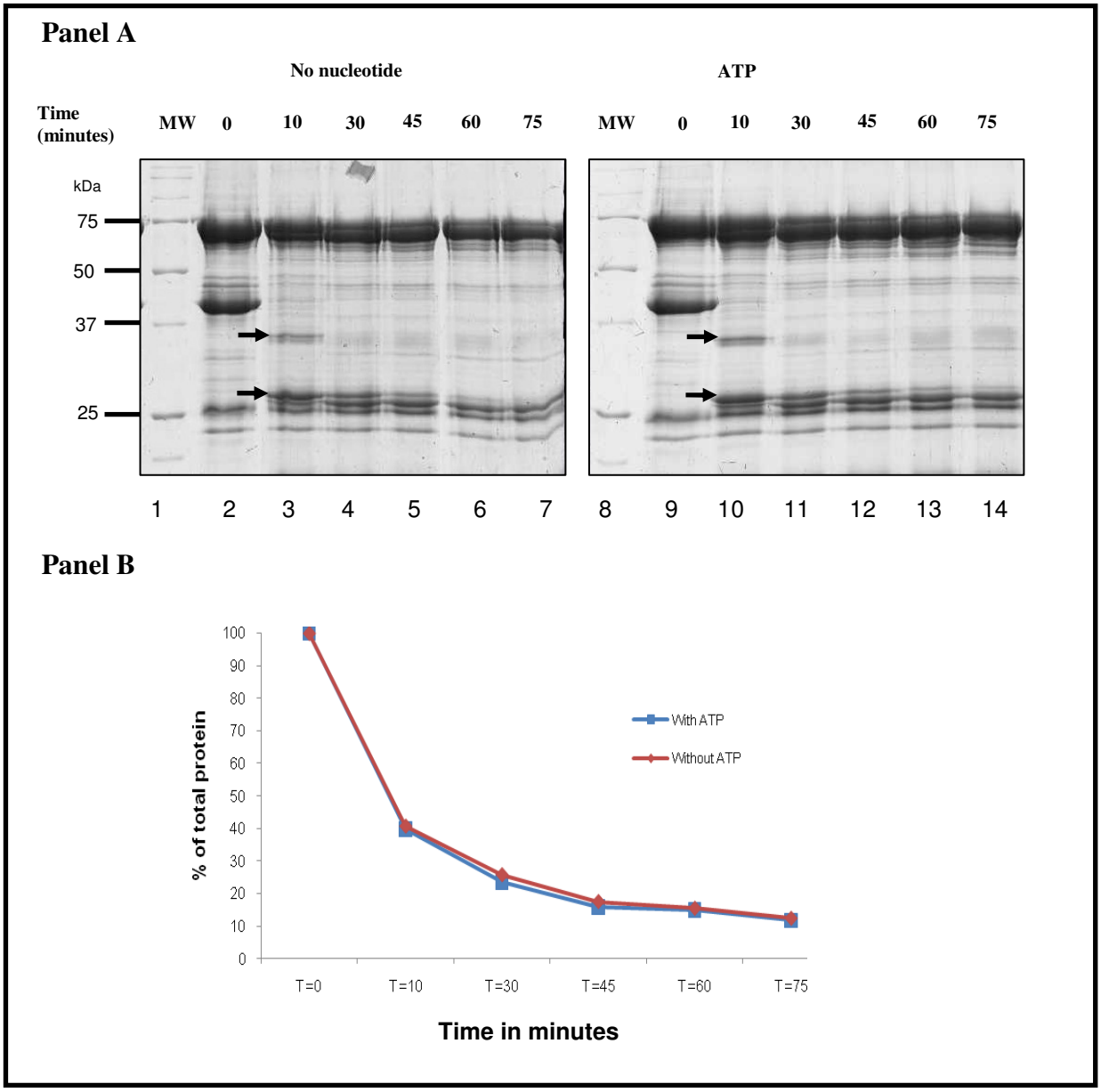

Figure 4.14: Time course for trypsin proteolysis for the rHH protein

Limited proteolysis of the recombinant complex was carried out using trypsin at 4°C. Digestion was started by the addition of trypsin to the reaction mix. 30 µg of the protein was incubated with 0.1 µg of trypsin. At specific time intervals, 15 µl aliquots were withdrawn from the reaction mix and the proteolysis was stopped by the addition of 0.5 µl of 10 mg/ml trypsin inhibitor prepared in 10 mM Tris-HCl pH 8.0. 5 µl of 4X SDS-PAGE loading dye was added and the sample was incubated at 95°C for 2 minutes and stored on ice until all reactions were completed. The proteins were resolved on a 12% polyacrylamide gel stained with Coomassie Blue.

Panel A) Lanes 1 and 9 is the control protein in the absence of trypsin, lane 2 Bio-Rad molecular weight markers, lanes 4-8 proteolysis products observed at t=10, 30, 45, 60 and 75 minutes respectively and lanes 10-14 proteolysis products formed in the presence of ATP at t=10, 30, 45, 60 and 75 minutes respectively. Putative HSJ1b proteolysis product observed at ~32-35 kDa is indicated by a black arrow

Panel B) Densitometric analysis of undigested Hsc70 after proteolysis by trypsin

4.3.3.4. Effect of nucleotides on the conformation of the complex

Hsp70 proteins have been shown to adopt three different conformations depending on the occupancy of the NBD (Buchberger, *et al*., 1995, Fung *et al*., 1996). To determine if Hsc70 complexed with HSJ1b also adopts different conformations, the tertiary structure was probed by partial digestion with chymotrypsin in the presence of various nucleotides and the fragments were separated by SDS-PAGE (Figure 4.15). The protein was digested with chymotrypsin for 10 minutes in the absence of nucleotides (lane 2, Figure 4.15) or in the presence of ATP (lane 3, Figure 4.15), ADP (lane 4, Figure 4.15) or AMP-PNP, a non hydrolysable analogue of ATP (lane 5, Figure 4.15). No significant difference could be observed in the proteolytic patterns of the protein in the presence of the different nucleotides.

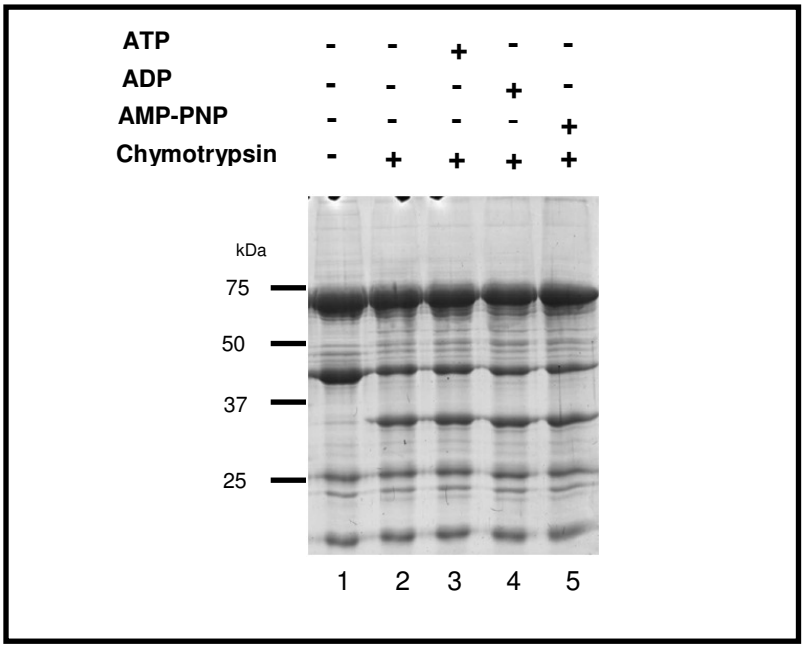

Figure 4.15: Effect of nucleotides on the proteolysis of the rHH protein by chymotrypsin

5 µg of the rHH protein was incubated with 0.016 µg with chymotrypsin at 4°C for 10 minutes. The digestions were performed in buffer containing 20 mM Tris-HCl pH 8.0, 50 mM potassium chloride, 3 mM magnesium chloride and 2 mM DTT for 15 minutes and the products were analysed on a 12% polyacrylamide gel stained with Coomassie Blue. Nucleotides were added at a concentration of 2 mM. Lane 1 is the control protein in the absence of chymotrypsin. Lane 2 is the proteolysis performed in the absence of nucleotide, lane 3 in the presence of ATP, lane 4 in the presence of ADP and lane 5 in the presence of AMP-PNP.

4.3.4. Oligomeric properties of the recombinant complex

4.3.4.1. Size exclusion chromatography

The oligomeric composition of the co-expressed Hsc70/HSJ1b protein was studied by size exclusion chromatography performed using a Superdex-200 gel filtration column calibrated using standard proteins. The standard curve obtained has been described in Section 2.10.4. The rHH Ni-NTA elution fractions were pooled and loaded onto the column. One ml fractions were collected and proteins were detected by measuring the protein concentration using Bradford assay (Bradford, 1976). The protein resolved into two elution peaks. The first peak was detected in the void volume, eluting between 30-44 ml with the peak fraction collected at 36 ml (represented as peak 1 on the chromatogram in panel A of Figure 4.16). The second peak in the included volume eluted between 46-60 ml. The peak fraction was obtained at 52 ml (represented as peak 2 on the chromatogram in panel A of Figure 4.16). The molecular weight of the protein species in peak 2 was calculated to be ~220 kDa from the calibration curve developed in Section 2.10.4. This is equivalent to a dimer of the rHH heterodimer (2 molecules of Hsc70 + 2 molecules of HSJ1b).

The fractions obtained from the Superdex-200 column were analysed by gel electrophoresis (Panel B, Figure 4.16). It was observed that both Hsc70 and HSJ1b subunits co-fractionate together in both elution peaks; however the stoichiometry of the two subunits varied for the two peaks. In peak 1 of SEC, the HSJ1b subunit appears to be the major species in the fraction, while in peak 2 of SEC, it is Hsc70. By visual inspection of the staining pattern on the gel, it appears that in peak 1 the ratio of Hsc70 and HSJ1b subunits seems to be 1:2 (Lanes 1-4, Panel B, Figure 4.16), while in peak 2, the Hsc70 subunit appears to be in excess over that of the HSJ1b subunit (Lanes 5-9, Panel B, Figure 4.16).

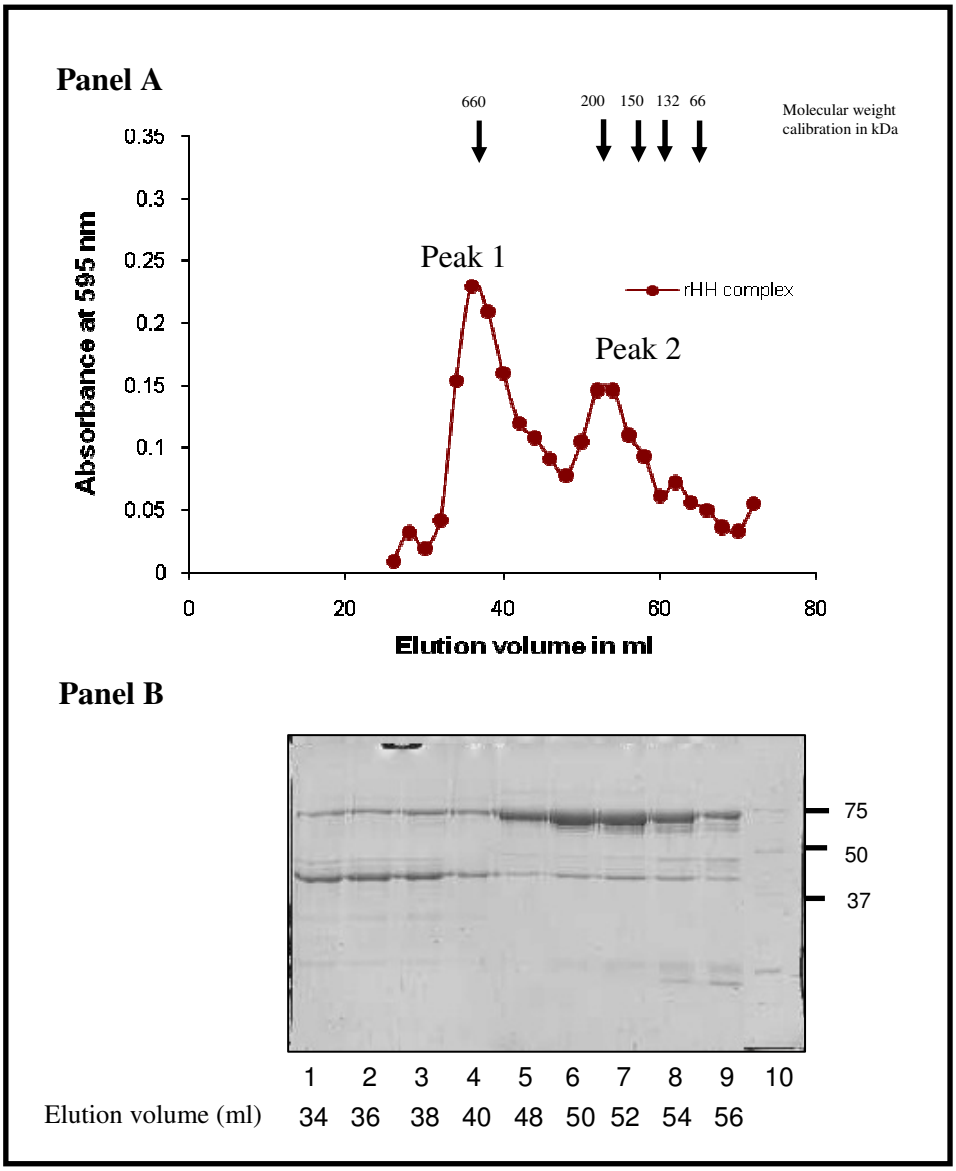

Figure 4.16: Size exclusion chromatography of the rHH complex.

Size exclusion chromatography was performed on a Superdex-200 column and the protein eluting from the column was collected as 1 ml fractions. The column volume (V_t) was 90 ml and the void volume (V_0) was estimated to be 36 ml. Absorbance of each fraction was determined using Bradford assay. 20 µl of protein from the indicated fractions was also analysed by SDS-PAGE gel electrophoresis.

Panel A: Elution profile of the rHH complex from the Superdex-200 column

Panel B: SDS-PAGE analysis of elution fractions. Lanes 1-4 are alternate fractions starting at fraction 34 until fraction 40, while alternate fractions starting at fraction 48-56 were loaded on lanes 5 -9 and lane 10 is the Bio-Rad precision plus molecular weight marker (broad range).

To determine if the two isolated peaks were functionally active, a thermal denaturation assay with 0.8 µM of luciferase was carried out as described in section 4.3.2.1. 1.27 µM of protein (calculated using MW of 110 kDa) from both the SEC peaks were used in the assay. The Hsc70/HSJ1b protein species from both peaks were found to be capable of protecting luciferase from thermal aggregation (Figure 4.17). However the percentage of luciferase retained in the soluble form was much lower for the isolated gel filtration peaks, when compared with the un-fractionated rHH protein after Ni-NTA chromatography. About 87% of the total luciferase remained soluble, when thermally denatured in the presence of the un-fractionated recombinant complex (columns 1 and 2, Figure 4.17). However with peak 1 ~50% luciferase was soluble (column 3, Figure 4.17), while peak 2 protected just over 40% (column 4, Figure 4.17). Both species showed a marginal increase in protection upon inclusion of ATP in the reaction mix (column 4 and 6, Figure 4.17), with peak 2 protecting almost 30% more luciferase (increase from 42.1% to 55.6%) upon addition of ATP. The reason for this observed functional difference between the fractionated and un-fractionated protein species is not clear.

.

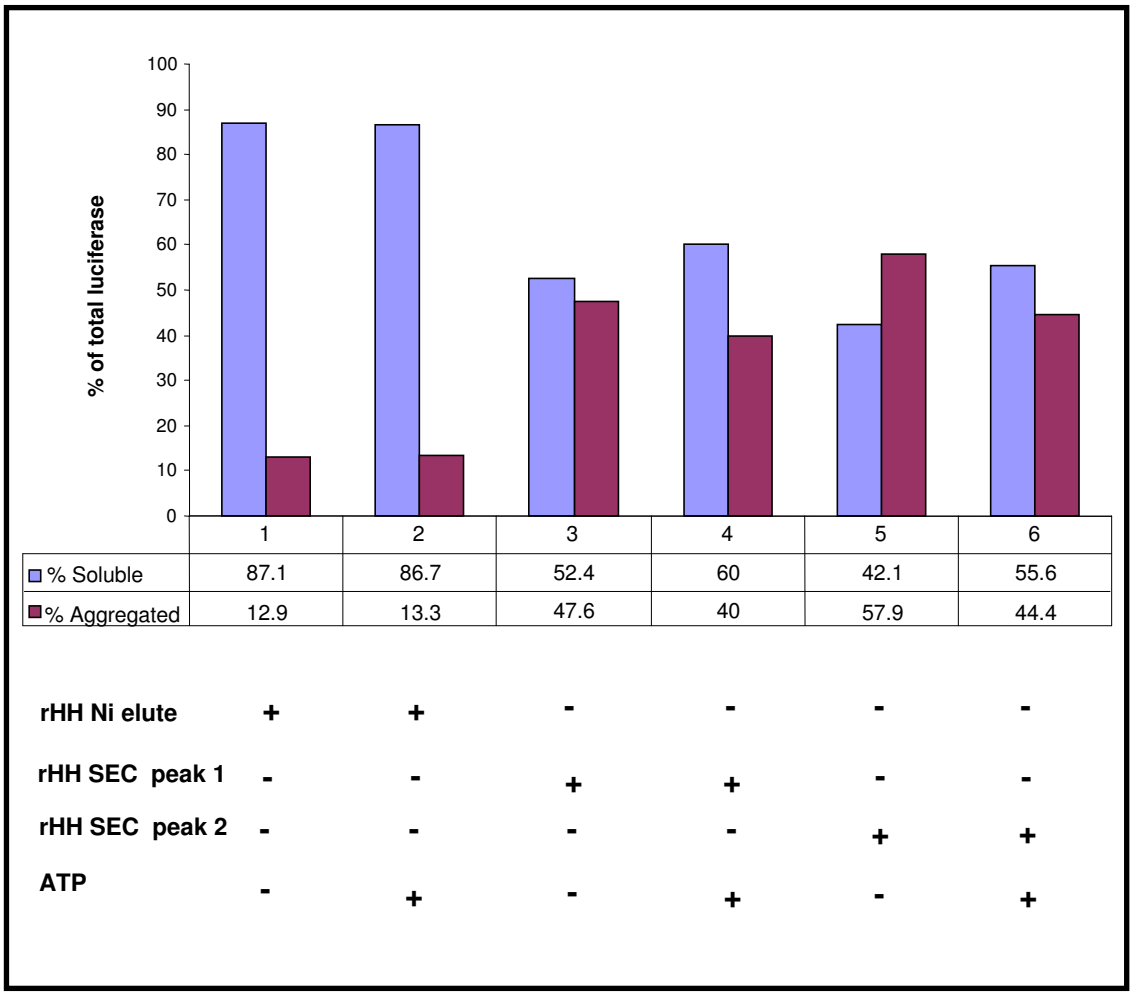

Figure 4.17: Functional activity of two peaks obtained after SEC of rHH.

Luciferase was thermally denatured at 42^{o}C for 10 minutes in the presence of the different rHH fractions and nucleotide. The reaction was spun down at 13,000 rpm to separate the soluble and aggregated fractions and analysed by SDS-PAGE. The amount of luciferase present in each fraction was quantified by densitometry and the percentage of soluble and aggregated luciferase for each reaction was calculated and plotted on MS Excel.

4.3.4.2. Sedimentation velocity analysis of peak 1

Hsc70 has been shown to oligomerise under a variety of conditions. One such factor which promotes the self association of Hsc70 is its association with Hsp40 partner protein. It was therefore necessary to determine if peak 1 obtained from size exclusion chromatography corresponds to well folded higher order oligomers or just undesirable aggregates. Peak 1 protein fractions were pooled and concentrated down to a final concentration of 0.8 mg/ml. The protein was then subjected to biophysical analysis by analytical ultracentrifugation (AUC). The experiment and analysis was performed by Dr. Dave Scott at the University of Nottingham. Sedimentation velocity analysis was performed at three different protein dilutions. Figure 4.18 is the sedimentation coefficient distribution obtained for all three dilutions of peak 1. The sedimentation peak at 10S represents the main protein peak and is consistent for all dilutions (represented by black arrow). Additionally, other peaks sedimenting faster than the main peak can also be observed. Philo, states that well resolved faster sedimenting peaks are indicative of aggregated protein species, while unresolved faster sedimenting peaks represent rapidly reversible self-associating oligomers (Philo, 2003). In the case of the peak 1 samples these peaks are not well resolved; thereby suggesting that peak 1 represents non-aggregated higher order oligomeric protein species. The molecular weight of the peak at 10S was calculated to be around 1.1 MDa.

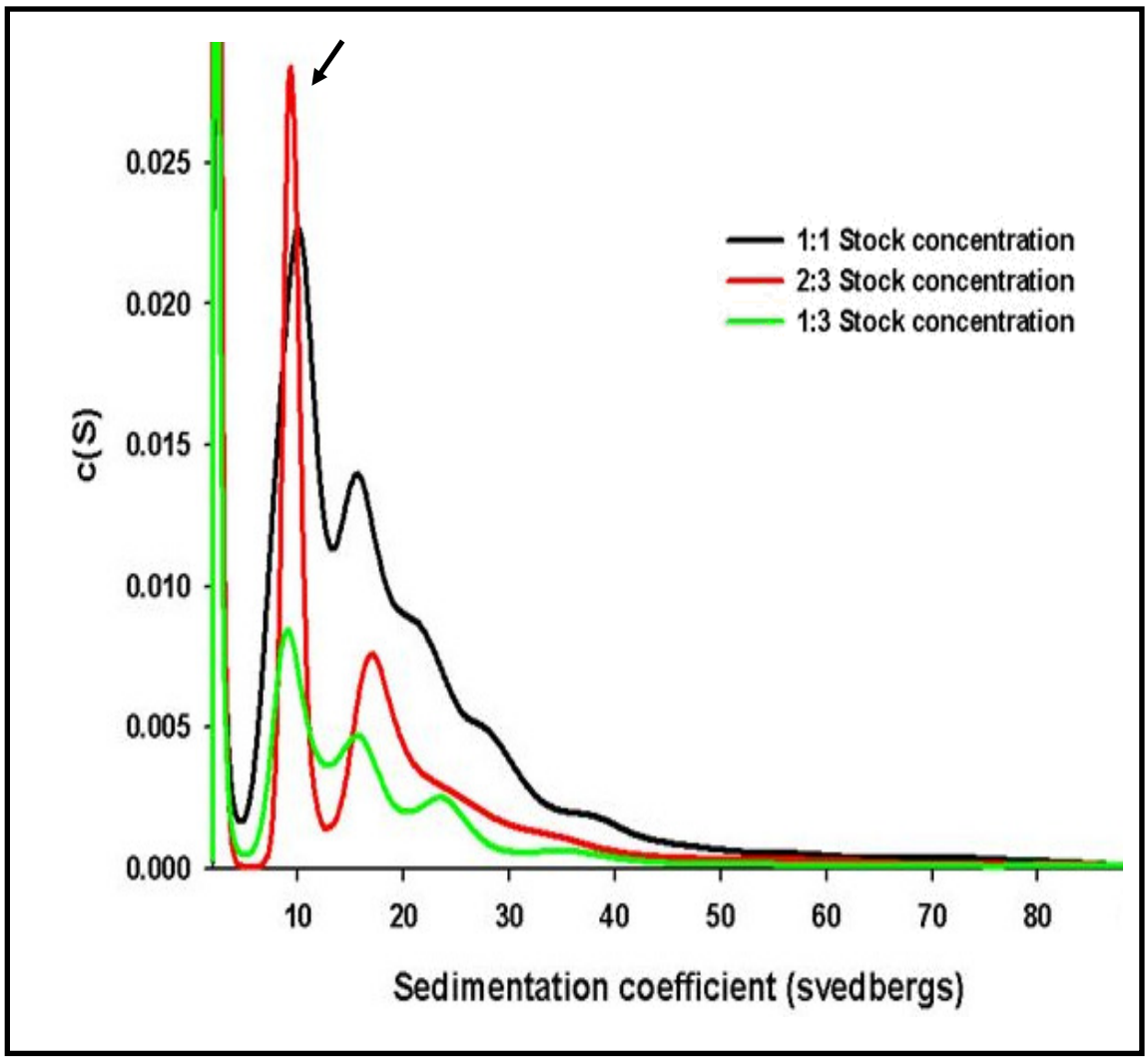

Figure 4.18: Sedimentation coefficient distribution for peak 1 of Hsc70/HSJ1b complex.

Peak 1 containing protein fractions were pooled and concentrated down to a final concentration of 0.8 mg/ml. Sedimentation velocity experiments were performed on a Beckman XL-A analytical ultracentrifuge (Beckman-Coulter) and run in the gel filtration buffer (20 mM Tris-HCl pH 8.0, 100 mM KCl) at different protein dilutions. Plots correspond to the calculated distribution of sedimentation coefficients, c(s) vs. sedimentation coefficient, S, in Svedberg units. The arrow mark indicates the position of the 10S peak.

4.3.5. Factors affecting oligomerisation of the rHH complex

From the previous sections, it was established that the two peaks obtained after SEC of rHH were in fact two functional forms of the complex. The next question was to understand the relationship between the two forms and what factors, if any, promoted the conversion of one form to the other. ATP and heat treatment at 42^{o}C with luciferase were identified as potential factors which could alter the oligomeric properties of the complex.

4.3.5.1. Effect of thermally denatured luciferase

The effect of binding to denatured substrate on the protein oligomerisation was studied using the soluble fraction obtained from the thermal aggregation assays carried out in the presence of ATP, using the protocols described in Section 4.3.2. Size exclusion chromatography was performed as before. Elution profiles were compared with that of the untreated rHH complex (Figure 4.19). As observed for the untreated rHH complex, a peak corresponding to the polymerised Hsc70/HSJ1b complex was observed in the void volume (represented as peak 1 on the chromatogram in panel A of Figure 4.19). Similarly, the ~220 kDa peak was also present; however for the protein incubated with denatured luciferase the peak eluted 2 ml earlier than usual. This could be due to the run conditions or because of luciferase binding to the protein.

Addition of thermally denatured luciferase affects the oligomerisation of the rHH complex, as reflected by the difference in proportion of peak 1 compared to peak 2. The protein associated with denatured substrate was found to resolve more as the ~220 kDa form compared to the untreated complex. A clearer picture emerges when the area under the peak was calculated for each peak and compared (Panel B, Figure 4.19). In the absence denatured luciferase, 64% of the rHH complex existed as oligomerised fraction. However interaction with thermally denatured luciferase reduced the percentage of oligomerisation to 28.4%. This reduction in oligomerisation was compensated by a corresponding increase in the ~220 kDa complex species. Thus denatured substrate promotes disassociation of the oligomeric peak 1 to form the ~ 220 kDa peak 2. The recovery of the protein from the Superdex column was extremely low and the ternary complex between the Hsc70/HSJ1b complex and luciferase could not be visualised by SDS-PAGE.

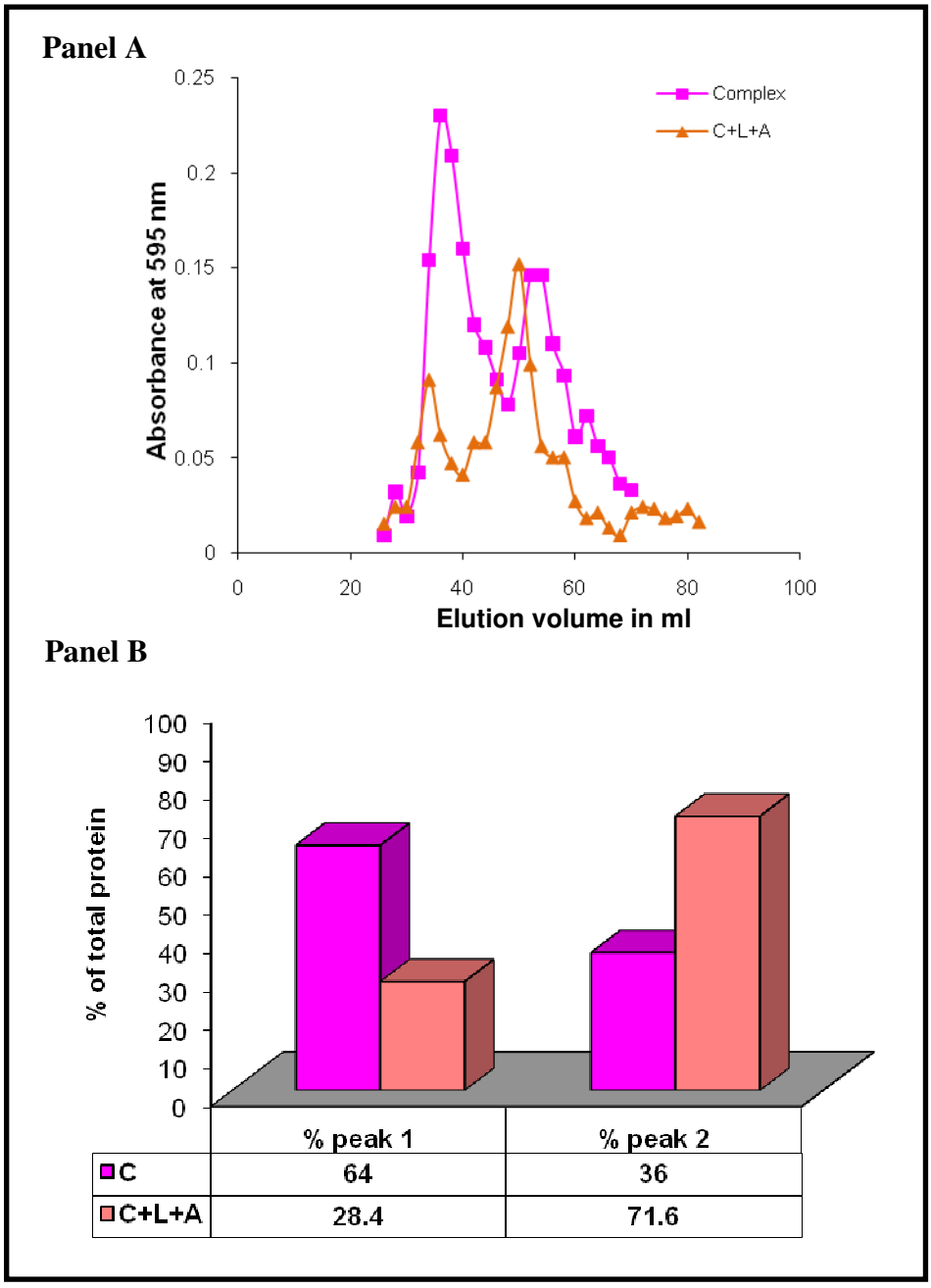

Figure 4.19: Effect of denatured substrate on oligomerisation of the rHH complex.

To obtain the C+L+A trace , thermal aggregation assay was set up as described in section 4.2.2 using 75 µg of the rHH protein with 50 µg of luciferase. The supernatant recovered after centrifugation at 13,000 rpm for 10 minutes was loaded onto the gel filtration column. The chromatography was performed in the assay buffer (20 mM Tris-HCl pH 8.0, 100 mM potassium chloride, 3 mM magnesium chloride and 2 mM DTT) following the protocol described previously.

Panel A: Comparison of the elution profile of the rHH complex (C) with complex treated with denatured luciferase in the presence of ATP (C+L+A).

Panel B: Distribution of the two peaks in C and C+L+A calculated using the area under the individual graphs obtained from panel A.

4.3.5.2. Effect of ATP

In order to study the effect of ATP has on the oligomeric composition of the complex; the protein was incubated with 2 mM ATP for 30 minutes at room temperature before being loaded onto the column. Elution profiles were compared with that of the untreated rHH complex (Figure 4.20). Comparison of the two profiles shows that the addition of ATP affects the extent of oligomerisation of the complex, as seen by the difference in proportion of peak 1 compared to peak 2. The protein associated with ATP was found to resolve more as the ~220 kDa form compared to the untreated protein. A clearer picture emerges when the area under the peak was calculated for each peak and compared (Panel B, Figure 4.20). Prior to addition of ATP 64% of the rHH complex existed as oligomerised fraction. However, addition of ATP reduced this to 40.5%. This reduction in oligomerisation was compensated by a corresponding increase in the ~220 kDa complex species. Thus ATP promotes disassociation of the oligomeric peak 1 to form the ~ 220 kDa peak 2.

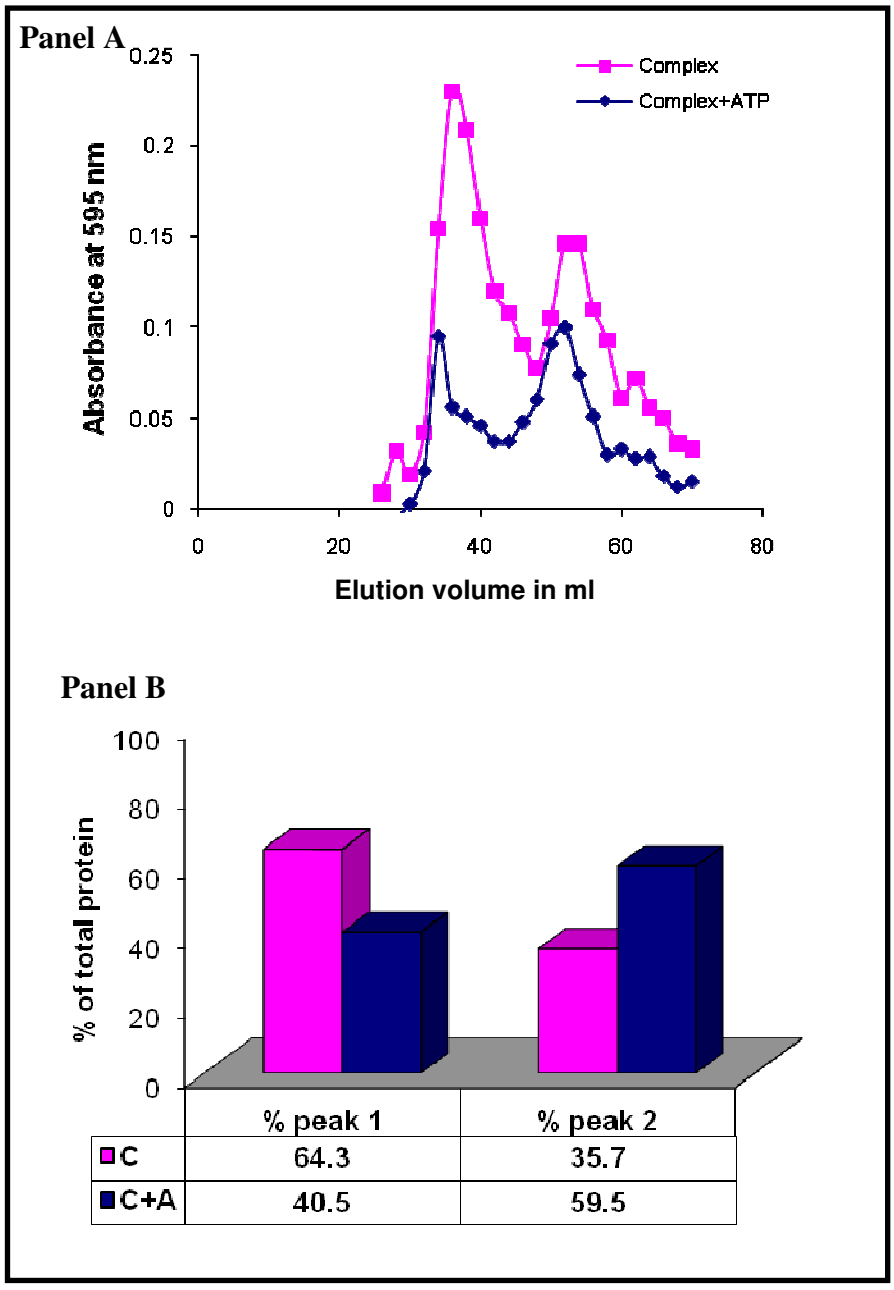

Figure 4.20: Effect of ATP on oligomerisation of the rHH complex.

The C+A trace was obtained by incubating 75 µg of the rHH for 30 minutes with 2 mM ATP at room temperature in buffer consisting of 20 mM Tris-HCl pH 8.0, 100 mM potassium chloride, 3 mM magnesium chloride and 2 mM DTT and then loaded onto the gel filtration column. The chromatography was performed in the assay buffer (20 mM Tris-HCl pH 8.0, 100 mM potassium chloride, 3 mM magnesium chloride and 2 mM DTT) following the protocol described previously.

Panel A: Comparison of the elution profile of the rHH complex (C) with complex treated with ATP (C+A)).

Panel B: Distribution of the two peaks in C and C+A calculated using the area under the individual graphs obtained from panel A.

The effect of ATP was studied further in detail to confirm that the increased proportion of ~220 kDa species was due to the breakdown of the oligomeric species. This was achieved by pooling the SEC peak 1 fractions and then treating with ATP for different time periods at room temperature. The samples were then analysed by gel filtration. In the first instance, the protein was incubated for 15 minutes at RT and its elution from the gel filtration column was analysed (blue trace in Figure 4.21). Clear signs of disassociation and formation of peak 2 can be observed. 15 minutes incubation with ATP resulted in the conversion of 23% of peak 1 into peak 2 (Panel B in Figure 4.21). Further incubation for another 15 minutes resulted in an additional 14% conversion (Panel B in Figure 4.21). However the maximum disassociation observed after 30 minutes is only a 37.3% conversion. This suggests a slow rate of conversion between the two forms. Probably a longer incubation time can induce further conversion, or the possibility exists that a percentage of the protein cannot be converted since it might be aggregated (as observed by the multiple peaks of AUC). In order to establish that the observed depolymerisation was not due to spontaneous disassociation of peak 1 upon re-chromatography, peak 1 protein fractions were pooled together and also re-chromatographed over the gel filtration column. From the chromatogram in Figure 4.21 (purple trace) it is clear that the elution profile of peak 1 remains unchanged and no spontaneous disassociation into peak 2 is detected. Therefore the observed disassociation in this experiment has to be ATP induced.

Panel A

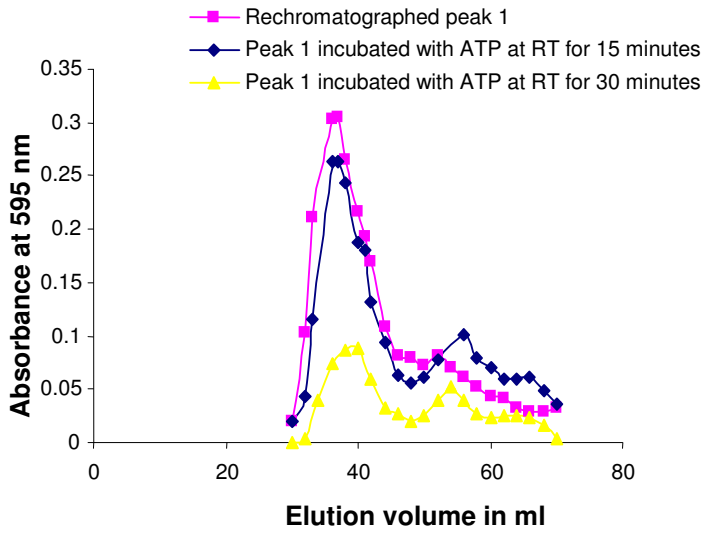

Panel B

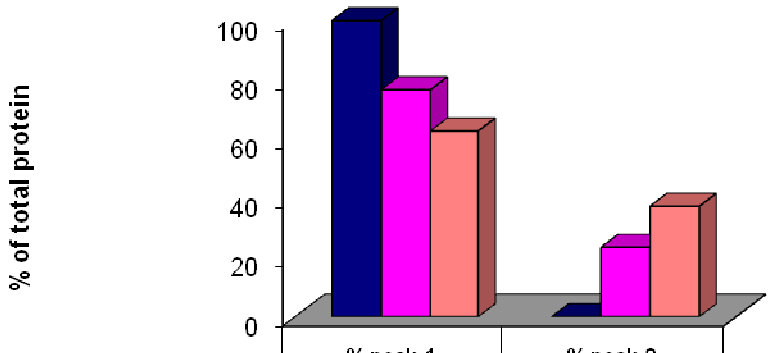

	% peak 1	% peak 2
Peak1	100	0
Peak 1 incubated with ATP for 15 min at RT	76.6	23.4
Peak 1 incubated with ATP for 30 minutes at RT	62.7	37.3

Figure 4.21: ATP induced disassociation of peak 1

The protein fractions of the oligomeric peak 1 were pooled and treated with 2 mM ATP for 15 and 30 minutes at room temperature in buffer consisting of 20 mM Tris-HCl pH 8.0, 100 mM Potassium chloride, 3 mM Magnesium chloride and 2 mM DTT. The reactions were subjected to SEC as described previously in section 4.3.6.1. The column was equilibrated with 20 mM Tris-HCl pH 8.0 plus 100 mM KCl. 1 mL fractions were collected after 25 ml of buffer had passed. The fractions were analysed for protein content using Bradford assay.

Panel A: Comparison of the elution profile of untreated peak 1 with protein treated with ATP for 15 minutes and 30 minutes respectively.

Panel B: Distribution of the two peaks calculated using the area under the individual graphs obtained from panel A.

Since ATP causes the oligomeric peak 1 to disassociate into peak 2, then could it also induce total disassociation of peak 2 into its individual components, – Hsc70 and HSJ1b? To answer this question, peak 2 fractions were pooled together and incubated for 30 minutes at room temperature with 2 mM ATP. The ATP treated protein was then loaded onto a Ni-NTA column and the bound proteins was eluted with 200 mM imidazole. The fractions were analysed by SDS-PAGE (Figure 4.22). If ATP results in the disassociation of the Hsc70 and HSJ1b subunits of peak 2, then the HSJ1b subunit should not be observed in the 200 mM elution fractions, as it is would no longer associated with the Hsc70 subunit. Analysis of the gel confirmed the same. Only Hsc70 was observed in the 200 mM elution fractions (lanes 5 and 6, Figure 4.22), while HSJ1b was observed in the flow through and wash fractions (Lanes 2 and 3, Figure 4.22).

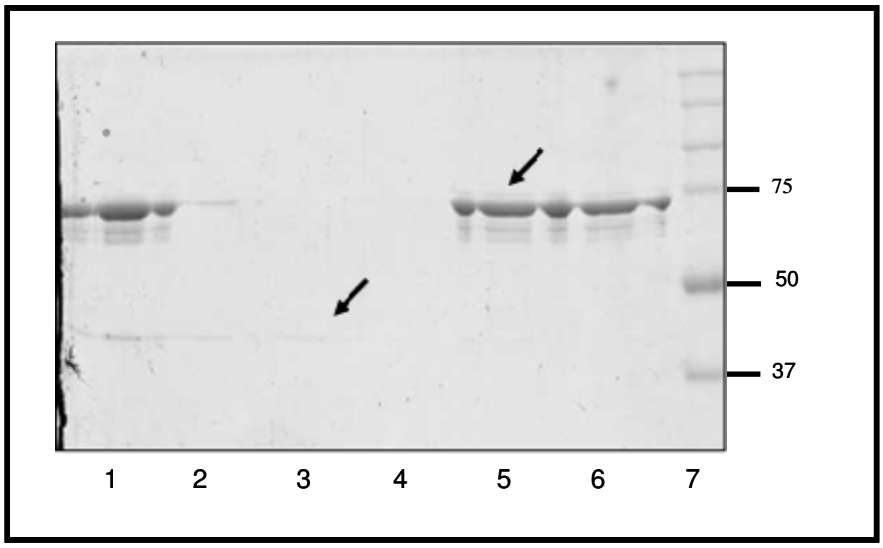

Figure 4.22: ATP induced disassociation of Hsc70 and HSJ1b subunits in peak 2 of SEC

The protein fractions of the peak 2 were pooled and treated with 2 mM ATP for 30 minutes at room temperature and applied to a Ni-NTA column equilibrated with buffer A (50 mM Tris-HCl pH 8.0, 100 mM NaCl). The protein was eluted in buffer A containing 200 mM imidazole. The polypeptide composition was analysed by SDS-PAGE (12% resolving gel) and the gel stained with Coomassie Brilliant Blue: Lane1 peak 2 protein loaded on the Ni column, lane 2 column flow through, lane 3 Wash with buffer A, lane 4 wash with 30 mM imidazole, lane 5 & lane 6 200mM imidazole elution, lane 7 Bio-Rad precision plus prestained molecular weight marker. The arrows indicate the elution position of the individual Hsc70 and HSJ1b subunits.

4.3.6. Structural studies of the full length complex

One of the primary goals of this work was to obtain structural information regarding the interactions of the Hsc70 and HSJ1b members of the HSP70 chaperone and HSP40 co-chaperone families. From size exclusion chromatography, it was determined that the ~220 kDa peak 2 fraction was suitable for X-ray crystallographic trials while the 1.1 MDa oligomeric peak 1 fraction could be an ideal target for preliminary electron microscopy analysis. The following sections describe the preliminary results from both experiments.

4.3.6.1. Crystallisation trials

An initial crystallisation screen for the peak 2 rHH fraction was set up using the Hampton Crystal Screens. These screens are macromolecular crystallisation kits composed of a selection of different crystallisation conditions, each condition containing different precipitants, salt and buffer solutions as suggested by Jancarik and Kim (Jancarik & Kim, 1991). Crystal screen and crystal screen 2 have 50 and 48 conditions, respectively. Crystallisation trials were set up at room temperature using the hanging drop vapour diffusion technique. The hanging drop method is one of the most popular crystallisation techniques. In this method, the protein is mixed with the reservoir solution (containing precipitants) and the drop is suspended from a cover slip and sealed over a well containing the reservoir solution. Super saturation of protein macromolecules is achieved by vapour-diffusion. This technique depends on the evaporation and diffusion of water between the well solution and protein sample, which have different precipitant concentration as a means of achieving super saturation and ultimately crystallisation (Benvenuti and Mangani, 2007). During the preliminary screening 96 drops were set up (the first 48 conditions from Hampton Screens I and II respectively). The drops were monitored for the presence of crystals. The outcome of the preliminary screen is presented in Figure 4.23 as a compilation of the drop photographs recorded at a single time point 2 months after the set up. Columns 1-6 correspond to drops set up Hampton crystal screen , and rest were set up with Hampton crystal screen 2. Light precipitation was observed in 33 drops and heavy amorphous precipitation in 11 conditions, while the rest of the drops were clear. However no crystals were obtained and further screening will be required to identify a potential crystallisation condition.

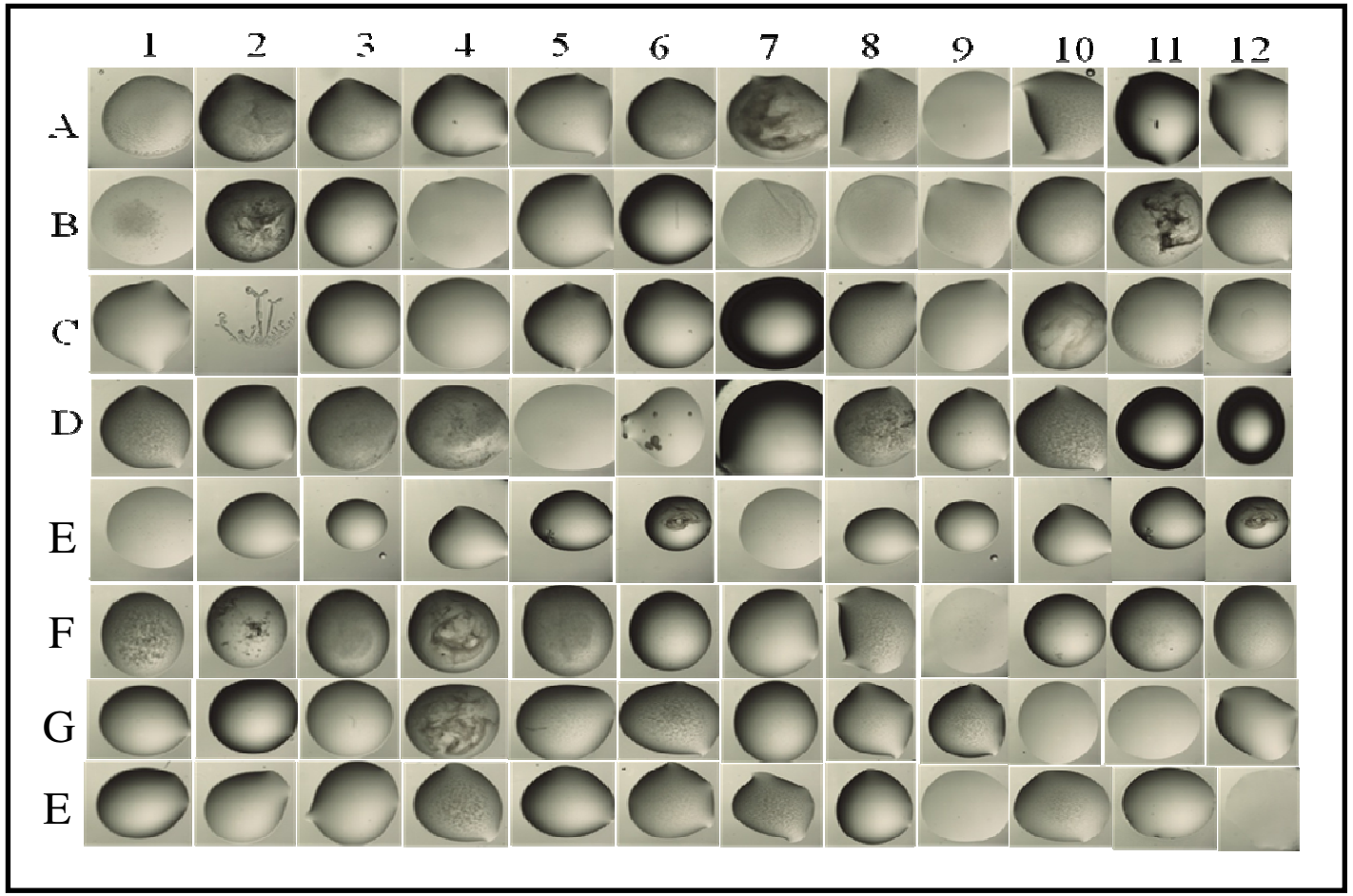

Figure 4.23: Hanging drop crystallisation trials of the rHH peak 2 SEC fraction with Hampton crystal screen I and II.

Protein at a concentration of 4 mg/ml was used for crystallisation trials. Initial trials were set up at room temperature via the hanging drop vapour diffusion method. The ~ 220 kDa protein was screened using the commercial Hampton Crystal Screens I and II. A total of 96 conditions were set up. Columns 1-6 correspond to the first 48 conditions of Hampton crystal screen and columns 7-12 correspond to that of Hampton crystal screen 2. The screens were periodically monitored and photographed for crystal growth.

4.3.6.2. Preliminary electron microscopy studies

Initially, the Hsc70-HSJ1b complex purified from the Ni-NTA affinity-column was subjected to negative staining by uranyl acetate and analysed by EM. The analysis was carried out by Dr.Corinne Smith at the University of Warwick. Panel A in Figure 4.24 is the image of the complex obtained at a protein concentration of 0.8 mg/ml. A good resolution was not obtained at this concentration. Serial dilution of the Ni-NTA protein sample was performed (1:5, 1:10, and 1:20), and then visualised by EM. Discrete particles could be observed at 1:20 dilution of the protein sample (Panel B in Figure 4.24). The majority of the particles appeared to be circular; a magnified view of which can be seen in Panel C of Figure 4.24. A few particles with a flower and stalk arrangement could also be observed (Panel D, Figure 4.24). This is possibly as a result of viewing the molecule from different orientation.

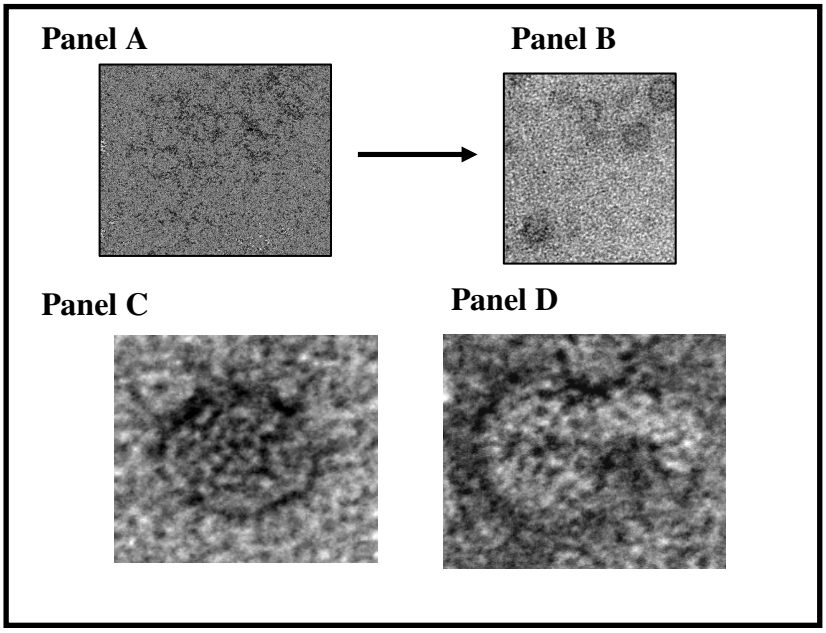

Figure 4.24: Negative staining and EM of the co-expressed Hsc70 and HSJ1b complex.

Protein samples were prepared for electron microscopy by dialysing the Ni-NTA elution fractions against 20 mM Tris-HCl pH 8.0, 50 mM potassium chloride overnight at 4^{o}C. The dialysed protein was concentrated down to 0.8 mg/ml and used for negative staining electron microscopy. The protein complex was negatively stained with freshly made 2% uranyl acetate on thin carbon-coated grids previously glow-discharged for 15 s. Panel A is the staining image before dilution. Panel B the image obtained after 1:20 dilution. Panel C is the magnified view of the circular particles while Panel D is view of particles with the flower and stalk arrangement.

Next negative staining was performed with the peak 1 fraction isolated by SEC to obtain images of this component of the rHH complex. Again imaging was started at a protein concentration of 0.8 mg/ml, and a further 1 in 20 dilution was required before discrete particles could be observed (Panel A, Figure 4.25). Two different particle types were observed, which have been enlarged in Panel B and C. Preliminary image classification studies have determined the size of the larger particles to be 260Å and that of the smaller one to be 162Å. These correspond to a molecular weight of 1.1 MDa and 420 kDa respectively. AUC had also previously estimated the molecular weight of peak 1 to be 1.1 MDa. From the sizing it appears that the smaller particles maybe disassociation products of the larger one, possibly due to the uranyl acetate staining. However more images need to be collected to carry out a more detailed study and possible reconstruction of the arrangement of Hsc70 and HSJ1b in the observed particles.

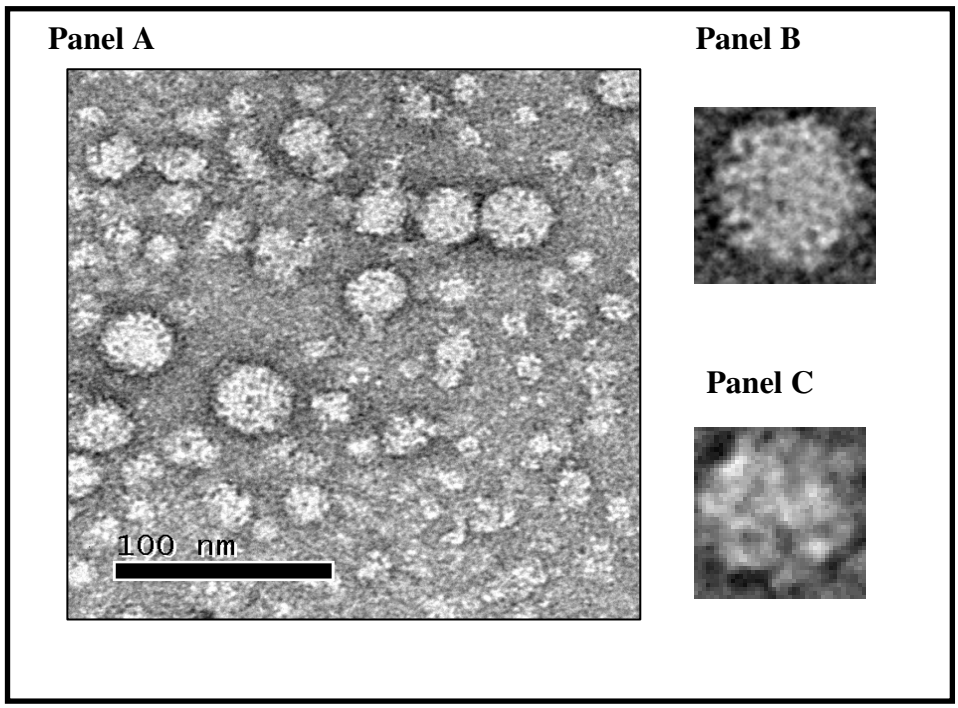

Figure 4.25: Negative staining of the peak 1 SEC fraction of the rHH complex.

SEC Peak 1 elution fractions were pooled together and concentrated down to 0.8 mg/ml and used for negative staining electron microscopy. The protein complex was negatively stained with freshly made 2% uranyl acetate on thin carbon-coated grids previously glow-discharged for 15 s. Panel A the image obtained after 1:20 dilution of the protein sample. Panel B is the magnified view of a larger particle while Panel C is the magnified view of smaller particles.

4.4. Discussion

Hsp70 proteins (both constitutive and inducible) under cellular conditions of stress bind to unfolding polypeptides. They prevent aggregation of these substrate proteins by binding to exposed hydrophobic residues and assist their refolding (Fink, 1999; Kampinga and Craig, 2010). A simple aggregation assay has been used routinely in the characterisation of chaperone proteins. Aggregation is either introduced using chemical agents such as urea and guanidium chloride, or by elevation of temperature (Daugherty *et al*., 1998; Nicoll *et al*., 2006). We demonstrated that the recombinant human Hsc70/HSJ1b complex had *in vitro* substrate protection capability using a luciferase based thermal aggregation assay. Elevation of temperatures to 42^{o}C causes aggregation of luciferase which has been shown to be reduced by the presence of chaperone proteins (Minami *et al*., 1996; Glover and Lindquist, 1998; Wang and Spector, 2001). In this assay, the rHH chaperone complex was successful in protecting 85% of the luciferase present. Minami *et al*., (1996) have reported that Hsc70/HDJ1 complex protected 70% luciferase, while Chamberlain *et al*., (1997) have demonstrated that the Hsc70/CSP1 complex could only maintain 50% of the luciferase in the soluble fraction. However this was observed to be ATP dependent, since in the absence of ATP, Hsc70/HDJ-1 proteins were only capable of protecting 25% of luciferase. However the rHH complex displayed an ATP independent activity. No significant improvement in activity was observed with the addition of ATP. This could possibly be due to the differences in how the protein complex was produced. In the previous studies, the chaperone complexes was reconstituted by combining the individual purified HSP70 and HSP40 family members and where ATP is required to initiate the formation of Hsp70-Hsp40 complex driven by the hydrolysis of ATP by the Hsp70 moiety (Russell *et al*., 1999), explaining the ATP dependent behaviour of the previous complexes. However in the case of the rHH protein, the preformed complex isolated from the Ni-NTA column is already in a competent state capable of protecting aggregating proteins, without any additional nucleotide requirement.

Another interesting observation was the difference in the amount of chaperone complex used for the successful protection of luciferase from thermal aggregation. In the case of the reconstituted Hsc70/HDJ-1 complex, the amount of Hsc70 (4.7 µM) used was in 47 fold excess, while HDJ-1 (3.2 µM) was 32 times in excess of the luciferase (0.1 µM) set up for aggregation, resulting in 70% luciferase protection

(Minami *et al*., 1996). In comparison, rHH was only 1.5 fold in excess to the luciferase present in the reaction and yet achieved 85% protection. Furthermore, thermal aggregation carried out in the presence of varying amount of luciferase, revealed that rHH could still protect more than 70% of the substrate even in reactions performed with 1:1 ratio of chaperone and luciferase. This clearly indicates that recombinant method of forming the Hsc70/HSJ1b complex is a more efficient chaperone system, compared to the systems previously studied.

Crystal structures of the ATPase domain of Hsp70 proteins of human and bovine origin have revealed that the Hsp70's are capable of binding to both calcium and magnesium metal ions (Flaherty *et al*., 1994, Sriram *et al*., 1997). We analysed the divalent cation requirements of the complex in substrate protection. To maintain luciferase protection, the protein requires the presence of either Ca^{2+} or Mg^{2+}. Replacement with another divalent metal, Ni^{2+} had a deleterious effect on the luciferase protection. However there was no preferential requirement for either Ca^{2+} or Mg^{2+} since replacing one with the other did not alter the levels of luciferase protection. A potential drawback of this study was the use of Ni^{2+} as the negative control. This is because it can potentially bind to the His tag on the Hsc70 and therefore hinder its interaction with the substrate. Also, at high concentrations Ni^{2+} has been shown to have a cytotoxic effect (Costa *et al*., 1994). For a more reliable interpretation, this experiment needs to be repeated with alternate divalent metal ions such as Mn^{2+}, Co^{2+} or Zn^{2+} and in the absence of divalent metal ions.

However despite maintaining almost 80% of thermally denatured luciferase in a soluble form, the rHH complex could not assist luciferase in regaining activity upon refolding at 25^{o}C. This is consistent with previous reports on the inability of reconstituted Hsc70/Hsp40 complexes to restore functional activity of thermally denatured luciferase (Frydman *et al*., 1992; Minami *et al*., 1996). Addition of diluted reticulocyte lysate has been shown to reactivate thermally denatured luciferase (Minami *et al*., 1996). However the exact component of reticulocyte lysate that enhances renaturation is as yet not completely understood (Minami *et al*., 1996). Thus although the co-expressed complex could protect 85% of luciferase from thermal aggregation in an ATP independent fashion, it was not successful in maintaining the substrate's functional activity.

Hsc70 on its own has very low basal ATPase activity (Russell *et al*., 1999). However cofactors such as Hsp40 proteins or unfolded substrate stimulate the rate of ATP hydrolysis (Laufen *et al*., 1999). Hsp40 co-chaperones have been reported to cause several fold increase in ATP hydrolysis (Russell *et al*., 1999). ATP hydrolysis converts Hsc70 into its ADP bound form which in turn stabilises the formation of ternary complex with unfolded substrate (Laufen *et al*., 1999). A 14-fold stimulation of Hsc70s' ATPase activity by Csp1 (Chamberlain and Burgoyne, 1997) and 7-fold stimulation of Hsc70s' ATPase activity by Hdj1 (Minami *et al*., 1996) have been reported. Unfolded protein, apocytochrome c has been shown to stimulate ATP hydrolysis of mammalian Hsc70 by 2-3 fold (Sadis and Hightower, 1992). Based on these findings we decided to evaluate the affect that binding to denatured luciferase has on the ATPase activity of Hsc70 in the rHH complex. A non-radioactive assay was chosen to detect phosphate release due to ATP hydrolysis. The ATP hydrolysis activity of the rHH complex was not significantly altered by denatured luciferase. A similar lack of stimulation was observed upon binding of denatured luciferase to the Hsc70/Csp1 complex. This was attributed to non-overlapping site of interaction between Csp1 and luciferase with Hsc70 (Chamberlain and Burgoyne, 1997). We believe that in the case of the rHH complex, Hsc70 in the presence of HSJ1b is already in a state fit to bind unfolded protein. Therefore, no further stimulation is observed upon interaction with luciferase, which could occur at a different site from HSJ1b.

This gives rise to an interesting question, how does the denatured substrate bind to the rHH complex without ATP and its hydrolysis. A plausible explanation would be if the purified Hsc70/HSJ1b complex contains endogenously bound nucleotide. The *T. thermophilus* DnaK and DnaJ complex purified as a hexameric complex was isolated without any bound nucleotide (Motohashi *et al*., 1994). This is the only other known report on the isolation of an intact Hsp70/Hsp40 complex. However in the case of the rHH complex, a convincing result could not be obtained regarding the nucleotide content of the rHH complex. Initial analysis was carried out by deriving the UV absorption spectrum of the purified complex. The observed A260/A280 ratio was calculated and found to be 1.4. Use of A260/A280 ratio to detect presence of nucleotide has been used previously by Wegele *et al*., to detect co-purification of nucleotides during the purification of yeast Hsp70 (Wegele *et al*., 2003). However using this method one cannot be certain by the presence of additional A260 absorbing

material, of the identity of the nucleic acid (ATP, other nucleotides, or RNA) bound to Hsc70. Therefore HPLC analysis to identify the bound nucleotide was undertaken. But this failed to convincingly indicate the absence/presence of any bound nucleotide, despite several attempts. However failure to detect any nucleotide should not lead to the automatic assumption that the rHH complex is formed in a nucleotide free state. There could also be certain experimental failures which could make the results obtained in the case of the rHH complex misleading. Gao *et al*., have reported that ATP and ADP binds very strongly to the Hsc70 and cannot be easily removed from the enzyme even after extensive dialysis or EDTA treatment (Gao *et al*., 1994). Nucleotide extraction for the HPLC analysis was carried out using the PCA extraction protocol. However, the efficiency of the extraction method was not evaluated and therefore failure to detect bound nucleotide could also be because of failure to extract the tightly bound nucleotide.

The NBD of Hsc70 can have three occupancy states: nucleotide free, ADP bound or ATP bound (Buchberger *et al*., 1995; Shaner and Morano, 2007). Hsc70 is predominantly in the ATP bound state, in the absence of Hsp40 co-chaperones. The rHH complex in our preparations co-elutes with a few contaminating protein species, which are found associated even after gel filtration. If Hsc70 was ATP bound, the contaminating protein species would not be expected to remain associated with Hsc70, since substrates have a high on/off rate when ATP is bound to Hsc70 (Bukau and Horwich 1998). This suggests that in the case of the rHH complex, the presence of bound ATP can be discounted. The rHH complex can either be nucleotide free or ADP bound. Both NBD occupancy states can satisfactorily explain the observed behaviour of the rHH complex as both forms exhibit high affinity for substrates (Schmid *et al.,* 1994, Gao *et al*., 1995). This would explain the observed luciferase protection in the absence of additional ATP. Thus the functional behaviours displayed by the rHH complex can be explained by the nature of occupancy of the NBD of Hsc70 in the rHH complex. Unfortunately, we have been unable to conclusively prove if it is ADP bound or nucleotide free.

The conformational features of the complex were probed by limited proteolysis using trypsin and chymotrysin. Exposed and flexible regions which are accessible to proteases more easily undergo cleavage first, while possible sites in the highly

structured core of the protein molecule either remain protected or undergo cleavage at a slower rate (Zappacosta, 1996). Proteolysis is therefore a useful tool to study the conformation of native proteins and associated transitions observed on substrate/cofactor/ligand binding (Hubbard, 1998). For both trypsin and chymotrysin, initial analysis was carried out at 30^{o}C. However at this temperature complete proteolysis of HSJ1b was observed within 10 minutes. This was not useful in furthering our understanding of the Hsc70/HSJ1b interactions. By reducing the temperature to 4^{o}C, the kinetics of the enzyme action appears to slow down and it was possible to observe the proteolysis of the Hsc70 and HSJ1b components.

Proteolysis of the Hsc70/HSJ1b complex by trypsin and chymotrypsin was monitored over a period of 75 minutes. The key observation was that irrespective of the protease used, the HSJ1b subunit was extremely susceptible to proteolysis, compared to the Hsc70 moiety. With chymotrypsin, the major proteolytic product of HSJ1b migrating at ~ 30 kDa was observed within 10 minutes from the start of the proteolysis and majority of the HSJ1b protein was converted into this fragment by the end of 75 minutes. Analysis of the HSJ1b protein sequence by GeneRunner software revealed 28 possible chymotrypsin cleavage sites. 27 out of the 28 sites are clustered together at the first 171 amino acids, while the 28th site is at Y261. Since the NH2-terminal region contains 28 potential chymotrypsin cleavage sites and yet gives rise to a single proteolysis fragment indicates that it must represent a well folded domain. With trypsin, complete proteolysis of HSJ1b was observed within 10 minutes of initiating the digestion. This was not surprising, since a total of 43 possible trypsin recognition sites were predicted by the Generunner software. These sites are uniformly distributed throughout the protein sequence, which explains the observed rapid proteolysis of HSJ1b, upon addition of trypsin.

The Hsc70 subunit on the other hand was more resistant to proteolysis. Even after 75 minutes of treatment with chymotrypsin, 80% of Hsc70 remained undigested. Chappel *et al*., (1986) have previously reported that chymotrypsin digestion of bovine Hsc70 resulted in a 60 kDa fragment which was subsequently proteolysed to form a 44 kDa fragment (Chappel *et al*., 1986). In the case of the rHH complex, two minor products observed at ~49 kDa and 52 kDa are the only indications of Hsc70 proteolysis by chymotrypsin, suggesting that Hsc70 adopts a different conformation in the presence

of the HSJ1b co-chaperone. There are a number of reports which have studied the influence of the Hsp40 moiety on the proteolysis of Hsp70 using trypsin. Bimston *et al*., (1998) reported that trypsin digestion of Hsc70 yields 58 kDa, 43 kDa, 20 kDa and 18 kDa fragments. The addition of Human DnaJ homologue (HDJ-1) did not seem to alter the proteolysis results (Bimston *et al*., 1998). However their report fails to discuss the state of the HDJ-1 moiety. With the rHH protein, Hsc70 undergoes proteolysis only at the N-terminal region, on the Factor XA site adjacent to the 10 X Histidine tag , resulting in a proteolysis product which differs from the undigested product (73 kDa) by only 1 or 2 kDa (~70-71 kDa). Analysis of the Hsc70 protein sequence by GeneRunner software predicts 82 potential trysin recognition sites, and yet it is extremely resistant to proteolysis. Therefore Hsc70 subunit of the rHH complex also appears to be well folded.

We studied whether any nucleotide-induced conformational changes to Hsc70 or to the stability of the complex could be observed. Hsp70 have been shown to adopt three distinct nucleotide dependent conformations: nucleotide-free, ADP-dependent, and ATP-dependent (Buchberger *et al*., 1995; Fung *et al*., 1996). In this study ATP, ADP and non-hydrolyzable ATP analogue, AMP-PNP were used. However the proteolysis patterns were identical to the ones obtained in the reaction where no additional nucleotide was added. Reactions with ATP were monitored for an extended over a period of 75 minutes using both trypsin and chymotrypsin; still no difference was detected between the nucleotide-free and ATP containing reactions. Partial trypsin digestion assay to test the influence of DnaJ on DnaK's conformation also shows that DnaJ does not noticeably alter DnaK's trypsin digestion pattern in the presence and absence of ATP (Wall *et al*., 1994). This was attributed to the possibility that DnaJ stimulated hydrolysis of ATP bound to DnaK prevented ATP binding/hydrolysis associated conformational change in DnaK or alternatively the conformational change experienced by DnaK was countered by rapid relaxation caused by DnaJ (Wall *et al*., 1994). This could be the explanation for the absence of nucleotide dependent conformational changes in the rHH complex.

Thus from the proteolysis data both the Hsc70 and HSJ1b subunits appear to be well folded. The altered chymotrypsin digestion pattern observed for Hsc70 indicates that Hsc70 displays alternate conformational features when associated with HSJ1b. Also,

the extreme susceptibility of HSJ1b suggests that, in the rHH complex, HSJ1b was the more exposed and therefore the more accessible of the two subunits.

Oligomerisation of the rHH complex was evaluated by size exclusion chromatography on a superdex-200 column, which has a fractionation range of 10,000-600,000 kDa. The rHH protein was found to resolve into two peaks. The first peak (which contained >60% of total protein) eluted in the void volume (>600 kDa), while the second peak fractionated with an estimated molecular weight of ~220 kDa. SDS-PAGE confirmed the co-fractionation of both Hsc70 and HSJ1b subunits in both the elution peaks of rHH. While the presence of the highly oligomerised fraction strongly hinted at polymerisation of Hsc70, the >600 kDa fraction could also represent protein aggregation. Using Analytical ultracentrifugation, it was successfully demonstrated that the >600 kDa protein fraction was indeed desirable protein oligomerisation and not undesirable protein aggregation. The major sedimentation species was observed at 10S, along with a few other minor sedimentation species (possible due to aggregation of the complex) and the estimated molecular weight for this species was 1.1 MDa.

Using size exclusion chromatography, Hsc70 has been previously shown to be a mixture of monomers, dimers, and high order oligomers in solution (Palleros *et al*., 1991; Kim *et al*., 1992; Benaroudj *et al*., 1994). This property is a well-documented feature of several members the Hsp70 protein family such as BiP (Blond-Elguindi *et al*., 1993), the constitutive Hsc70 (Benaroudj *et al*., 1994), the inducible Hsp70 (Brown *et al*., 1993) and DnaK (Schönfeld *et al*., 1995). One important factor that influences the equilibrium towards oligomerisation is the Hsp40 co-chaperone proteins. King *et al*., (1995) successfully demonstrated that Hsc70 polymerised in the presence of yeast DnaJ (YDJ1) but required ATP for this activity (King *et al*., 1995). Similarly Jiang *et al*., (1997) have reported about auxilin (DnaJ homologue) induced polymerization of Hsc70, by shifting the elution profile of the Hsc70 into the void volume of the gel filtration column. The existence of interaction between Hsc70 and the DnaJ homologues during the polymerization event is controversial. Barring auxilin, most DnaJ homologues have been reported to bind very weakly to Hsc70 (King *et al*., 1995; Jiang *et al*., 1997; King *et al*., 1999). Auxilin was shown to form a complex with Hsc70 which then elutes in the void volume. At the same time, Angelidis *et al*., 2001 have shown the existence of monomeric and aggregated forms of Hsp70s *in vivo* using

non-denaturing gradient analysis, and association of Hsp40 takes place preferentially through the monomeric Hsc70.

The 1.1 MDa co-polymer species could be due to formation of the Hsc70/HSJ1b complex or as a result of HSJ1b induced polymerisation of Hsc70 and subsequent complex formation. However we do not have conclusive data to prove that the 1.1 Mda protein species is a polymerisation product, since Hsc70 polymerisation by Hsp40 has been shown to occur only in the presence of ATP; ADP, AMP-PNP, and nucleotide free conditions did not promote the Hsp70 polymerisation (King *et al*., 1995). In the case of the rHH, we are not entirely sure about the factors promoting the polymerisation. It might be driven by of cellular ATP present during the protein expression, since no additional ATP was added during the course of the study.

Thus the Hsc70/HSJ1b complex appears to be a heterogenous mix of ~220 kDa and hetero-oligomeric co-polymer species, and these two species actually represent two different states of association between Hsc70 and HSJ1b. The only other report on the isolation of an intact complex between DnaK and DnaJ was isolated from the bacteria *Thermus thermophilus*. The molecular weight of this complex was estimated to be 310 kDa using gel filtration column, and no other oligomeric co-polymer was reported (Motohashi *et al*., 1994). For the first time the co-existence of both the oligomeric and non-oligomeric state of interaction between the Hsc70 and Hsp40 has been demonstrated. That, this represented a true state of interaction was further validated by the detection of functional activity for both forms of the complex. Both protein species could protect almost 50% of luciferase from thermal denaturation in their own right, which further corroborates our claim that these are two functional interaction states between Hsc70 and HSJ1b proteins.

The relationship between the oligomeric and ~220 kDa forms of the complex was further investigated. It has been reported that the equilibrium between monomeric and oligomeric Hsc70 species is influenced by nucleotides and unfolded proteins (Benaroudj *et al*., 1996). Hsc70 in the presence of nucleotide (ADP) and absence of any nucleotide, is observed to be a mixture of monomer, dimers and higher oligomers, while ATP and unfolded proteins shift the equilibrium in favour of the monomeric form of Hsc70 (Carlino *et al*., 1992; Toledo *et al*., 1993; Palleros *et al*., 1993). Therefore the effect of unfolded substrate and ATP on the oligomeric composition of

the rHH complex was studied. First the protein was heat treated (at 42^{o}C) in the presence of luciferase, and its effect on the oligomeric composition was studied by SEC. Hsc70, *in vivo,* exits in an aggregated form at 37 °C, which persists after heat treatment, however denatured luciferase was detected interacting with only the non-aggregated forms (Angelidis *et al*., 1999). SEC of the rHH complex after heat treatment revealed the existence of both the polymerised and ~220 kDa forms, however with a ~two-fold increase in the proportion of ~220 kDa species. This signifies substrate dependent conversion of the oligomeric Hsc70/HSJ1b complex to the ~220 kDa Hsc70/HSJ1b complex. Similarly, ATP dependent depolymerisation was also observed, where the oligomeric form breaks down to form the ~220 kDa Hsc70/HSJ1b complex which when treated with ATP, disassociates into the individual Hsc70 and HSJ1b subunits.

Our observations could signify a potential physiological relevance. Polymerisation of Hsc70 has been identified as a possible regulatory event, which maintains the chaperone in an inactive state (King *et al*., 1995a). Studies performed with BiP (Hsp70 from the endoplasmic reticulum) found that polymerised BiP was observed to be free of protein substrates, while the monomeric form was found associated with protein substrate (Freiden *et al*., 1992). King *et al*., have suggested that the observed *in vitro* polymerisation of Hsp70 proteins by their Hsp40 cofactors could be of physiological relevance too (King *et al*., 1999). Angelidis *et al*., 1999 have shown the existence of monomeric and aggregated forms of Hsp70s *in vivo* using non-denaturing gradient analysis. Thus the two forms observed by gel filtration of the rHH complex could represent possible *in vivo* interaction states (illustrated in Figure 4.26). The complex of 70 and 40 exists in a storage form (polymer) and active form (~220 kDa). Addition of ATP or substrate, first converts the complex into the active form. Further treatment with ATP causes disassociation of the complex. The ~220 kDa form represents an unexplored but potentially significant intermediate 70/40 interaction state in the *in vivo* scenario.

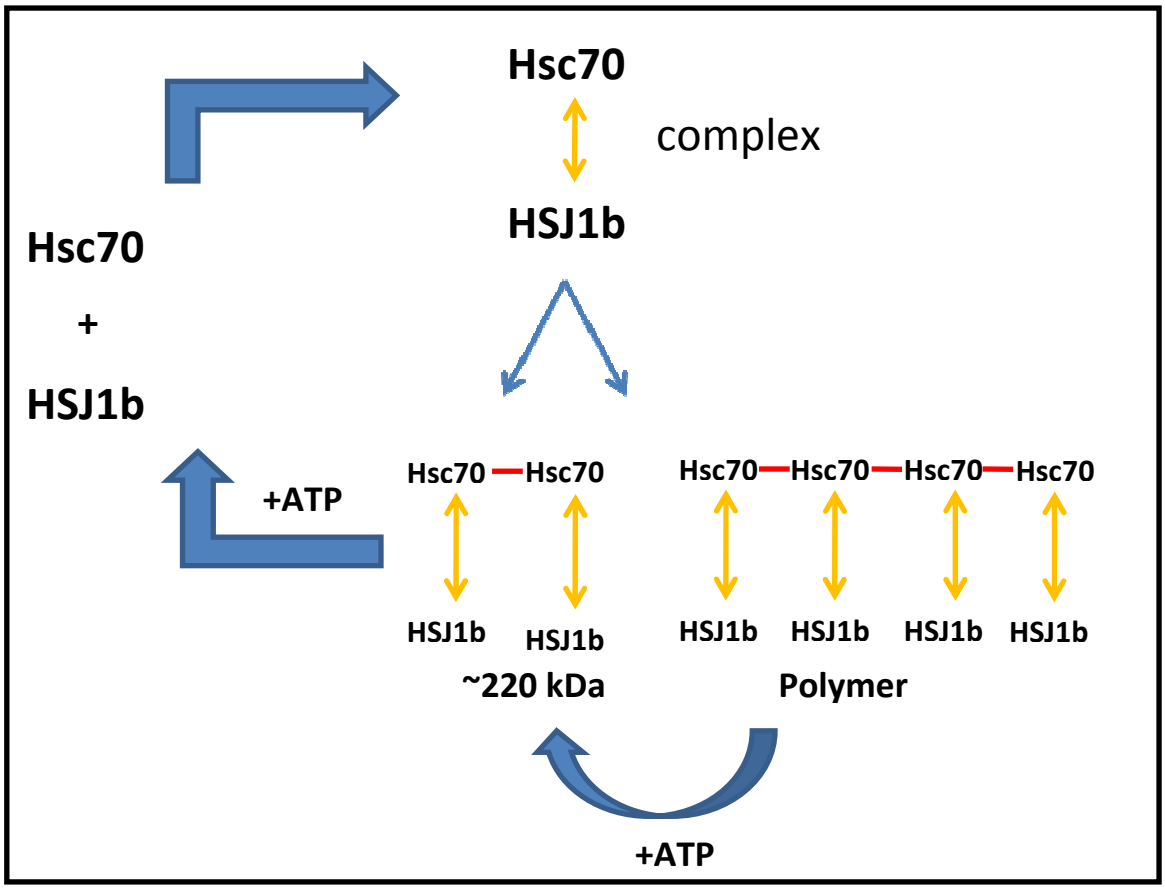

Figure 4.26: Physiological relevance for the two forms of the Hsc70/HSJ1b complex isolated by SEC

Preliminary structural studies on the co-expressed proteins were carried out by crystallography and negative EM staining. The 220 kDa gel filtration fraction was studied by X-ray crystallography. However no potential crystallisation condition was identified. The large size of the peak 1 from SEC allowed us to pursue preliminary structural analysis by electron microscopy. Negative EM staining normally enables specimens to adsorb to a carbon support film in one or a limited number of preferred orientations (Ohi *et al*., 2004). Previously, electron microscopy analysis of T.DnaK.DnaJ complex has been reported as a trigonal particle with a central cavity (Motohashi *et al*., 1994). Their results revealed homogeneous circular shaped particles with a diameter of 115 Å. Preliminary results obtained from negative staining of the rHH protein Ni NTA elution fraction revealed mostly circular particles. However a few particles resembling a bunch of flowers and its stalk were also observed, which could represent an alternate view of the protein complex. The preliminary results from negative staining are extremely encouraging, and are a first step towards determining the structure of the Hsc70/HSJ1b complex.

Chapter 5

Comparison of the recombinant Hsc70/HSJ1b complex with the reconstituted Hsc70/HSJ1b *in vitro* complex

CHAPTER 5: Comparison of the recombinant Hsc70/HSJ1b complex with the reconstituted Hsc70/HSJ1b *in vitro* complex

5.1. Introduction

Biochemical studies on the interaction of HSP70 and HSP40 family members have been routinely carried out using a reconstituted protein complex formed by combining the individual chaperone and co-chaperone components in the presence of ATP, which drives the formation of the complex (Jiang *et al*., 1997; Lu and Cyr, 1998; Laufen *et al*., 1999). A reconstituted Hsc70/HDJ-1 complex was used by Minami *et al*., (1996) to study the effects of the human DnaJ homologue (HDJ-1) on the chaperone functions of the human Hsc70 protein (Minami *et al*., 1996). Using a similar methodology, Chamberlain and Burgoyne, (1997) have studied the importance of the HPD motif in the DnaJ-like cysteine string proteins to interaction with Hsc70 (Chamberlain and Burgoyne, 1997). The work by Pleckaityte and co-workers is another example of the use of reconstituted protein system, where they have demonstrated using gel filtration that complex formation between Hsp70 and Hsp40 from *Meiothermus ruber* absolutely requires ATP for its assembly (Pleckaityte *et al*., 2003)

In Chapter 3, isolation of a recombinant form of the Hsc70/HSJ1b (rHH) complex was described. The functional behaviour of this complex was studied and has been discussed in detail in Chapter 4. The characterisation studies carried out for the rHH complex suggests that its behaviour does not concur with studies carried out using a reconstituted complex. Could the recombinant complex represent an alternative model of the chaperone/co-chaperone interactions? In order to establish this, a reconstituted Hsc70/HSJ1b complex was generated as described by Minami *et al*., and others (Minami *et al*., 1996; Chamberlain and Burgoyne, 1997). The properties of the rHH complex was then compared with the reconstituted *in vitro* form. The comparison was based on the two complex's substrate protection efficiency, conformational differences probed by partial proteolysis and polymerisation properties determined by size exclusion chromatography. This chapter details the outcome of this comparative study and its bearing on using the recombinant complex as a model protein to study and understand the Hsc70 chaperone and HSJ1b co-chaperone interactions.

5.2. Material and Methods

5.2.1. Expression of human Hsc70 and HSJ1b genes

Hsc70 and HSJ1b proteins were expressed using the pET16b-Hsc70 and pET16b-HSJ1b constructs (described in Chapter 3). Protein expression was carried out in *E. coli* BL21(DE3). The plasmids were transformed into *E. coli* BL21(DE3) cells and a single colony was used for overnight inoculation into LB broth containing 100 µg/ml of ampicillin, grown at 37°C. Up to 4% of the overnight seed culture was used to inoculate the large scale cultures the next day. Growth and induction was performed as described in Chapter 2, section 2.10.1. Briefly, cells were grown at 37°C to an OD_{595} of 0.6-0.8. Protein expression was induced by the addition of IPTG to a final concentration of 0.4 mM. After induction, cells were grown for further 3 hrs. Cells were harvested as described Chapter 2, section 2.10.1 and the cell pellet was re-suspended in lysis buffer (50 mM Tris-HCl pH 8.0, 250 mM NaCl, 5 mM imidazole and 5% glycerol (v/v)) and stored at -80°C until required.

5.2.2. Purification of human Hsc70 and HSJ1b

Purification of the recombinant Hsc70 and HSJ1b proteins was performed following the protocol for the purification of poly-histidine tagged proteins described in section 2.10.2 in Chapter 2. Briefly, cells were lysed, centrifuged and the soluble supernatant fraction was applied to a 4 ml Ni-NTA column, which was pre-equilibrated with the lysis buffer. The column was then washed with 5 CV of lysis buffer and again with 5 CV of lysis buffer containing 30 mM imidazole. Hsc70 and HSJ1b proteins were eluted from the Ni column with 3 CV's of elution buffer (lysis buffer plus 200 mM imidazole). A typical yield of 4-5 mg of protein was obtained per litre of culture for both Hsc70 and HSJ1b. The elution profiles of the proteins were analysed on a 12% SDS-PAGE gel as described in section 2.l0.5 in Chapter 2. Fractions of nickel purified Hsc70 were pooled and dialysed against buffer containing 20 mM Tris-HCl pH 8.0, 50 mM potassium chloride overnight at 4°C.

5.2.3. ATP treatment of HSJ1b

The 200 mM imidazole elution fractions containing HSJ1b protein were pooled and incubated with 1mM ATP, 1 mM DTT and 10 mM $MgCl_2$ for 30 minutes at room temperature with rocking. The ATP treated HSJ1b protein was diluted two-fold with

10 mM Tris-HCl pH 8.0 prior to loading onto a 4 ml Ni-NTA column pre-washed with 10 CV of equilibration buffer (50 mM Tris-HCl pH 8.0, 200 mM NaCl). The column was then washed with 5 CV of equilibration buffer and followed by a second wash with 5 CV of equilibration buffer plus 20 mM imidazole. The protein was finally eluted in 1 ml fractions in 3 CV of equilibration buffer containing 200 mM imidazole. The elution profile was monitored by SDS-PAGE analysis. Peak fractions of the ATP-treated HSJ1b were pooled together and dialysed against buffer containing 20 mM Tris-HCl pH 8.0, 50 mM potassium chloride overnight at 4^{o}C prior to use in assays.

5.2.4. Thermal aggregation assay

A thermal aggregation assay was performed as described in Chapter 4, section 4.2.3, with luciferase as the substrate. 15 µl reactions were set up and the assay was carried out with the indicated combination of chaperones (2.1 µg each of Hsc70, HSJ1b and rHH complex) in the presence/absence of ATP. Luciferase (0.8 µM) was incubated with the indicated chaperones in a buffer containing 20 mM Tris-HCl pH 8.0, 50 mM KCl, 3 mM $MgCl_2$ and 2 mM DTT for 5 min at room temperature. The reactions were incubated at 42^{o}C for 10 min. The soluble and aggregated fractions were then separated by centrifugation and analysed by SDS-PAGE electrophoresis. The percentage of luciferase present in the soluble and aggregated fraction was quantified from the gel by densitometry.

5.2.5. Partial proteolysis studies

The protocol used for the partial proteolysis studies has been described in detail in Chapter 4, Section 4.2.5. Briefly, the protein was incubated with trypsin or chymotrypsin at a protease to protein ratio of 1:300 (w/w) in assay buffer containing 20 mM Tris-HCl pH 8.0, 50 mM KCl, 3 mM $MgCl_2$ and 2 mM DTT. ATP was added where required at a concentration of 2 mM. The individual protein concentrations used for the chymotrypsin and trypsin proteolysis experiments have been tabulated in Table 5.1. Chymotrypsin reactions were performed at 4^{o}C for 10 minutes, while trypsin proteolysis was carried out at 25^{o}C for 15 minutes. The reactions were stopped at specified time points by the addition of trypsin inhibitor and proteolysis products were analysed on a 12% SDS-PAGE gel.

Protein	Amount of protein used in µg	
	Chymotrypsin	Trypsin
Hsc70	2.5	NA
HSJ1b	2.5	NA
***In vitro* complex (Hsc70+HSJ1b)**	2.5 of Hsc70 + 2.5 of HSJ1b	4.4 of Hsc70 + 2.2 of HSJ1b
Recombinant complex (rHH)	4.4	4.4

Table 5.1: Amount of protein used for trypsin and chymotrypsin proteolysis reactions.

5.2.6. Size exclusion chromatography

Size exclusion chromatography was performed using a Superdex-200 column. The column was equilibrated with 20 mM Tris-HCl pH 8.0 buffer containing 100 mM potassium chloride,1 mM ATP, 10 mM $MgCl_2$ and 5 mM beta-mercaptoethanol. 214 µg of Hsc70 was incubated with 142 µg of HSJ1b in the presence of 2 mM ATP and 10 mM $MgCl_2$ for 30 minutes and then loaded onto a size exclusion column. 1 ml fractions were collected and alternate fractions were analysed for protein content using Bradford assay. A plot of the absorbance on the y-axis versus the elution volume on the x-axis was used to monitor the chromatography. The peak fractions were also analysed by SDS-PAGE electrophoresis.

5.3. Results

5.3.1. Purification of recombinant Hsc70

For the purpose of protein production, the gene was transformed into *E. coli* BL21(DE3). Cells were grown at 37°C and protein production was induced by the addition of IPTG. Recombinant Hsc70 was isolated by Ni-NTA chromatography. The purified Hsc70 protein was eluted with 200 mM imidazole and analysed by SDS-PAGE electrophoresis (Figure 5.1). Hsc70 eluting from the column was observed migrating at 73 kDa on the gel (lane 5 and 6, Figure 5.1). The elution fractions were pooled and dialysed against buffer containing 20 mM Tris-HCl pH 8.0, 50 mM potassium chloride overnight at 4°C to remove the imidazole content.

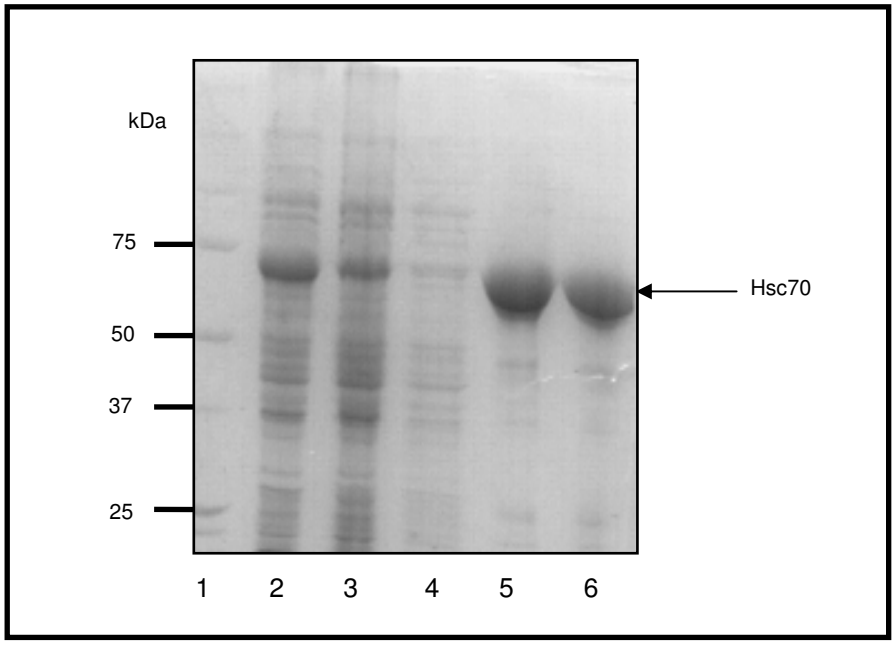

Figure 5.1: Chromatography profile of Hsc70 on Ni-NTA resin

Human Hsc70 was expressed in *E. coli* BL21(DE3) cells by induction with 0.4 mM IPTG for three hours at 37°C. The lysed, soluble extract was applied to a Ni-NTA column, extensively washed with 50 mM Tris-HCl pH 8.0, 250 mM NaCl, 5 mM β-Mercaptoethanol buffer containing 30 mM imidazole and eluted with 50 mM Tris-HCl pH 8.0, 250 mM NaCl, 5 mM β-Mercaptoethanol containing 200 mM imidazole. The polypeptide composition was analysed by SDS-PAGE (12% resolving gel), stained with Coomassie Brilliant Blue and photographed: Lane 1 contains Bio-Rad molecular weight marker, lane2 soluble fraction, lane 3 cell pellet, lane 4 column flow through and lane 5&6 200 mM imidazole elution.

5.3.2. Purification of recombinant HSJ1b

Expression of HSJ1b was carried out in BL21(DE3) cells. Growth was carried out at 37^{o}C and protein expression was induced by the addition of IPTG to a final concentration of 0.4 mM. HSJ1b protein present in the soluble extract was purified by Ni-NTA agarose chromatography. The ~44 kDa HSJ1b protein was eluted with 200 mM imidazole and confirmed by SDS-PAGE analysis (lane 6, Figure 5.2).

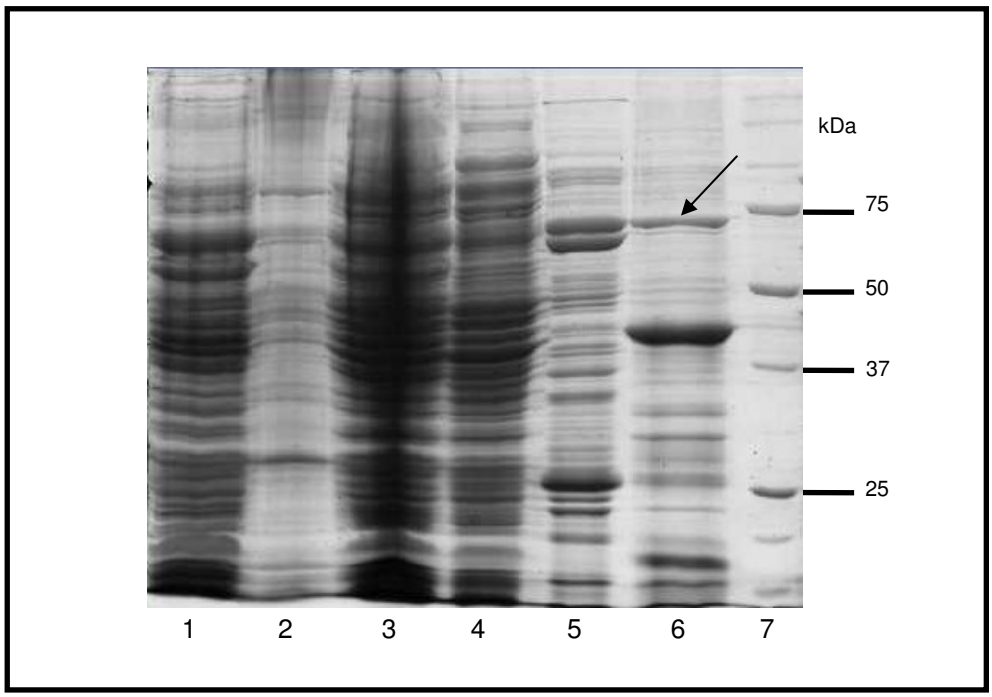

Figure 5.2: HSJ1b purification by Ni-NTA chromatography.

Human HSJ1b was expressed in *E.coli* BL21(DE3) and induced with 0.4 mM IPTG for three hours at 37^{o}C. The lysed, soluble extract was applied to a Ni-NTA column and eluted with buffer 50 mM Tris-HCl pH 8.0, 250 mM NaCl, 5% glycerol containing 200 mM imidazole. The polypeptide composition was analysed by SDS-PAGE (12% resolving gel) and the gel stained with Coomassie Brilliant Blue: lane 1 soluble fraction, lane 2 cell pellet, lane 3 column flow through, lane 4 column wash, lane 5 column wash with 30 mM imidazole, lane 6 200 mM imidazole elution and lane 7 protein molecular weight marker. The ~70 kDa contaminating species is indicated by an arrow.

5.3.3. ATP treatment of HSJ1b

A ~70 kDa band was observed to be co-eluting with the HSJ1b protein eluting from the Ni-NTA column (indicated by an arrow on lane 6, Figure 5.2). Western blot analysis performed on the purified HSJ1b protein using a DnaK antibody confirmed it to be *E.coli* DnaK (data not shown). Chamberlain and Burgoyne, (1997) reported a similar contamination during the expression of recombinant cysteine string proteins. They recommend the use of an Mg.ATP wash step to destabilise this interaction (Chamberlain and Burgoyne, 1997). A similar approach was adopted and an additional wash step with 2 mM ATP was included during the Ni-NTA purification step (data not shown). However this was not effective in removing the ~70 kDa contaminating species. Therefore the protein was first eluted from the Ni-agarose column and then incubated with 1 mM ATP for 30 minutes at room temperature. The ATP treated HSJ1b protein was then diluted two fold to reduce the imidazole content and then bound to a second Ni-NTA column and eluted with 200 mM imidazole.

The elution of the ATP treated HSJ1b protein after Ni-NTA chromatography was assessed on a 12% gel (Figure 5.3). From the gel it was observed that the DnaK species was found in the unbound and wash fractions (lane 2 and 3, Figure 5.3). It was also observed that a fraction of the ATP-treated HSJ1b was present in the flow through fraction (indicated by a * on lane 2, Figure 5.3). This could possibly be due to the fact that the protein was loaded on the column with 50 mM imidazole (after dilution), which might have prevented all of the protein from binding to the Ni agarose. The HSJ1b protein eluting from the column was found to be free from the contaminating ~70 kDa species (lane 5, Figure 5.3). Elution fractions (5-12) were pooled and dialysed against buffer containing 20 mM Tris-HCl pH 8.0, 50 mM potassium chloride overnight at 4^{o}C to remove the imidazole.

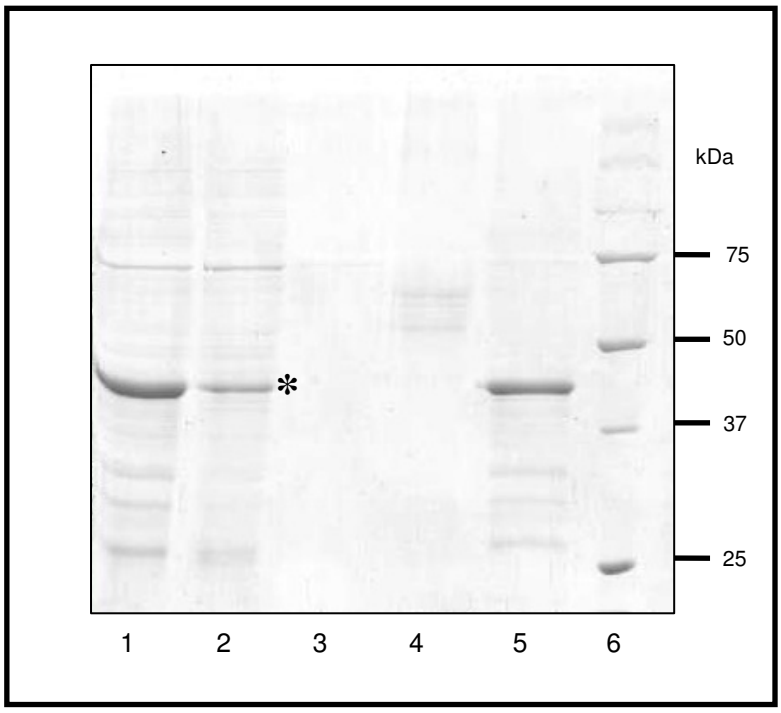

Figure 5.3: Elution profile of ATP treated HSJ1b from Ni-NTA column.

Human HSJ1b purified by Ni-NTA chromatography was incubated with 2 mM ATP, 10 mM $MgCl_2$ and 1 mM DTT for 30 minutes at room temperature. The protein was re-purified by a second Ni-NTA chromatographic step to obtain HSJ1b free from contaminating DnaK protein. The ATP treated HSJ1b protein was diluted two fold with 10 mM Tris-HCl pH 8.0 prior to loading onto a 4 ml Ni-NTA column pre-washed with 10 CV of equilibration buffer (50 mM Tris-HCl pH 8.0, 200 mM NaCl). The column was then washed with 5 CV of equilibration buffer and followed by a second wash with 5 CV of equilibration buffer plus 20 mM imidazole. The protein was finally eluted in 1 ml fractions in 3 CV of equilibration buffer containing 200 mM imidazole. The protein was analysed by SDS-PAGE. Lane 1 ATP treated HSJ1b loaded onto the column, lane 2 column flow through, lane 3 wash, lane 4 column wash with 20 mM imidazole, lane 5 200 mM imidazole elution fractions and lane 6 molecular weight marker proteins. HSJ1b is indicated by an asterisk.

5.3.4. Comparative study on the recombinant complex and the in vitro complex

The dialyzed Hsc70 and HSJ1b proteins were combined at specific ratios (the values are specified in the following sections) and complex formation was initiated by the addition of 2 mM ATP. This reconstituted complex will be referred hence forth as the *in vitro* Hsc70/HSJ1b complex. The recombinant rHH complex was purified as described in Chapter 3. Representative Hsc70 (lane 1, Figure 5.4), HSJ1b (lane 2, Figure 5.4), *in vitro* Hsc70/HSJ1b complex (lane 3, Figure 5.4) and rHH (lane 4, Figure 5.4) proteins samples used in this study were analysed by SDS-PAGE (Figure 5.4). The proteins prepared for the assay were observed to >85% pure, which was deemed sufficient for the following studies. The protein complexes were assessed based on their substrate protection efficiency, conformational properties and Hsc70 polymerisation.

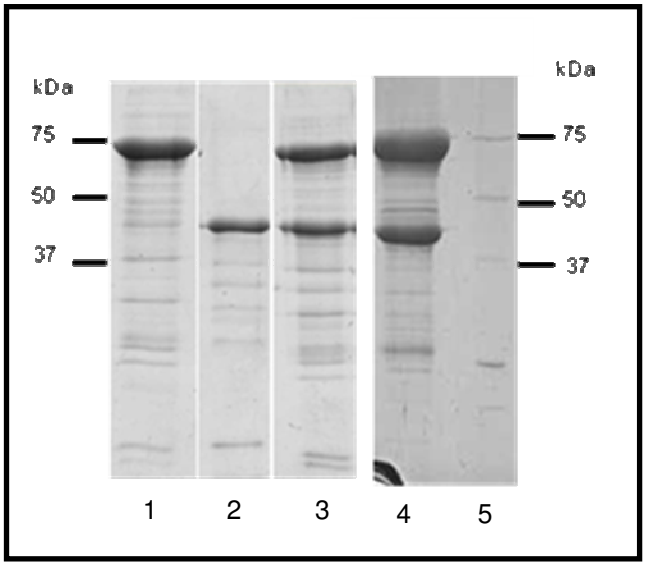

Figure 5.4: SDS-PAGE analysis of the Hsc70, HSJ1b, *in vitro* Hsc70/HSJ1b and rHH proteins.

Hsc70 and HSJ1b Ni-NTA elution fractions were pooled together and dialysed against buffer containing 20 mM Tris-HCl pH 8.0, 50 mM potassium chloride overnight at 4^{o}C. The dialysed proteins were separately concentrated in a 30 kDa cut-off centricon prior to use in assays. The *in vitro* complex was formed by combining Hsc70 and HSJ1b in a 1:1 ratio in the presence of 2 mM ATP. Lane1 is loaded with purified Hsc70 protein, lane 2 is purified HSJ1b protein, lane 3 is the reconstituted *in vitro* complex, lane 4 aliquot of the rHH complex and lane 5 Bio-Rad precision plus prestained molecular weight marker.

5.3.4.1. Prevention of protein aggregation

An efficient test system for chaperone activity is the ability of the chaperone protein to prevent aggregation of a substrate protein (Forreiter and Nover, 1998). According to Minami *et al*., neither the Hsp70 nor the Hsp40 protein alone was capable of protecting substrates such as luciferase from thermal stress. The combined action of a reconstituted Hsp70 and Hsp40 protein system in the presence of ATP was required to maintain luciferase in a soluble state (Minami *et al*., 1996). The thermal aggregation assay was carried out as described in the materials and methods section. The effect of proteins (Hsc70 and HSJ1b), either acting alone or as a complex (*in vitro* or recombinant) on maintaining the solubility of luciferase during heat denaturation was studied. The assays were performed both in the presence/absence of ATP to understand the effect of the nucleotide on the chaperone function. Aggregation of luciferase was induced by elevating the temperature to 42^{o}C. After 10 minutes the reactions were centrifuged to separate the soluble and aggregated fractions. Samples were analysed by SDS-PAGE electrophoresis and the amount of luciferase in each reaction was quantified by densitometry. Figure 5.5 is the plot of the percentage of luciferase detected in the soluble and insoluble fractions for reactions performed with the different chaperone proteins. In Chapter 4, section 4.3.1, we have shown that in the absence of chaperone proteins, 81.4% of luciferase is rendered insoluble at 42^{o}C. The presence of Hsc70 during thermal aggregation protected almost 60% of luciferase (reaction 3, Figure 5.5), while HSJ1b alone protected <50% of luciferase present in the reaction (reaction 1, Figure 5.5). The addition of ATP to these reactions resulted in the detection of an extra 10% luciferase in the soluble fraction (reactions 2 and 4 respectively, Figure 5.5). When Hsc70 and HSJ1b were added together in the absence of ATP, the resulting *in vitro* complex could maintain just over 50% of luciferase in the soluble fraction. The rHH complex prevented almost 85.7% of luciferase from thermal denaturation (reactions 5 and 7, Figure 5.5), a 62% increase compared to the *in vitro* reaction. However when Hsc70 and HSJ1b were added together in the presence of ATP, the resulting *in vitro* complex could maintain >70% of the substrate in the soluble fraction, an additional 20% increase (from 52.3% to 73.6%) in substrate protection. The rHH complex was unaffected by the addition of ATP as reported in Chapter 4 (reactions 6 and 8, Figure 5.5).

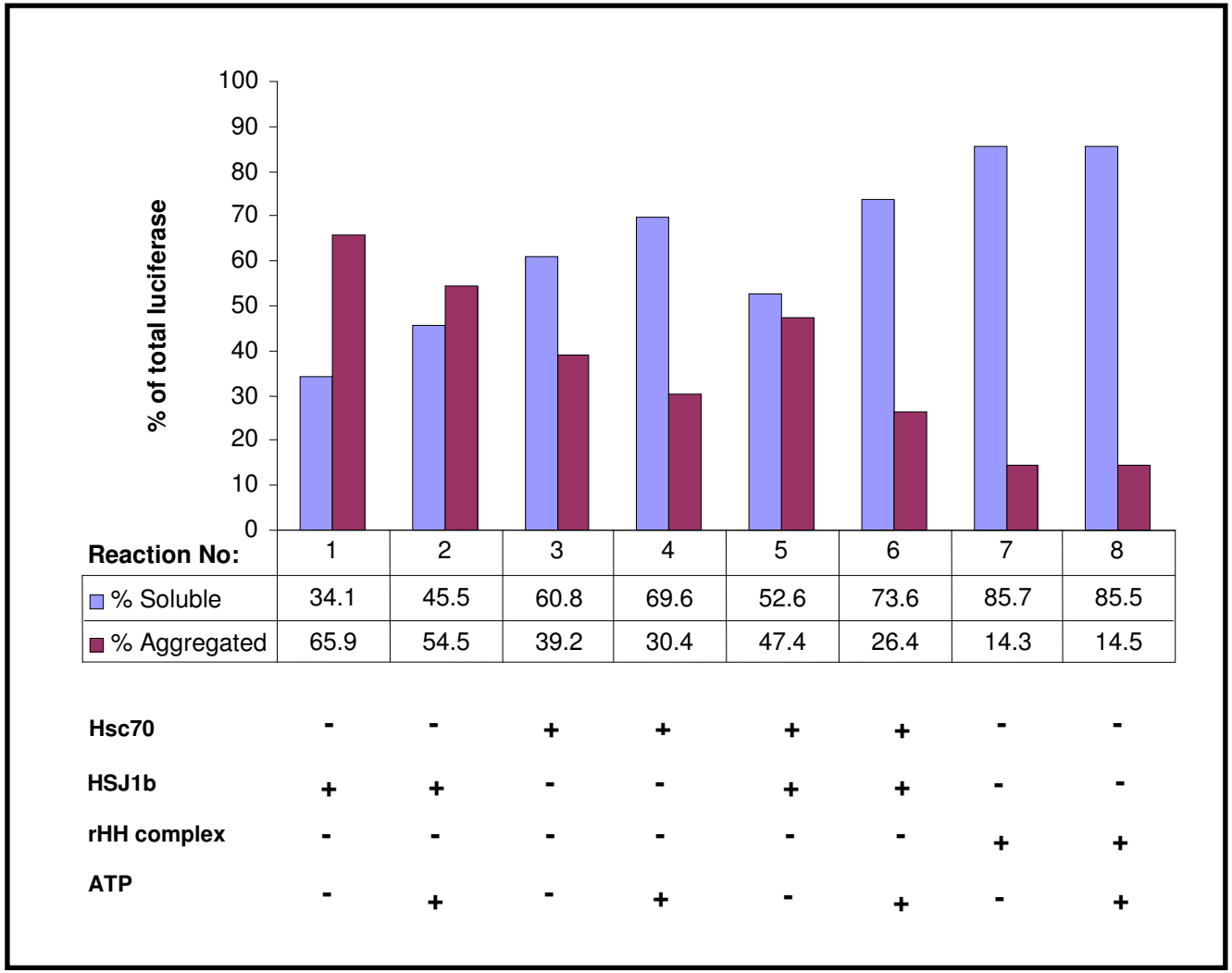

Reaction No:	1	2	3	4	5	6	7	8
% Soluble	34.1	45.5	60.8	69.6	52.6	73.6	85.7	85.5
% Aggregated	65.9	54.5	39.2	30.4	47.4	26.4	14.3	14.5
Hsc70	-	-	+	+	+	+	-	-
HSJ1b	+	+	-	-	+	+	-	-
rHH complex	-	-	-	-	-	-	+	+
ATP	-	+	-	+	-	+	-	+

Figure 5.5: Prevention of protein aggregation studied using Hsc70, HSJ1b, *in vitro* Hsc70/HSJ1b complex and the rHH proteins.

0.8 µm of luciferase was thermally denatured at 42^{o}C for 10 minutes in the presence/absence of the 2.1 µg each of Hsc70, HSJ1b, rHH complex and *in vitro* complex formed by combining 2.1 µg each of Hsc70 and HSJ1b. For the reactions containing ATP, the nucleotide was added at a concentration of 2mM. The reaction was spun down at 13,000 rpm to separate the soluble and aggregated fractions and analysed by SDS-PAGE. The amount of luciferase present in each fraction was quantified by densitometry and the percentage of soluble and aggregated luciferase for each reaction was calculated and plotted on MS Excel.

It was interesting to next look at the effect thermal stress at 42°C had on the solubility of the individual chaperone proteins i.e., Hsc70 and HSJ1b. The amount of Hsc70 and HSJ1b present in the insoluble fraction was measured using as described previously. Figure 5.6 is a plot of the percentage of Hsc70 aggregation during the course of the assay at 42°C. When the reactions were performed with Hsc70 on its own or in the presence of HSJ1b, but in the absence of ATP, almost 27% and 31% respectively of Hsc70 was detected in the pellet fraction of the assay (reactions 1 and 3, Figure 5.6). Addition of ATP to these reactions (reactions 2 and 4, Figure 5.6) marginally improves the Hsc70 solubility. However, Hsc70 from the rHH complex appears to be more resilient to thermal denaturation, as only ~13% of Hsc70 was found in the insoluble fraction and its solubility is not ATP dependent (reactions 5 and 6, Figure 5.6).

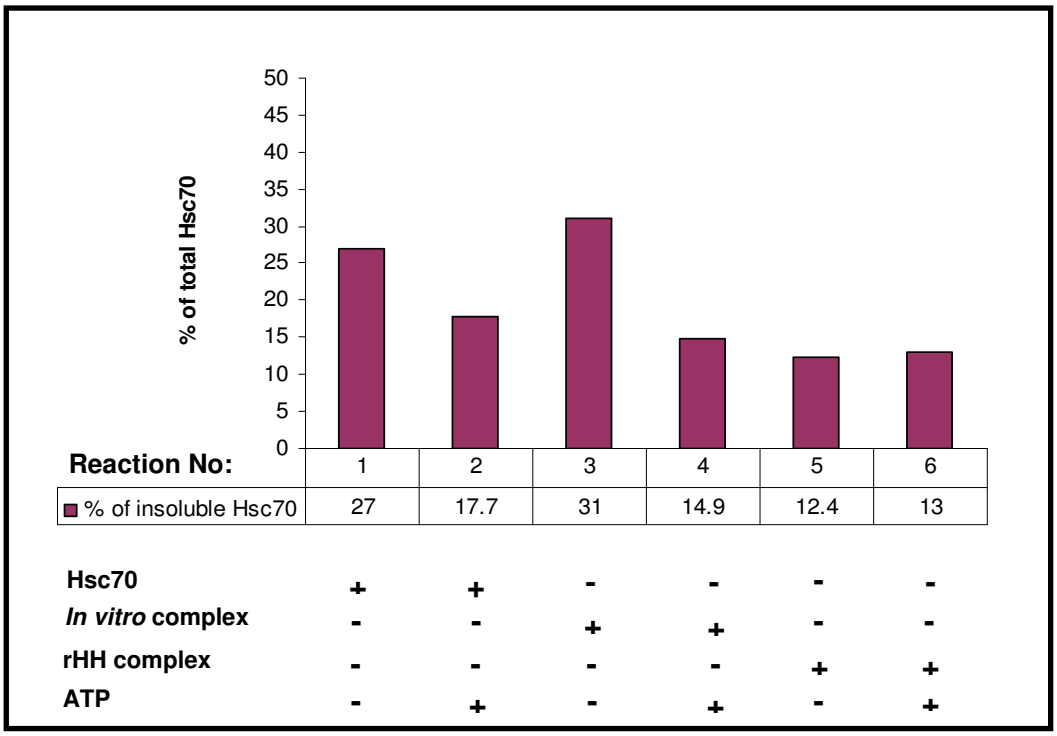

Figure 5.6: Percentage of Hsc70 rendered insoluble during the thermal aggregation assay.

Luciferase was thermally denatured at 42°C for 10 minutes in the presence of the indicated chaperones and 2mM ATP. The reaction was spun down at 13,000 rpm to separate the soluble and aggregated fractions. The insoluble and soluble fractions obtained from the luciferase aggregation assay were analysed on a 12% SDS-PAGE gel. Hsc70 in the insoluble fraction of the gel, for each reaction, was measured using densitometry and plotted as percentage of total Hsc70 present in both the soluble and insoluble fractions.

.

Similarly, the percentage of HSJ1b rendered insoluble during the thermal aggregation was estimated. Figure 5.7 is the graph of the percentage of HSJ1b detected in the insoluble fraction of the assay. In the reaction performed in the presence of only HSJ1b 33.3% of the protein was insoluble (reaction 1, Figure 5.7). A similar percentage of HSJ1b (36.3 %) was aggregated when coupled with Hsc70 but in the absence of ATP (reaction 2, Figure 5.7). Addition of ATP causes only a 3% increase in solubility of HSJ1b when coupled with Hsc70 in the presence of ATP (the *in vitro* complex, reaction 3, Figure 5.7). It appears that the solubility of HSJ1b is unaffected by the presence of its Hsc70 chaperone partner, in the case of *in vitro* complex. HSJ1b complexed as the rHH complex however was 67% less insoluble than its counterpart from the *in vitro* complex. As determined for its Hsc70 partner in the previous section, only ~ 14% of HSJ1b was insoluble (reactions 4 and 5, Figure 5.7).

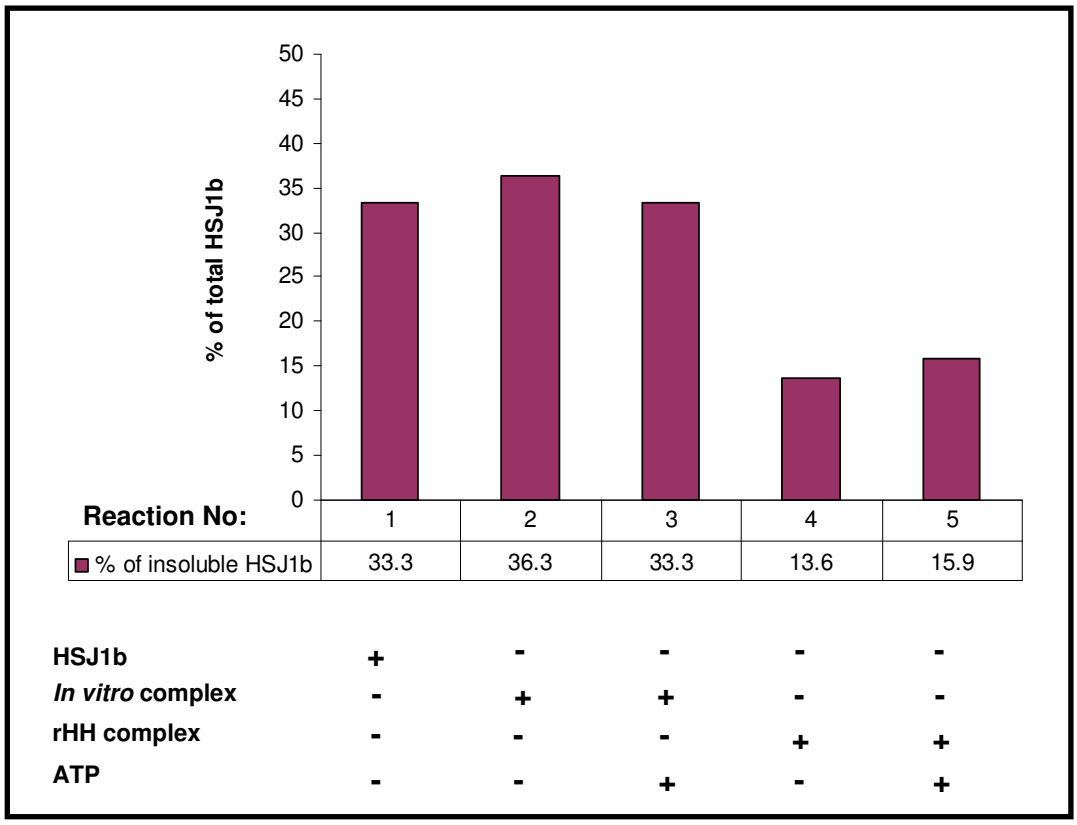

Figure 5.7: Percentage of HSJ1b rendered insoluble during the thermal aggregation assay.

Luciferase was thermally denatured at 42°C for 10 minutes in the presence of the indicated chaperones and nucleotide. The reaction was spun down at 13,000 rpm to separate the soluble and aggregated fractions and analysed by SDS-PAGE. HSJ1b in the insoluble fraction of the gel, for each reaction, was measured using densitometry and plotted as percentage of total HSJ1b present in both the soluble and insoluble fractions.

From the above analysis, a correlation can be shown between the solubility of luciferase and the solubility of both the Hsc70 and HSJ1b proteins. Increased solubility of just the Hsc70 is not sufficient for improving the solubility of luciferase, as was observed with the *in vitro* complex. Higher solubility of both Hsc70 and HSJ1b subunits of the rHH complex may therefore explains the higher levels of luciferase protection observed with the recombinant Hsc70/HSJ1b complex.

From the percentage of soluble substrate (luciferase), Hsc70 and HSJ1b calculated from the previous sections the ratio of interaction between the chaperone-co chaperone –substrate moieties during thermal stress was calculated. The results have been tabulated in Table 5.2.

Reactions		**Actual Ratio**	**Approximated ratio**
Hsc70	**L**	L:H 1:1.2	1:1
	L+ ATP	L:H 1:1.2	1:1
HSJ1b	**L**	L:J 1:2	1:2
***In vitro* complex**	**L**	L:H:J 1:1.3:1.2	1:1:1
	L+ ATP	L:H:J 1:1.2:0.9	1:1:1
rHH complex	**L**	L:H:J 1:1:1	1:1:1
	L+ ATP	L:H:J 1:1:1	1:1:1

Table 5.2: Observed ratio of interaction between Hsc70, HSJ1b and luciferase.

The ratio was obtained using the densitometric values from Figure 5.5 to 5.7. L represents luciferase, H-Hsc70 and J-HSJ1b.

All decimal fractions were approximated to nearest whole number. Observed fractions could be the consequence of using densitometry for the quantification, which is influenced by variation in gel staining and destaining. In both complexes, the three interacting components of the reaction i.e. Hsc70, HSJ1b and luciferase come together in a 1:1:1 ratio. Hsc70 on its own bound to luciferase in a 1:1 ratio and HSJ1b appears to interact in a 2 to 1 ratio with luciferase.

5.3.4.2. Conformational differences

Limited proteolysis experiments were conducted to probe the potential differences in the conformational features of the *in vitro* complex and the recombinant rHH form. The experiment was performed for all four proteins (Hsc70, HSJ1b, the *in vitro* complex and the recombinant complex) using the proteases trypsin and chymotrypsin. Proteolysis of the individual Hsc70 and HSJ1b proteins served as references to decipher changes in the pattern of proteolytic fragments for Hsc70 or HSJ1b as a consequence of complex formation.

Limited proteolysis by chymotrypsin

All four proteins, i.e. Hsc70, HSJ1b, *in vitro* and recombinant complexes were digested by chymotrypsin for 10 minutes at 4^{o}C. The digestion products were visualised by SDS-PAGE electrophoresis (Figure 5.8). Panel A shows the digestion products obtained for Hsc70, panel B for HSJ1b, while panel C and D represent the digestion patterns for the *in vitro* and rHH complexes respectively. From the gel it was observed that although Hsc70 was undergoing proteolysis (as observed by decreasing intensity of the 73 kDa band in lanes 2 and 3, panel A, Figure 5.8) no major proteolysis product could be observed. Detection of minor digestion products was difficult because of the presence of minor contaminating protein species (panel A, lanes 2 and 3, Figure 5.8). However enrichment of a ~ 60 kDa, 50 kDa and ~40 kDa species could be observed (indicated by a * in panel A, lanes 2 and 3, Figure 5.8). HSJ1b on the other hand undergoes very quick proteolysis at 4^{o}C, resulting in a fragment approximately 30 kDa in molecular weight (represented by an arrow mark in panel B, lane 2, Figure 5.8). Chymotrypsin proteolysis of the *in vitro* and recombinant complex results in near identical digestion profiles. In both cases, the Hsc70 component appears to be largely resistant to proteolysis and no proteolysis product indicative of Hsc70 digestion is observed (panel C and D, Figure 5.8. As with the individual HSJ1b proteolysis reactions, in the complexed state also, the HSJ1b subunit was more sensitive to cleavage by chymotrypsin and resulted in a 30 kDa fragment (represented by arrow mark, panel C and panel D, Figure 5.8).

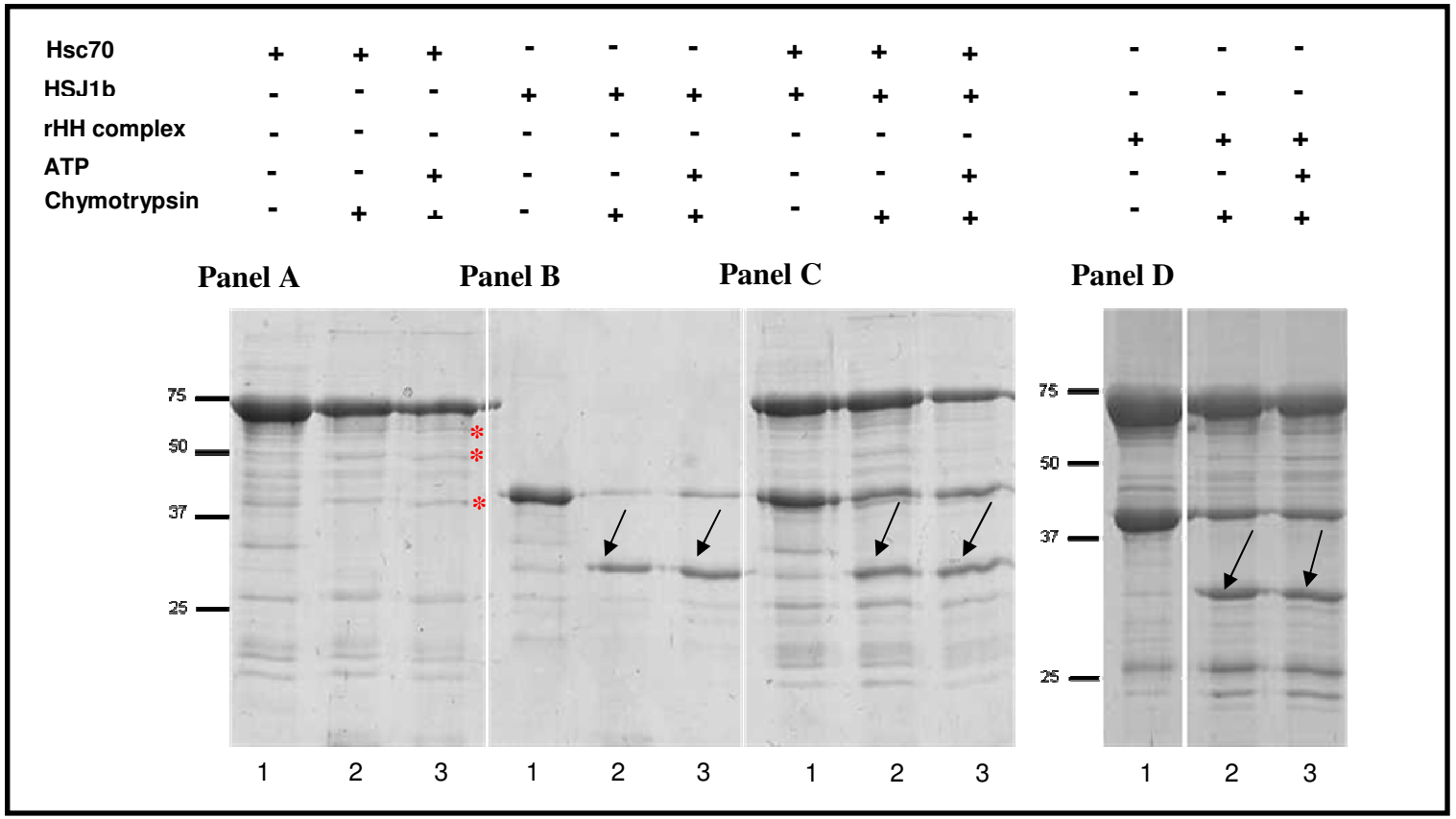

Figure 5.8: Limited proteolysis studies using chymotrypsin protease

2.5 µg of Hsc70, 2.5 µg of HSJ1b, and 4.4 µg of rHH were incubated with chymotrypsin at 4°C in the presence and absence of ATP (2 mM). For the *in vitro* complex 2.5 µg of Hsc70 was combined with 2.5 µg of HSJ1b.The digestions were performed in buffer containing 20 mM Tris-HCl pH 8.0, 50 mM potassium chloride, 3 mM magnesium chloride and 2 mM DTT for 10 min. The digestion products were analysed on a 12% polyacrylamide gel stained with Coomassie Blue. The first track on the left hand side (lane 1) in each panel is the control protein in the absence of chymotrypsin. Lane 2 in each panel is the proteolysis performed in the absence of ATP and lane 3 in the presence of ATP. Panel A: Chymotrysin digestion of Hsc70. Panel B: Chymotrysin digestion of HSJ1b. Panel C: Chymotrysin digestion of the *in vitro* complex. Panel D: Chymotrysin digestion of rHH complex. The arrowhead indicates the putative digestion product of HSJ1b. The * indicates the putative digestion product of Hsc70.

In order to determine if the state of association between Hsc70 and HSJ1b altered their sensitivity to chymotrypsin, densitomeric tracing of the uncleaved Hsc70 and HSJ1b protein remaining following partial chymotrypsin digestion was calculated. Hsc70 either on its own or as a complex (*in vitro* or rHH) did not show any visible signs of proteolysis and no major proteolysis product could be detected on the SDS-PAGE. Despite this almost ~65% of uncomplexed Hsc70 remains uncleaved in the absence of ATP. This is reduced to 46% upon addition of ATP to the proteolysis reaction. This suggests that in the presence of ATP, the Hsc70 protein's open conformation is more accessible to chymotrypsin digestion. For the *in vitro* complex, when Hsc70 was combined with HSJ1b in the absence of ATP, 84.7% of Hsc70 was undigested. Addition of ATP causes a 58% increase in cleavage of Hsc70, suggesting that the *in vitro* complex of Hsc70 and HSJ1b in the presence of ATP adopts an open conformation. In contrast, 86 % of the Hsc70 subunit from the rHH complex in the absence of ATP, and, 77% in the presence of ATP was resistant to chymotrypsin proteolysis. This suggests that the Hsc70 subunit of the rHH complex adopts an alternate conformation compared to that of the free Hsc70 and the *in vitro* complex.

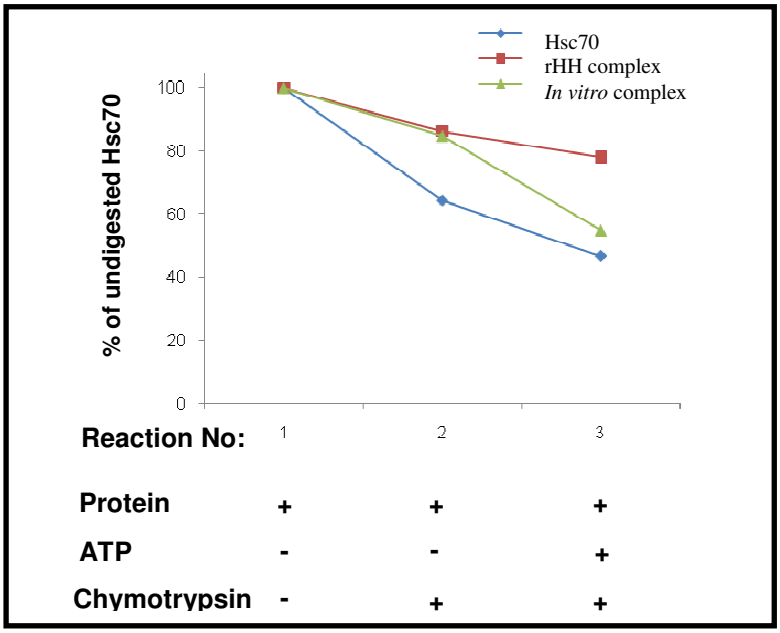

Figure 5.9: Densitometric analysis of undigested Hsc70 after proteolysis by chymotrypsin

Partial proteolysis by chymotrypsin was performed as described in section 5.2.4 and the digestion products were analysed on a 12% polyacrylamide gel stained with Coomassie Blue. Densitometric traces of the Hsc70 subunits from the gel (using figure 5.8) allowed the quantification of the amount of Hsc70 undigested as a percentage of Hsc70 protein in the control reaction. Reaction 1 is the amount of protein in the control reaction not treated with the protease and is assigned 100%, reaction 2 is chymotrypsin proteolysis performed in the absence of ATP and reaction 3 chymotrypsin proteolysis performed in the presence of 2mM ATP.

Similarly using densitometry, the percentage of undigested HSJ1b protein was measured for all three reactions (Figure 5.8). Almost 82% of HSJ1b was degraded down to its ~30 kDa fragment when proteolysis was performed in the absence of Hsc70. Irrespective of the nature of the complex (*in vitro* or recombinant) the presence Hsc70 chaperone partner reduced the rate of proteolysis of HSJ1b. In the absence of ATP, almost 54% of HSJ1b from the *in vitro* complex remained undigested, which was just 7% higher than that observed for the recombinant complex (reaction 2, figure 5.8). The presence of ATP during proteolysis increased the sensitivity of HSJ1b of the *in vitro* complex by 20% (reaction 3, figure 5.8). Thus susceptibility of HSJ1b to proteolysis appears to reduce in the presence of its Hsc70 partner.

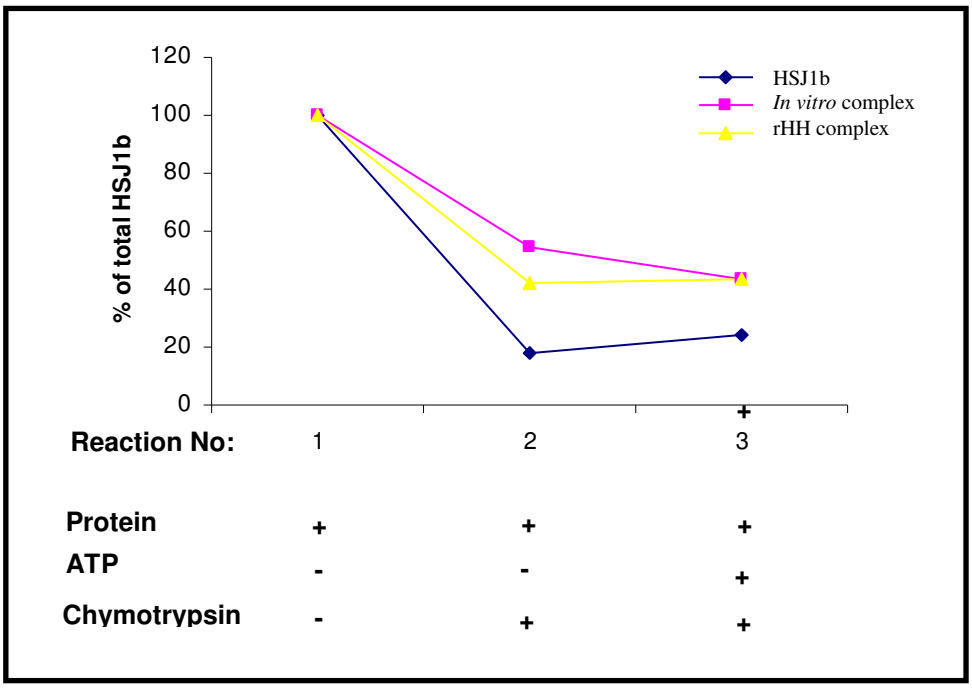

Figure 5.10: Densitometric analysis of undigested HSJ1b after proteolysis by chymotrypsin

Partial proteolysis by chymotrypsin was performed for 10 minutes at 4°C in the presence and absence of ATP (2 mM). The digestion products were analysed on a 12% polyacrylamide gel stained with Coomassie Blue. Densitometric traces of the HSJ1b fractions from the SDS-PAGE gel (using figure 5.8) allowed comparison of the amount of HSJ1b left undigested at the end of the proteolysis reaction as a percentage of HSJ1b protein in the control reaction. Reaction 1 is the amount of protein in the control reaction not treated with the protease and is assigned 100%, reaction 2 is chymotrypsin proteolysis performed in the absence of ATP and reaction 3 chymotrypsin proteolysis performed in the presence of 2mM ATP.

Limited proteolysis by trypsin

Since the proteolysis experiment with chymotrypsin was inconclusive, proteolysis with trypsin were undertaken. Reactions were performed at 25^{o}C in the presence and absence of ATP as per the protocol of Chamberlain and Burgoyne (Chamberlain and Burgoyne, 1997) and the proteolysis fragments were assessed as described in the previous section. Trypsin digestion of the *in vitro* complex in the absence of ATP resulted in 4 major polypeptide species (Figure 5.11). The first species was observed migrating very close to the undigested Hsc70 protein species at 73 kDa (as seen in panel A, comparing the control in lane 1 to the trypsin treated samples in lane 2 and 3, Figure 5.11). Another three groups of proteolytic cleavage products migrated at approximately 60 kDa, 52-55 kDa and 40-44 kDa. Addition of ATP did not make any difference to the sensitivity of the *in vitro* complex to tryptic digestion (lane 2, panel A, Figure 5.11).

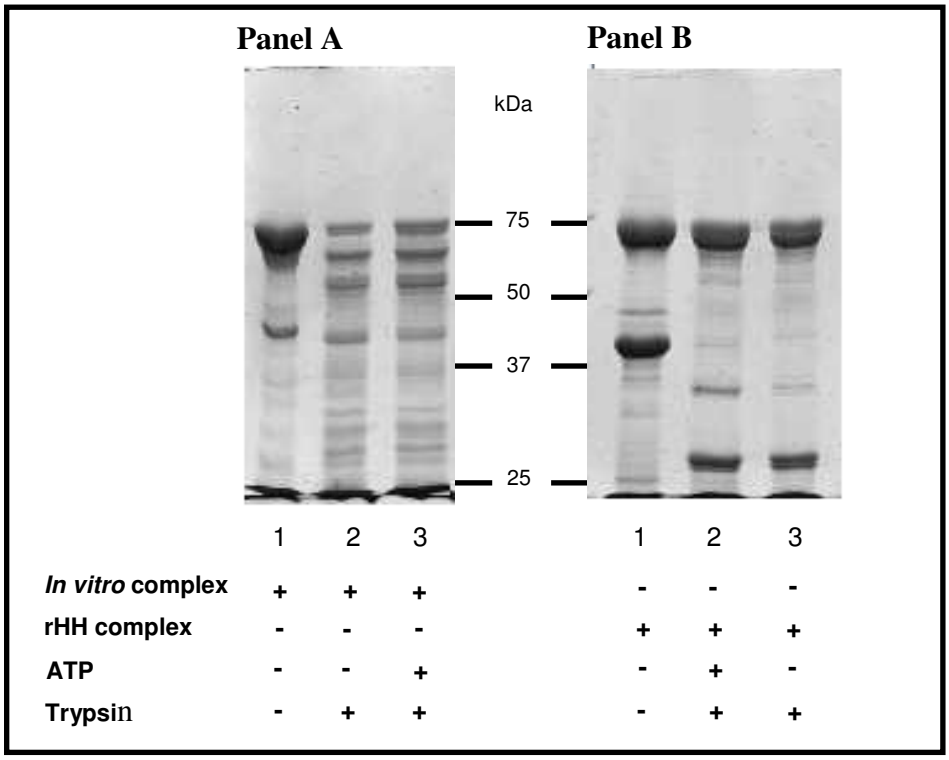

Figure 5.11: Limited proteolysis studies of the *in vitro* and rHH proteins using trypsin protease

The two complexes were incubated with trypsin in a ratio of 1:300 (w/w) for 15 minutes at in the presence and absence of ATP (2 mM). The digestion products were analysed on a 12% polyacrylamide gel stained with Coomassie Blue. Panel A: Trysin digestion of the *in vitro* complex. Panel B: Trysin digestion of rHH complex. The first track on the left hand side in each panel is the control protein in the absence of trypsin. Lane 2 in each panel is the proteolysis performed in the absence of ATP and lane 3 in the presence of ATP.

Similarly, the rHH complex was subjected to partial proteolysis by trypsin and the digestion products were analysed by SDS-PAGE electrophoresis (panel B Figure 5.11). Contrary to what was observed for the *in vitro* complex, Hsc70 of the rHH complex was resistant while HSJ1b was more sensitive to trypsin. Two main groups of proteolytic cleavage products were detected; one migrating at 73 kDa and the other at 25 - 27 kDa. A close examination of the 73 kDa band reveals that the band actually comprises of two closely migrating species rather than one (lane 3, panel B, Figure 5.11). This was similar to the observations made on the *in vitro* complex. Addition of ATP causes subtle changes in the digestion pattern. An additional cleavage product migrating at approximately 30 kDa is observed (lane 2, panel B, Figure 5.11).

The striking difference between the *in vitro* and the rHH complexes is the sensitivity of Hsc70 to proteolysis. The percentage of undigested Hsc70 protein in both the complexes was calculated (Figure 5.12). In the absence of ATP, almost 73% of Hsc70 from the rHH complex remained undigested compared to only 28.2% observed for the *in vitro* complex (reaction 2, Figure 5.12). The addition of ATP increased the amount of undigested Hsc70 of the *in vitro* complex to 41.9%, while the effect of ATP on the Hsc70 subunit of the rHH complex was negligible (~2%, reaction 3, Figure 5.12). A similar comparison on the sensitivity of the HSJ1b fraction could not be made because of the ambiguous nature of the identity of the 40-44 kDa species present in the proteolysis reaction of the *in vitro* complex. It has been reported that one of the proteolysis fragments resulting from trypsin digest of DnaK migrates at 40-44 kDa (Liberek *et al*., 1991). This coincides with the migration position of the HSJ1b protein itself.

An important conclusion that can be drawn from the trypsin proteolysis is the apparent difference in the assembly of HSJ1b with respect to HSc70 for the two complexes. From the proteolysis it is apparent that the conformation adopted by the rHH complex renders Hsc70 less susceptible to proteolytic attack by trypsin, contrary to what was observed for the *in vitro* complex.

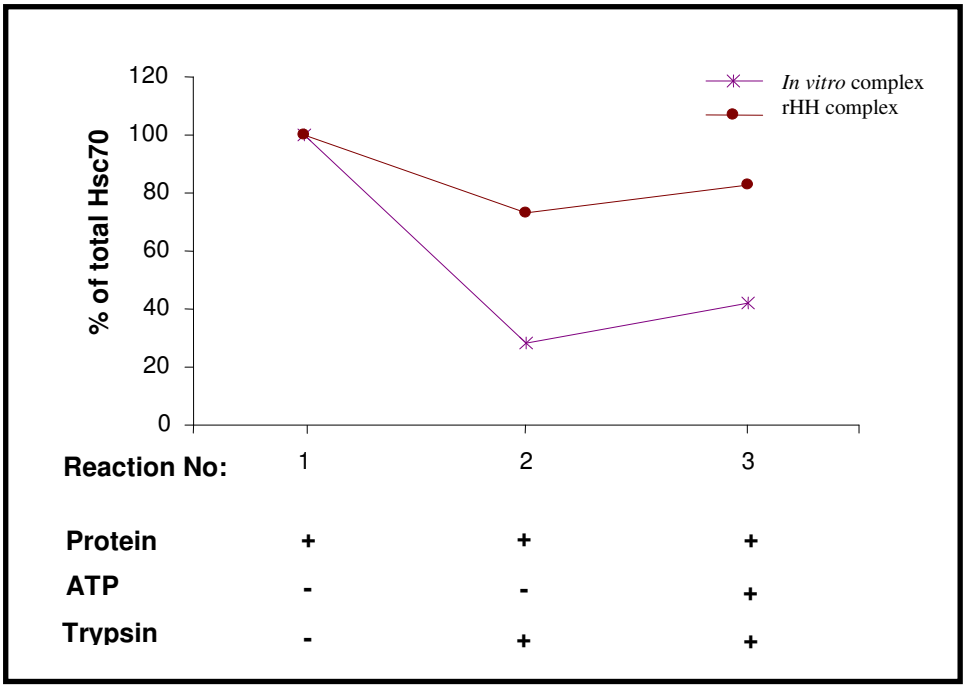

Figure 5.12: Densitometric analysis of Hsc70 left undigested after trypsin digestion of the *in vitro* and recombinant complex.

Partial proteolysis by trypsin was performed for 15 minutes at 20°C in the presence and absence of ATP (2 mM). The digestion products were analysed on a 12% polyacrylamide gel stained with Coomassie Blue. Traces for the Hsc70 fractions were plotted from denstometric analysis of the SDS-PAGE gel and compared with the percentage of Hsc70 present in the reaction prior to digestion (reaction 1). Reaction 2 is trypsin reaction performed in the absence of ATP and in the presence of ATP (reaction 3).

5.3.5. Oligomerisation studies

We next decided to study by size exclusion chromatography the extent of oligomerisation and complex formation when Hsc70 and HSJ1b were reconstituted as an *in vitro* complex. Hsc70 and HSJ1b were combined in 2:1(w/w) in the presence of ATP and loaded onto a Superdex-200 column. The column was equilibrated in the buffer specified in section 5.2.6 and the chromatography was performed in buffer containing ATP (Panel A, Figure 5.13). As observed for the rHH complex, a peak corresponding to the polymerised Hsc70/HSJ1b complex was observed in the void volume (represented as peak 1 on the chromatogram in panel A of Figure 5.13). In contrast to the well resolved ~220kDa peak obtained for the rHH, the peak in the included volume for the *in vitro* complex was poorly resolved and extended over almost 16 ml from fraction 48-60 ml and an additional shoulder peak eluting from 60-72 mls (represented as peak 2 on the chromatogram in panel A of Figure 5.13). This suggests a degree of instability in the interactions of the protein components. However analysis of the fractions obtained from the Superdex-200 column by SDS-PAGE (Panel B, Figure 5.13) confirms the presence of both the Hsc70 and HSJ1b subunits in both the resolved peaks. Visual inspection of the SDS gel revealed that although both Hsc70 and HSJ1b subunits co-fractionate together in both elution peaks for both the complexes, the stoichiometry of the two subunits for the two peaks were different. In peak 1 the Hsc70 and HSJ1b subunits appear to be in a 1:1 ratio (Lanes 1-4, Panel B, Figure 5.13), while for peak2, this ratio appears to varying across the fractions for the *in vitro* (Lanes 5-9, Panel B, Figure 5.13), which reiterates our doubts regarding the stability of this fraction.

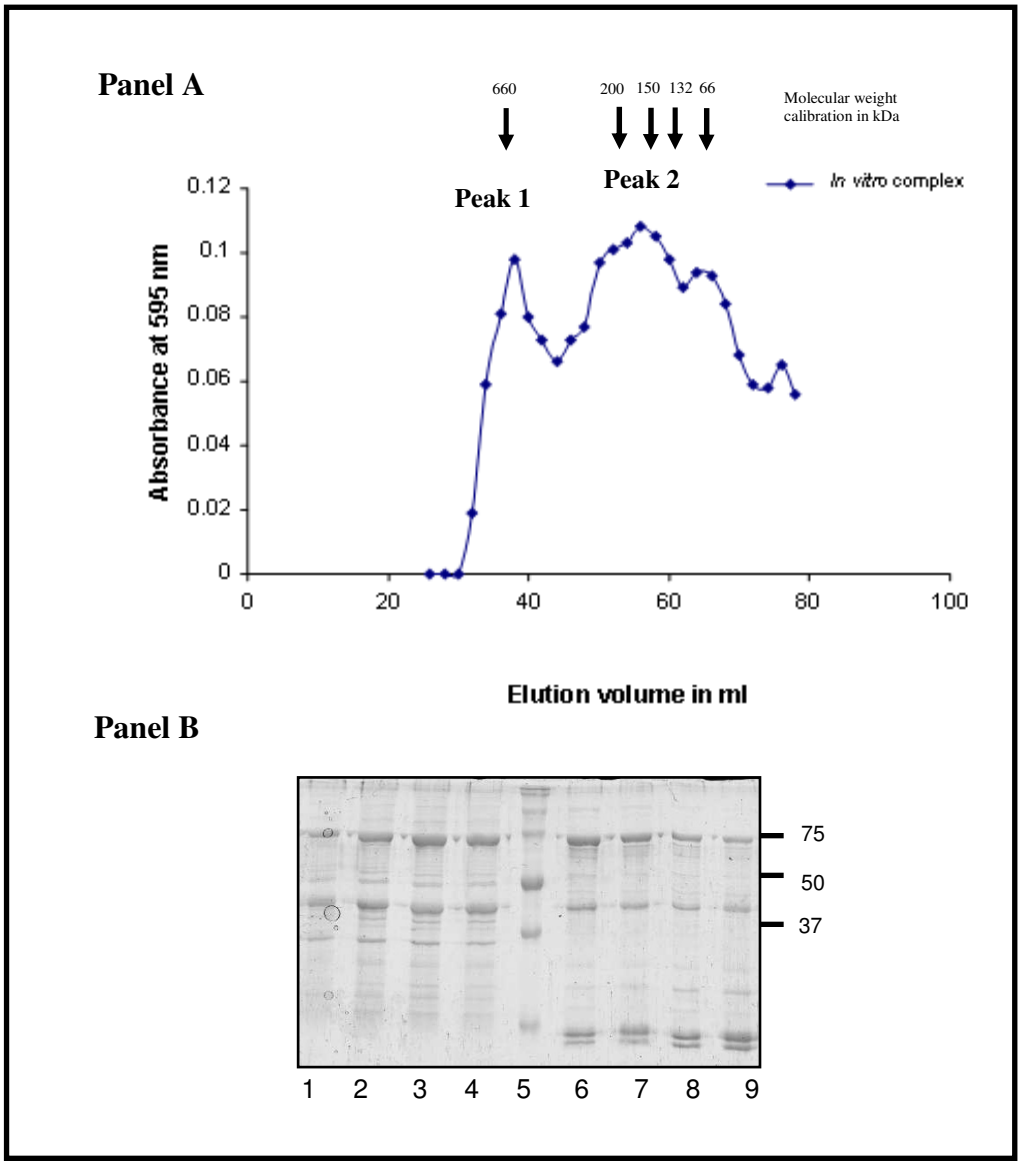

Figure 5.13: Oligomeristion studies of the *in vitro* complex using size exclusion chromatography

Size exclusion chromatography was performed on a Superdex-200 column. Hsc70 and HSJ1b were combined in the presence of ATP and loaded onto the column. The column was equilibrated in the buffer specified in section 5.2.6 and the chromatography was performed in buffer containing ATP. The protein eluting from the column was collected as 1 ml fractions. The absorbance of each fraction was determined using Bradford assay. Plot of absorbance at 595 nm for the fractions on the Y-axis versus the elution volume (X-axis) was used to develop the elution profile chromatogram.
Panel A: Elution profile of the *in vitro* complex from the Superdex-200 column.
Panel B: SDS-PAGE analysis of the elution of the *in vitro* complex from the gel filtration column
Lanes 1-4 fractions 36-39, lane 5 is the Bio-Rad precision plus prestained molecular weight marker (broad range) and lanes 6-10 are fractions 56-59.

In order to confirm that an *in vitro* complex was indeed formed, SEC of the purified recombinant chaperones. Hsc70 and HSJ1b was performed and compared with the elution profiles for rHH and *in vitro* complex. HSJ1b (figure 5.14, trace in teal) primarily eluted as a dimer, but approximately 50% of the protein was detected in the void volume, suggesting protein aggregation. Similarly, a large proportion of Hsc70 (Figure 5.14, trace in blue) was also aggregated and detected in the void volume. The rest of the Hsc70 protein eluted as a broad unresolved peak corresponding to species having a molecular mass of approximately 150-250 kDa. The formation of an *in vitro* complex between Hsc70 and HSJ1b in the presence of ATP did not result in the appearance of a distinct additional peak which would suggest that Hsc70 and HSJ1b assemble and interact in an ATP-dependent manner. Instead peak 2 was broad and extended over more than 20 ml, and overlapping, when compared, with both the individual Hsc70 and HSJ1b elution profiles (indicated by arrow marks in panel B in Figure 5.14). This again gives credence to our doubts regarding the stability of the interaction of the Hsc70 and HSJ1b *in vitro* complex.

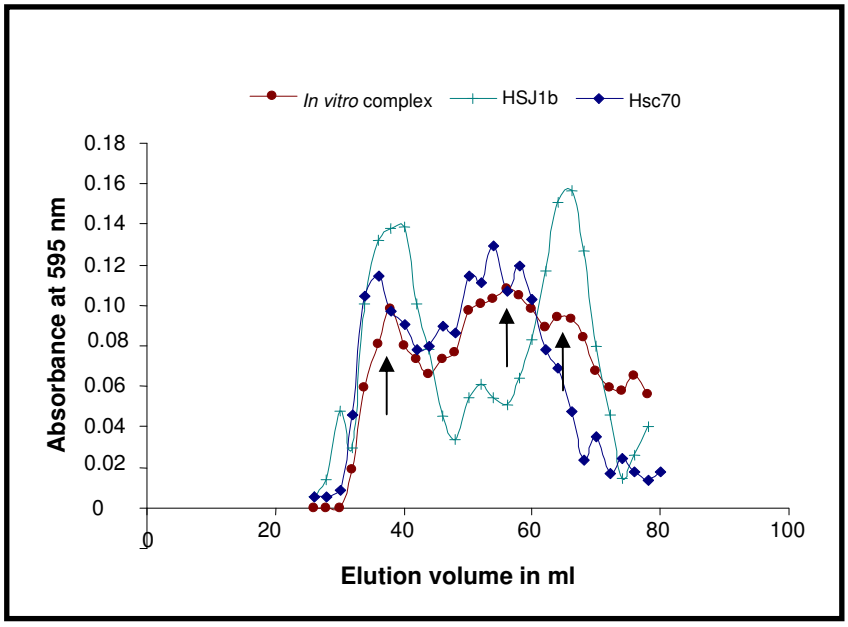

Figure 5.14: Comparison of the elution profile of Hsc70 and HSJ1b with the *in vitro* complex.

Size exclusion chromatography was performed on a Superdex-200 column. 50 µg of Hsc70 and HSJ1b were separately loaded onto the column. The column was equilibrated and run in 20 mM Tris-HCl pH 8.0 plus 100 mM potassium chloride. 1 mL fractions were collected after 25 ml of buffer had passed. Absorbance of each fraction was determined using Bradford assay. The elution chromatograms for Hsc70 and HSJ1b were then superposed with the elution profile obtained for the *in vitro* complex (ref Figure 5.13).

Similarly the elution profile of the rHH complex was compared with the individual profiles of Hsc70 and HSJ1b (Figure 5.15). In Chapter 4, from SEC analysis, the rHH protein was determined to be composed of two protein fractions; one a very large species in the void volume and the second a dimer of a heterodimer at ~ 220 kDa. Upon comparison with the elution profiles of individual Hsc70 (Figure 5.14, trace in blue) and HSJ1b polypeptides (Figure 5.15, trace in teal), it was observed that the elution position of the 220 kDa fraction, overlapped partly with the Hsc70's broad elution peak, but not with that of the HSJ1b elution. However SDS-PAGE analysis performed in chapter 4 has confirmed the presence of both Hsc70 and HSJ1b subunits, thereby indicating that the ~220 kDa species represents a distinct additional peak bought about by the assembly and interaction of Hsc70 and HSJ1b into a dimer of a heterodimer.

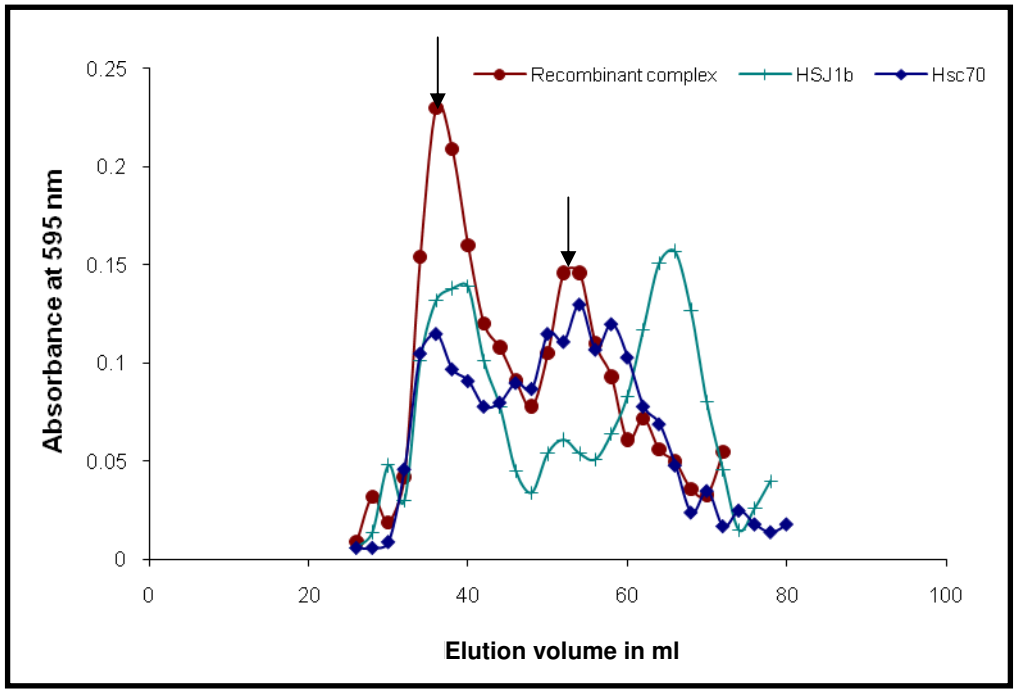

Figure 5.15: Comparison of the elution profile of Hsc70 and HSJ1b with the rHH complex on SEC.

Size exclusion chromatography was performed on a Superdex-200 column. 50 µg of Hsc70 and HSJ1b were separately loaded onto the column. The column was equilibrated and run in 20 mM Tris-HCl pH 8.0 plus 100 mM potassium chloride. 1 mL fractions were collected after 25 ml of buffer had passed. Absorbance of each fraction was determined using Bradford assay. The elution profiles of Hsc70 and HSJ1b were then superposed with the elution profile obtained for the rHH complex (ref Figure 4.16).

In Chapter 4, analytical ultracentrifugation confirmed that the elution peak in the void was apparently a non-aggregated higher order oligomer. This oligomeric fraction may be attributed to the polymerisation effect of Hsp40 proteins on Hsp70 (King *et al*., 1995). In the absence of AUC data for the *in vitro* complex, it is difficult to determine if the first peak obtained for the *in vitro* complex is an aggregate or a non-aggregated higher order oligomer as determined for the rHH protein. Working on the assumption that it represented non-aggregated protein, the differences in oligomerisation composition between the rHH and *in vitro* protein complexes was quantified. Panel A in Figure 5.16 is a superposition of the elution profiles of the *in vitro* and rHH complexes from the Superdex 200 column, and the boundaries used to demarcate the two peaks have been indicated by the boxed area. Peak 1 has been defined by the blue box and peak 2 has been defined by the red box. The area under the curve for the two peaks was calculated using this boxed area and the values plotted as percentage of total protein in peak1 and peak 2 (panel B, Figure 5.16). Interestingly for the rHH complex the percent of protein eluting as the highly oligomerised peak 1 (panel B, Figure 5.16) was almost two times that occupied by peak 1 of the *in vitro* complex (64% and 38% respectively). The exact opposite relation was observed for the peak 2 (panel B, Figure 5.16); the *in vitro* complex predominantly exists as the non aggregated form (62%) as opposed to the 38% calculated for the rHH protein (Figure 5.16). However the correlation between the greater oligomerisation and the observed functional superiority of rHH is not yet clear.

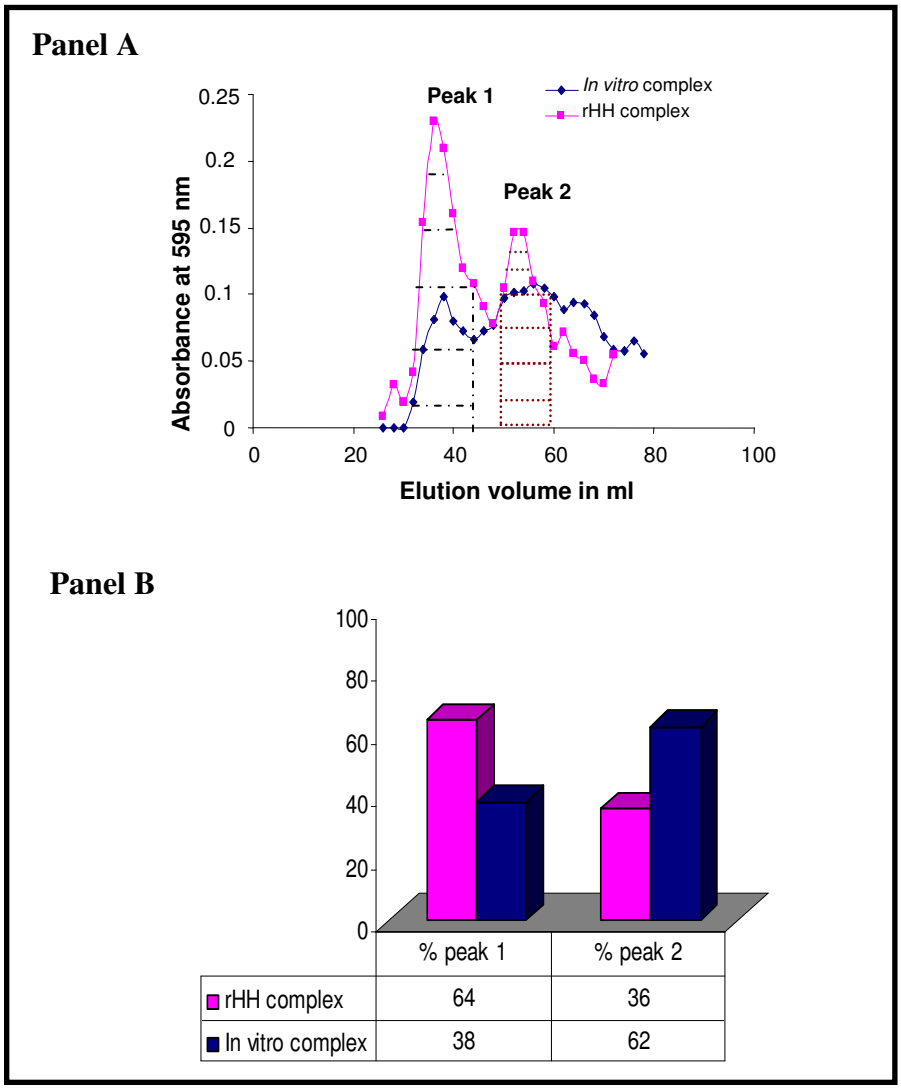

Figure 5.16: Proportion of rHH and *in vitro* complex as peak 1 and peak 2.

Size exclusion chromatography was performed on a superdex 200 column. The column was equilibrated and run in 20 mM Tris-HCl pH 8.0 plus 100 mM potassium chloride. 1 mL fractions were collected after 25 ml of buffer had passed. Absorbance of each fraction was determined using Bradford assay.

Panel A: Comparison of the elution profile of the *in vitro* complex with the rHH complex.

Panel B: Distribution of the two peaks for the two complexes was determined by calculating the area under the peaks.

5.4. Discussion

The interactions between the HSP40 and HSP70 families have been widely studied using a reconstituted Hsp70/Hsp40 *in vitro* system. Mammalian Hsc70/Hsp40, yeast Ssalp/Ydjlp and the Hsc70/Csp are just a few examples of the chaperone/co-chaperone complexes studied using this method (Levy *et al*., 1995; Minami *et al*., 1996; Chamberlain and Burgoyne, 1997). Usually, the *in vitro* complex is formed by combining the individual purified HSP70 and HSP40 family members. Complex formation is driven by the addition of ATP which initiates the formation of an Hsp70-Hsp40 complex driven by the hydrolysis of ATP by the Hsp70 moiety (Russell *et al*., 1999). In this chapter a comparative study of the recombinant rHH complex and the *in vitro* complex was carried out.

To generate an *in vitro* complex, Hsc70 and HSJ1b proteins had to be independently purified. The *Hsc70* and *HSJ1b* genes cloned into the pET-16b vector were successfully over-expressed in *E.coli*. The proteins were expressed with a 10 X histidine tag, such that both proteins could be purified using Ni-NTA chromatography. HSJ1b required an additional purification step to remove a major contaminating protein species at 70 kDa. This was confirmed to be the *E.coli* Hsp70 chaperone protein, DnaK. Chamberlain and Burgoyne, (1997) reported a similar contamination during the expression of recombinant cysteine string proteins (Chamberlain and Burgoyne, 1997). An additional Mg.ATP wash step in the Ni-NTA chromatography was unsuccessful in eliminating all the contaminating protein. HSJ1b was therefore eluted from a preliminary Ni-NTA column and then treated with Mg.ATP for an extended period of time. The ATP treated HSJ1b protein was separated from the contaminating DnaK species by an additional Ni-NTA chromatographic step. HSJ1b isolated by this method was observed to be free from DnaK contamination. Purified Hsc70 and HSJ1b proteins were reconstituted together to form an *in vitro* complex and studied along with the rHH complex from Chapter 3. The two complexes differed in two aspects. The first being the HSJ1b subunit in the rHH complex is untagged, while HSJ1b for the *in vitro* complex retains the 10 X histidine tag. However previous studies have reported that both the His tagged and untagged Hsp40 behaved identically in functional assays (Minami *et al*., 1996). Therefore we decided against cleaving the His tag from the recombinant HSJ1b and proceeded to use the His tagged HSJ1b

protein. The second difference was that the *in vitro* complex was formed by combining the dialysed Hsc70 and HSJ1b proteins; whereas the rHH protein was not dialysed and contained 200 mM imidazole used for the Ni-NTA elution. However we have observed that the presence of imidazole or its removal by dialysis does not influence the functioning of the rHH complex (determined using the thermal aggregation assay, data not shown). Based on this reasoning, it was decided that these differences will not influence or bias the results of our study.

Suppression of substrate aggregation is an essential chaperone activity (Forreiter and Nover, 1998). The functional efficiency of the *in vitro* and recombinant complexes was investigated by a thermal aggregation assay. Firefly luciferase has been used routinely as the substrate protein for such aggregation studies, where the elevation of temperatures to 42^{o}C causes aggregation of luciferase. This aggregation can be reduced by the presence of chaperone proteins (Minami *et al*., 1996; Glover and Lindquist, 1998; Wang and Spector, 2001). Using thermal aggregation assays Minami *et al*., 1996 have studied the regulation of mammalian Hsc70 by the DnaJ homologue (HDJ1). They reported that the reconstituted Hsc70/HDJ1 complex exhibited an ATP dependent increase in luciferase protection levels. In the presence of ATP, the Hsc70/HDJ1 complex's luciferase protection was enhanced by approximately two fold (Minami *et al*., 1996). In contrast to these finding, it was observed that the protection capability of the rHH complex used in this study was not nucleotide dependent. The recombinant chaperone complex was successful in protecting (85%), of luciferase which was unaffected by the addition of ATP. Luciferase protection by the individual Hsc70 and Hsc70/HSJ1b *in vitro* complex was consistent with the observations of Minami *et al*. and exhibited an ATP induced increase in luciferase protection. The observed increase in protection was however not as dramatic as the two fold increase reported by Minami *et al*.

Hsc70 and Hsc70/HSJ1b *in vitro* complex proteins exhibited substrate protection even in the absence of ATP (60.8% and 52.6% respectively). A possible explanation for this observation could be the purification protocol used for the isolation of Hsc70. Minami *et al*., purified Hsc70 from bovine brain following the original protocol reported by Schlossman *et al.* This method recommends treating the purified Hsc70 with EDTA to improve the ATP dependent activity of the extracted Hsc70 protein (Schlossman *et al.,*

1984). Hsc70 used during the course of this study was expressed recombinantly in *E.coli* and purified by single step Ni-NTA chromatography. Therefore the purified protein might comprise of a mixed population of ATP dependent and independent forms, explaining the observation of functional activity in the absence of ATP.

Recombinant HSJ1b protein used in this study was also found to be capable of maintaining up to 35% of luciferase soluble, suggesting that HSJ1b can possibly functional as a chaperone on its own merit. Though the mammalian DnaJ homologue (Hdj1) was unable to function as a chaperone (Minami *et al*.,), other Hsp40's such as the *E.coli* DnaJ have been shown to behave as chaperones (Szabo *et al*., 1996; Langer *et al*., 1992). However further investigation is required to confirm HSJ1b's chaperone capabilities.

A correlation was observed between the solubility of the individual Hsc70 and HSJ1b subunits and the solubility of luciferase. For the *in vitro* complex the percentage solubility of Hsc70 subunit was directly proportional to the solubility of luciferase. Addition of ATP results in an increase in solubility of Hsc70 which translates into increased solubility of the substrate. Most interesting was that this did not result in an increased solubility of its co-chaperone partner-HSJ1b. This raises an interesting question on the role of HSJ1b during substrate protection in the *in vitro* form of the complex in the presence of ATP. The Hsc70 and HSJ1b proteins involved in forming the rHH complex were more resilient to higher temperatures, with almost 85% of both the proteins present in the soluble fraction. Thus a higher solubility of both Hsc70 and HSJ1b is required for the higher levels of luciferase protection as observed with the recombinant Hsc70/HSJ1b complex. This could explain the observed difference in luciferase protection between the two complexes.

This then raises questions on the possible differences in the mechanism of interaction of the Hsc70 and HSJ1b proteins of the *in vitro* and rHH complex with the denatured substrate. Formation of the *in vitro* complex is initiated by the addition of ATP and the Hsc70/HSJ1b ternary complex is a post ATP hydrolysis product. Though we have not been able to prove conclusively the nucleotide content of the rHH complex, we believe the complex isolated from the Ni-NTA column is already in a competent state to protect aggregating proteins, without any additional nucleotide requirement. This then

strongly suggests that the two complexes are binding denatured luciferase in seemingly different ways.

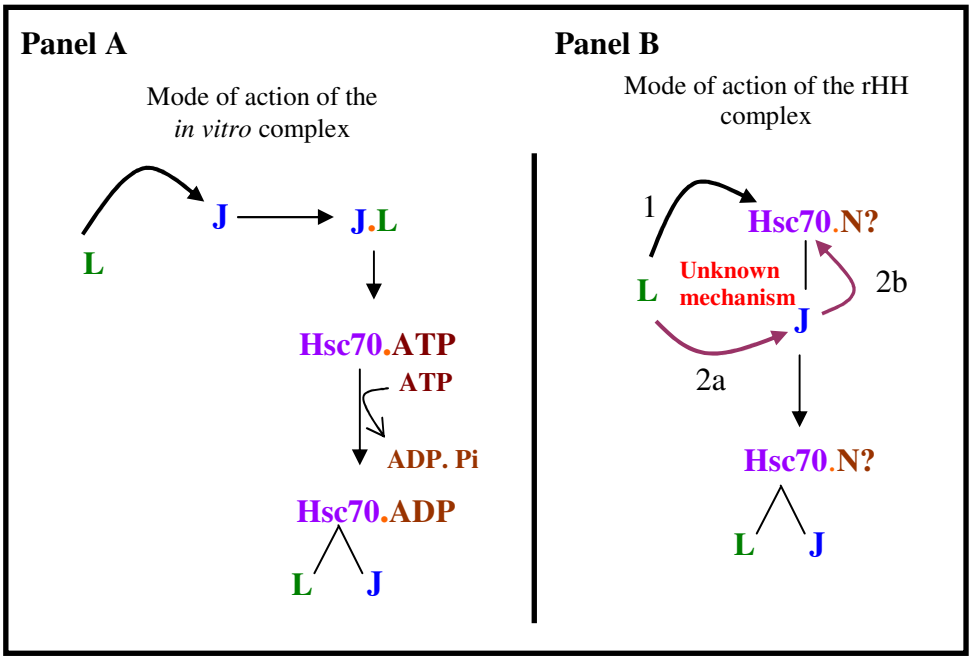

Figure 5.17: Proposed mechanism of action of HSJ1b assisted Hsc70 binding to denatured substrate (using luciferase as an example).

Panel A) Sequence of events leading to formation of the ternary complex of Hsc70, HSJ1b (**J**) and luciferase (**L**) for the *in vitro* complex. **Panel B**) Two potential mechanisms (indicated by 1 and 2) for the formation of the ternary complex of Hsc70 possibly bound to nucleotide N, HSJ1b (**J**) and luciferase (**L**) in the rHH complex.

According to Szabo *et al*. (1994), luciferase initially binds to DnaJ, which initiates ATP hydrolysis by DnaK to form a Luciferase-DnaK-DnaJ complex (Szabo *et al*., 1994). Panel A in Figure 5.17 illustrates the mode of action for the *in vitro* complex according to Szabo *et al*. Although this model might explain the observations for the *in vitro* complex reconstituted from Hsc70 and HSJ1b, it fails to convincingly explain the mode of action for the preformed recombinant (rHH) complex. Panel B illustrates a hypothetical mode of interaction for luciferase with the rHH complex. It explores the possibility that luciferase binds directly to the pre-existing Hsc70/HSJ1b complex. Two routes are possible; either the unfolded substrate (i.e. luciferase) binds directly to the Hsc70 subunit of the complex (labelled 1 in panel B, Figure 5.17), or the substrate first binds to the HSJ1b subunit of the complex (labelled 2a in panel B, Figure 5.17) which then hands it over to Hsc70 (labelled 2b in panel B, Figure 5.17). More work is required to confirm the exact mechanism.

The two complexes exhibited dissimilar substrate protection, which could be due to differing conformations. These potential differences between the recombinant Hsc70/HSJ1b complex and the *in vitro* complex were probed by limited proteolysis. This technique is used routinely to study the conformation of native proteins and associated transitions observed on substrate /cofactor/ ligand binding (Hubbard, 1998). In this study, the enzymes chymotrypsin and trypsin were used so that two types of specificity could be probed. Chymotrypsin cleaves peptides at the carboxyl side of tyrosine, tryptophan, and phenylalanine residues (amino acids contain aromatic rings) while trypsin predominantly cleaves peptide chains at the carboxyl side of the amino acids lysine and arginine (Stryer *et al*., 2002).

Chappel *et al*., (1986) reported that chymotrypsin digestion of bovine Hsc70 at 37^{o}C resulted in a 60 kDa fragment which was subsequently proteolysed to form a 44 kDa fragment. We expected the proteolysis pattern from our study to be different from that reported by Chappel *et al*. due to variations in the temperature used for the proteolysis experiments. While their results were reported at 37^{o}C, our study was performed at 4^{o}C. We found that Hsc70 was sensitive to proteolysis by chymotrypsin and more than 50% of Hsc70 was proteolysed in the presence of ATP. However no major proteolysis products could be detected. Three very minor proteolytic fragments (at approximately 60 kDa, 50 kDa and 40 kDa) could also be observed. But owing to the inherent contamination of the protein sample, the validity of these observations is uncertain. A longer incubation time may have been more insightful. Chymotrypsin digestion of HSJ1b produced only one detectable fragment at approximately 30 kDa. Analysis of the HSJ1b protein sequence by GeneRunner software revealed 28 possible chymotrypsin recognition sites. 27 out of the 28 sites are clustered together in the first 171 amino acids, while the 28th site is at Y261. Comparing the sequence analysis with the observed proteolytic fragment sizes, it appears that the primary site of cleavage is either Y51 or Y261. However this prediction is based solely in bioinformatic analysis of the distribution of chymotrypsin sites on the protein sequence and needs to be confirmed by N-terminal sequencing or MS/MS of the fragment.

Partial proteolysis of the *in vitro* and recombinant complex by chymotrypsin however revealed no detectable difference between the digest patterns. In both the cases, the Hsc70 component of the complex appears to be resistant to proteolysis and no

discernible cleavage products from the proteolysis of Hsc70 were observed. Based on our digestion of HSJ1b alone, it is believed that the major cleavage product migrating at ~30 kDa originated from the HSJ1b fraction. Although the basic pattern of digestion was consistent for both complexes, there was a difference in the extent of digestion of the HSJ1b protein between the complexed and the uncomplexed state. HSJ1b on its own was extremely vulnerable to chymotrypsin, resulting in the cleavage of almost 82% of HSJ1b over the time course of the experiment. However as part of the complexes, HSJ1b cleavage was slower as suggested by an increase in the percentage of residual HSJ1b- 55% and 42% for the *in vitro* and recombinant complex respectively. The interaction with Hsc70 has a stabilising effect, by either protecting the cleavage site on HSJ1b or by inducing a conformational change in HSJ1b which then alters protease sensitivity.

Since proteolysis by chymotrypsin failed to reveal any conformational differences between the two protein complexes, proteolysis by trypsin was undertaken. Partial tryptic proteolysis was performed on the reconstituted *in vitro* complex and rHH complex at 30^{o}C. The Hsc70 subunits in both the rHH and the *in vitro* gave rise to a ~70-71 kDa fragment which differed from the undigested product (73 kDa) by only 1 or 2 kDa. In Chapter 4, an analysis of the Hsc70 protein sequence by the Generunner software established that the only potential cleavage site which can give rise to a 71 kDa product, does not occur in the native Hsc70 protein sequence, but in the Factor Xa site which follows the N-terminal His•Tag® sequence contributed by the pET-16b expression vector. The resulting 71 kDa product is therefore the native Hsc70 without the histidine tag. In addition, the *in vitro* complex gave rise to three other major proteolytic products. Two of the fragments observed at ~60 kDa and ~52 kDa respectively were presumptively the cleavage products of Hsc70. The third fragment at ~ 40-44 kDa is of disputable origin, as it could possibly be a cleavage product of Hsc70 or remnants of undigested HSJ1b protein. The addition of ATP did not affect the digest pattern, therefore showing no evidence of a conformational change during the assembly of the *in vitro* complex. Other than the ~71 kDa product, the Hsc70 subunit of the rHH was completely resistant to tryptic digestion under these experimental conditions. Instead the HSJ1b subunit of the rHH was almost completely digested. Proteolysis of rHH resulted in only two prominent digestion fragments, one at ~35 kDa, and other at ~27 kDa both apparently originating from the HSJ1b subunit.

Addition of ATP resulted in the disappearance of the 35 kDa fragments indicative of probably a conformational shift resulting in quicker proteolysis of HSJ1b. Bioinformatic analysis of the HSJ1b sequence using GeneRunner software revealed 43 trypsin recognition sites, uniformly distributed across the protein sequence. Therefore this could not provide any reliable clues about a potential site of cleavage which could result in a ~27 kDa fragment. Bimston *et al*., (1998) reported that trypsin digestion of Hsp70 yields 58 kDa, 43 kDa, 20 kDa and 18 kDa fragments, which concurs with some of the Hsc70 proteolysis fragments obtained for the *in vitro* complex. The addition of Human DnaJ homologue (HDJ-1) did not seem to alter the proteolysis results (Bimston *et al*., 1998). However their report fails to discuss the state of the HDJ-1 moiety. In contrast, Chamberlain *et al*., (1997) reported that digestion of Hsc70 was significantly enhanced in the presence of cysteine string proteins 1 (Csp1) and ATP. Csp1 itself was extremely sensitive to the proteolysis and was undetectable by SDS-PAGE (Chamberlain *et al*., 1997). Contrastingly, in our experiments we observe that Hsc70 is in fact less susceptible to tryptic digestion in the presence of HSJ1b and ATP. But the digestion of Hsc70 is faster when ATP is not present; implying that in the presence of HSJ1b and ATP Hsc70 adpots a "closed" conformation, protecting it from proteolysis.

Data obtained from these proteolysis studies indicate a difference between the *in vitro* and recombinant complexes at a structural level. The Hsc70 with its HSJ1b partner isolated recombinantly clearly adopts a different conformation compared to the model *in vitro* complex which has been routinely used in the study of the chaperone/co-chaperone complex. However, more structural work is required to validate these observations. Perhaps N-terminal sequencing of the digest fragments is a way forward to identifying the regions on the proteins showing conformational mobility.

Oligomerisation of the rHH complex has been extensively discussed in chapter 4. So we next decided to evaluate and compare the extent of complex formation and oligomerisation under *in vitro* conditions. Pleckaityte and co-workers have studied the behaviour of the Hsp70 and Hsp40, when combined together in the presence and absence of ATP (Pleckaityte *et al*., 2003). In the absence of ATP, they did not observe an additional elution peak, which could be attributed to complex formation (Pleckaityte *et al*., 2003). Additionally, biochemical analysis by Minami *et al*., also

reported that protection of denatured substrate from thermal aggregation requires the combined action of the reconstituted Hsc70 and Hsp40 protein system and ATP (Minami *et al*., 1996) Therefore in this study, we have restricted ourselves to study the nature of the complex formation between Hsc70 and HSJ1b under *in vitro* conditions only in the presence of ATP.

During SEC the rHH protein was found to resolve into two peaks. The first peak eluted in the void volume, while the second peak fractionated at an estimated molecular weight of ~220 kDa. The oligomeric nature of the first peak from the void volume was studied by analytical ultracentrifugation and was confirmed to be a non- aggregated protein species, presumably arising from the polymerisation of the HSJ1b with the Hsc70. A similar peak is observed for the *in vitro* complex, suggesting successful polymerisation of the two proteins under *in vitro* conditions. In the absence of AUC data, it is difficult to determine if the first peak obtained for the *in vitro* complex is an aggregate or a non-aggregated higher order oligomer as determined for the rHH protein. For the second peak, although the elution volumes for both the complexes approximately matched, the resolution of the second peak for the *in vitro* complex was very poor, as observed from the broad nature of the elution. An estimate of the molecular weight of the second peak *in vitro* complex cannot be made due to the broad nature of the elution spectra. An interesting difference between the two complexes was the difference in the extent of oligomerisation of the two complexes. Based on the percentage distribution of the two peaks for the two complexes, it is apparent that the rHH complex exists predominantly in the oligomerised state, while the *in vitro* complex shows as much as 40% lesser oligomerisation. This suggests Hsc70/HSJ1b oligomerisation is more profound in the recombinant scenario than the *in vitro* one. The functional significance of this disparity, although not immediately clear/confirmed, could potentially explain the various functional and conformational differences that have been observed during the course of this study.

A comparative study was also performed with the elution profile of the individual Hsc70 and HSJ1b polypeptides, to determine if the the peak 2 in the retention volume is an additional elution peak, distinct from the elution profiles of the individual Hsc70 and HSJ1b. If so, it can concluded that this additional peak is due to the assembly of the Hsc70/HSJ1b complex, albeit an unstable one. Hsc70 has been observed to exist as

a mixture of monomer, dimers and higher order oligomers when bound to ADP, and as a monomer in the presence of ATP (Carlino *et al*., 1992; Toledo *et al*., 1993; Palleros *et al*., 1993). Recombinant Hsc70 used in our studies was found exist as a heterogeneous mixture of dimers and trimers, suggesting that it was probably in an ADP bound state. This correlates with our observations from the thermal aggregation assay where Hsc70 was found to be functionally competent even in the absence of ATP. Recombinant HSJ1b eluted as a dimer. Type I and II Hsp40's have been shown to exist as dimers in solution, and is also functionally essential. Disruption of its dimerisation capabilities results in defective chaperone functions for both types of Hsp40s (Sha *et al*., 2000; Li *et al*., 2003). Another feature that was observed in the SEC profiles of both Hsc70 and HSJ1b was that a large proportion of both the proteins eluted in the void volume, indicating protein aggregation. This could be time induced, due to storage at 4^{o}C during the course of the study. Similar time induced aggregation of Hsc70 has also been reported by Borges & Ramos (2006), who have observed during the course of their study that long term storage of the protein affected the homogeneity of the protein.

When the individual Hsc70 and HSJ1b elution profiles were superposed with that of the reconstituted Hsc70/HSJ1b, the peak 2 in the retention volume coincided with the elution profiles of both the individual Hsc70 and HSJ1b. On comparing our results with the reported SEC elution profile for the Hsp70/Hsp40 complex from *M. ruber*, it was observed that the authors have also obtained a broad peak coinciding with the individual elution profiles of the Hsp70 and Hsp40 (Pleckaityte *et al*., 2003). Only an additional small shoulder can be observed with this broad peak, which in their report has been attributed to the formation of the complex (Pleckaityte *et al*., 2003). However due to the broad nature of elution for the peak 2 of the *in vitro* Hsc70/HSJ1b it was difficult to ascertain the presence of an additional unique peak, which could be indicative of the assembly and formation of a complex.

Summarising, in this chapter we compared the behaviour of the recombinant complex (rHH) with the reconstituted *in vitro* complex with respect to their substrate protection efficiency, conformational properties and degree of oligomerisation. The two complexes generated by two different protocols display significantly differences in their functional properties. Under our experimental conditions, the rHH complex was not only superior to the *in vitro* complex in protecting unfolded substrate; the assembly of the Hsc70/HSJ1b complex also appears to be conformationally dissimilar to that of the *in vitro* complex. Taking together all these factors, the recombinant Hsc70/HSJ1b complex is an attractive model to study the mechanisms of assembly and working in the formation of the Hsc70 chaperone and HSJ1b co-chaperone complex.

Chapter 6
Analysis of domain variants of Hsc70 and their complexes for functional and structural studies

CHAPTER 6: Analysis of domain variants of Hsc70 and their complexes for functional and structural studies

6.1 Introduction

One of the primary aims of this thesis was to obtain structural data to elucidate the interactions of the Hsc70 and HSJ1b proteins. Results from Chapter 4 indicated that the full length Hsc70 /HSJ1b complex isolated using the co-expression strategy was a mixture of oligomeric and a ~220 kDa protein species. Preliminary structural analysis of the oligomeric species was performed by electron microscopy. The ~220 kDa fraction, although suitable for crystallography, did not yield any promising results from initial trials performed with Hampton sparse matrix screens.

An alternate approach to obtain structural information was therefore to dissect the Hsc70 protein into functional domain modules which could continue to bind to HSJ1b and identify a construct suitable for crystallography. The domain architecture of Hsc70 has been discussed in detail in Chapter 1. Briefly, Hsc70 is composed of 3 domains. The N-terminal region has the 44 kDa nucleotide binding domain (NBD) while the C-terminal region can further divided into two domains – an 18 kDa peptide binding domain (PBD) and a 10 kDa region which is believed to act as a lid over the peptide binding domain (Chappell *et alI*., 1987; Flaherty *et al*., 1990 Huang *et al*., 1993 and Zhu *et al*., 1996).

Using a yeast two hybrid system, Demand *et al*., have identified potential binding sites for the various cofactor proteins such as Hsp40, Hip, Hop and Bag. Figure 6.1 maps the potential sites of interaction between the Hsc70 domain and its co-chaperone partners in the eukaryotic Hsp70 system. Demand *et al.*, reported that the C-terminal region of Hsc70 hosts distinct binding sites for both Hsp40 and Hop, while Hip exclusively bind to the NBD (Demand *et al*., 1998). BAG-1 binds to the NBD of Hsc70 in cooperation with the Hsp40, but competes with Hip for the binding site (Höhfeld *et al*., 1997). CHIP (carboxyl terminus of Hsc70-interacting protein) as the name suggests has been found to bind to Hsc70 fragments containing amino acids 540 to 650 and absence of the amino acids abolished this interaction (Ballinger *et al*., 1999).

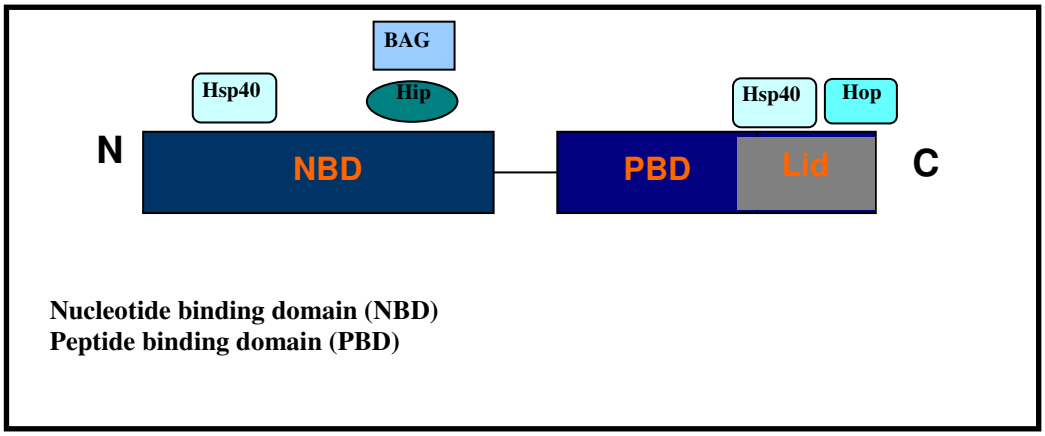

Figure 6.1: Map of potential co-chaperone binding sites on Hsc70

The C-terminal region of Hsc70 hosts distinct binding sites for both Hsp40 and Hop, while Hip exclusively binds to the NBD (Demand *et al*., 1998). BAG-1 binds to the NBD of Hsc70 in cooperation with the Hsp40, but competes with Hip for the binding site (Höhfeld *et al*., 1997).

From the study of Demand *et al*., it was clear that Hsp40 is capable of binding to both the N and C-terminal regions of Hsc70. Therefore in this Chapter, work was carried out to generate the domain variants of Hsc70 which were still capable of forming a complex with HSJ1b. These complexes of the domain variants with HSJ1b were isolated by Ni-NTA chromatography. The results section of this chapter is divided into two parts. Part A describes the purification of the domain complexes with HSJ1b and the biochemical analysis carried out to understand the role of the different domains in the complex formation with HSJ1b. Part B deals with the X-ray crystallography work carried out with one of the domain complexes.

6.2 Materials and Methods

6.2.1. Amplification of domain modules

Primer design

Primers were designed to amplify the N-terminal 60 kDa fragment (N60), the nucleotide binding domain (NBD), C-terminal region (CTR) and the CTR deletion of the C-terminal 10 kDa lid region (CTRΔC) from the coding region of the full length *Hsc70* gene. The regions amplified by the primers are highlighted in Figure 6.2.

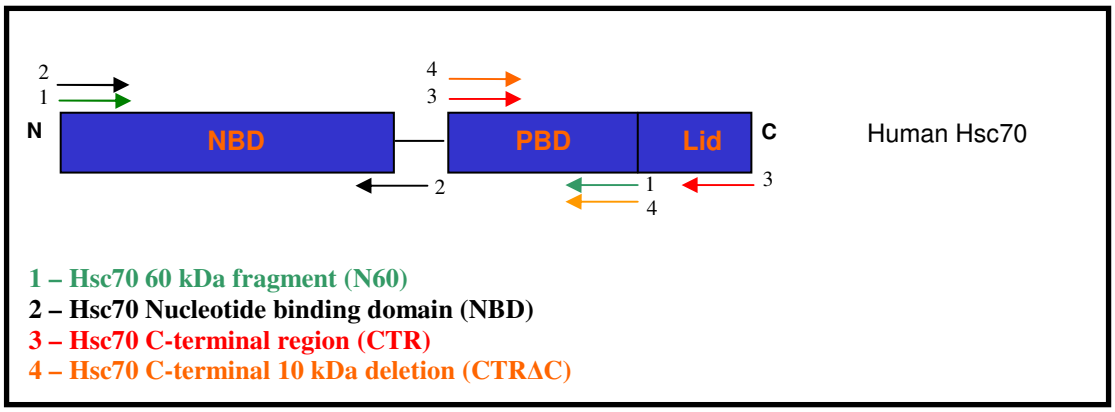

Figure 6.2: Amplification of Hsc70 domain modules

Four functional domain modules were identified and primers were designed to amplify the desired region. The four different colour arrow sets represents the four regions amplified using the full length pGEMt-*Hsc70* plasmid as template.

The primers designed for the amplification of each domain are listed in Table 6.1. *Nde*I and *Bam*HI restriction sites were introduced at the 5' and at the 3' ends respectively of each of the amplified products to enable directional cloning of the fragments into a suitable vector.

Domain	Primers (5' to 3' end)		Product size
N60	Fwd	GGATCCATATGTCCAAGGGACTGCAGTTGG	1659 bp
	Rev	GATCGGATCCTTAGGCATGTTGCTGCTGG	
NBD	Fwd	GGATCCATATGTCCAAGGGACTGCAGTTGG	1167 bp
	Rev	GATCGGATCCTCACTCAGACTTGTCTCCAGACAAGA	
CTR	Fwd	GATCCATATGGTACTGCTGCTGGACGT	789 bp
	Rev	GATCGGATCCTTAATCAACCTCTTCAATGGTGG	
CTRΔC	Fwd	GATCCATATGGTACTGCTGCTGGACGT	492 bp
	Rev	GATCGGATCCTTAGGCATGTTGCTGCTGG	

Table 6.1: Primer sequence, restriction sites and PCR product size for the domain fragments

Base pairs underlined and highlighted in red indicate the restriction endonuclease recognition sequence introduced into the primers to enable directional cloning of the PCR products.

PCR conditions

The construction of the pGEMt-*Hsc70* plasmid has been described in Chapter 3. This plasmid was used as the template for all the PCR reactions, and all amplifications were carried out using the 2X Phusion™ High-Fidelity PCR Master Mix containing the proof-reading enzyme, Phusion High-Fidelity DNA Polymerase (NEB). The parameters used for the PCR amplification reactions are listed in Table 6.2.

Segment	Number of cycles	Temperature (^{o}C)	Time in minutes
Initial denaturation	1	95	1
Denaturation, primer annealing and extension	30	95 60 72	1 1 2 for N60 1.2 for NBD 1 for CTR 0.5 for CTRΔC
Final extension	1	72	7
Final Hold	1	4	Indefinite

Table 6.2: PCR conditions for the amplification of the domain modules of the Human *Hsc70* gene

6.2.2. Insertion of domain fragments into pET-16b vector

The individual domain modules were cloned into the pET-16b bacterial expression vector. The amplified PCR products and pET-16b vector was digested with *Nde*I and *Bam*HI and prepared for ligation as per protocols described in chapter 2. The vector and insert were ligated in a 1:3 ratio and transformed into *E. coli* DH5α cells using protocols previously described in Chapter 2. Clones were confirmed by restriction digestion analysis of plasmid DNA isolated from transformed colonies (protocol described in chapter 2). DNA sequences were verified by sequencing the plasmids at the Advanced Biotechnology Centre (ABC), Imperial College, UK. The plasmids will be henceforth referred to as pET-16b-N60, pET-16b-NBD, pET-16b-CTR and pET-16b-CTRΔC.

6.2.3. Co-transformation of the Hsc70 domain modules with HSJ1b plasmid

For normal expression studies, pET-16b-N60, pET-16b-NBD, pET-16b-CTR and pET-16b-CTRΔC plasmids carrying the N60, NBD, CTR and CTRΔC fragments were co-transformed with the pET-24a-*HSJ1b* plasmid into the *E. coli* expression strain BL21(DE3). For the studies requiring the incorporation of Seleno-l-methionine (SelMet), the pET-16b-NBD clones were co-transformed with the pET-24a-HSJ1b plasmid into the *E. coli* methionine auxotroph expression strain- B384(DE3). Transformation was carried out as per the protocol described in Chapter 2 and the transformed cells were plated onto LB plates containing 50 µg/ml ampicillin and 25 µg/ml kanamycin and incubated overnight at 37^{o}C.

6.2.4. Co-expression and purification

Co-expression studies were carried out at 37^{o}C using the protocol described in Chapter 3, section 3.2.8. Cells were grown in LB media up to an OD at A595 of 0.6-0.8. Protein expression was induced by the addition of IPTG to a final concentration of 0.4 mM. After induction, cells were grown for a further 3 hrs. Cells were harvested as described Chapter 2, Section 2.10.1 and the cell pellet was re-suspended in lysis buffer (50 mM Tris-HCl pH 8.0, 100 mM NaCl, 5 mM imidazole and 5% (v/v) glycerol) and stored at -80^{o}C until required. Ni-NTA purification of the respective domain complexes was performed according to the protocol described for the purification of

polyhistidine tagged proteins in Section 2.10.2 of Chapter 2. The elution profiles of the recombinant proteins were analysed on a 12% SDS-PAGE gel.

6.2.5. Expression and purification of Seleno-l-methionine labelled protein

A single colony was grown overnight in 10 ml LB broth supplemented with 50 µg/ml of ampicillin and 25 µg/ml kanamycin at 37^{o}C in a shaking incubator. The overnight culture was harvested at 3000 rpm for 10 minutes and the cell pellet was washed three times with 10 ml of autoclaved water. The pellet was finally resuspended in 2 ml of water and used to inoculate 1 l of SelenoMet Medium Base containing SelenoMet Nutrient Mix, l-selenomethionine (40 mg/ml), 50 µg/ml ampicillin and 25 µg/ml kanamycin. The prepared SelenoMet Medium was provided by Dr. Steve Smerdon from NIMR, Mill Hill.

Cultures were grown at 37^{o}C until an OD of 0.6-0.7 was reached, whereupon protein expression was induced by the addition of 0.4 mM IPTG. Induction was continued overnight at 20^{o}C. Cells were harvested as described in Chapter 2, Section 2.11.1 and the cell pellet was resuspended in lysis buffer (50 mM Tris-HCl pH 8.0, 100 mM NaCl, 5 mM imidazole, 5% (v/v) glycerol and 5 mM beta-mercaptoethanol) and stored at -80^{o}C until required. SelMet-labelled protein was purified by Ni-NTA chromatography as described in Section 2.10.2 in Chapter 2. However the eluted protein was supplemented with 1 mM DTT to prevent oxidation of the selenium.

6.2.6. Ion exchange chromatography

The NBD/J protein elution fractions from the Ni-NTA column were diluted with 50 mM Tris-HCl pH 8.0 to reduce the NaCl concentration to 25 mM. Ion exchange chromatography was performed on a 20 ml Q sepharose column (Sigma). The column was equilibrated with 50 mM Tris-HCl pH 8.0, 25 mM NaCl and 5% (v/v) glycerol. The protein was applied to the column and then washed with 2 CVs of equilibration buffer. The protein was step eluted with equilibration buffer containing 50, 100, 250, 500 and 1000 mM NaCl. The elution profile was monitored via SDS-PAGE. In the case of selMet-labelled protein 1 mM DTT was included in the chromatography buffers.

6.2.7. Size exclusion chromatography

Size exclusion chromatography was performed on a 90 ml Superdex-200 column. The column was equilibrated with 20 mM Tris-HCl pH 8.0 with 100 mM KCl. In the case of selMet-labelled protein 1 mM DTT was included in the buffer. One ml fractions were collected after 25 ml of buffer had passed. The fractions were analysed for protein content using the Bradford assay using BSA as a standard. A graph of the absorbance on the y-axis and the elution volume on the x-axis was plotted. The peak fractions were analysed by SDS-PAGE electrophoresis.

6.2.8. Partial proteolysis studies

Proteolysis experiments were performed as described previously in chapter 4, section 4.2.5. Briefly, 4.4 µg of purified complex was digested with chymotrypsin in a protease to protein ratio of 1:300 (w/w) at 4°C for 10 minutes. The digestion products were analysed by SDS-PAGE on a 12% polyacrylamide gel and compared with undigested protein.

6.2.9. Thermal aggregation assay

15 µl reactions were set up, containing 1.27 µM of each domain complex and 0.8 µM of the substrate-luciferase. The assay was carried out as described in Chapter 4, section 4.2.3. The reactions were subjected to thermal shock at 42^{o}C for 10 minutes. The insoluble and soluble fractions were separated by centrifugation at 13,000 rpm and analysed by SDS-PAGE electrophoresis. The percentage of luciferase in the soluble and aggregated fraction was quantified from the gel by densitometry.

6.2.10. Protein crystallisation

Purified protein was concentrated using a centricon YM-30 centrifugal Filter Devices (Millipore). The final protein concentration was determined via the Bradford protein assay (Bradford, 1976) using BSA as a standard. Protein at a concentration of 5 mg/ml was used for initial screening. Crystallisation was set up at room temperature using the hanging-drop vapour-diffusion method. One µl of protein solution was mixed with the same amount of precipitant and the drops were equilibrated against 500 µl of reservoir solution. Preliminary trials were carried out with Crystal Screen and Crystal Screen 2 from Hampton Research (Cudney *et al.*, 1994; Jancarik & Kim, 1991).

6.3 Results

PART A: ROLE OF THE DIFFERENT DOMAINS IN THE INTERACTION WITH HSJ1B

In order to evaluate the influence of the individual Hsc70 domains in its interaction with HSJ1b, a 60 kDa N-terminal fragment (N60) which lacks the 10 kDa region of the C-terminus, the nucleotide binding domain (NBD), C-terminal region (CTR) and the CTR deletion of the C-terminal 10 kDa lid region (CTRΔC) were generated and used in this study. A schematic overview of the domain variants of Hsc70 is presented in Figure 6.3.

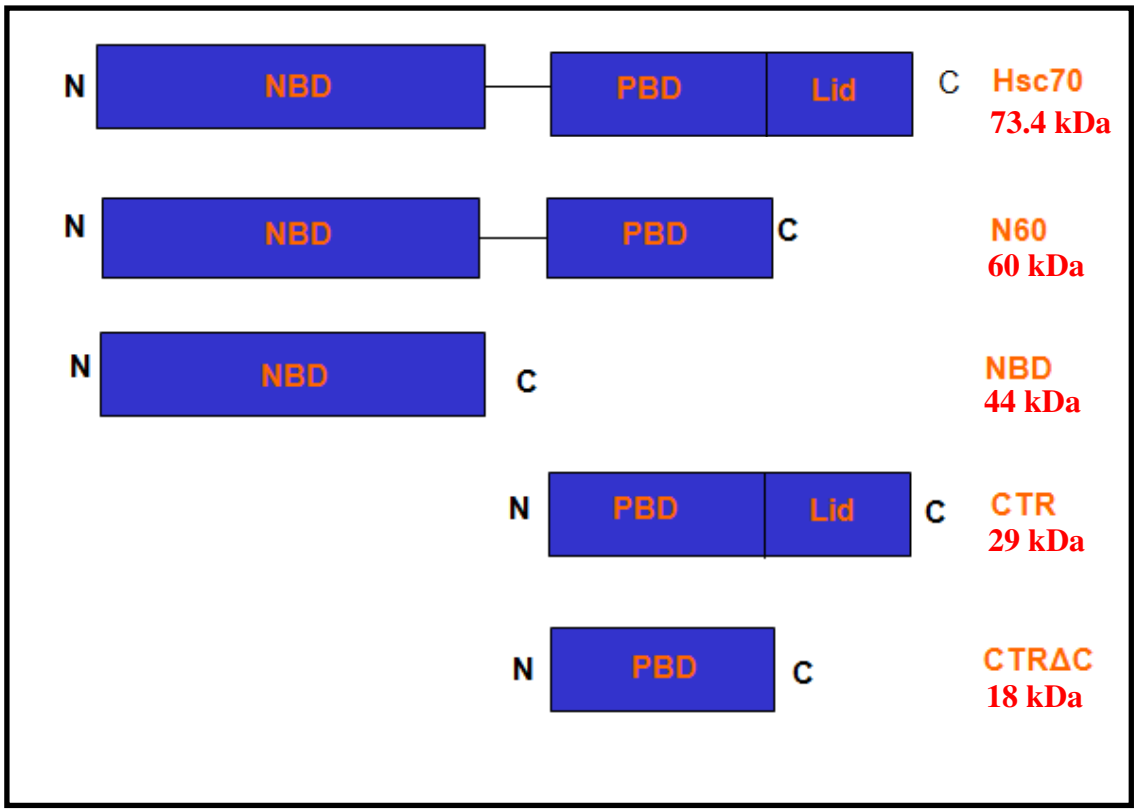

Figure 6.3: **Domain architecture of full length Hsc70 and its domain variants.**

6.3.1 PCR amplification of the domains

Using the pGEMt-Hsc70 plasmid as template, regions coding for the N60 fragment, NBD, CTR and CTRΔC modules were amplified. PCR amplification reactions for all four fragments were analysed on a 0.8% (w/v) agarose gel (Figure 6.4). From the nucleotide sequences the fragment sizes were calculated to be 1659 base pairs for the N60 fragment, 1167 base pairs for the NBD, 789 base pairs for the CTR and 492 base pairs for the C-terminal deletion mutant (CTRΔC). Product sizes were confirmed by agarose electrophoresis (Figure 6.4). Panel A in Figure 6.4 confirms the successful amplification N60 fragment. Panel B shows the successful amplification of the NBD (lane 1, Panel B, Figure 6.4). Panel C confirms the amplification of the CTR (lane 1, Panel C, Figure 6.4) and the (CTRΔC) (lane 2, Panel C, Figure 6.4).

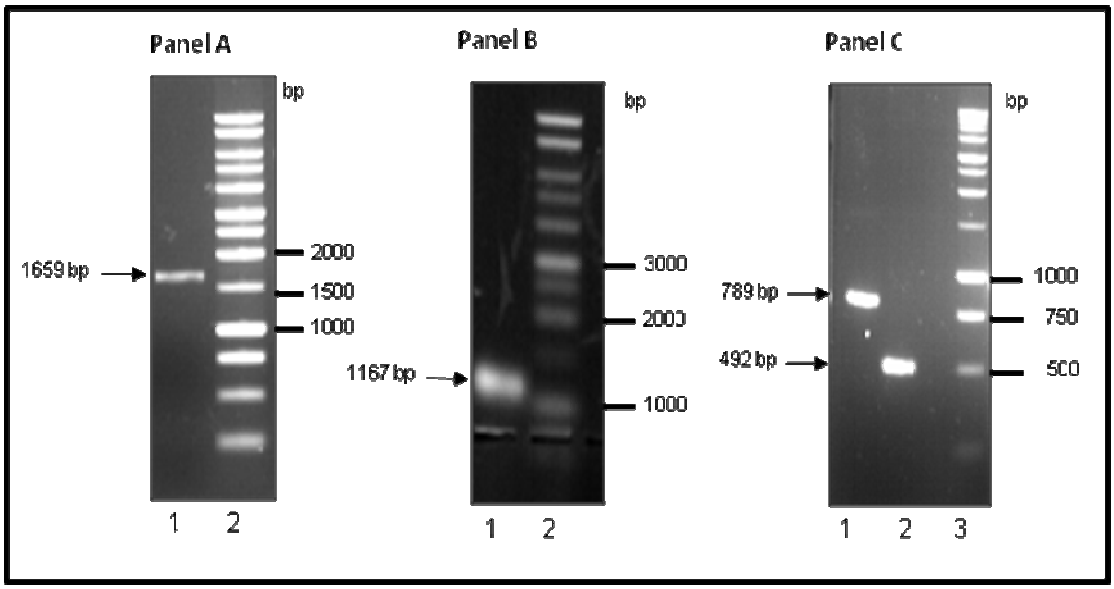

Figure 6.4: PCR amplification of Hsc70 domains

PCR reactions to amplify the required coding regions were set up as described in section 6.2.1 using the pGEMt-*Hsc70* plasmid as the template. 10 µl of each PCR product was subjected to electrophoresis on a 0.8% (w/v) agarose gel to confirm amplification of the expected size product.
Panel A) Amplification of the N60 fragment of Hsc70
Lane 1 shows 10 µl of the PCR product for the N60 fragment of Hsc70, lane 2 contains 6 µl of Promega 1Kb DNA Ladder (molecular weight marker).
Panel B) Amplification of the NBD of Hsc70
Lane 1 is 10 µl of the NBD PCR product; lane 2 contains 6 µl of Promega 1Kb DNA Ladder.
Panel C) Amplification of the CTR and CTRΔC domains of Hsc70
Lane 1 is amplified CTR product, lane 2 is amplification of CTRΔC region and lane 3 contains 6 µl of Promega 1Kb DNA Ladder (molecular weight marker).

6.3.2 Insertion of the Hsc70 domain fragments into pET-16b

The amplified PCR product for each domain fragment was purified and digested with the enzymes *Nde*I and *Bam*HI. The fragments were ligated with pET-16b vector digested at the *Nde*I and *Bam*HI restriction sites. Plasmids pET-16b-N60, pET-NBD, pET-16b-CTR and pET-16b-CTRΔC were subsequently generated. The clones were confirmed by restriction enzyme digestion of the isolated plasmids with *Nde*I and *Bam*HI. The reactions were visualised by agarose gel electrophoresis (Figure 6.5). Panel A in Figure 6.5 shows the successful release of the expected insert size from the pET-16b-N60 clone (lanes 3 and 4), Panel B confirms insert release for the pET-16b-NBD clones (lanes 2 and 3), Panel C confirms the insertion of the CTR gene fragment into the pET-16b vector in plasmids 1 and 3 (lane 2 and 4), while plasmid 2 (lane 3) does not have the desired insert. Similarly, lanes 2 and 3 of Panel D confirm the presence of the CTRΔC fragment in pET-16b.

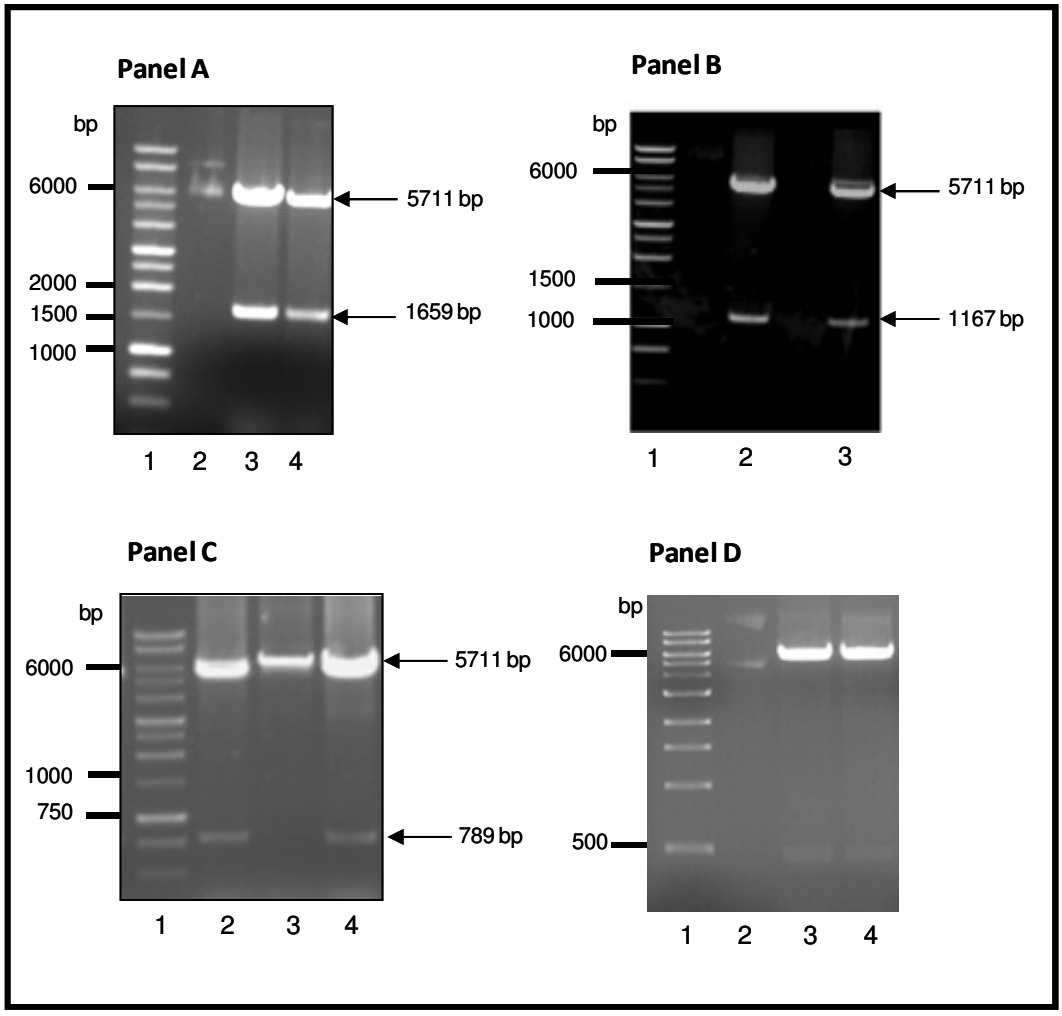

Figure 6.5: Confirmation of cloning of the *Hsc70* domain fragments into the pET-16b vector

Single white colonies inoculated and grown overnight with ampicillin were used for plasmid extraction by alkaline lysis. 15 µl of the extracted DNA was used for restriction digestion by *Nde*I and *Bam*HI enzymes and visualized on a 0.8% agarose gel. The DNA was visualised by staining with ethidium bromide at 0.5 ug/ml and photographed under UV illumination.

Panel A) Confirmation of N60 clones
Lane 1 contains 6 µl of Promega 1Kb DNA Ladder (molecular weight marker), lane 2 is plasmid 1 prior to restriction digest, lane 3 *Nde*I and *Bam*HI digestion of the plasmid 1 and lane 4 *Nde*I and *Bam*HI digestion of the plasmid 2.

Panel B) Confirmation of NBD clones
Lane 1 contains 6 µl of Promega 1 Kb DNA Ladder (molecular weight marker), lanes 2 and 3 are *Nde*I and *Bam*HI digestion of clones 1 and 2.

Panel C) Confirmation of CTR clones
Lane 1 contains 6 µl of Promega 1 Kb DNA Ladder (molecular weight marker) lanes 2, 3 and 4 are *Nde*I and *Bam*HI digestion of clones 1,2 and 3.

Panel D) Confirmation of CTRΔC clone
Lane 1 contains 6 µl of NEB 1 Kb DNA Ladder, lane 2 is plasmid 1 prior to restriction digest, lane 3 *Nde*I and *Bam*HI digestion of the plasmid 1 and lane 4 and *Bam*HI digestion of the plasmid 2.

6.3.3 Purification of the domain complexes

6.3.3.1 Ni-NTA chromatography

Plasmids pET-16b-N60, pET-16b-NBD, pET-16b-CTR and pET-16b-CTRΔC were each co-transformed with the pET-24a-HSJ1b plasmid and co-expressed in *E. coli* BL21(DE3) cells. Co-expressed N60/J, NBD/J, CTR/J and CTRΔC/J polypeptides were isolated by Ni-NTA chromatography. The proteins were eluted from the Ni-NTA column at an imidazole concentration of 200 mM and were analysed by SDS-PAGE (Figure 6.6). From the four panels in Figure 6.6 it can be seen that all four domains and HSJ1b remained bound to the column after extensive washing and co-eluted when 200 mM imidazole was applied to the column. This strongly suggests that all pairs of polypeptides form a complex when co-expressed. Panel A in Figure 6.6 shows the elution profile of N60/J complex. The eluted complex was composed of a 60 kDa polypeptide and a ~40 kDa polypeptide (molecular weight corresponding to the N60 fragment and migration position of HSJ1b respectively, lanes 6-8, Figure 6.6). Panel B in Figure 6.6 shows the elution profile of the NBD/J complex from the Ni-NTA column. The NBD has a calculated molecular weight of 44 kDa and the HSJ1b, as reported in chapter 3, migrates anomalously at ~40 kDa. Under the electrophoretic conditions of this study the two protein components of the NBD/J complex were observed to migrates as a single band at approximately 44 kDa and the two individual protein bands could not be distinguished (lanes 6 and 7, Figure 6.6). Panel C in Figure 6.6 shows the elution profile of the CTR/J complex from the Ni-NTA column. The eluted complex was composed of a 29 kDa CTR polypeptide and a 40 kDa HSJ1b polypeptide (molecular weight corresponding to CTR fragment and migration position of HSJ1b respectively, lanes 7-9, Figure 6.6). Panel D in Figure 6.6 is the elution profile of the CTRΔC/J complex from the Ni-NTA column. The eluted complex was composed of a 18 kDa polypeptide and a 40 kDa polypeptide (molecular weight corresponding to CTRΔC fragment and migration position of HSJ1b respectively, lane 8, Figure 6.6).

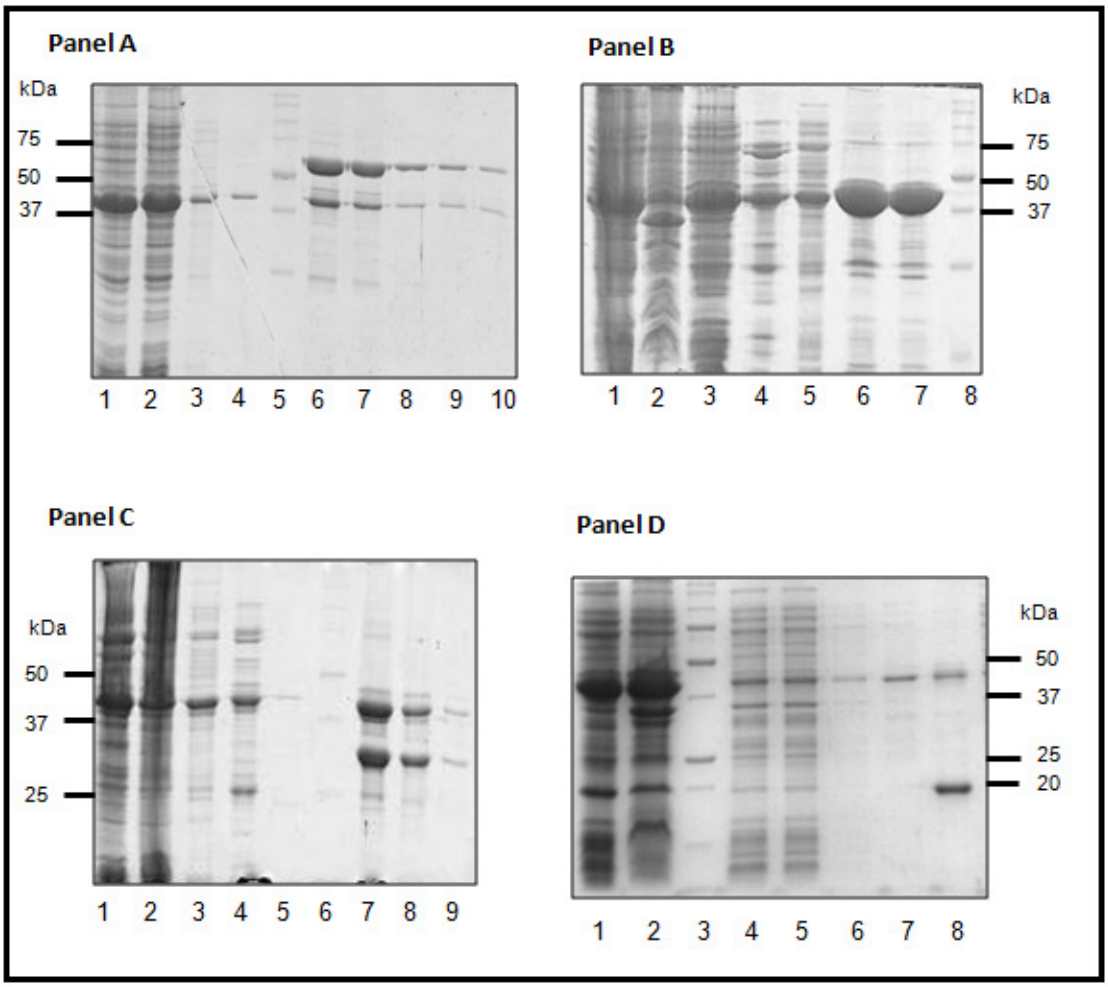

Figure 6.6: Purification of the various Hsc70 domain complexes with the full length HSJ1b.

Recombinant complexes were expressed in *E. coli* BL21(DE3) cells by induction with 0.4 mM IPTG for three hours at 37°C. The lysed, soluble extract was applied to a Ni-NTA column, extensively washed with buffer A and eluted with buffer (50 mM Tris-HCl pH 8.0, 100 mM NaCl, 5 mM imidazole and 5% glycerol) containing 200 mM imidazole. The polypeptide composition was analysed by SDS-PAGE (12% resolving gel), stained with Coomassie Brilliant Blue and photographed.

Panel A: Isolation of N60/J complex by Ni-NTA chromatography
Lane 1 soluble extract, lane 2 insoluble pellet, lane 3 column flow through, lane 4 wash with 30 mM imidazole, lane 5 Bio-Rad precision plus prestained molecular weight marker (broad range), lane 6-10 200 mM imidazole elution fractions.

Panel B: Isolation of NBD/J complex by Ni-NTA chromatography
Lane 1 soluble extract, lane 2 insoluble pellet, lane 3 column flow through, lane 4 wash with buffer A, lane 5 Wash with 30 mM imidazole, lanes 6 & lane 7 200 mM imidazole elution and lane 8 Bio-Rad precision plus prestained molecular weight marker.

Panel C: Isolation of CTR/J complex by Ni-NTA chromatography
Lane 1 soluble extract, lane 2 insoluble pellet, lane 3 column flow through, lane 4 wash with buffer A, lane 5 Wash with 30 mM imidazole, lane 6 Bio-Rad precision plus prestained molecular weight marker, lane 7-9 200 mM imidazole elution fractions.

Panel D: Isolation of CTRΔC/J complex by Ni-NTA chromatography
Lane 1 soluble extract, lane 2 insoluble pellet, lane 3 Bio-Rad precision plus prestained molecular weight marker, lane 4 column flow through, lane 5 wash with buffer, lane 6 overflow from lane 5, lane 7 Wash with 30 mM imidazole, lane 8 200 mM imidazole elution fraction.

The amount of co-expressed HSJ1b polypeptide eluting from Ni-NTA resin was observed to differ between the various domain constructs. Both the N-terminal and the C-terminal regions of the Hsc70 protein host a binding site for its Hsp40 co-chaperone (Demand *et al*., 1998; Suh *et al*., 1998). Truncation of the full length Hsc70 into its various domains therefore may not alter its interaction and/or binding with the co-chaperone protein. In the case of the co-expressed complexes, altered binding of the domain variants to HSJ1b was studied by quantifying the proportion of HSJ1b polypeptide co-eluting with Hsc70 from the nickel column using densitometry. The proportion of Hsc70 to HSJ1b was then calculated as percentage of the total (Hsc70+HSJ1b) proteins (Figure 6.7). It was noticed that there was only a very slight difference in the proportion of HSJ1b bound by the N60 fragment (34%) compared to the full length Hsc70 (40%). The CTR region was found to be associated a slightly higher percentage of HSJ1b; almost 11% more than the full length Hsc70. The CTRΔC/J complex has almost 50% less bound HSJ1b than CTR, indicating that the deletion of the C-terminal 10 kDa region has a deleterious effect on the HSJ1b interaction with the isolated CTR domain. However deletion of this 10 kDa region does not seem to overtly affect the interaction of the N60 fragment with HSJ1b, indicating that the NBD rather than the distal 10 kDa region is the major site of HSJ1b binding.

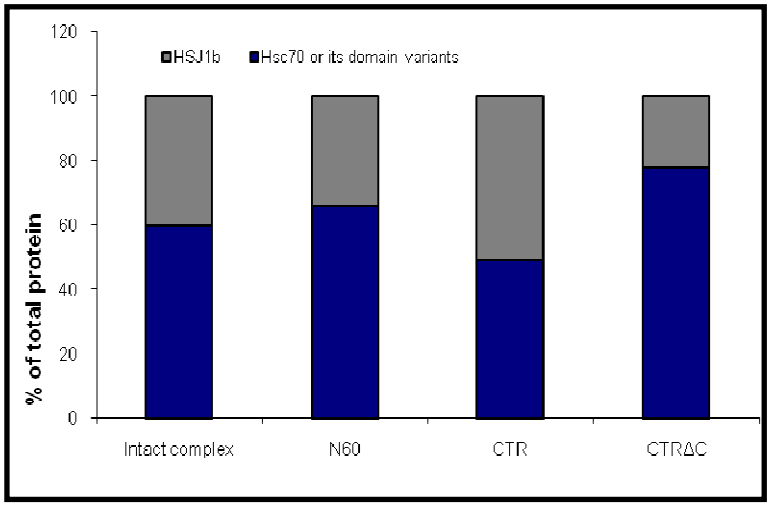

Figure 6.7: Effect of Hsc70 domain truncation on its association with HSJ1b protein.

Each domain construct was co-expressed with HSJ1b and purified over the Ni-NTA column as described in the previous sections. The eluted proteins were visualised on a 12% SDS-PAGE gel, and the Hsc70 and HSJ1b polypeptides were quantified by densitometry. Variation in the proportion of HSJ1b co-eluting with the domain variants and full length Hsc70 from the Ni-NTA column was represented as percentage of total (Hsc70+HSJ1b) protein.

The Ni-NTA fractions of all 4 domain complexes were then subjected to the next purification step – size exclusion chromatography (discussed in section 6.3.3.2). Except for the NBD/J complex, the SEC was successful in separating most of the contaminating polypeptides for the other domain complexes. Therefore, Ion exchange chromatography was undertaken to further purify the NBD/J protein obtained after Ni-NTA chromatography so that a pure complex that could be obtained for crystallographic analysis. The predicted pI for the NBD/J complex is 6.42 suggesting that the protein can bind to the anion exchange resin, Q-sepharose. The protein was eluted using a step gradient of NaCl up to 1 M concentration. At 100 mM NaCl, elution of the complex was observed (Lanes 4 and 5, Figure 6.8). Lanes 6 and 7 represent elution fractions obtained using 250 mM NaCl while the sample run in lane 8 was obtained at 500 mM NaCl. The 100 mM elution fractions were pooled and concentrated to bring down the volume prior to loading onto the gel filtration column.

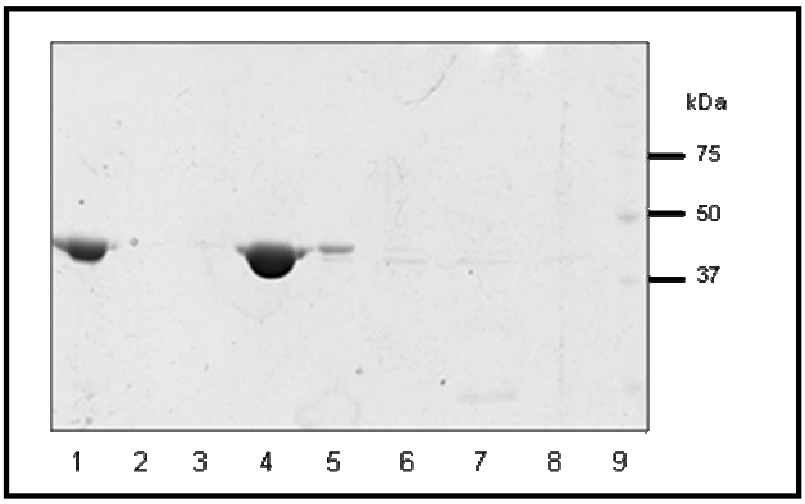

Figure 6.8: Ion exchange chromatography of the NBD/J complex.

Ion Exchange chromatography was performed using a Q sepharose ion exchange resin. NBD/J complex obtained from Ni-NTA chromatography was bound to Q-sepharose pre-equilibrated with 50 mM Tris-HCl pH 8.0, 25 mM NaCl and 5% (v/v) glycerol. The bound protein was eluted with an NaCl step gradient from 0-500 mM in equilibration buffer. Lane 1 NBD/J complex load, lane 2 flow through from the column, lane 3 50 mM NaCl wash, lanes 4 & 5 100 mM NaCl elution fractions, lanes 6 & 7 250 mM NaCl elution fractions, lane 8 500 mM NaCl elution, lane 9 Bio-Rad precision plus prestained molecular weight marker proteins.

6.3.3.2 Size exclusion chromatography

SEC was performed to fulfil two purposes. One was to assess the homogeneity of the protein since this is an essential requirement for protein crystallography. Aggregation of protein has been shown to inhibit crystallisation (Littlechild, 1991). Therefore, size-exclusion chromatography (SEC) was performed to assess the oligomeric compositions of the purified proteins and also to separate any higher order oligomers/aggregates from the protein.

The Ni-NTA elution fractions were pooled and loaded onto a Superdex-200 gel filtration column equilibrated with the buffer specified. 1 ml fractions were collected and proteins were detected by measuring the protein concentration using Bradford assay. When the N60/J complex was subjected to SEC, the complex resolved into two peaks (Panel A, Figure 6.9); Peak 1 at 38 ml was reminiscent of the polymerised peak observed for the full length rHH complex (see Chapter 4). The polypeptide composition of the N60/J peak 1 was confirmed by SDS-PAGE to contain both the N60 and HSJ1b protein subunits (lanes 1-3, Panel A, Figure 6.10). The second peak at 54 ml has an estimated molecular weight of approximately of 185 kDa, which corresponds to the molecular weight of a trimer of the 60 kDa subunits (3*60=180) only. SDS-PAGE confirms that the N60/J peak2 protein fractions comprised predominantly of the 60 kDa fragment (lanes 4-9, Panel A, Figure 6.10).

The NBD/J complex gave rise to a single homogenous peak with an apparent molecular weight of 130 kDa (Panel B, Figure 6.9). SDS-PAGE revealed a single band migrating at approximately 44 kDa – the shared migration pattern of both the NBD and HSJ1b (Panel B, Figure 6.10). The NBD/J complex was selected for further structural studies based on its clean and homogenous elution from the gel filtration column.

The CTR/J complex resolved into two fractions (Panel C, Figure 6.9); the apparent molecular weight of peak 1 of the CTR/J complex was 560 kDa and represented higher order oligomers of the complex, while Peak 2 was poorly resolved between 49-71 ml (Panel C, Figure 6.9). Analysis by SDS-PAGE (Panel C, Figure 6.10) shows that both peaks contained CTR and HSJ1b moieties, but the diffused nature of resolution of second peak suggests possibly a weak interaction between the two protein subunits.

When the CTRΔC/J complex was subjected to SEC, the protein complex resolved into two fractions over the Superdex-200 column (Panel D, Figure 6.9). Interestingly, analysis of the fractions by SDS-PAGE revealed that the CTRΔC/J peak 1 fractions comprised only of the HSJ1b protein (lanes 2-4, Panel D, Figure 6.10) and peak 2 was composed entirely of the PBDΔC fragment (lanes 6-9, Panel D, Figure 6.10). It appears that the CTRΔC/J could not maintain its complexed state over the gel filtration column and disassociated into the individual CTRΔC fragment and HSJ1b protein. We believe that this could be due to the removal of the C-terminal 10 kDa fragment, which weakens/disrupts the binding of HSJ1b to CTRΔC. Table 6.3 summarises the estimated molecular mass for the 4 domain complexes as per their resolution over the Superdex-200 column.

Protein Sample	Peak Elution Volume in ml	Calculated Molecular Mass in kDa
Peak 1 N60/J	38	655
Peak 2 N60/J	54	185
NBD/J	59	135
Peak 1 CTR/J	41	417
Peak 2 CTR/J	49-71	276-48
Peak 1 CTRΔC/J	38	655
Peak 2 CTRΔC/J	64	84

Table 6.3: Molecular weight determination of the protein species in the peaks resolved from size exclusion chromatography.

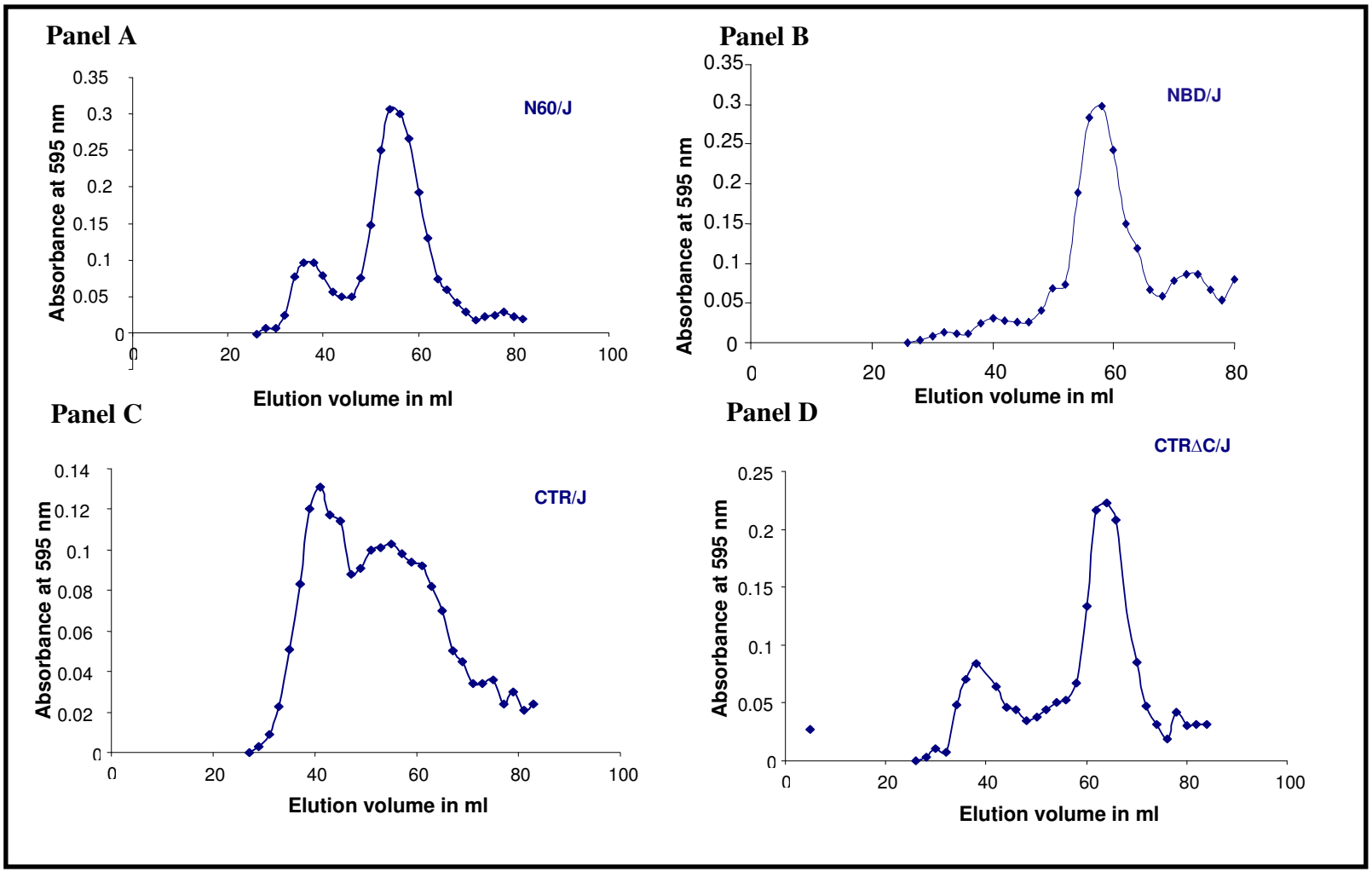

Figure 6.9: Size exclusion chromatography of the domain complexes

Size exclusion chromatography was performed on a Superdex-200 column and the protein eluting from the column was collected as 1 ml fractions. Absorbance of each fraction was determined using Bradford assay. Plot of Absorbance at 595 nm for the fractions on the Y-axis versus the elution volume (X-axis) was used to develop the elution profile chromatogram.
Panel A: Elution profile of the N60/J complex from the Superdex-200 column. **Panel B:** Elution profile of the NBD/J complex from the Superdex-200 column.
Panel C: Elution profile of the CTR/J complex from the Superdex-200 column. **Panel D:** Elution profile of the CTRΔC/J complex from the Superdex-200 column.

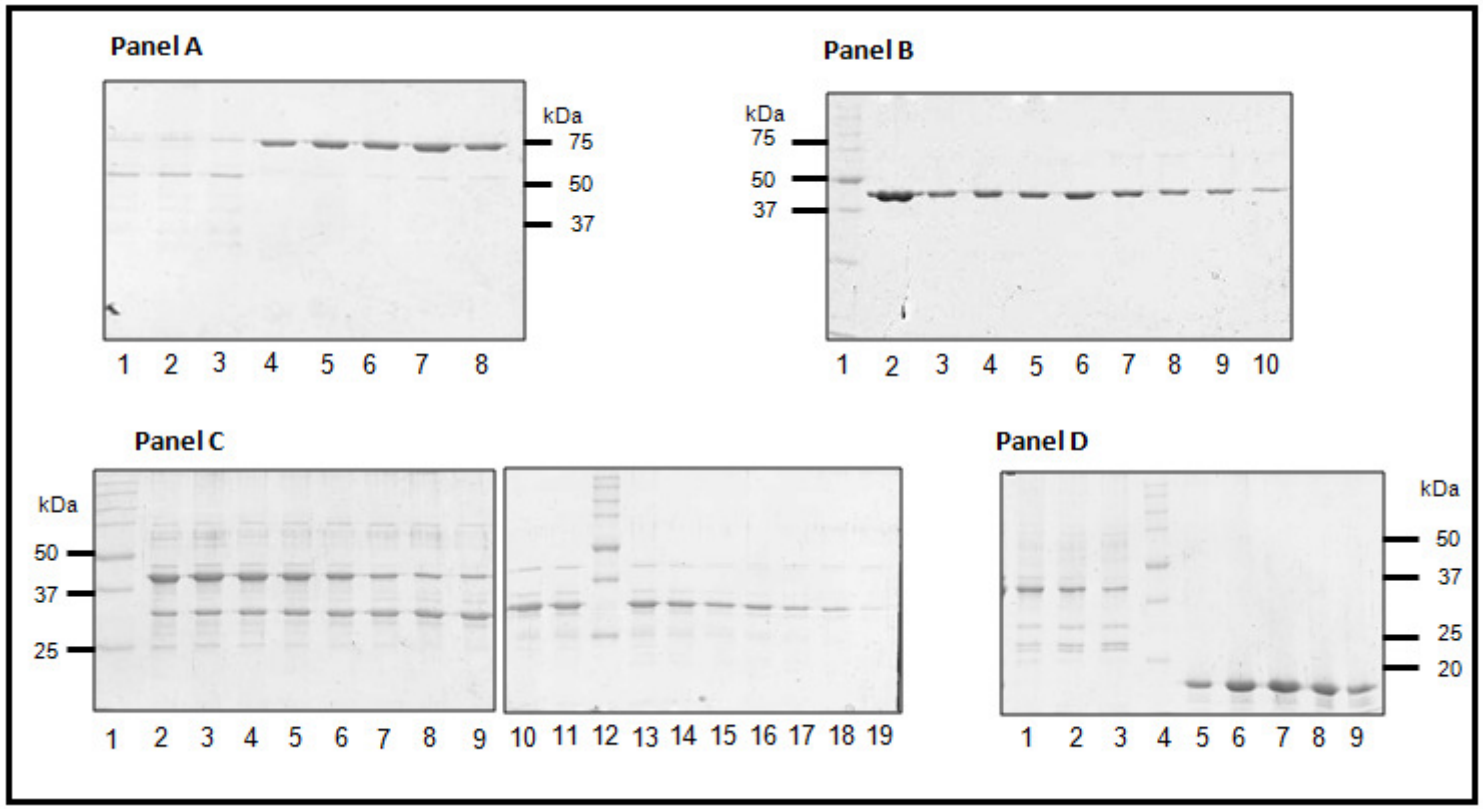

Figure 6.10: SDS-Page analysis of the peak obtained during gel filtration of the individual Hsc70 domain/HSJ1b complexes.

Panel A: N60/J SEC fractions. Lanes 1-3 elution from fractions 36, 37 and 38 respectively, lanes 4-8 protein elution from fraction 60, 57, 56, 55 and 54
Panel B: NBD/J elution fractions. Lane 1 is the Bio-Rad precision plus prestained molecular weight marker, lane 2 is sample of protein loaded onto the column, lanes 3-10 protein elutions from fraction 56 to fraction 63.
Panel C: CTR/J SEC fractions. Lane 1 is the Bio-Rad precision plus prestained molecular weight marker, lanes 2-9 alternate fractions starting at fraction 39 – 52, lane 10 fraction 53, lane 11 is the Bio-Rad precision plus prestained molecular weight marker, lane 12-19 protein elution's from fraction 54 to fraction 61.
Panel D: CTRΔC/J elution fractions Lane 1 is sample of protein loaded onto the column, lanes 2-4 elution from fraction 38,40 and 42 respectively, lane 5 is the Bio-Rad precision plus prestained molecular weight marker, lanes 6-10 protein elution from fraction 60, 62, 64, 66 and 68.

Next, using the data obtained from the size exclusion chromatography studies, the region on Hsc70 essential for its binding to HSJ1b and extent of oligomerisation was studied. The gel filtration profiles of the domain complexes were compared with the full length rHH complex and the results of the comparison are shown in Figure 6.11. The comparison was performed with the NBD/J, CTR/J and N60/J complexes and not with the CTRΔC/J complex since we had established in the previous section that it does not form a stable complex with HSJ1b.

From Panel A, Figure 6.11, it is apparent that although the isolated N-terminal NBD was capable of binding to HSJ1b, the gel filtration profile of the NBD/J complex was devoid of any higher order oligomeric protein species. On the other hand the isolated C-terminal CTR is found to be perfectly capable of undergoing oligomerisation similar to the full length complex (Panel B, Figure 6.11). The degree of oligomerisation of the CTR/J complex was approximately 70% that of the intact rHH complex (Panel D, Figure 6.11). From Panel A and B it can be concluded that oligomerisation of Hsc70 and HSJ1b complex requires the C-terminal of Hsc70.

The next step was to pinpoint which region in the CTR - the C-terminal 18 kDa PBD or the 10 kDa lid region, was responsible for the oligomerisation. This was ascertained using the N60/J complex, since the N60 fragment differs from the full length Hsc70 only by the deletion of the C-terminal 10 kDa lid domain. From Panel C in Figure 6.11, it is clearly seen that although the presence of the 18 kDa PBD partially restored oligomerisation, however the observed oligomerisation was only one third of the capabilities of the full length rHH complex (Panel D, Figure 6.11). Therefore, the presence of the 18 kDa PBD alone is not sufficient to induce polymerisation and the C-terminal 10 kDa appears to be vital for the polymerisation of the complex.

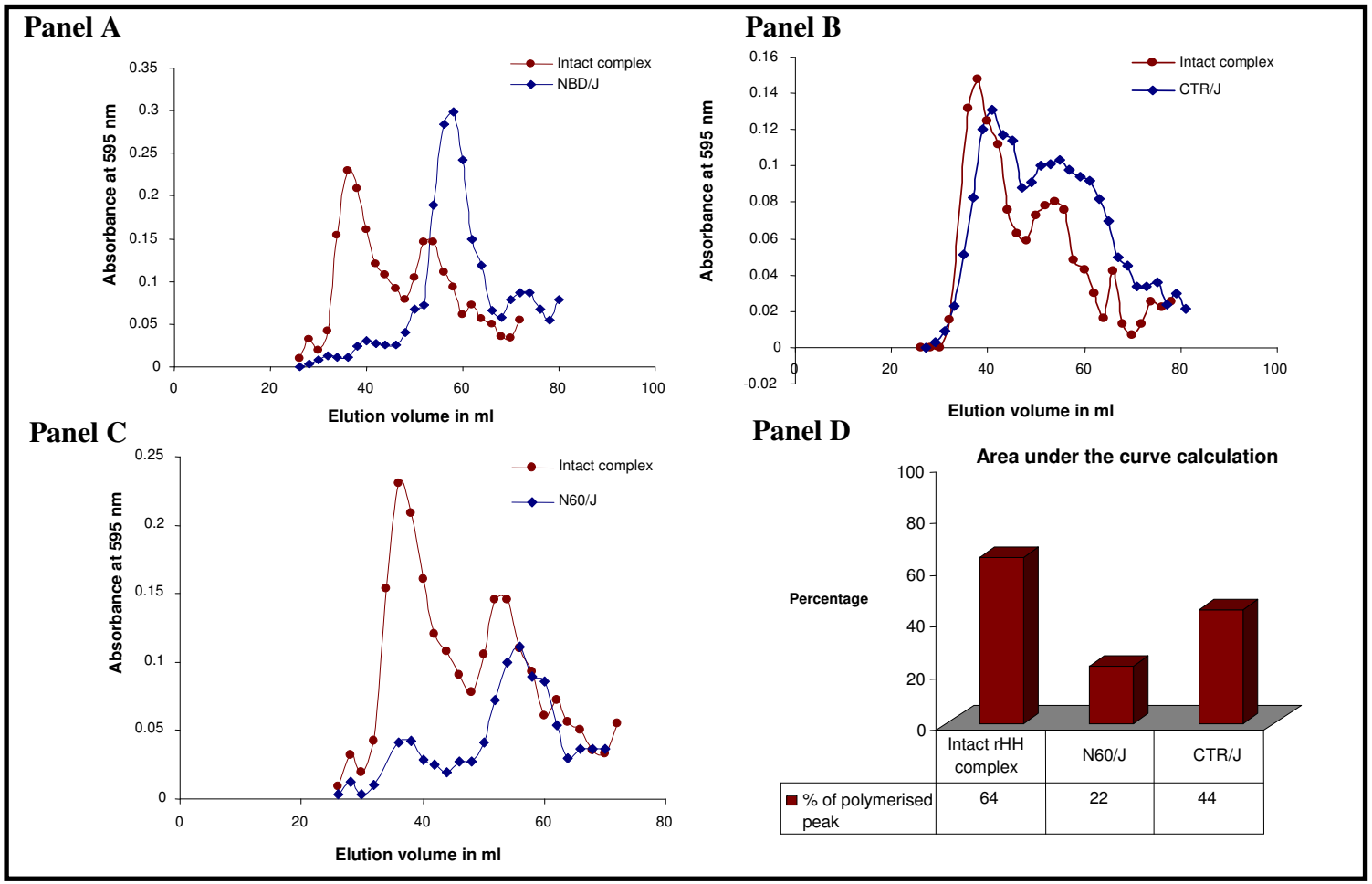

Figure 6.11: Comparison of SEC profiles of the individual Hsc70 domain/HSJ1b complexes with the SEC profile of full length complex

Size exclusion chromatography was performed on a superdex 200 column. 1 ml fractions were collected from the column after 25 ml of buffer had passed. Protein concentration of alternate samples was determined by Bradford assay, and the concentration was plotted to obtain the elution trace for each complex.
Panel A: Comparison of the chromatogram of the full length rHH complex with NBD/J. **Panel B:** Comparison of the chromatogram of the full length rHH complex with CTR/J. **Panel C:** Comparison of the chromatogram of the full length rHH complex with N60/J. **Panel D:** Degree of polymeristaion of the domain complexes. Area under peak 1 was calculated from the elution chromatogram plotted for each domain complex and percentage of total protein existing as a higher oligomeric species was calculated and plotted using MS Excel.

6.3.4 Changes in functional properties due to 10 kDa C-terminal deletion

From the SEC data, it was concluded that the 10 kDa C-terminal fragment of Hsc70 is essential for stable HSJ1b binding, and also functional oligomerisation of the rHH complex. The effect the deletion of this 10 kDa region has on the functional properties of the chaperone/co-chaperone complex was studied using the N60/J domain complex in comparison with the full length rHH complex. Two assays were used; first, was the thermal aggregation assay to study the capacity of the complexes to protect denatured substrate and second, was a modified malachite green colourimetric assay to monitor stimulation of ATP hydrolysis in both the protein complexes.

6.3.4.1 Protection of luciferase from thermal aggregation

Thermal aggregation studies were carried out as described in the previous chapters using luciferase as substrate. Aggregation of luciferase was initiated by elevating the temperature to 42^{o}C. The percentage of soluble and insoluble luciferase, after thermal aggregation, was measured densitometrically and plotted as percentage of total luciferase in the reaction (Figure 6.12). It was previously established that in the absence of the chaperone proteins, 81.4% of luciferase aggregated during a 10 minute incubation at 42 °C (refer Chapter4, section 4.3.1). However, when the full length rHH complex was present during thermal inactivation, 85.7% of the total luciferase protein remained soluble (reaction 3, Figure 6.12). This was reduced to 40% when the N60/J complex was used instead of the intact rHH complex without the addition of ATP (reaction 1, Figure 6.12). Intriguingly, the N60/J complex displayed a >70% ATP dependent increase in luciferase protection (increase from 40% to 68.2%, reaction 2 in Figure 6.12). This ATP dependent increase in luciferase solubility has so far not been observed for the full length complex. Ungewickell *et al* have previously shown that the N60 fragment is sufficient for the the binding of auxilin and for the *in vitro* uncoating of clathrin-coated vesicles (Ungewickell *et al*., 1997). In our case, the N60/J complex is sufficient for protecting luciferase from aggregation, although not to the same extent as the intact rHH complex. Also, the N60/J and the rHH show differences in their ATP requirements for substrate protection, suggesting mechanistic differences in the two protein complexes.

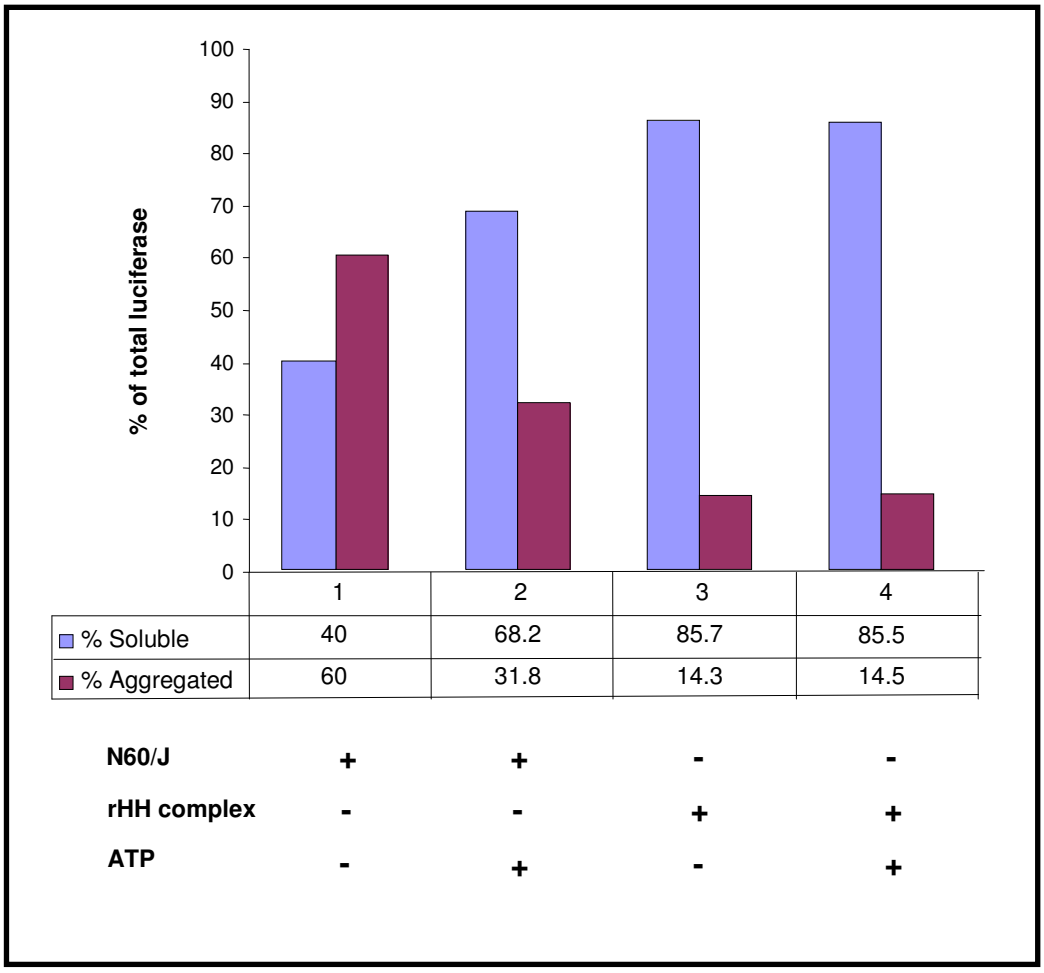

Figure 6.12: Luciferase protection studies using N60/J and full length rHH complexes.

Luciferase was thermally denatured at 42°C for 10 minutes in the presence of the indicated chaperones and nucleotide. The reaction was spun down at 13,000 rpm to separate the soluble and aggregated fractions and analysed by SDS-PAGE. The amount of luciferase present in each fraction was quantified by densitometry and the percentage of soluble and aggregated luciferase for each reaction was calculated and plotted using MS Excel.

6.3.4.2 ATP-Hydrolysis assay

We next compared the effect of the C-terminal 10 kDa truncation on the ATPase activity of the full length rHH complex using the N60/J complex. Stimulation of the basal ATPase activity was evaluated by measuring the phosphate released from the system using a modified malachite green colourimetric assay. Upon addition of 2 mM ATP, 41 nmols of Pi/mg/min was released by the rHH complex, compared to the 22 nmols of Pi/mg/min measured for the N60/J complex (Figure 6.13). The phosphate release measurements for the N60/J complex was approximately 50% less than that observed for the full length complex. Thus in the case of the Hsc70 and HSJ1b complex, the deletion of the of the 10-kDa fragment from the C terminus of Hsc70 does not completely abolish its ATPase activity, but it does have a deleterious effect on it.

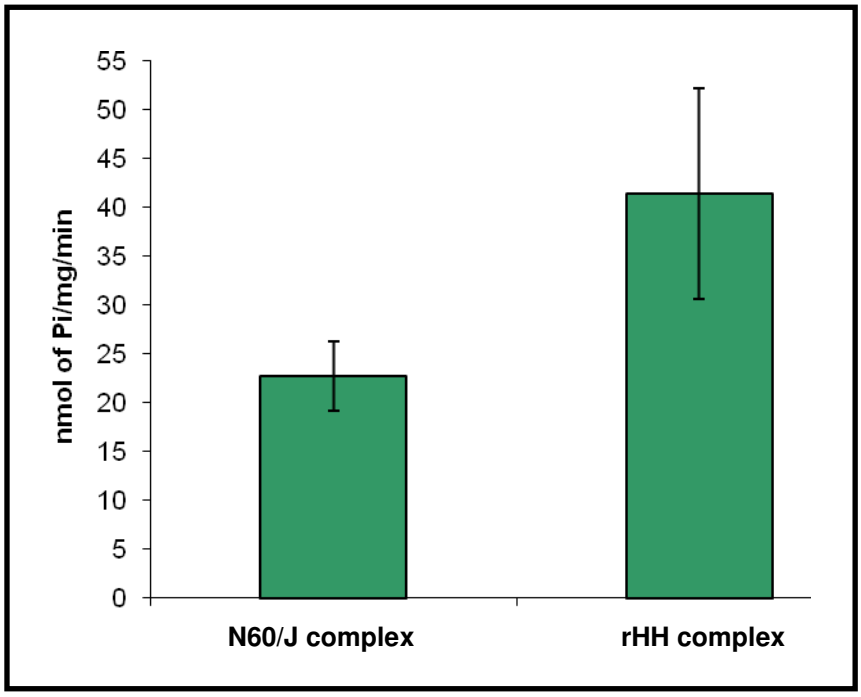

Figure 6.13: ATP hydrolytic capability of N60/J amd full length rHH complexes

The rHH and N60/J complex proteins (0.5 mM) were incubated with 2 mM ATP at 37^{o}C, and the amount of phosphate release was monitored colourimetrically using a modified Malachite Green non-radioactive assay. Readings were taken at 620 nm and phosphate release was calculated from the phosphate standard curve. Three independent experiments were performed, and the average and standard deviation were calculated.

6.3.5 Conformational changes due to 10 kDa C-terminal deletion

Limited proteolysis experiments were conducted to probe the potential differences in the conformational features of the N60/J complex and the recombinant rHH form. The digestion products were visualised by SDS-PAGE electrophoresis (Figure 6.14). Panel A shows the digestion products obtained for the N60/J complex and panel B for the intact rHH complex. From the time course experiments carried out in Chapter 4, it was observed that proteolysis could be observed within 10 minutes of incubation with chymotrypsin, and therefore this time period was considered to be sufficient for our studies with the N60/J complex. Our previous studies have also shown that in the rHH complex, the Hsc70 component appears to be largely resistant to proteolysis, while the HSJ1b subunit clearly was more sensitive to cleavage by chymotrypsin resulting in a ~28-30 kDa cleavage product (represented by arrow marks in Panel B, Figure 6.14). The proteolysis pattern obtained for the N60/J complex partly resembled that of the full length rHH complex. The characteristic ~28-30 kDa HSJ1b cleavage product was observed, but more interestingly the N60 fragment of Hsc70 also showed signs of proteolysis (represented by * lane 2 and 3, Panel A, Figure 6.14), which were not detected with the full length Hsc70. This indicates that the C-terminal 10 kDa fragment of Hsc70 may play a role of a shield to protect the Hsc70 full length protein from proteolysis, as observed for the rHH protein. Removal of this domain (as is the case for the N60 fragment) renders the Hsc70 protein moiety susceptible to the protease chymotrypsin. Thus the distal C-terminal 10 kDa region appears to be crucial for the chaperone/co-chaperone interaction, since the removal of this zone alters both the functional and conformational properties of the Hsc70/HSJ1b interaction.

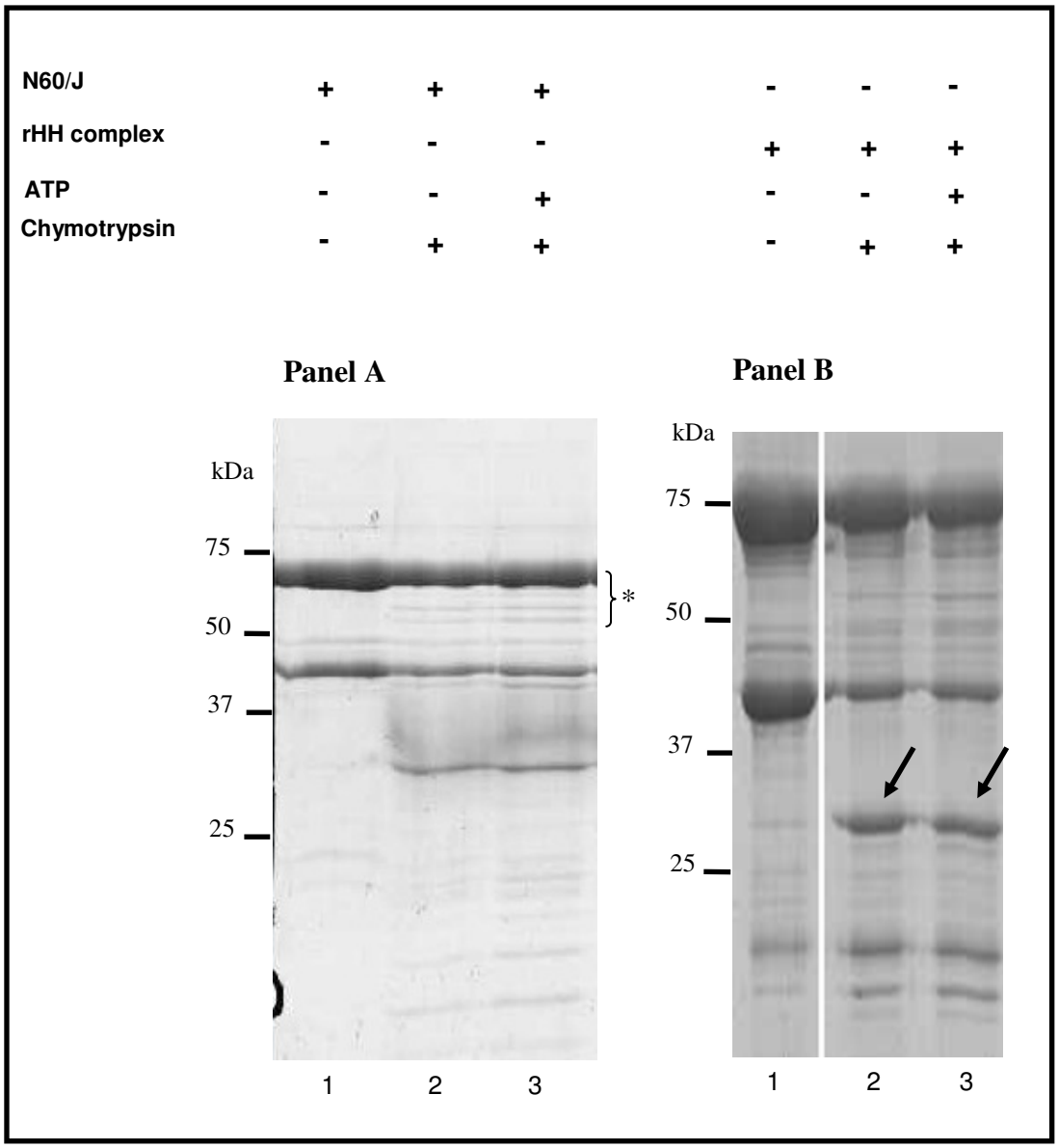

Figure 6.14: Limited proteolysis studies of N60/J amd full length rHH complexes using chymotrypsin protease

4.4 µg of both the protein complexes were incubated with chymotrypsin at 4°C in the presence and absence of ATP (2 mM). The digestions were performed in buffer containing 20 mM Tris-HCl pH 8.0, 50 mM potassium chloride, 3 mM magnesium chloride and 2 mM DTT for 10 min. The digestion products were analysed on a 12% polyacrylamide gel stained with Coomassie Blue. The first track on the left hand side (lane 1) in each panel is the control protein in the absence of chymotrypsin. Lane 2 in each panel is the proteolysis performed in the absence of ATP and lane 3 in the presence of ATP. **Panel A:** Chymotrysin digestion of the N60/J complex. Putative N60 domain proteolysis products are indicated by a *** Panel B:** Chymotrysin digestion of rHH complex. The arrowhead indicates the major digestion product of HSJ1b.

PART B: STRUCTURAL STUDIES

6.3.6 Structural studies of the domain complexes

Based on size exclusion chromatography the NBD/J complex was found to be the most promising construct for structural studies. In order to determine if the NBD/J complex was functionally active, ATPase activity was measured using a modified malachite green colourimetric assay. It was observed from the phosphate release measurements that the NBD/J complex exhibited approximately 7 fold lower phosphate release (Figure 6.15). This is not unusual, as it has been previously demonstrated that the ATP hydrolysis activity of the isolated NBD is not stimulated by Hsp40 co-chaperones (Laufen *et al*., 1999).

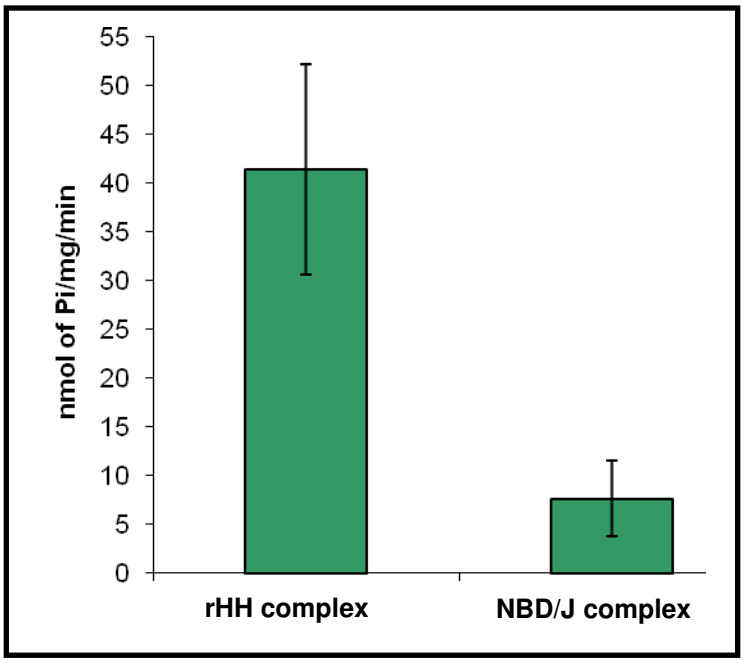

Figure 6.15: ATPase activity of the NBD/J complex compared with the rHH complex

The full length rHH and NBD/J complex proteins (0.5 mM) were incubated with 2 mM ATP at 37^{o}C, and the amount of phosphate release was monitored colourimetrically using a modified Malachite Green non-radioactive assay. Readings were taken at 620 nm and phosphate release was calculated from the phosphate standard curve. Three independent experiments were performed, and the average and standard deviation were calculated.

6.3.6.1 Crystallisation of NBD/J complex

The 135 kDa NBD/J peak fractions from SEC were pooled and concentrated with a 30 kDa cut off centricon. The purity of the protein was confirmed by SDS-PAGE before the crystallisation trials were undertaken (Lane 1, Figure 6.16). On a 15% gel, both the HSJ1b and NBD polypeptides could be distinguished and the protein prepared for crystallisation trials was estimated to be >95% pure.

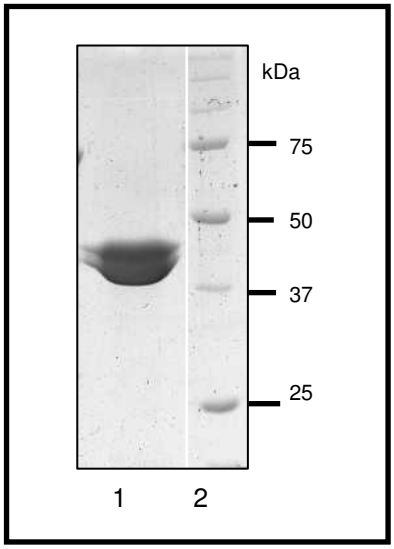

Figure 6.16: SDS-PAGE analysis of the concentrated NBD/J protein

Elution fractions from the SEC were pooled together and concentrated in a 30 kDa cut-off centricon. Prior to setting up the crystallisation trials, 1 µl of the concentrated protein was then loaded on 15 % SDS-PAGE gel to check the sample purity. Lane1 is loaded with 1 µl of the concentrated NBD/J complex and lane 2 Bio-Rad precision plus prestained molecular weight marker.

The NBD/J protein was screened using the commercial Hampton Crystal Screens 1 and 2 using protein at a concentration of 5 mg/ml. This was determined to be the optimal concentration for crystallisation trials as instant precipitation was observed in crystallisation trials set with a protein concentration above 5 mg/ml. Initial crystallisation trials were set up using the hanging drop vapour diffusion method. One µl of the protein was mixed with an equal volume of reservoir buffer and the trays were incubated at room temperature. Crystals were observed after 5 days in the conditions listed in Table 6.4. Further screens were also set up at the Molecular structure facility at NIMR, London, but no other crystals were obtained.

	Condition 15	Condition 22
Buffer, pH	0.1 M Sodium cacodylate trihydrate pH 6.5	0.1 M Tris hydrochloride pH 8.5
Precipitant	30% (w/v) PEG 8000	30% (w/v) PEG 4000
Salt	0.2 M Ammonium sulphate	0.2 M Sodium acetate trihydrate

Table 6.4: Crystallisation conditions identified for the NBD/J complex from Hampton Crystal Screen 1

The crystals obtained from conditions 15 and 22 of Hampton crystal screen are shown in Figure 6.17. Crystals from condition 15 appeared as overlapping plates (Panel A, Figure 6.17) and condition 22 gave rise to wafer thin needle-like crystals (Panel B, Figure 6.17). For low-temperature measurement, the crystals were dipped into a drop of cryo solution prepared by the addition of glycerol as cryoprotectant at a final concentration of 20% (wvv) to the identified crystallization solution, flash frozen in a nitrogen-gas cryostream at 113 K and stored until diffraction analysis.

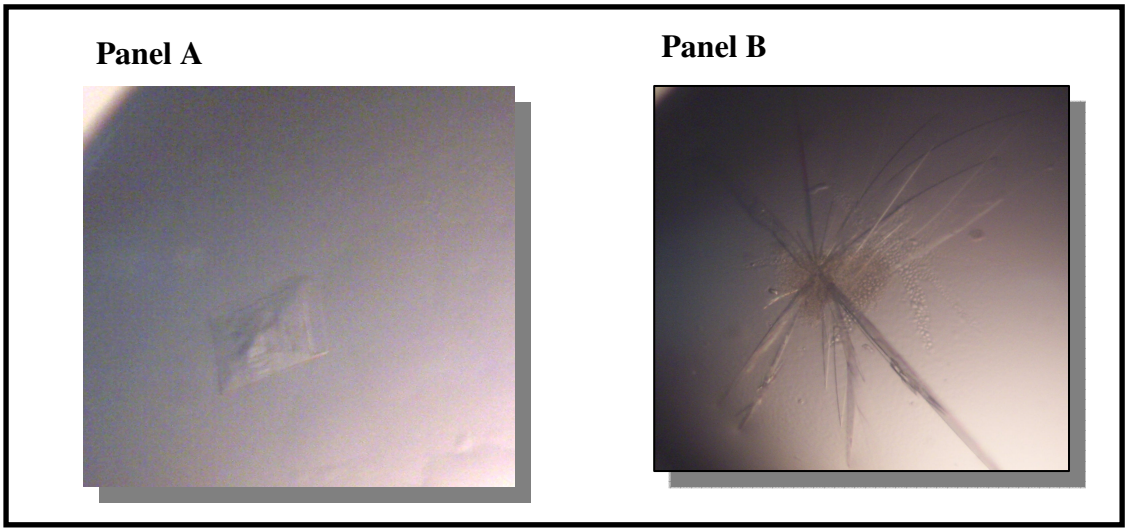

Figure 6.17: NBD/J crystals obtained from screening with Hampton Crystal screen 1.

Crystals were obtained using the hanging drop vapour diffusion method, with NBD/J co-expressed protein at 5 mg/ml, under Hampton crystal screen 1 conditions 15 (Panel A) 0.1 M sodium cacodylate trihydrate pH 6.5, 30% (v/v) PEG 8000, 0.2 M ammonium sulphate and 22 (Panel B) 0.1 M Tris hydrochloride pH 8.5, 30% (v/v) PEG 4000, 0.2 M sodium acetate trihydrate.

6.3.7 Structure solution for crystals from condition 22

X-ray analyses were performed at the Diamond synchrotron facility at Oxford. The crystal diffracted up to 2.75 Å. The structure was analysed at NIMR, Mill Hill by Dr.Steve Smerdon, who provided us with the refined structure to carry out further analysis. Figure 6.18 shows the typical diffraction pattern for the crystals obtained from condition 22. The collected data was processed using the HKL-2000 program package using DENZO (Otwinowsky and Minor, 1997) and the resulting intensities scaled using SCALEPACK (Otwinowsky and Minor, 1997).

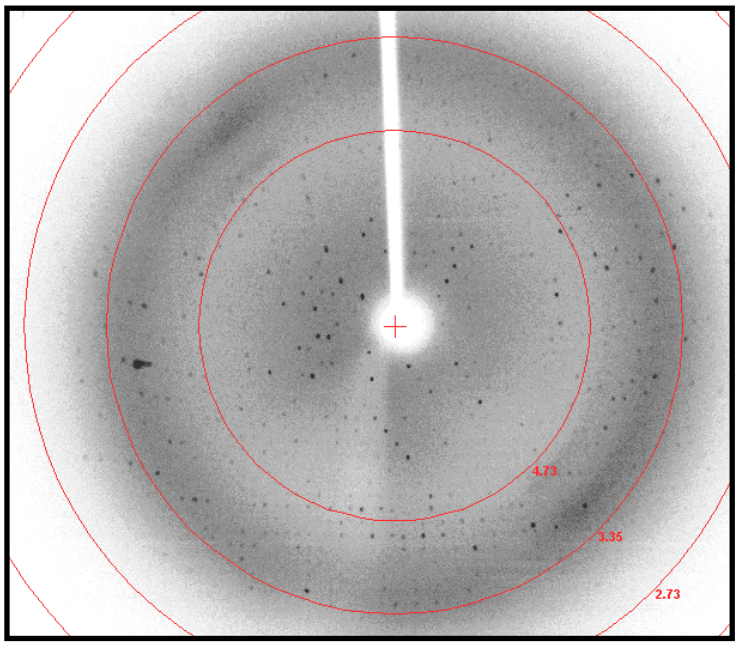

Figure 6.18: Diffraction pattern of NBD/J crystals obtained from condition 22 of Hampton crystal screen .

The solvent content of the crystal was determined by calculating the Mathews' coefficient (Matthews, 1968). Based on the solvent content and the expected molecular weight of the protein sample, an estimate can be made on the number of molecules in the asymmetric unit. The calculation was performed using the matthews_coef program from the CCP4 programme suite (Dodson *et al*., 1997). Working with a molecular weight of 79.7 kDa (44 kDa for the Hsc70 NBD + 35.7 kDa for HSJ1b), the solvent content calculated allowed for the presence of 2 molecules in the asymmetric unit. The structure solution was initiated by molecular replacement using MOLREP (Vagin & Teplyakov, 1997). The bovine Hsc70 ATPase domain with bound ADP (PDB id: 3HSC) was used as the model for molecular replacement. The electron density map was examined using WinCoot (Emsley and Cowtan, 2004). The structure solution

obtained from the data collected for the condition 22 crystal matched exactly with the structure of 3HSC. No extra density was observed either for the HSJ1b protein or for any bound nucleotide. Crystals obtained from Condition 22 were therefore the unliganded NBD without its HSJ1b partner. The model developed was subjected to molecular refinement using REFMAC. The cell parameters details are shown in Table 6.5.

Apo-Hsc70 NBD	
Space group	$P12_11$
Cell parameters (Å)	a 73.2
	b 77.8
	c 75.3
	α 90
	β 100.6
	γ 90
Resolution range (Å)	14.934 - 2.756
Total No. of reflections	21513

Table 6.5: Cell parameters for the Apo form of the Nucleotide binding domain of Hsc70

The stereochemical quality of the protein structure was analysed by running the PROCHECK v.3.5.4 suite of programs (Laskowski *et al*., 1993) on the Stuctural Analysis and Verification Server. Figure 6.19 is the Ramachandran's plot generated for the structure. Ramachandran's map is the plot of the phi and psi angles of the amino acids to yield a conformational map (Ramachandran *et al*., 1963). The structure has 87.8% of the residue in the core region (red region on the plot, labelled A, B, L in Figure 6.19), 11.3% residues in the additional allowed regions (labelled a, b, l, p in Figure 6.19), 0.75% residues in the generously allowed regions [labelled ~a, ~b, ~l, ~p in Figure 6.19] and just 0.1% in the disallowed region.

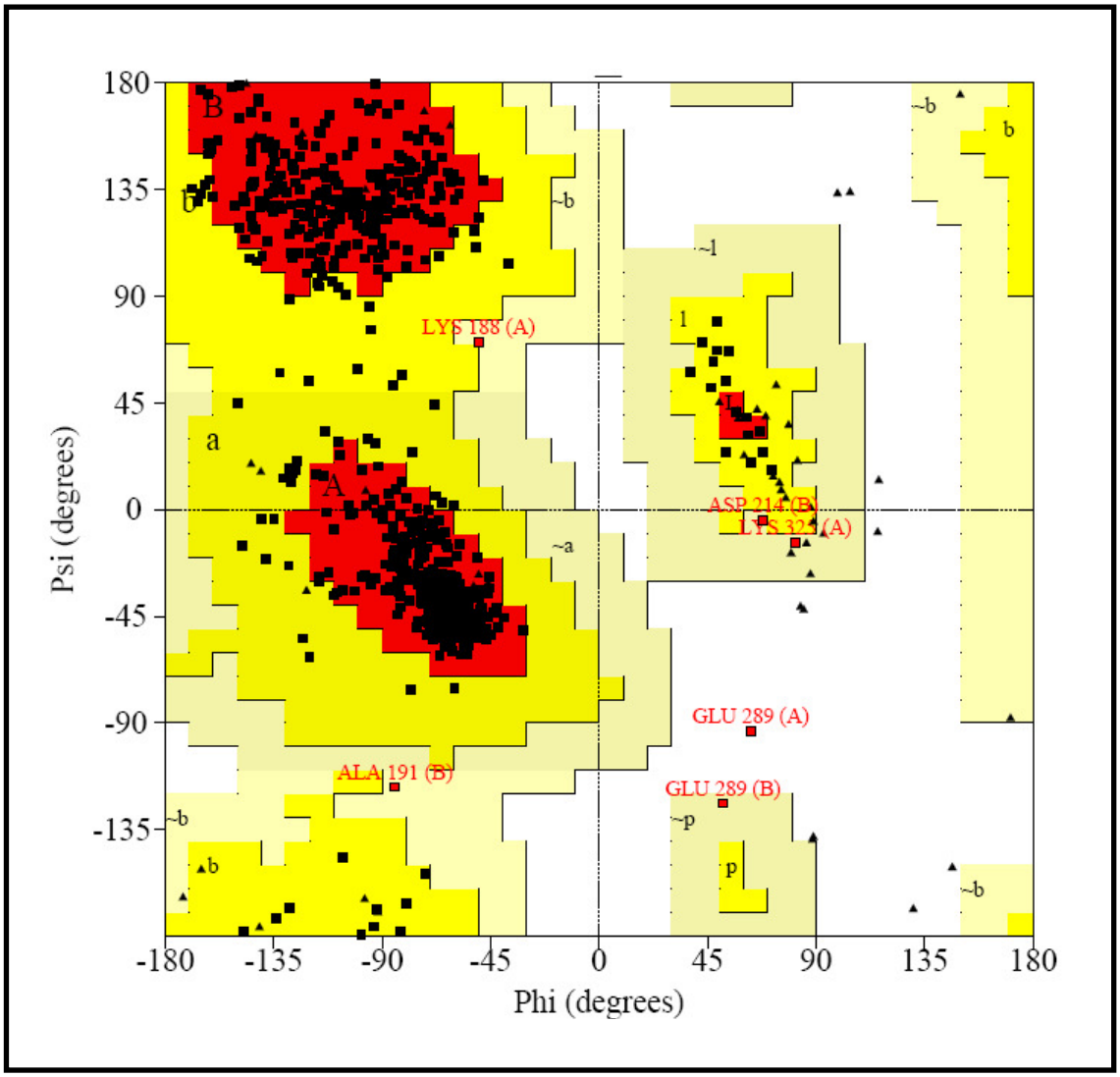

Figure 6.19: Ramachandran plot of the apo form of the nucleotide binding domain of Human Hsc70.

The Ramachandran plot was generated using the PROCHECK v.3.5.4 suite of programs on the Stuctural Analysis and Verification Server. The colouring/shading on the plot represents the different regions described in Morris *et al.*, (1992). The red areas correspond to the "core favoured" regions, the yellow areas corresponds to the additional allowed regions, while the off-white areas represent the generously allowed regions. Residues in generously allowed and disallowed regions are labelled in red.

6.3.8 General features of the apo-NBD structure

Preliminary crystallographic analysis showed that the protein crystal belongs to the monoclinic lattice. Further processing and scaling confirmed the space group to be $P12_11$. The cell parameters are a = 73.2 Å, b =77.8 Å, c = 75.3 Å, $\alpha = \gamma = 90^o$, $\beta = 100.6^o$. The crystal has two chains (A and B) in the asymmetric unit (Figure 6.20). In Figure 6.20 a cartoon representation of chain A and chain B of the apo form of the NBD is shown. The sub-domains were assigned based on previous structural characterisations of the nucleotide bound NBD structures (Flaherty *et al*., 1994; Zhang and Zuiderweg, 2004). The Hsc70 NBD comprises of two lobes. Lobe I extends from residue 1-188 and 361-384, while lobe II is formed of the remaining residues. Each lobe can be further distinguished into two sub-domains – IA (coloured red in Figure 6.20) and IB (coloured yellow in Figure 6.20) for lobe I and IIA (coloured green in Figure 6.20) and IIB (coloured orange in Figure 6.20) for lobe II (Zhang and Zuiderweg, 2004).

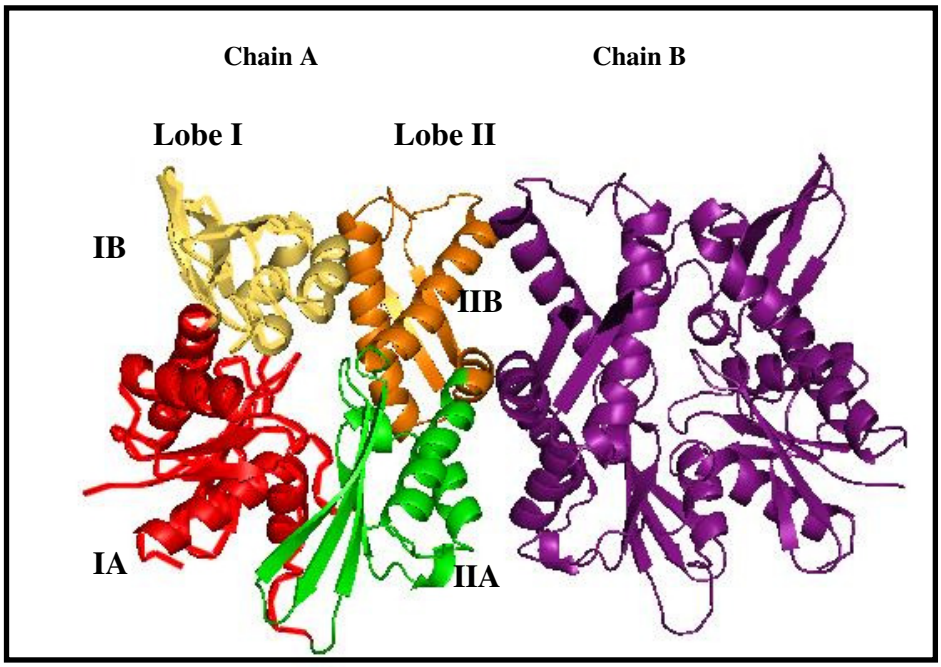

Figure 6.20: Structure of the apo form of the Nucleotide binding domain (NBD) of Human Hsc70.

Ribbon representation of the NBD of human Hsc70 generated by Pymol. Chain A and B are both shown. The division of the NBD into lobe I and II and the assignment of sub-domains IA, IB and IIA, IIB are depicted in red, yellow, green and orange respectively on Chain A. Chain B is shown in purple.

The structure was analysed using the Protein Interfaces, Surfaces and Assemblies (PISA) service, version 1.18 (Krissinel and Henrick, 2007) offered on the Protein Databank in Europe (PDBe) site. PISA is an interactive tool for the exploration of macromolecular interfaces and prediction of probable quaternary structures. The solvation energy (ΔG) and buried surface area for the two chains were calculated. The results are tabulated in Table 6.6. For chain A, of the total 382 amino acids in the protein chain 346 of them are surface exposed residues. The solvent accessible area for this chain is 17508.5 $Å^2$ and the solvation energy for folding (ΔG) is -352 Kcal/mol. As expected, the corresponding values obtained for Chain B match very closely to those of Chain A. Analysis of protein interfaces between Chain A and B did not reveal any specific interactions that could result in the formation of stable quaternary structures. Therefore the dimeric structure obtained is most probably due to the crystal packing and not indicative of the quaternary structure adopted by the protein in solution.

Chain	Surface		ΔG, Kcal/mol
	N_{res}	Area, $Å^2$	
A	346	17508.5	-352.0
B	350	17455.9	-352.4

Table 6.6: Solvation energy and solvent-accessible surface area of the two chains A and B of the apo form of the Nucleotide binding domain (NBD) of Human Hsc70.

N_{res} is the number of amino acids present on the surface of the protein, **ΔG** is the solvation energy for folding and the **Area** represents solvent-accessible surface area of the structure, in $Å^2$.

6.3.9 Alignment studies

Next, comparison of the apo form of the nucleotide binding domain with selected nucleotide bound entries in the Protein Data Bank (PDB) was carried out using the Protein structure comparison service (SSM) at European Bioinformatics Institute (http://www.ebi.ac.uk/msd-srv/ssm) authored by E. Krissinel and K. Henrick. The structures used in the analysis are as follows: (i) Bovine Hsc70 NBD in the ADP bound state (3HSC), (ii) E175S mutant of bovine Hsc70 NBD in the ADP bound state (1NGA), (iii) Bovine Hsc70 NBD in the ANP (Phosphoaminophosphonic acid-

adenylate ester) bound state (1NGI) and (iv) D199S mutant of bovine Hsc70 NBD in the ATP bound state (1NGE). These structures are referred to by their PDB codes in the following sections.

6.3.9.1 Overall alignment

The conformation of the apo and liganded forms of the Hsc70 NBDs were compared using the Secondary Structure Matching tool (Krissinel and Henrick, 2004) from the PDBe services. The programme compares 3-dimensional structures of proteins and provides the Cα alignment of the compared structures. The apo structure of the Hsc70 NBD superimposed well with the liganded conformations, with an average r.m.s. deviation of 0.7 Å for the main-chain Cα atoms. The root mean square deviation (RMSD) values and corresponding Q-scores for each of the structure used in the study is tabulated in Table 6.7. The Q-score is a quality function of Cα-alignment, and takes into account the alignment length and RMSD. A Q-score of 1 is possible only in the case of identical structures (Krissinel and Henrick, 2004). From the RMS deviation and the Q-score (tabulated in Table 6.7) obtained for the superimposition of the apo NBD with other structures from the Pdb database, we can draw the conclusion that the differences in the Cα chain of the liganded and unliganded states of the NBD is minimal.

PDB Identifier	Protein information	RMSD	Q-score
3hsc:A	Bovine Hsc70 NBD with bound ADP	0.747	0.922
1ngi:A	Bovine Hsc70 NBD +ANP +Ca^{2+}	0.715	0.9117
1nga:A	Bovine Hsc70 apo NBD +ADP +Mg^{2+}	0.764	0.9243
1nge:A	Bovine Hsc70 apo NBD +ATP +Mg^{2+}	0.736	0.9088

Table 6.7: RMSD and Q-scores for the Cα alignment of the apo form of the NBD with the nucleotide bound forms

This was not surprising since previous studies analysing the native and mutant NBD's in complex with different nucleotides have not revealed conformational changes between the different nucleotide dependent forms (O'Brien and McKay, 1993, Flaherty *et al*., 1994). Alignment of 11 bovine Hsc70 NBDs, with different nucleotide occupancy, all superimposed with a pairwise RMSD of <0.5Å, suggesting structural rigidity of the NBD (Zhang and Zuiderweg, 2004). Figure 6.21 shows a pairwise

overall alignment of the apo NBD structure obtained in this study (coloured blue) with the ADP bound structure of the bovine Hsc70 (Pdb id:3HSC, coloured red), which illustrates this observation. As expected, no major structural changes could be detected.

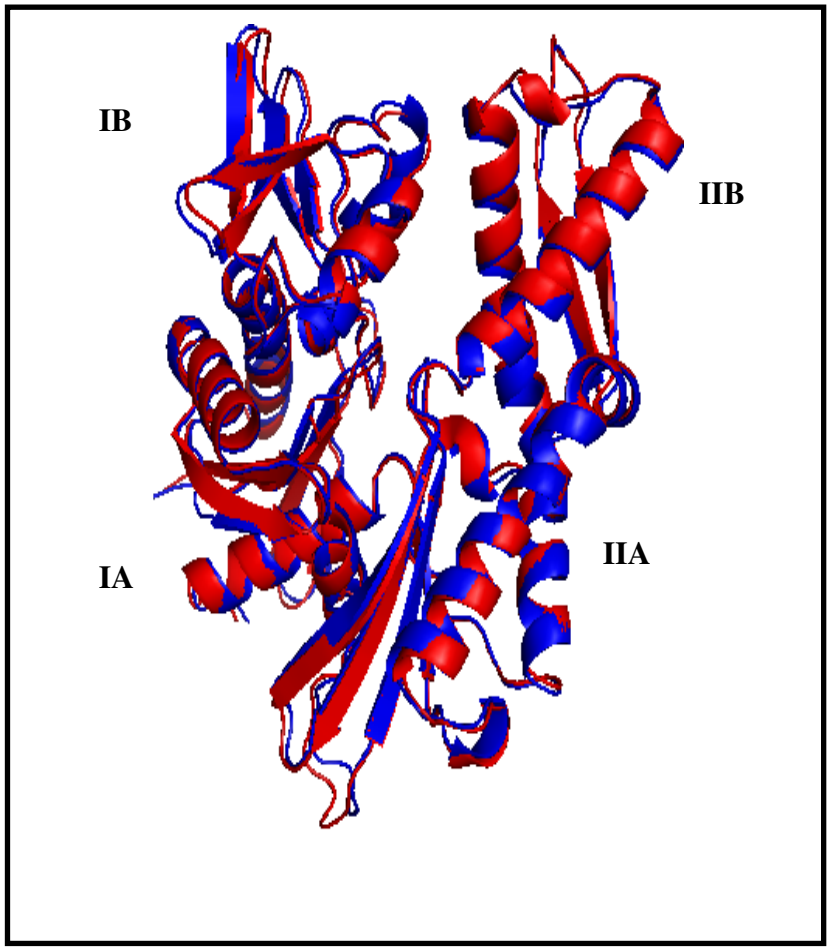

Figure 6.21: Overall alignment of the human Hsc70 apo-NBD with the bovine ADP bound form (3HSC)

Chain A of the human apo-NBD structure was superimposed with the ADP bound structure (pdb id:3HSC). The figure shows an overlay of the ribbon representations with the apo-NBD represented in blue while the ADP bound form is in red. The image was generated using Pymol.

6.3.9.2 Sub-domain alignment

Although the crystal structures have not shown major conformational changes between the different nucleotide bound states, NMR analysis has revealed the existence of flexibility and movement in the NBD (Zhang and Zuiderweg, 2004). Therefore, instead of studying the overall movement of the whole NBD, the relative movement of the two sub-domains of the NBD i.e lobe I and lobe II was assessed. A comparison was carried out between the human apo structure and the bovine ADP bound structure (Pdb id: 3HSC). The crystal structures were both visually analysed and structurally superimposed using PyMOL.22 (DeLano, 2002). The two structures were studied by firstly superimposing the Lobe I of the NBD, and then the matrix thus obtained was used to transform the whole molecule. Figure 6.22 shows that the two structures which were very closely aligned (refer Figure 6.21), now records a displacement of lobe II of the NBD with respect to lobe I. Inspection of lobe II in Figure 6.22 shows a previously undetected movement in the loop and helical regions of the sub-domain IIB of lobe II (indicated by an arrow) depending on the liganded/unliganded state of the NBD.

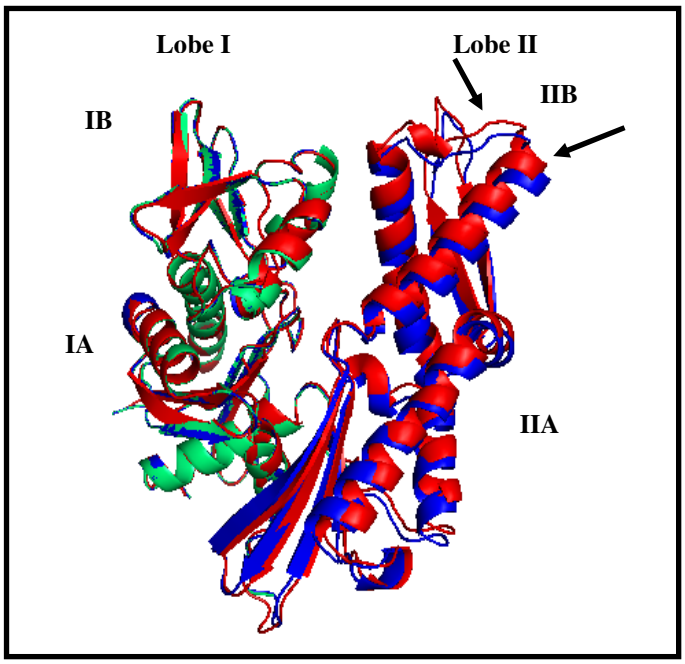

Figure 6.22: Sub-domain alignment of the human Hsc70 apo NBD with the ADP bound form

The superimpositions were generated by Pymol. The figure shows an overlay of the ribbon representations of apo-NBD (blue) with the ADP bound NBD (Pdb id: 3HSC, red). Lobe I residues (shown in green) alone were aligned and the transformed matrix was applied to the whole molecule. The resulting superimposition reveals displacement in lobe II.

Distance measurements showed that some of the residues in the helix and loop connecting helix I and II of 3HSC were displaced by > than 2Å. Figure 6.23 shows the displacement of sub-domain IIB of lobe II of 3HSC (trace in red) with respect to the apo form (trace in blue). Distances between a few equivalent Cα atoms in the loop region of sub-domain IIB in lobe II are indicated in the figure.

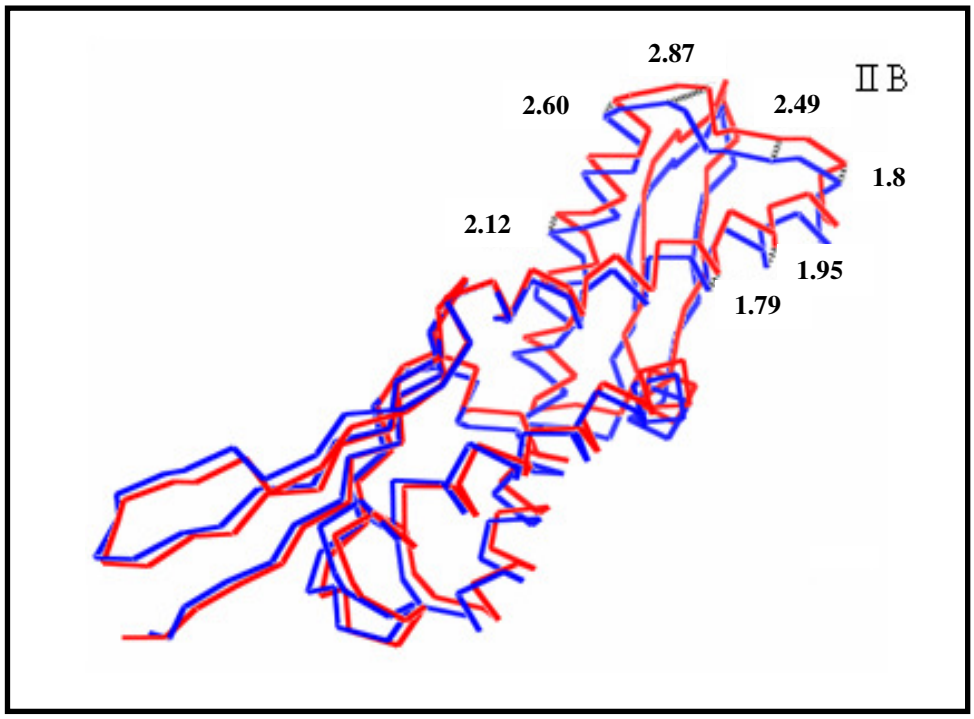

Figure 6.23: Superimposed Cα trace of the apo form of human Hsc70 and the bovine ADP bound form

The ADP bound (Pdb id: 3HSC) and the apo NBD structures are shown in red and blue, respectively. The two structures were superimposed as described previously using lobe I residues and the relative movement of lobe II was observed. The distances (in Å) between a few equivalent Cα atoms in the two states are marked in the sub-domain IIB of lobe II.

Similar alignment studies of the human apo NBD structure were also performed with 1NGI, 1NGA and 1NGE structures which were the ANP, ADP and ATP bound forms of the bovine NBD. The results obtained were similar to that obtained with the 3HSC structure (data not shown). This clearly indicates that the lobe II of the apo state of the NBD takes up an alternate position to that observed in the liganded state, irrespective of the bound ligand (ADP, ANP or ATP). Flexibility in sub-domain IIB has been reported in the crystal structure of the bovine Hsc70 NBD bound to the BAG domain (Sondermann *et al*., 2001). The movement observed in sub-domain IIB assumes

additional significance since it lines the nucleotide binding cleft along with sub-domain IB (Zhang and Zuiderweg, 2004).

6.3.9.3 Alignment of residues involved in inter sub-domain interaction

The nucleotide binding domain structure has been observed to adopt two conformations. The "closed" form has been observed in crystal structures obtained in the nucleotide bound state (Flaherty *et al*., 1990, 1994; O'Brien *et al*., 1996; Zhu *et al*., 1996; Chang *et al*., 2008) and in the nucleotide free state (Jiang *et al*., 2007; Shida *et al*., 2010). The "open" form has been reported for the human Hsc70 NBD/BAG domain complex (Sondermann *et al*., 2001), the bovine Hsc70 nucleotide-free NBD-SBD fragment (Jiang *et al*., 2007) and the human Hsp70 NBD and ATP-bound yeast Sse1 complex (Polier *et al*., 2008). Shida *et al*., have identified that in the closed conformation, an interaction exists between the Glu268 from sub-domain IIB with Tyr15 and Lys56 from sub-domains IA and IB, respectively, which is absent in the open conformation. They concluded that this interaction is with Glu268 is crucial for maintaining the geometry of the closed form. We therefore looked into the existence of interaction between the Glu268 and Tyr15 and Lys56. Using Pymol, the distance between Glu268 and Tyr15 and Lys56 was measured (Figure 6.25). Glu268 is 5.11 Å from Tyr15 and 6.23 Å from Lys56. From these measurements, it can be concluded that Glu268 is too far away to interact with either Tyr15 or Lys56, and therefore the apo form of Hsc70 NBD exists in an open conformation.

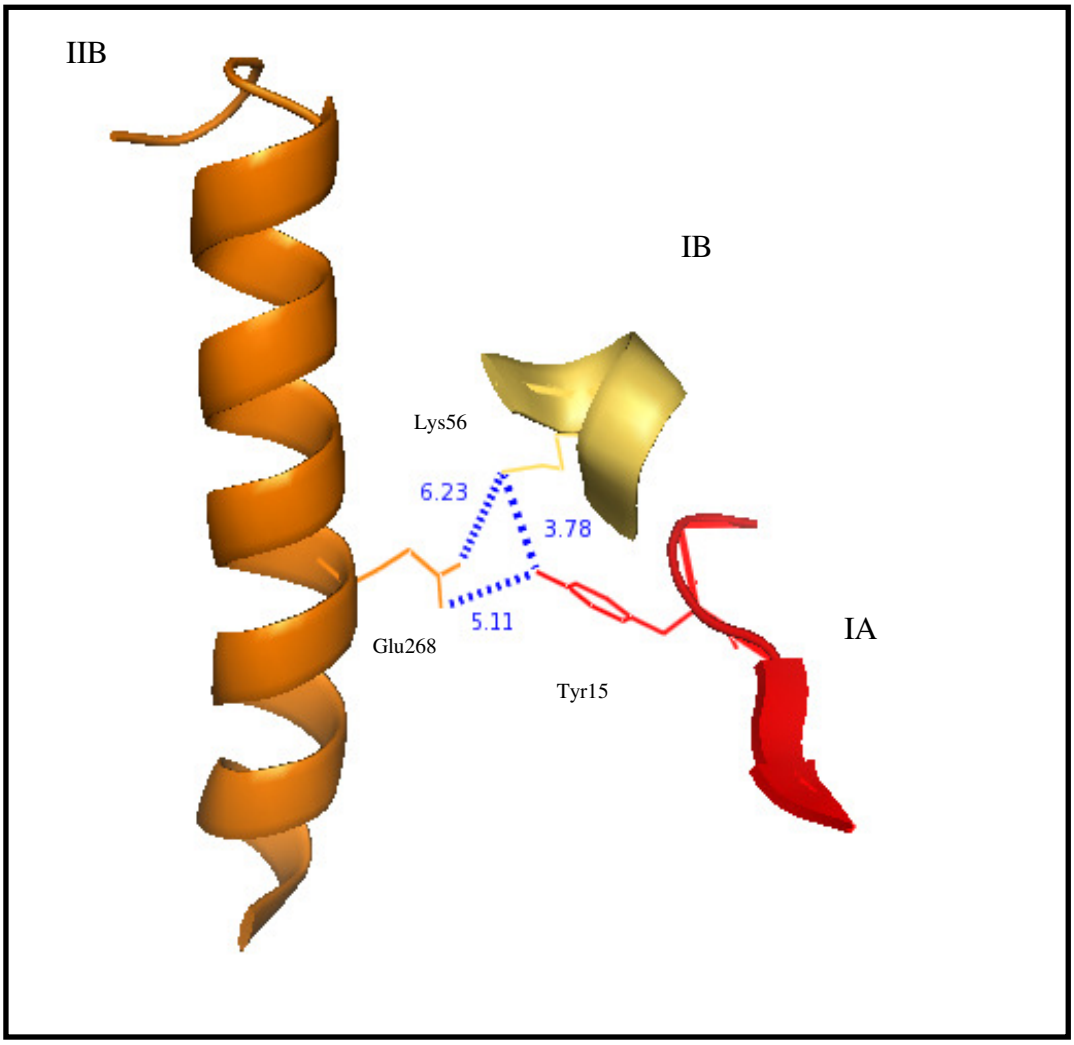

Figure 6.24: Distance of Glu268 from Tyr15 and Lys56 in the open-form NBD

The distances between Glu268 from sub-domain IIB to Tyr15 and Lys56 from sub-domains IA and IB were measured using Pymol. The sub-domains IA, IB and IIB are depicted in red, yellow and orange respectively. Glu268, Tyr15 and Lys56 are depicted in stick mode. The distances(in Å) between the residues are displayed on the blue dashed lines.

6.3.9.4 Alignment of residues involved in ligand binding

NMR studies on the NBD from the Hsp70 of *Thermus thermophilus* revealed that conformational changes observed in the apo state are localised in the ligand binding site. (Revington *et al*., 2004) In particular sub-domain IA and IIB have been implicated (Revington *et al*., 2004). In the previous section relative movement of lobe II with respect to lobe I was established, therefore the next step was to analyse the effect of this displacement in the ligand binding site. The side chains of the NBD involved in making polar contacts with ADP was identified using the 3HSC structure. The PISA service on the PDBe site was used for this purpose. Using Pymol, the 3HSC residues involved in ligand binding were aligned with the corresponding residues from apo NBD structure (Figure 6.25). Panel A in Figure 6.25 reveals the position of the amino acids necessary to make contact with ADP and their relative position with respect to ADP in the 3HSC crystal structure. Panel B in Figure 6.25 now displays the relative position of the equivalent residues of the aligned apo NBD structure with respect to 3HSC. Residues from the apo structure are in blue and the corresponding residues from 3HSC are in red. The relative shift in the positioning of these residues in the apo state from their ligand bound state positions was measured (Panel B of Figure 6.25).

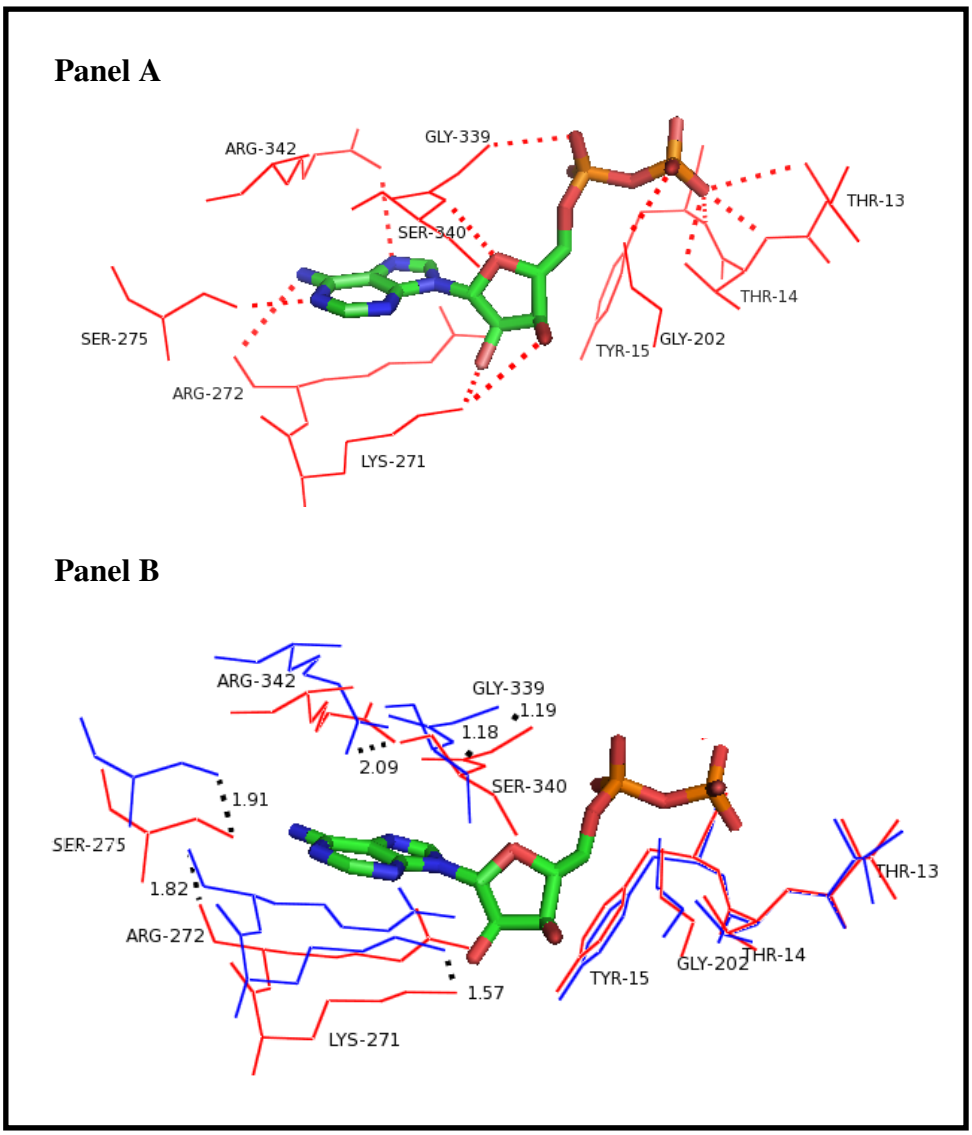

Figure 6.25: Displacement of residues involved in nucleotide binding

Residues involved in making polar contacts with ADP were identified suing the 3HSC structure. Selected amino acids residues and ADP are depicted in stick mode. Residues from 3HSC are depicted in red and those from the apo-NBD are in blue Hydrogen bonding interactions between nucleotide and the 3HSC residues are displayed as red dashed lines. The difference in positioning of equivalent residues from 3HSC and apo-NBD are emphasised by black dotted lines. The distanc (in Å) between the equivalent residues from 3HSC and apo-NBD is also shown. The figure was generated using PyMol.
Panel A shows the positioning and mode of interactions of the identified residues from 3HSC with ADP. **Panel B** shows the relative position of the equivalent residues of the apo structure when aligned sub-domain wise with 3HSC

Some of the residues such as Arg342, Ser 275, Arg 272 and Lys 271 were displaced by more than 1.5Å. The effect of such a displacement in the positioning of the key residues in the nucleotide binding cleft on their interaction with ADP was studied. This was achieved by measuring the hypothetical hydrogen bonding distance between the displaced residues of the apo structure and corresponding atom on ADP (Table 6.8). The position on the amino acid from which the measurements were made is also indicated within brackets in column 3 of Table 6.8. These values were then compared with the known values obtained for the 3HSC structure. The values are tabulated in Table 6.7. Ser 275, Gly 339, Ser 340 and Lys 271 (coloured red in Table 6.8) show an increase in hydrogen bonding distance in the apo form of almost 1 Å. This suggests that conformation of the nucleotide binding cleft in the apo NBD form displaces some of the key residues such that it is not conducive to forming contacts with this ligand.

No	Position on ADP	Residue Information	Distance between the amino acid and ADP in 3HSC	Distance between the amino acid and ADP in the apo state
1	ADP [N6]	ARG 272[O]	3.71	3.30
2	ADP [N1]	SER 275[OG]	2.69	3.89
3	ADP [O1B]	GLY 202[N]	3.04	2.75
4	ADP [O3B]	TYR 15[N]	2.82	3.08
5	ADP [O3B]	THR 13[N]	3.47	3.21
6	ADP [O3B]	THR 14[N]	2.71	2.72
7	ADP [O3B]	THR 14[OG1]	2.51	2.71
8	ADP [O1A]	GLY 339[N]	2.91	3.97
9	ADP [O4']	SER 340[N]	3.50	4.36
10	ADP [O3']	LYS 271[NZ]	3.48	3.75
11	ADP [O2']	LYS 271[NZ]	2.60	3.35
12	ADP [N7]	ARG 342[NH1]	3.38	3.09

Table 6.8: The hydrogen bonding distance (Å) between the residues involved with nucleotide binding and ADP.

Residues in red are displaced by almost 1 Å in the apo NBD structure when compared with the bovine ADP bound structure (3HSC).

6.3.10 Structure solution for crystals from condition 15

The structure of crystals obtained from condition 15 was analysed by Dr. Steve Smerdon at the NIMR facility, Mill Hill. The crystal diffracted up to 2.2 Å. Figure 6.26 shows the typical diffraction pattern for the crystals. Preliminary crystallographic analyses showed that the protein crystal belongs to the monoclinic lattice and further processing and scaling confirmed the space group to be $P12_11$. The cell parameters are a = 61.8 Å, b = 86.06 Å, c = 114.3 Å, $\alpha = \gamma = 90^o$, $\beta = 96.7^o$. The collected data was processed and scaled as described in the earlier section. Structure solution was initiated by molecular replacement using MOLREP using the Hsc70 ATPase domain with bound ADP (PDB id: 3HSC) as a phasing model. However molecular replacement was unsuccessful and no satisfactory solution could be obtained.

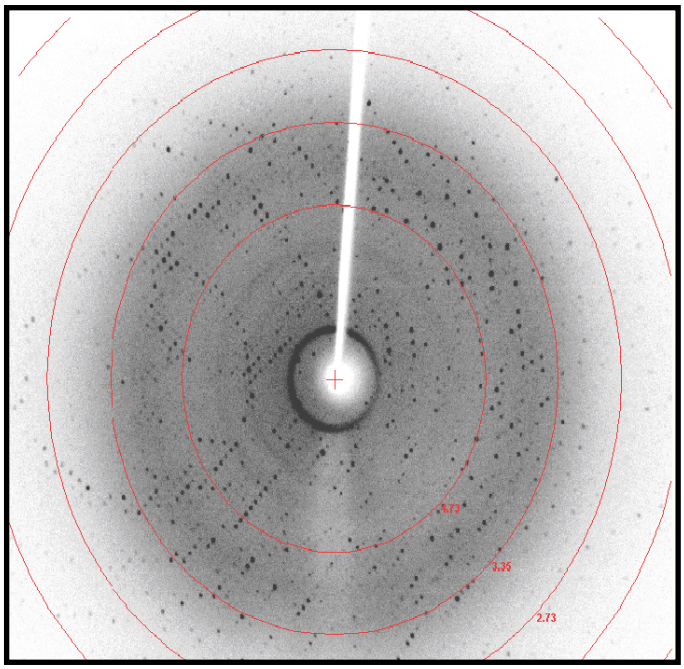

Figure 6.26: Diffraction pattern of NBD/J crystal obtained from condition 15 of Hampton crystal screen

As a means of obtaining phase information which was required to solve the structure for the protein in crystals obtained from condition 15, production of seleno-l-methionine substituted NBD/J protein was undertaken. SelMet labelling was achieved by inhibition of methionine biosynthesis (Doublié, 1997), in a methionine auxotrophic *E. coli* strain, in this case B834 [DE3]. The NBD/J complex was expressed in a minimal medium supplemented with SelMet as described in Materials and Methods (section 6.2.5) to produce proteins where the methionine residues are replaced with seleno-L-methionine. The NBD/J complex was purified using the same sequential chromatographic steps as those used for the native protein. Figure 6.27 compares the gel filtration elution profile of the SelMet labelled NBD/J protein with the native protein to confirm that the oligomerisation of the NBD/J complex remains unchanged with the incorporation of the selenium label.

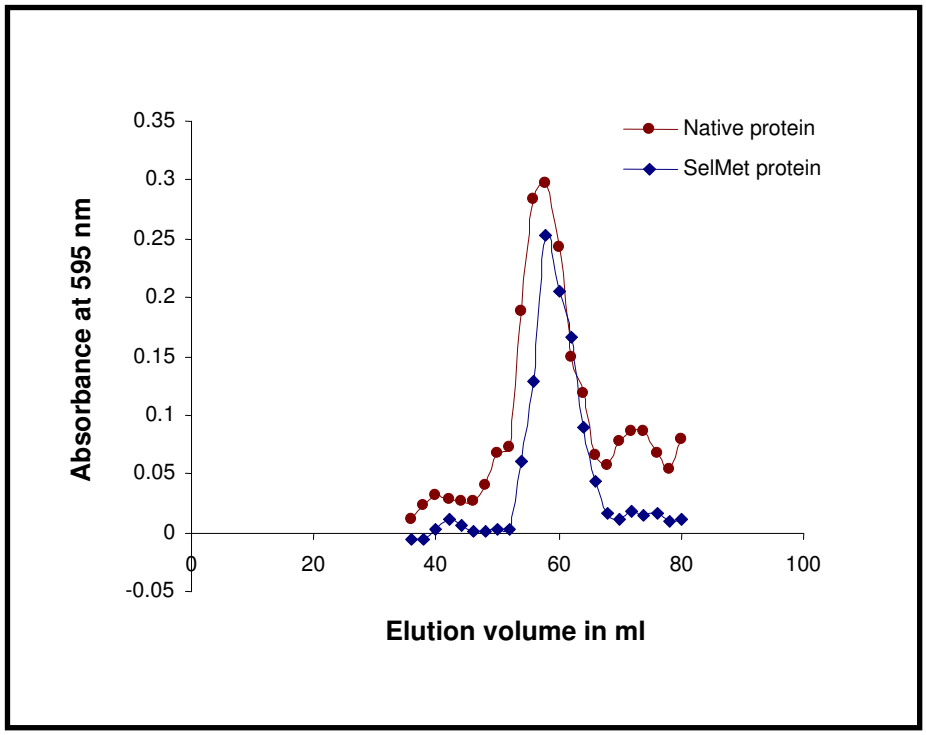

Figure 6.27: Comparison of the SEC elution profile of the native NBD/J complex with the SelMet labelled NBD/J complex.

Native NBD/J protein was expressed in BL21(DE3) and SelMet labelled NBD/J protein was expressed in B834 [DE3]. Both proteins were purified from Ni-NTA and Ion exchange chromatography following the protocols described previously. Size exclusion chromatography was performed on a Superdex-200 column and the protein eluting from the column was collected as 1 ml fractions. The absorbance of each fraction was determined using Bradford assay.

Protein from the size exclusion chromatography was concentrated as before and trials were set up at a protein concentration of 5 mg/ml. Using the crystallistaion condition identified for the native protein a single crystal was obtained which was deformed and therefore not usable. Panel A in Figure 6.28 is an image of the crystal obtained. Repeated attempts at crystallising the SelMet NBD/J protein resulted in crystalline clusters from which a single crystal could not be isolated. Panel B in Figure 6.28 is an example of the clusters observed in the drops. Therefore, optimisation of the crystallisation condition was undertaken at the Molecular Structure facility, NIMR by Ms. Lesley Haire. Crystals were obtained using the condition 20% (vwv) PEG8K, 0.2 M ammonium sulphate and 0.1 M MOPS pH 7.5. Panel C in Figure 6.27 represents the seleno-l-methionine-labelled crystals of NBD/J protein. However no selenium signal could be detected from the data collected using these crystals and therefore the structure remains unsolved.

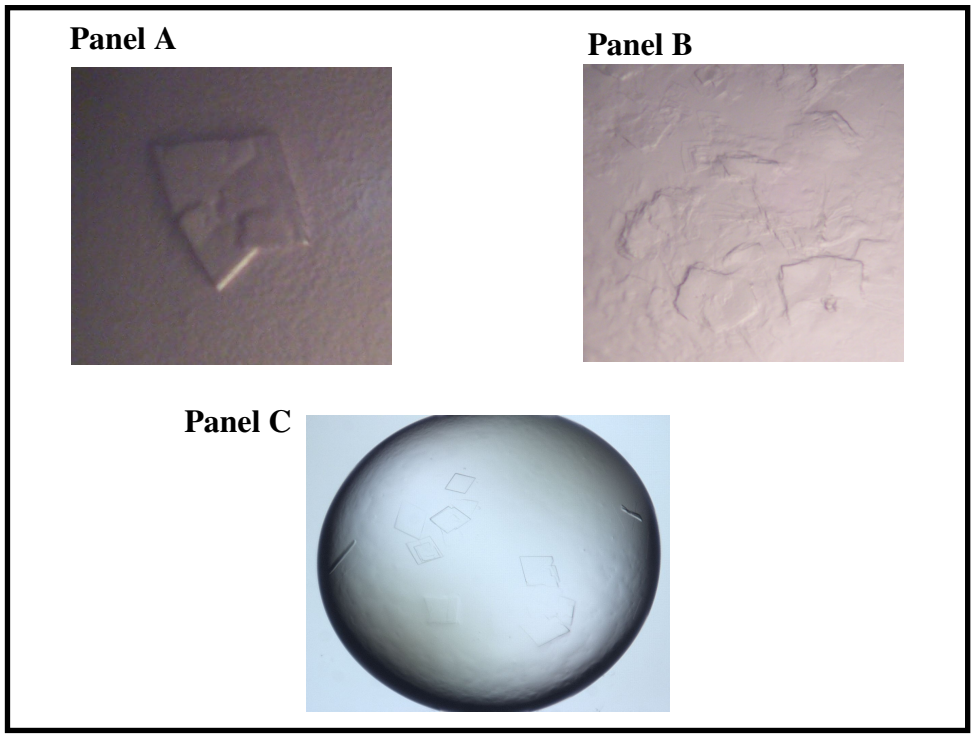

Figure 6.28: Optimisation of crystallisation conditions to obtain crystals of the selenium labelled NBD/J protein.

The deformed crystals in Panel A and B were obtained when crystallised under the same crystallisation condition as the native crystals. Panel C represents the well defined crystals obtained after optimisation of crystallisation conditions.

6.4 Discussion

In this chapter, the biochemical and structural work carried out using domain variants of the Hsc70 protein has been described. Studying the behaviour of the domains in complex with HSJ1b will contribute to understanding the nature of the interaction of the full length Hsc70 with HSJ1b.

In order to evaluate the role of the individual Hsc70 domains in thier interaction with the HSJ1b partner protein, the 44 kDa N-terminal nucleotide binding domain (NBD) and the C-terminal hydrophobic region (CTR) were expressed individually. The N-terminal region has the 44 kDa NBD and is involved in nucleotide binding and hydrolysis (Chappell *et al.,* 1987; Flaherty *et al*., 1990 and Huang *et al*., 1993). The isolated 44 kDa NBD exists as a monomer and has been crystallised in ATP and ADP bound forms (DeLuca-Flaherty *et al*., 1988; Flaherty *et al*., 1990). The K_m values obtained for ATP hydrolysis by the NBD in isolation have been observed to be equal to that of the full length Hsc70 (O'Brien *et al*., 1993). NMR studies (Garimella *et al*., 2006) and biochemical analysis using BIAcore (Suh *et al*., 1998) have determined that the NBD hosts the primary site of interaction for the J-domain of the Hsp40 co-chaperone family.

The C-terminal region (CTR) is further divided into two domains – an 18 kDa peptide binding region (PBD) involved in recognition of substrate moieties and a 10 kDa region which is believed to act as a lid over the peptide binding domain (Zhu *et al*., 1996). Wang *et al*., have demonstrated using the S-peptide of RNase-A as substrate, that the 18 kDa PBD is sufficient for peptide binding. The 18 kDa fragment displayed an affinity of 8 μM, which matched the value obtained for the full length Hsc70 (Wang *et al*., 1993). The requirement of the 10 kDa lid fragment for the functioning of the Hsc70 has been debated. Reports in the literature have concluded that the 10 kDa lid region might not be relevant for Hsc70's chaperone functions (Ungewickell *et al*., 1997; Wilbanks *et al*., 1995). However, Demand *et al*., have used the yeast two hybrid system to demonstrate that the 10 kDa C-terminal region of Hsc70 provides non overlapping binding sites for interacting protein cofactors such as the Hsp40 family members and Hop (Hsc70-Hsp90-organizing protein, Demand *et al*., 1998).

It has already been established that the isolated C-terminal region of the Hsc70 can be highly oligomerised and therefore been implicated for the self-association property of the full length Hsc70 (Benaroudj *et al*., 1997). However there are conflicting reports as to whether self-association in Hsc70 is brought about by the 18 kDa peptide binding domain or the 10 kDa lid region. Using sedimentation velocity and gel filtration studies, Fouchaq and co-workers came to the conclusion that Hsc70 oligomerisation was due to the 18 kDa PBD (Fouchaq at al., 1999), while the crystal structure of the 10 kDa lid region demonstrated that this region played a role in the self association of Hsc70 (Chou *et al*., 2003). Therefore, to understand the oligomerisatin of rHH complex, two c-terminal deletion mutants were engineered. Tsai *et al*, 1994 reported that deletion of the C-terminal 10 kDa region generates a functional 60 kDa fragment which displays ATPase properties similar to that of the full length Hsc70 protein (Tsai *et al*., 1994). A 60 kDa N-terminal fragment (N60) which lacks the 10 kDa fragment of the C-terminus was constructed. A second deletion mutant was also made of the CTR lacking the 10 kDa lid region (CTRΔC), essentially the isolated PBD.

Thus 4 fragments of Hsc70 i.e NBD, CTR, N60 and CTRΔC were selected for the domain-wise study on the interactions of Hsc70 with HSJ1b. All four constructs were successfully amplified and cloned into the pET-16b vector. Each domain fragment was co-expressed with HSJ1b (referred to as 'J' in these complexes) and the N60/J, NBD/J, CTR/J and CTRΔC/J complexes were subsequently isolated by Ni-NTA chromatography.

Gassler *et al*., used SPR spectroscopy to assess the physical interaction between the NBD, CTR and N60 fragments of *E.coli* DnaK with DnaJ (Gassler *et al*., 1998). DnaJ was shown to interact with either the full length DnaK or the N60 fragment and not with the other isolated domains (Gassler *et al*., 1998). However NMR perturbation experiments had previously shown evidence of physical association of the J-domain of DnaJ with the DnaK's NBD (Greene *at al*., 1998). Although no direct evidence is available to show the binding of mammalian Hsp40's to the isolated CTR, the distal 10 kDa region has been shown to host a secondary site of interaction with the Hsp40 family members, as identified by Demand *et al*., using the yeast two hybrid systems (Demand *et al*., 1998).

The co-expression system used previously to successfully isolate the full length Hsc70 and HSJ1b protein complex was employed to see if it is possible to isolate the complexes between HSJ1b and Hsc70 domains. From the analysis of the co-expressed protein elutions from the Ni-NTA, all four domain fragments co-eluted with HSJ1b. While N60/J, NBD/J and CTR/J complexes were expected, detection of CTRΔC/J was unexpected since the 18 kDa PBD is not known to host any interaction sites for Hsp40 family members. Subsequently, size exclusion chromatography confirmed that while 60/J, NBD/J and CTR/J were stable complexes, CTRΔC/J was not. The CTRΔC/J complex disassociated over the gel filtration column.

Closer analysis of the isolated complexes of the deletion mutants however revealed that the deletion mutants exhibited altered levels of binding to HSJ1b. Removal of the 10 kDa C-terminal region in the N60 construct marginally reduced its ability to bind HSJ1b when compared with the intact Hsc70 (ref figure 6.7). While binding of HSJ1b to the CTR mutant was comparable to that of the full length Hsc70, the CTRΔC/ J showed almost 50% reduction in the amount of bound HSJ1b. This clearly suggests that, although the Hsc70 NBD is the primary site of interaction between Hsc70 and HSJ1b, the binding of HSJ1b to Hsc70 is also mediated via the 10 kDa C-terminal region and deletion of this region weakens and disrupts the binding.

Oligomeric properties of the domain complexes

Polymerisation of Hsc70 has been suggested to be a regulatory event necessary to maintain the chaperone in an inactive state (King *et al*., 1995a). Sucrose density gradient and non denaturing electrophoresis studies performed on cell lysates containing BiP (Hsp70 from the endoplasmic reticulum) indicates that polymerised BiP was observed to be free of protein substrates, while the monomeric form was found associated with protein substrate (Freiden *et al.*, 1992). In the previous chapter, it was observed that the the rHH protein resolves into two fraction over the gel filtration column. The first peak eluted in the void volume, while the second peak fractionated at an estimated molecular weight of ~220 kDa. The oligomeric peak 1 from the SEC could be a result of the polymerisation of the Hsc70 by HSJ1b, and subsequent co-polymer formation. HSJ1b subunit was found associated with the Hsc70 subunit in both the polymeric SEC fractions. An important area of focus in this chapter

was to therefore establish the region on Hsc70 essential for this polymerisation that was observed during the course of this study.

Oligomerisation state of the isolated N60/J, NBD/J, CTR/J and CTRΔC/J complexes was studied by size exclusion chromatography. The NBD/J complex was completely non-oligomeric. This indicated that the perceived polymerisation event was driven by the C-terminal region of Hsc70. This was confirmed by gel filtration of the CTR/J complex. 44% of CTR/J protein existed as higher order oligomers, compared to the 64% calculated for the intact Hsc70/HSJ1b complex. However, only 22% of the N60/J complex existed in a polymerised state. The N60 fragment has both the NBD and PBD and only lacks the 10 kDa C-terminal portion of Hsc70. The reduced polymerisation of the N60/J, despite the presence of the 18 kDa PBD of the CTR, incriminates the 10 kDa C-terminal region in the polymerisation of the Hsc70 in the presence of HSJ1b.

The results presented in this chapter clearly indicate that the deletion of this distal 10 kDa lid region directly affects the formation of the Hsc70 polymer with HSJ1b co-polymer as observed by the gel filtration profiles of N60/J and CTRΔC/J complexes.. Previously the 10 kDa lid region (from rat) has been implicated for its role in the self-association of Hsc70 (Chou *et al*., 2003). This is the first report on its possible role in HSJ1b mediated polymeristaion of Hsc70. It remains to be confirmed if the observations holds true for other members of the Hsp40 family or if this was specific for the interaction of Hsc70 and HSJ1b proteins.

Functional and conformational changes due to deletion of 10 kDa lid region

The effect the deletion of the C-terminal 10 kDa region has on the functional properties of the Hsc70/HSJ1b complex was studied using the luciferase protection assay and by measuring the ATPase activity or the N60/J domain complex and the full length, rHH complex. The N60/J complex showed evidence of ATP dependent protection luciferase from thermal stress. Almost 70% of luciferase was maintained soluble by the N60/J complex in the presence of ATP. The ATP hydrolysis activity (measured by phosphate release) of the N60/J complex was 50% less than that obtained for the full length rHH complex. Contradictory reports are available on the functional capabilities of the N60 fragment, and the effect of the missing distal 10 kDa C-terminal lid region. Leng *et al*., demonstrated that the ATPase activity of the bovine N60 fragment can be successfully stimulated with the rat DnaJ-like protein, RDJ1

(Leng *et al*.,1998). Similarly, Ungewickell *et al*., have shown that auxillin J-domain interacts with the N60 fragment and is successful in the uncoating of clathrin baskets (Ungewickell *et al*., 1997). This was in direct contradiction to previous results from Chappel *et al*., who reported that the bovine Hsc70's N-terminal 60 kDa fragment did not have clathrin binding activity (Chappel *et al*., 1987). Furthermore, Hu and Wang reported that a stable complex of the N60 fragment with S-carboxymethyl α-lactalbumin (CMLA), an unfolded protein could not be detected by native gel electrophoresis (Hu and Wang, 1996). From the results for our functional studies on the N60/J complex, it was observed that the N60/J complex used in this study could function as a chaperone, albeit in a reduced capacity, and this therefore suggests that the distal 10 kDa region plays an important functional role.

Conformational differences between the two constructs were studied by partial proteolysis. A key feature identified in the studies carried out on the intact Hsc70/HSJ1b complex is the susceptibility of the HSJ1b to digestion by chymotrypsin. This feature was conserved in the N60/J complex. Interestingly, the N60 moiety of the N60/J complex also showed signs of proteolysis. This was not the case for the full length rHH complex; Hsc70 appeared to be totally impervious to digestion under similar experimental conditions. This indicates that the conformation adopted by the N60/J results in the exposure of a chymotrypsin site(s) on the Hsc70 fragment which were previously protected. Since the main difference between the full length Hsc70 and the N60 fragments is the 10 kDa lid region, this region might conceal chymotrypsin recognition sites on the full length Hsc70 which become exposed in the N60 fragment and therefore makes it susceptible to proteolysis.

A few important conclusions can be drawn from the biochemical studies conducted on the complexes of the domain fragment with HSJ1b.

1) Using the co-expression system, a physical interaction of the isolated N-terminal NBD and C-terminal region (CTR) with HSJ1b has been shown. The interaction with the CTR is dependent on the distal 10 kDa region, because CTRΔC was incapable of stably binding with HSJ1b. Removal of the 10 kDa region clearly impacts the interaction of HSJ1b with the Hsc70 modules, which agrees with the prediction of Demand *et al*., that it hosts a binding site for the Hsp40 cofactor.

2) The C-terminal 10 kDa lid region has been implicated in self association of Hsc70. The studies carried out this chapter reveal for the first time that this region also plays an integral role in the HSJ1b mediated polymerisation of Hsc70, and the subsequent co-polymer formation.

These conclusions provide useful insights especially regarding the regions on the Hsc70 critical for mediating the interaction with its Hsp40 co-chaperone partner, in this case HSJ1b.

X-ray crystallographic studies

Of the four domain complexes studied only the NBD/J complex was studied by X-ray crystallography. X-ray crystallography is a powerful tool to determine the 3-dimensional structure of proteins (Smyth and Martin, 2000). However the bottleneck in this process is growing protein crystals of sufficient size and quality suitable for diffraction studies. Under appropriate conditions the solubility of the protein in the sample can be manipulated to reach a state of supersaturation, which favours the formation of crystals (Gernert *et al*., 1988). One of the most important factors for protein crystallisation is the sample purity and homogeneity. Protein contamination or the presence of aggregates can inhibit crystal growth (McPherson, 1999). Based on the observations of the gel filtration profiles of each complex, only the NBD/J complex eluted as a homogenous peak and was also estimated to be > 98% pure when assessed by gel electrophoresis. Electrophoresis on a 15% SDS gel over an extended time period also resolved the closely migrating NDB and HSJ1b protein bands, confirming the presence of both protein species. Taking these facts into consideration, only the NBD/J complex domain complex was deemed suitable for cyrtsallographic studies

Prior to crystallisation the protein was concentrated and observed to be stable during concentration. At higher concentrations the protein was no longer soluble and precipitated out of solution. Therefore crystallisation trials were performed at a protein concentration of 5 mg/ml. The formation of protein crystals is dependent on a large number of variables including the type of buffer and pH of buffer, precipitant, salt solution, concentration of protein and temperature (Smyth and Martin, 2000).

Initial crystallisation trials were performed using a sparse matrix screen. These are collection of crystallisation conditions which have been shown to produce protein

crystals and were conceptualised by Jancarik and Kim (Jancarik and Kim, 1991). Several commercial screens are available which allows screening around a vast range of parameters. The initial screen for the NBD/J complex was carried out using the Hampton Crystal Screens. Crystal screen 1 and crystal screen 2 have 50 and 48 conditions respectively. Crystallisation trials were set up using the hanging drop vapour diffusion technique. Crystals were obtained under 2 of the Hampton crystal screen conditions – condition 15 and condition 22. The structure solution for the crystals obtained from condition 22 was straightforward and was solved by Molecular replacement (MR). MR uses the phase information from a previously solved crystal structure similar to the unknown structure and performs mathematical operations to generate a model for the unknown structure (Tickle and Driessen, 1996). Several structures of the NBD of the Hsp70 proteins are available in the PDB database. The ADP bound form of the bovine Hsc70 NBD (Pdb id: 3HSC) was used to generate a starting model for the structure solution. However, no extra density corresponding to the HSJ1b protein could be detected. Crystals obtained under condition 22 therefore contained just the individual NBD and not a complex of NBD and HSJ1b. Interestingly the NBD showed no density for any nucleotide; therefore the crystal represented the apo state of the Human Hsc70's nucleotide binding domain (1-386 amino acids).

This is the first report for the apo structure of the NBD from the Human Hsc70. In 2007, Jiang *et al*., published the apo structure of the NBD from bovine Hsc70, along with the structure of the complex of bovine NBD and auxilin's J- domain. Structural analysis carried out during the course of our study revealed that the structure of the Human apo NBD is identical to that of the Bovine apo NBD, possibly due to the high levels of homology in the amino acid sequence. Limited proteolysis studies carried out by Buchberger *et al*., 1995, shows that DnaK (*E. coli* Hsp70) exhibits three conformations dictated by the absence of nucleotide, ATP bound state and ADP bound state respectively (Buchberger *et al*., 1995). Similar observations were made from the proteolysis experiments carried out using Hsp70 from *Saccharomyces cerevisiae* (Ssa1p, Fung *et al*., 1996). Intriguingly no significant difference in the overall conformation could be detected between the apo form and the nucleotide bound forms when structural superimposition of the NBD structures was carried out. The lack of detectable conformational change can be explained by the observations of Buchberger *et al*., that nucleotide dependent conformation change is dependent on interdomain

communication and probably localised in the C-terminal region of DnaK (Buchberger *et al*., 1995).

Next analysis was carried out to study the possibility of subtle sub-domain movements which could remain undetected when studying the overall alignment. Relative movement of lobe II with respect to lobe I of the apo structure was compared with the ADP bound structure (3HSC). The alignment studies revealed movement in sub-domain II B of lobe II in the apo NBD. This was an interesting observation because the structure of DnaK's NBD in complex with GrpE crystallised in the nucleotide free form also displays an outward rotation of sub-domain II B rotated by almost 14^{o} (Harrison *et al*., 1997). A similar shift in this sub-domain was detected in the structure of the Hsc70 NBD in the presence of BAG-1domain (Sondermann *et al*., 2001). An NMR study the 44-kDa Hsc70 NBD from *Bos taurus* in the ADP.Pi state revealed that the NBD is dynamic and the four sub-domains (IA, IB, IIA, IIB) can reorient themselves, depending on the experimental conditions (Zhang and Zuiderweg, 2004). They suggest that the relative movement of both domains IB and IIB plays a role in nucleotide binding and release (Zhang and Zuiderweg, 2004). Therefore we carried out a study into the positioning of residues implicated in ligand binding and discovered they were displaced in the apo structure, compared to the ADP bound form. Some of the residues like Arg342, Ser 275, Arg 272 and Lys 271 were displaced by more than 1 Å. These are all crucial residues which make up the adenine binding pocket. For example, Arg272 is involved in forming a salt bridge across to Glu268 (Flaherty *et al*., 1991). The Glu268 in turn has been implicated to be crucial for the inter sub-domain interaction (Shida *et al*., 2010). Inter sub-domain interactions of the Glu268 with Tyr15 and Lys56 define the closed state of the NBD. In the open form this interaction is absent. The previously reported structures of the apo NBD of bovine Hsc70 and human Hsp70 display a closed conformation (Jiang *et al*., 2007; Shida *et al*., 2010). Intriguingly, the apo structure obtained during the course of this study was observed to be in the open conformation. The "open" form has been reported for the Hsc70 NBD/BAG domain complex (Sondermann *et al*., 2001), the Hsc70 nucleotide-free NBD-SBD fragment (Jiang *et al*., 2005) and the Hsp70 NBD/ATP-bound Sse1 complex (Polier *et al*., 2008), indicating that the presence of co-factor or the SBD promotes this conformation. It is possible that since the human Hsc70 NBD in our study was crystallised in the presence of the HSJ1b cofactor, it has adopted the open

conformation, in its apo state. The NBD did not crystallise in complex with the HSJ1b, possibly due to potential differences in solubility of the two proteins. However, despite the differences in the sub-domain interactions observed between the nucleotide free form of Hsc70's NBD and the ADP bound form, the physiological and functional significance of a nucleotide free state for Hsc70 *in vivo* is not yet clear.

Determination of a structure solution for the protein crystals obtained from condition 15 of Hampton crystal screen was unfortunately not as straightforward as the previous case. Although the crystal gave high resolution diffraction data (2.2 Å), a structure solution was not forthcoming. MR was attempted with several starting models such as the ADP bound NBD (3HSC), the bovine Hsc70's NBD in complex with the J-domain (2qwn) and the J-domain of Human Hsp40 (1HDJ). All attempts failed to provide a solution. From the many trials it is apparent that the crystal most probably did not contain the NBD fragment and therefore might not represent the complex of NBD and HSJ1b. It therefore raises the possibility that the protein crystallised under condition 15 is the Human HSJ1b protein. To date there is no full length structure reported for any member of the Hsp40 family. There are several structures of the various domains in isolation such as the conserved J-domain, carboxyl terminus and zinc finger-like domain as well as the peptide binding fragment (Qian *et al*., 1996; Lu and Cry, 1998; Huang *et al*., 1999 and Li *et al*., 2003). It is possible that MR with the J-domain structures were unsuccessful because the J-domain corresponds to only 78 amino acids on the HSJ1b sequence and is therefore too small to provide a MR solution.

Since the MR experiments failed to provide the phase information required for solving the structure, Selenomethionine (SelMet) labelling of the NBD/J protein was undertaken. Selenomethionine is an amino acid containing selenium, and is incorporated into the protein in the place of the amino acid methionine (Cowie and Cohen, 1957). Structure of the SelMet incorporated crystals can be determined by multi-wavelength anomalous diffraction (MAD) methods (Doublie, 1997; Hendrickson, 1991). Selenium is a heavy atom and is useful in providing phase information for the structure (Strub *et al*., 2003). Another important factor to consider, is the number of methionines in the protein sequence. A good rule of thumb is to verify that the protein being labelled has at least one methionine for every 10 kDa of the protein. This is necessary for efficient and detectable incorporation of selenium. From

an analysis of the protein sequences for the NBD fragment (44 kDa) and HSJ1b (35.5 kDa) there are six and three methionines respectively, which should be sufficient for the detection of the signal. The NBD/J protein was co-expressed in *E. coli* strains auxotrophic for methionine, and purified following the same purification protocols as the native protein. Size exclusion chromatography confirmed that elution profile of the native NBD/J and SelMet labelled protein was the same. Optimisation of the original crystallisation condition was required to obtain crystals of the SelMet incorporated NBD/J protein. However analysis of the diffraction data collected from the SelMet crystals revealed that the incorporation of selenium is very low and therefore failed to help provide a structure solution.

Results from this chapter raise important questions on the actual role of the distal 10 kDa region in the interaction of the Hsc70 and HSJ1b. This region appears to be crucial for the chaperone/co-chaperone interaction, since the removal of this zone alters binding, functional and conformational properties of the 70/40 interaction. Also, the structure of the NBD of the human Hsc70 in its Apo form was successfully solved in its open conformation. Diffraction data has been collected for native and SelMet labelled crystals obtained under a different crystallisation condition. However the structure remains elusive.

Chapter 7
Conclusions and Future work

CHAPTER 7: Conclusions and Future Work

7.1 Summary of Results

The main objective of this thesis was to produce a stable form of an Hsc70/HSJ1b complex which could be used in the elucidation of the structural details of the interactions between the Hsp70 and Hsp40 protein families. The first hurdle towards achieving this aim was the production of a stable Hsp70-Hsp40 complex protein which could be used for structural studies and biophysical analysis.

In **Chapter 3**, we reported the successful purification of an intact Hsp70/Hsp40 complex from bacteria using a co-expression system. We expressed and purified a recombinant Hsp70/Hsp40 complex from *E.coli* using human Hsc70 and HSJ1b as representatives of the Hsp70 and Hsp40 families respectively. The human Hsc70 was amplified from cDNA prepared from HB4a cells and inserted into the pET-16b vector, allowing the Hsc70 protein to be expressed with an N-terminal 10 x histidine tag. The full length human HSJ1b gene was cloned into the pET-24a vector with a stop codon immediately after the coding sequence, and therefore the HSJ1b protein was expressed with neither an N-terminal nor C-terminal Histidine tag. The Hsc70/HSJ1b complex was isolated using a single step Ni-NTA chromatography. Both Hsc70 and HJj1b subunits were observed in the higher concentration imidazole elution fractions. The untagged HSJ1b protein could only elute with such high imidazole levels only if it was complexed with the 70 kDa histidine tagged Hsc70. The complex formation between the two subunits was further confirmed by 2-dimensional electrophoresis. Thus, we have used a novel method for the purification of recombinant chaperone/co-chaperone complex formed *in vivo* (albeit under recombinant conditions) without any external manipulation.

Biochemical characterization of the recombinant complex, rHH, was carried out in **Chapter 4**. The chaperone activity of rHH complex was assessed by its ability to prevent thermal aggregation of a substrate (luciferase in this study). It was observed that revealed that the chaperone complex can protect ~85% of substrate protein (luciferase) from thermal aggregation, and retain it in the soluble fraction but this

luciferase was found to be inactive. It was observed that the recombinant complex was capable of preventing luciferase aggregation up to a molar ratio of 1:1 beyond which the efficiency reduced by almost 60%. The first important observation from this chapter was that the rHH complex appears to function in an ATP independent fashion. The presence of denatured substrate did not alter the ATPase activity of Hsc70. The lack of a requirement for ATP or ATP hydrolysis displayed by the rHH complex was an interesting finding, since most studies performed with a reconstituted Hsp70/Hsp40 chaperone/co-chaperone complex have stressed on the importance of ATP for the functioning of the complex. The rHH complex is already in a competent state to protect aggregating proteins, without any additional nucleotide requirement. The functional behaviours displayed by the rHH complex could be explained only if the NBD of Hsc70 in the rHH complex contained a bound nucleotide. Unfortunately, we have been unable to conclusively prove if the NBD is ATP/ADP bound or nucleotide free.

Limited proteolysis experiments provided useful insights into the arrangements of the HSJ1b subunits with respect to Hsc70 in the rHH complex. Both subunits appear to be well folded, but the HSJ1b was extremely susceptible to proteolysis while Hsc70 was resistant. This suggests that the HSJ1b subunit was more exposed and therefore more accessible of the two subunits. It is possible that in the quaternary structure, the HSJ1b plays the role of a shield, which prevents the proteolysis of the core Hsc70 subunits.

Analysis of the rHH complex by gel filtration, revealed the existence of two forms of the complex. SDS-PAGE analysis confirmed the presence of both the Hsc70 and HSJ1b subunits in both the rHH forms. The first form (peak 1), although eluting in the void volume of the superdex 200 column, was confirmed to be non-aggregated by analytical ultracentrifugation and its molecular weight was estimated to be 1.1 MDa. This fraction represented higher order oligomers of the rHH complex, which we believe represents the product of Hsc70 polymerisation by HSJ1b. The second form (peak 2) had an estimated molecular weight of 220 kDa, indicating the rHH complex existed as a dimer of an Hsc70/HSJ1b dimer. Using ATP, we have shown the cyclic disassociation of peak 1 to form peak 2, which in turn disassociates into the individual Hsc70 and HSJ1b components. It is not clear if the observed disassociation is due to ATP binding or ATP hydrolysis. A similar conversion of peak 1 to peak 2 was

observed in the presence of denatured luciferase. The full length complex was found to be unsuitable for X-ray crystallographic studies due to its highly heterogenous oligomeric composition. Instead electron mcroscopic studies were pursued. Preliminary results from negative staining have proved to be very exciting and intresting. However due to heterogeneity of the peak 1 fractions, caused probably due to the dissociation of the complex during the uranyl acetate staining procedure, further image processing could not be pursued.

Most investigations into the interactions of the Hsp70 proteins with their Hsp40 co-chaperone partners have used a reconstituted system. The data from our characterisation studies of the recombinant complex did not concur with the published reports carried out using a reconstituted complex. Therefore it was necessary to ascertain if the observations from our study was unique for the recombinant complex, or if it was due to the choice of Hsp70 and Hsp40 proteins used in our study. For this purpose, in **Chapter 5**, an *in vitro* Hsc70/HSJ1b complex was formed by reconstitution, and its functional properties were studied and compared with that of the recombinant system. Interestingly, the *in vitro* system displayed ATP dependent luciferase protection, as reported previously for the reconstituted systems such as Hsc70/HDJ-1 proteins, Hsp70 and Hsp40 proteins from *Meiothermus rubber* and Hsc70/CSP interactions. Conformational differences were observed between the two systems when treated with the protease trypsin. The Hsc70 and HSJ1b subunits interact differently in the two models, since the Hsc70 subunit appears to be more sensitive to proteolysis in the *in vitro* complex than in the rHH complex. Thus the recombinant Hsc70/HSJ1b complex is potentially a more robust model to study the mechanisms of assembly and working in the formation of the Hsc70 chaperone and HSJ1b co-chaperone complex.

We next generated domain variants of Hsc70 capable of binding to HSJ1b in **Chapter 6** to study the regions on the Hsc70 critical for mediating the interaction with its Hsp40 co-chaperone partner, in this case HSJ1b. It was observed that removal of the distal C-terminal 10 kDa region impacts on the interaction of HSJ1b with Hsc70 and that furthermore this region is crucial for the formation of the Hsc70/HSJ1b co-polymer. This region was further found to be conformationally essential, since deletion of this

10 kDa fragment, left the remaining N-terminal 60 kDa vulnerable to proteolytic cleavge.

The NBD/J domain complex was determined to be suitable for X-ray crystallographic studies, because of its purity and homogeneity. Crystallisation trials yielded two protein crystals from condition 15 and 22 of Hampton crystal screen . Both crystals belonged to the P_1211space group. A structure solution for the data collected from crystals of condition 22 was initiated by molecular replacement using the bovine Hsc70 ATPase domain with bound ADP (PDB id: 3HSC) as the model. The structure was determined to be the unliganded Hsc70 NBD without its HSJ1b partner. This is the first report for the apo structure of the NBD from the Human Hsc70. The structure of the Human apo NBD was found to be identical to that of the bovine apo NBD, possibly due to the high level of homology in the amino acid sequence. When structural superposition was carried out between the apo form and the nucleotide bound structures available in the PDB database, no significant difference in the overall conformation was observed. However, we detected displacement of sub-domain II B of lobe II in the apo NBD, when the relative movement of the two sub-domains of the NBD was assessed relative to the position of their position in the bovine NBD structure. Another interesting finding was regarding the residues involved in the inter sub-domain interactions - Glu268 from sub-domain IIB with Tyr15 and Lys56 from sub-domains IA and IB, respectively. Our structure was observed to be in the open conformation, signified by the lack of interaction between the Tyr15, Lys56 and Glu268. This is a novel conformation for the nucleotide-free NBD structure because all previous open conformations of the NBD have been reported in the presence of the Hsp70 co-factors (Sondermann *et al*., 2001; Polier *et al*., 2008) or the SBD (Jiang *et al*., 2005).

A structural solution for the data collected from crystals of condition 15 diffracting with a resolution of up to 2.2 Å could not be obtained using existing methodology. All attempts using molecular replacement have so far failed to provide a solution. From the many trials with the existing structures in the PDB database, it is apparent that the crystal probably does not contain the NBD fragment and therefore might not represent a complex of NBD and HSJ1b. However it does raise the interesting possibility that the protein crystallised under condition 15 is the human HSJ1b protein and to date

there is no full length structure reported for any member of the Hsp40 family. SelMet labelling of the NBD/J protein was undertaken to obtain the phase information required for solving the structure. Crystals of the labelled protein were successfully obtained. However data collection revealed that the signal from the incorporation of selenium was poor and therefore failed to help provide a structure solution.

7.2 Future work

The recombinant complex is an attractive tool to further our understanding of the Hsp70/Hsp40 interactions from a fresh perspective. The future line of investigation will look to improve our functional and structural understanding of the recombinant complex and has been explained in detail in the following section.

- **Identification of endogenously bound nucleotide**

So far in this study we have been unsuccessful in identifying if the recombinant complex was isolated with a bound nucleotide. However this information is crucial to better understand the behaviour of the complex with respect to substrate protection and ATP hydrolysis. This can be undertaken by HPLC as discussed in this thesis. However the efficiency of different nucleotide extraction methods needs to be optimised. Mass spectroscopy might be another alternative.

- **Repeating SelMet labelling studies for the NBD/J complex**

Selenium labelling of the NBD/J complex was undertaken in an attempt to solve the structure for the crystals obtained from condition 15 of Hampton crystal screen . However this experiment was performed only once, and was not sucessfull the first time. Therfore SelMet labelling needs to be repeated to confirm if structure determination is possible using the existing methodology. Failing this, alternative phasing techniques such as heavy metal derivatives of the crystals may be undertaken.

- **Improving sample homogeneity for electron microscopy**

Preliminary analysis of the rHH protein by negative staining revealed discrete particles. However the particles were hetergeneous in size and shape. Improving sample homogeneity for EM work will be the focus of our future work. The smaller particles observed indicate possible dissociation from the larger complex possibly as a

result of uranyl acetate staining and therefore fixation with glutaraldehyde will be undertaken to see if this can reduce the proportion of disassociation.

References

References

AITKEN, A. & LEARMONTH, M. (1996). Protein Determination by UV Absorption. *In:* WALKER, J. M. (ed.) *The Protein Protocols Handbook.* Humana Press.

ALBERTI, S., ESSER, C. & HOHFELD, J. (2003). BAG-1--a nucleotide exchange factor of Hsc70 with multiple cellular functions. *Cell Stress & Chaperones,* 8**,** 225-231.

ANDRÉASSON, C., FIAUX, J., RAMPELT, H., MAYER, M. P. & BUKAU, B. (2008). Hsp110 Is a Nucleotide-activated Exchange Factor for Hsp70. *Journal of Biological Chemistry,* 283**,** 8877-8884.

ANFINSEN, C. B. (1973). Principles That Govern Folding of Protein Chains. *Science,* 181**,** 223-230.

ANGELIDIS, C., LAZARIDIS, I. & PAGOULATOS, G. (1999). Aggregation of hsp70 and hsc70 in vivo is distinct and temperature-dependent and their chaperone function is directly related to non-aggregated forms. *European Journal of Biochemistry,* 259**,** 505-512.

BALLINGER, C. A., CONNELL, P., WU, Y. X., HU, Z. Y., THOMPSON, L. J., YIN, L. Y. & PATTERSON, C. (1999). Identification of CHIP, a novel tetratricopeptide repeat-containing protein that interacts with heat shock proteins and negatively regulates chaperone functions. *Molecular and Cellular Biology,* 19**,** 4535-4545.

BARRAL, J. M., BROADLEY, S. A., SCHAFFAR, G. & HARTL, F. U. (2004). Roles of molecular chaperones in protein misfolding diseases. *Seminars in Cell & Developmental Biology,* 15**,** 17-29.

BECKER, J. & CRAIG, E. (1994). Heat-shock proteins as molecular chaperones. *European Journal of Biochemistry,* 219**,** 11-23.

BENAROUDJ, N., BO, F., TRINIOLLES, F., GHELIS, C. & LADJIMI, M. (1994). Overexpression in Escherichia coli, purification and characterization of the molecular chaperone HSC70. *European Journal of Biochemistry,* 221**,** 121-128.

BENAROUDJ, N., FOUCHAQ, B. & LADJIMI, M. M. (1997). The COOH-terminal peptide binding domain is essential for self-association of the molecular chaperone HSC70. *Journal of Biological Chemistry,* 272**,** 8744-8751.

BENAROUDJ, N., TRINIOLLES, F. & LADJIMI, M. M. (1996). Effect of nucleotides, peptides, and unfolded proteins on the self-association of the molecular chaperone HSC70. *Journal of Biological Chemistry,* 271**,** 18471-18476.

BENVENUTI, M. & MANGANI, S. (2007). Crystallization of soluble proteins in vapor diffusion for x-ray crystallography. *Nat Protoc,* 2**,** 1633-1651.

BIMSTON, D., SONG, J. H., WINCHESTER, D., TAKAYAMA, S., REED, J. C. & MORIMOTO, R. I. (1998). BAG-1, a negative regulator of Hsp70 chaperone activity, uncouples nucleotide hydrolysis from substrate release. *EMBO Journal,* 17**,** 6871-6878.

BLATCH, G. L. & LASSLE, M. (1999). The tetratricopeptide repeat: a structural motif mediating protein-protein interactions. *Bioessays,* 21**,** 932-939.

BLOND-ELGUINDI, S., CWIRLA, S. E., DOWER, W. J., LIPSHUTZ, R. J., SPRANG, S. R., SAMBROOK, J. F. & GETHING, M. J. (1993). Affinity panning of a library of peptides displayed on bacteriophages reveals the binding specificity of BiP. *Cell,* 75**,** 717-728.

BLOND-ELGUINDI, S., FOURIE, A. M., SAMBROOK, J. F. & GETHING, M. J. (1993). Peptide-dependent stimulation of the ATPase activity of the molecular chaperone BiP is the result of conversion of oligomers to active monomers. *Journal of Biological Chemistry,* 268**,** 12730-12735.

BOORSTEIN, W. R., ZIEGELHOFFER, T. & CRAIG, E. A. (1994). Molecular evolution of the HSP70 multigene family. *J Mol Evol,* 38**,** 1-17.

BORGES, J. C. & RAMOS, C. H. (2006). Spectroscopic and thermodynamic measurements of nucleotide-induced changes in the human 70-kDa heat shock cognate protein. *Archives of Biochemistry and Biophysics,* 452**,** 46-54.

BORK, P., SANDER, C., VALENCIA, A. & BUKAU, B. (1992). A Module of the Dnaj Heat-Shock Proteins Found in Malaria Parasites. *Trends in Biochemical Sciences,* 17**,** 129-129.

BOSHOFF, A., NICOLL, W. S., HENNESSY, F., LUDEWIG, M., DANIEL, S., MODISAKENG, K. W., SHONHAI, A., MCNAMARA, C., BRADLEY, G. & BLATCH, G. L. (2004). Molecular chaperones in biology, medicine and protein biotechnology. *South African Journal of Science,* 100**,** 665-677.

BRADFORD, M. (1976). A rapid and sensitive method for the quantitation of microgram quantities of protein utilizing the principle of protein-dye binding. *Analytical Biochemistry,* 72**,** 248-254.

BRANDEN, C-I. & TOOZE, J. (1999). Introduction to protein structure. 2nd Edition.

Garland Publishing.

BREHMER, D., RUDIGER, S., GASSLER, C. S., KLOSTERMEIER, D., PACKSCHIES, L., REINSTEIN, J., MAYER, M. P. & BUKAU, B. (2001). Tuning of chaperone activity of Hsp70 proteins by modulation of nucleotide exchange. *Nature Structural Biology,* 8**,** 427-432.

BRODSKY, J., HAMAMOTO, S., FELDHEIM, D. & SCHEKMAN, R. (1993). Reconstitution of protein translocation from solubilized yeast membranes reveals topologically distinct roles for BiP and cytosolic Hsc70. *Journal of Cell Biology,* 120**,** 95.

BROWN, C. R., MARTIN, R. L., HANSEN, W. J., BECKMANN, R. P. & WELCH, W. J. (1993). The constitutive and stress inducible forms of hsp 70 exhibit functional similarities and interact with one another in an ATP-dependent fashion. *The Journal of Cell Biology,* 120**,** 1101-1112.

BUCHBERGER, A., THEYSSEN, H., SCHRODER, H., MCCARTY, J. S., VIRGALLITA, G., MILKEREIT, P., REINSTEIN, J. & BUKAU, B. (1995). Nucleotide-induced conformational changes in the ATPase and substrate binding domains of the DnaK chaperone provide evidence for interdomain communication. *Journal of Biological Chemistry,* 270**,** 16903-16910.

BUKAU, B. (1993). Regulation of the Escherichia coli heat-shock response. *Molecular Microbiology,* 9**,** 671-680.

BUKAU, B. & HORWICH, A. L. (1998). The Hsp70 and Hsp60 chaperone machines. *Cell,* 92**,** 351-366.

BUKAU, B., WEISSMAN, J. & HORWICH, A. (2006). Molecular chaperones and protein quality control. *Cell,* 125**,** 443-451.

BURKHOLDER, W. F., ZHAO, X., ZHU, X., HENDRICKSON, W. A., GRAGEROV, A. & GOTTESMAN, M. E. (1996). Mutations in the C-terminal fragment of DnaK affecting peptide binding. *Proceedings of the National Academy of Sciences of the United States of America,* 93**,** 10632-10637.

CAPLAN, A. (2003). What is a co-chaperone? *Cell Stress & Chaperones,* 8**,** 105.

CAPLAN, A. J., CYR, D. M. & DOUGLAS, M. G. (1993). Eukaryotic homologues of Escherichia coli dnaJ: a diverse protein family that functions with hsp70 stress proteins. *Mol Biol Cell,* 4**,** 555-563.

CARLINO, A., TOLEDO, H., SKALERIS, D., DELISIO, R., WEISSBACH, H. & BROT, N. (1992). Interactions of liver Grp78 and Escherichia coli recombinant Grp78 with ATP: multiple species and disaggregation. *Proceedings of the National Academy of Sciences of the United States of America,* 89**,** 2081.

CHAMBERLAIN, L. H. & BURGOYNE, R. D. (1997). The molecular chaperone function of the secretory vesicle cysteine string proteins. *Journal of Biological Chemistry,* 272**,** 31420-31426.

CHANG, Y. W., SUN, Y. J., WANG, C. & HSIAO, C. D. (2008). Crystal structures of the 70-kDa heat shock proteins in domain disjoining conformation. *Journal of Biological Chemistry,* 283**,** 15502-15511.

CHAPPELL, T. G., KONFORTI, B. B., SCHMID, S. L. & ROTHMAN, J. E. (1987). The ATPase core of a clathrin uncoating protein. *Journal of Biological Chemistry,* 262**,** 746-751.

CHAPPELL, T. G., WELCH, W. J., SCHLOSSMAN, D. M., PALTER, K. B., SCHLESINGER, M. J. & ROTHMAN, J. E. (1986). Uncoating ATPase is a member of the 70 kilodalton family of stress proteins. *Cell,* 45**,** 3-13.

CHAPPLE, J., SPUY, J., POOPALASUNDARAM, S. & CHEETHAM, M. (2004). Neuronal DnaJ proteins HSJ1a and HSJ1b: a role in linking the Hsp70 chaperone machine to the ubiquitin–proteasome system? *Biochemical Society Transactions,* 32**,** 640-642.

CHAPPLE, J. P. & CHEETHAM, M. E. (2003). The chaperone environment at the cytoplasmic face of the endoplasmic reticulum can modulate rhodopsin processing and inclusion formation. *Journal of Biological Chemistry,* 278**,** 19087-19094.

CHEETHAM, M. E. & CAPLAN, A. J. (1998). Structure, function and evolution of DnaJ: conservation and adaptation of chaperone function. *Cell Stress & Chaperones,* 3**,** 28-36.

CHIANG, H. L. & DICE, J. F. (1988). Peptide Sequences That Target Proteins for Enhanced Degradation during Serum Withdrawal. *Journal of Biological Chemistry,* 263**,** 6797-6805.

CHOU, C. C., FOROUHAR, F., YEH, Y. H., SHR, H. L., WANG, C. & HSIAO, C. D. (2003). Crystal structure of the C-terminal 10-kDa subdomain of Hsc70. *Journal of Biological Chemistry,* 278**,** 30311-30316.

CHUNG, K. T., SHEN, Y. & HENDERSHOT, L. M. (2002). BAP, a mammalian BiP-associated protein, is a nucleotide exchange factor that regulates the ATPase activity of BiP. *Journal of Biological Chemistry,* 277**,** 47557-47563.

CONWAY DE MACARIO, E. & MACARIO, A. J. (1994). Heat-shock response in Archaea. *Trends Biotechnol,* 12**,** 512-518.

COSTA, M., ZHUANG, Z., HUANG, X., COSENTINO, S., KLEIN, C. & SALNIKOW, K. (1994). Molecular mechanisms of nickel carcinogenesis. *Science of the Total Environment,* 148**,** 191-199.

COTTO, J., KLINE, M. & MORIMOTO, R. (1996). Activation of heat shock factor 1 DNA binding precedes stress-induced serine phosphorylation. *Journal of Biological Chemistry,* 271**,** 3355.

COWIE, D. & COHEN, G. (1957). Biosynthesis by Escherichia coli of active altered proteins containing selenium instead of sulfur. *Biochimica et biophysica acta,* 26**,** 252-261.

COWING, D. W., BARDWELL, J. C., CRAIG, E. A., WOOLFORD, C., HENDRIX, R. W. & GROSS, C. A. (1985). Consensus sequence for Escherichia coli heat shock gene promoters. *Proc Natl Acad Sci U S A,* 82**,** 2679-2683.

CREIGHTON, T. E. (1978). Experimental studies of protein folding and unfolding. *Prog Biophys Mol Biol,* 33**,** 231-297.

CREIGHTON, T. E. (1993). Proteins: Structures and Molecular Properties, 2nd edition. *New York: W. H. Freeman*.

CSERMELY, P., SCHNAIDER, T., SO''TI, C., PROHÁSZKA, Z. & NARDAI, G. (1998). The 90-kDa Molecular Chaperone Family:: Structure, Function, and Clinical Applications. A Comprehensive Review. *Pharmacology & Therapeutics,* 79**,** 129-168.

CUDNEY, R., PATEL, S., WEISGRABER, K., NEWHOUSE, Y. & MCPHERSON, A. (1994). Screening and optimization strategies for macromolecular crystal growth. *Acta Crystallographica Section D: Biological Crystallography,* 50**,** 414-423.

CYR, D. M., LANGER, T. & DOUGLAS, M. G. (1994). DnaJ-like proteins: molecular chaperones and specific regulators of Hsp70. *Trends Biochem Sci,* 19**,** 176-181.

CYR, D. M., LU, X. & DOUGLAS, M. G. (1992). Regulation of Hsp70 function by a eukaryotic DnaJ homolog. *Journal of Biological Chemistry,* 267**,** 20927-20931.

DAUGHERTY, D. L., ROZEMA, D., HANSON, P. E. & GELLMAN, S. H. (1998). Artificial chaperone-assisted refolding of citrate synthase. *Journal of Biological Chemistry,* 273**,** 33961-33971.

DELANO, W. 2002. The PyMOL molecular graphics system.

DELUCA-FLAHERTY, C., FLAHERTY, K. M., MCINTOSH, L. J., BAHRAMI, B. & MCKAY, D. B. (1988). Crystals of an ATPase fragment of bovine clathrin uncoating ATPase. *Journal of Molecular Biology,* 200**,** 749-750.

DEMAND, J., LUDERS, J. & HOHFELD, J. (1998). The carboxy-terminal domain of Hsc70 provides binding sites for a distinct set of chaperone cofactors. *Molecular and Cellular Biology,* 18**,** 2023.

DEMELER, B. (2005). UltraScan: a comprehensive data analysis software package for analytical ultracentrifugation experiments. *Analytical Ultracentrifugation: Techniques And Methods***,** 210-229.

DESHAIES, R. J., KOCH, B. D., WERNER-WASHBURNE, M., CRAIG, E. A. & SCHEKMAN, R. (1988). A subfamily of stress proteins facilitates translocation of secretory and mitochondrial precursor polypeptides. *Nature,* 332**,** 800-805.

DIAMANT, S., BEN-ZVI, A. P., BUKAU, B. & GOLOUBINOFF, P. (2000). Size-dependent disaggregation of stable protein aggregates by the DnaK chaperone machinery. *Journal of Biological Chemistry,* 275**,** 21107-21113.

DINGWALL, C. & LASKEY, R. (1992). The nuclear membrane. *Science,* 258**,** 942-947.

DODSON, E. J., WINN, M. & RALPH, A. (1997). Collaborative computational project, number 4: Providing programs for protein crystallography. *Macromolecular Crystallography, Pt B,* 277**,** 620-633.

DOUBLIE, S. (1997). Preparation of selenomethionyl proteins for phase determination. *Methods in Enzymology,* 276**,** 523-530.

EASTON, D., KANEKO, Y. & SUBJECK, J. (2000). The Hsp110 and Grp170 stress proteins: newly recognized relatives of the Hsp70s. *Cell Stress & Chaperones,* 5**,** 276.

ELLIS, J. (1987). Proteins as molecular chaperones. *Nature,* 328**,** 378-379.

ELLIS, R. J. (1990). Molecular Chaperones - the Plant Connection. *Science,* 250**,** 954-959.

ELLIS, R. J. & HARTL, F. U. (1996). Protein folding in the cell: competing models of chaperonin function. *FASEB J,* 10**,** 20-26.

EMSLEY, P. & COWTAN, K. (2004). Coot: model-building tools for molecular graphics. *Acta Crystallographica Section D-Biological Crystallography,* 60**,** 2126-2132.

FINK, A. L. (1999). Chaperone-mediated protein folding. *Physiological Reviews,* 79**,** 425-449.

FINKELSTEIN, D., STRAUSBERG, S. & MCALISTER, L. (1982). Alterations of transcription during heat shock of Saccharomyces cerevisiae. *Journal of Biological Chemistry,* 257**,** 8405.

FLAHERTY, K., WILBANKS, S., DELUCA-FLAHERTY, C. & MCKAY, D. (1994). Structural basis of the 70-kilodalton heat shock cognate protein ATP hydrolytic activity. II. Structure of the active site with ADP or ATP bound to wild type and mutant ATPase fragment. *Journal of Biological Chemistry,* 269**,** 12899.

FLAHERTY, K. M., DELUCA-FLAHERTY, C. & MCKAY, D. B. (1990). Three-dimensional structure of the ATPase fragment of a 70K heat-shock cognate protein. *Nature,* 346**,** 623-628.

FLAHERTY, K. M., WILBANKS, S. M., DELUCA-FLAHERTY, C. & MCKAY, D. B. (1994). Structural basis of the 70-kilodalton heat shock cognate protein ATP hydrolytic activity. II. Structure of the active site with ADP or ATP bound to wild type and mutant ATPase fragment. *Journal of Biological Chemistry,* 269**,** 12899-12907.

FLYNN, G., CHAPPELL, T. & ROTHMAN, J. (1989). Peptide binding and release by proteins implicated as catalysts of protein assembly. *Science,* 245**,** 385.

FORREITER, C. & NOVER, L. (1998). Heat induced stress proteins and the concept of molecular chaperones. *Journal of biosciences,* 23**,** 287-302.

FOUCHAQ, B., BENAROUDJ, N., EBEL, C. & LADJIMI, M. M. (1999). Oligomerization of the 17-kDa peptide-binding domain of the molecular chaperone HSC70. *European Journal of Biochemistry,* 259**,** 379-384.

FREIDEN, P., GAUT, J. & HENDERSHOT, L. (1992). Interconversion of three differentially modified and assembled forms of BiP. *The EMBO journal,* 11**,** 63.

FRYDMAN, J., NIMMESGERN, E., ERDJUMENT-BROMAGE, H., WALL, J., TEMPST, P. & HARTL, F. (1992). Function in protein folding of TRiC, a cytosolic ring complex containing TCP-1 and structurally related subunits. *The EMBO journal,* 11**,** 4767.

FRYDMAN, J., NIMMESGERN, E., OHTSUKA, K. & HARTL, F. U. (1994). Folding of nascent polypeptide chains in a high molecular mass assembly with molecular chaperones. *Nature,* 370**,** 111-117.

FUNG, K. L., HILGENBERG, L., WANG, N. M. & CHIRICO, W. J. (1996). Conformations of the nucleotide and polypeptide binding domains of a cytosolic Hsp70 molecular chaperone are coupled. *Journal of Biological Chemistry,* 271**,** 21559-21565.

GAO, B., EISENBERG, E. & GREENE, L. (1995). Interaction of nucleotide-free Hsc70 with clathrin and peptide and effect of ATP analogues. *Biochemistry,* 34**,** 11882-11888.

GAO, B., GREENE, L. & EISENBERG, E. (1994). Characterization of nucleotide-free uncoating ATPase and its binding to ATP, ADP, and ATP analogues. *Biochemistry,* 33**,** 2048-2054.

GAO, X. & HU, H. (2008). Quality control of the proteins associated with neurodegenerative diseases. *Acta Biochim Biophys Sin (Shanghai),* 40**,** 612-618.

GARIMELLA, R., LIU, X., QIAO, W., LIANG, X. Y., ZUIDERWEG, E. R. P., RILEY, M. I. & VAN DOREN, S. R. (2006). Hsc70 contacts helix III of the J domain from polyomavirus T antigens: Addressing a dilemma in the chaperone hypothesis of how they release E2F from pRb. *Biochemistry,* 45**,** 6917-6929.

GASSLER, C. S., BUCHBERGER, A., LAUFEN, T., MAYER, M. P., SCHRODER, H., VALENCIA, A. & BUKAU, B. (1998). Mutations in the DnaK chaperone affecting interaction with the DnaJ cochaperone. *Proc Natl Acad Sci U S A,* 95**,** 15229-15234.

GASSLER, C. S., WIEDERKEHR, T., BREHMER, D., BUKAU, B. & MAYER, M. P. (2001). Bag-1M accelerates nucleotide release for human Hsc70 and Hsp70 and can act concentration-dependent as positive and negative cofactor. *Journal of Biological Chemistry,* 276**,** 32538-32544.

GENEVAUX, P., SCHWAGER, F., GEORGOPOULOS, C. & KELLEY, W. L. (2002). Scanning mutagenesis identifies amino acid residues essential for the in vivo activity of the Escherichia coli DnaJ (Hsp40) J-domain. *Genetics,* 162**,** 1045-1053.

GERNERT, K. M., SMITH, R. & CARTER, D. C. (1988). A simple apparatus for controlling nucleation and size in protein crystal growth. *Anal Biochem,* 168**,** 141-147.

GLOVER, J. & LINDQUIST, S. (1998). Hsp104, Hsp70, and Hsp40:: A Novel Chaperone System that Rescues Previously Aggregated Proteins. *Cell,* 94**,** 73-82.

GLÜCK, J. M., HOFFMANN, S., KOENIG, B. W. & WILLBOLD, D. (2010). Single Vector System for Efficient N-myristoylation of Recombinant Proteins in <italic>E. coli</italic>. *PLoS ONE,* 5**,** e10081.

GOLDBERGER, R., EPSTEIN, C. & ANFINSEN, C. (1963). Acceleration of reactivation of reduced bovine pancreatic ribonuclease by a microsomal system from rat liver. *Journal of Biological Chemistry,* 238**,** 628.

GÖRG, A., WEISS, W. & DUNN, M. (2004). Current two-dimensional electrophoresis technology for proteomics. *Proteomics,* 4**,** 3665-3685.

GRAGEROV, A., ZENG, L., ZHAO, X., BURKHOLDER, W. & GOTTESMAN, M. E. (1994). Specificity of DnaK-peptide binding. *Journal of Molecular Biology,* 235**,** 848-854.

GREENE, M. K., MASKOS, K. & LANDRY, S. J. (1998). Role of the J-domain in the cooperation of Hsp40 with Hsp70. *Proceedings of the National Academy of Sciences of the United States of America,* 95**,** 6108-6113.

GREENER, T., ZHAO, X., NOJIMA, H., EISENBERG, E. & GREENE, L. E. (2000). Role of cyclin G-associated kinase in uncoating clathrin-coated vesicles from non-neuronal cells. *Journal of Biological Chemistry,* 275**,** 1365-1370.

GROSSMAN, A. D., ERICKSON, J. W. & GROSS, C. A. (1984). The htpR gene product of E. coli is a sigma factor for heat-shock promoters. *Cell,* 38**,** 383-390.

GUPTA, R. S. & SINGH, B. (1992). Cloning of the HSP70 gene from Halobacterium marismortui: relatedness of archaebacterial HSP70 to its eubacterial homologs and a model for the evolution of the HSP70 gene. *J Bacteriol,* 174**,** 4594-4605.

GYRD-HANSEN, M., NYLANDSTED, J. & JAATTELA, M. (2004). Heat shock protein 70 promotes cancer cell viability by safeguarding lysosomal integrity. *Cell Cycle,* 3**,** 1484–1485.

HAAS, I. & WABL, M. (1983). Immunoglobulin heavy chain binding protein.

HAHN, G. M. & LI, G. C. (1982). Thermotolerance and heat shock proteins in mammalian cells. *Radiat Res,* 92**,** 452-457.

HAN, W. & CHRISTEN, P. (2001). Mutations in the interdomain linker region of DnaK abolish the chaperone action of the DnaK/DnaJ/GrpE system. *FEBS Letters,* 497**,** 55-58.

HARRISON, C. J., HAYER-HARTL, M., DI LIBERTO, M., HARTL, F. & KURIYAN, J. (1997). Crystal structure of the nucleotide exchange factor GrpE bound to the ATPase domain of the molecular chaperone DnaK. *Science,* 276**,** 431-435.

HARTL, F. U. (1996). Molecular chaperones in cellular protein folding. *Nature,* 381**,** 571-579.

HELD, P. (2008). Measure Your Purity: Assessment of Nucleic Acid Purity via UV Absorbance. *Darmstadt*, Allemagne, Git.

HENDRICKSON, W. (1991). Determination of macromolecular structures from anomalous diffraction of synchrotron radiation. *Science,* 254**,** 51.

HENNESSY, F., NICOLL, W., ZIMMERMANN, R., CHEETHAM, M. & BLATCH, G. (2005). Not all J domains are created equal: implications for the specificity of Hsp40-Hsp70 interactions. *Protein Science,* 14**,** 1697-1709.

HENSOLD, J., HUNT, C., CALDERWOOD, S., HOUSMAN, D. & KINGSTON, R. (1990). DNA binding of heat shock factor to the heat shock element is insufficient for transcriptional activation in murine erythroleukemia cells. *Molecular and Cellular Biology,* 10**,** 1600.

HILL, R., FLANAGAN, J. & PRESTEGARD, J. (1995). 1H and 15N magnetic resonance assignments, secondary structure, and tertiary fold of Escherichia coli DnaJ (1-78). *Biochemistry,* 34**,** 5587-5596.

HOHFELD, J. & JENTSCH, S. (1997). GrpE-like regulation of the hsc70 chaperone by the anti-apoptotic protein BAG-1. *EMBO Journal,* 16**,** 6209-6216.

HOHFELD, J., MINAMI, Y. & HARTL, F. U. (1995). Hip, a Novel Cochaperone Involved in the Eukaryotic Hsc70/Hsp40 Reaction Cycle. *Cell,* 83**,** 589-598.

HU, S. M. & WANG, C. (1996). Involvement of the 10-kDa C-terminal fragment of hsc70 in complexing with unfolded protein. *Archives of Biochemistry and Biophysics,* 332**,** 163-169.

HUANG, K., FLANAGAN, J. & PRESTEGARD, J. (1999). The influence of C-terminal extension on the structure of the "J-domain" in E. coli DnaJ. *Protein Science,* 8**,** 203-214.

HUANG, S., TSAI, M., TZOU, Y., WU, W. & WANG, C. (1993). Aspartyl residue 10 is essential for ATPase activity of rat hsc70. *Journal of Biological Chemistry,* 268**,** 2063.

HUBBARD, S. J. (1998). The structural aspects of limited proteolysis of native proteins. *Biochimica Et Biophysica Acta-Protein Structure and Molecular Enzymology,* 1382**,** 191-206.

JANCARIK, J. & KIM, S. (1991). Sparse matrix sampling: a screening method for crystallization of proteins. *Journal of Applied Crystallography,* 24**,** 409-411.

JIANG, J., MAES, E. G., TAYLOR, A. B., WANG, L., HINCK, A. P., LAFER, E. M. & SOUSA, R. (2007). Structural basis of J cochaperone binding and regulation of Hsp70. *Molecular Cell,* 28**,** 422-433.

JIANG, J., PRASAD, K., LAFER, E. & SOUSA, R. (2005). Structural basis of interdomain communication in the Hsc70 chaperone. *Molecular Cell,* 20**,** 513-524.

JIANG, R. F., GREENER, T., BAROUCH, W., GREENE, L. & EISENBERG, E. (1997). Interaction of auxilin with the molecular chaperone, Hsc70. *Journal of Biological Chemistry,* 272**,** 6141-6145.

JOHNSON, J. L. & CRAIG, E. A. (2001). An essential role for the substrate-binding region of Hsp40s in Saccharomyces cerevisiae. *J Cell Biol,* 152**,** 851-856.

JOHNSTON, K., CLEMENTS, A., VENKATARAMANI, R., TRIEVEL, R. & MARMORSTEIN, R. (2000). Coexpression of proteins in bacteria using T7-based expression plasmids: expression of heteromeric cell-cycle and transcriptional regulatory complexes. *Protein Expression and Purification,* 20**,** 435-443.

JOLLY, C. & MORIMOTO, R. I. (2000). Role of the heat shock response and molecular chaperones in oncogenesis and cell death. *J Natl Cancer Inst,* 92**,** 1564-1572.

KABANI, M., BECKERICH, J. M. & BRODSKY, J. L. (2002). Nucleotide exchange factor for the yeast Hsp70 molecular chaperone Ssa1p. *Molecular and Cellular Biology,* 22**,** 4677-4689.

KAMPINGA, H. H. & CRAIG, E. A. (2010). `The HSP70 chaperone machinery: J proteins as drivers of functional specificity. *Nature Reviews Molecular Cell Biology,* 11**,** 579-592.

KARZAI, A. & MCMACKEN, R. (1996). A bipartite signaling mechanism involved in DnaJ-mediated activation of the Escherichia coli DnaK protein. *Journal of Biological Chemistry,* 271**,** 11236.

KIANG, J. G. & TSOKOS, G. C. (1998). Heat shock protein 70 kDa: Molecular biology, biochemistry, and physiology. *Pharmacology & Therapeutics,* 80**,** 183-201.

KIM, D., LEE, Y. J. & CORRY, P. M. (1992). Constitutive HSP70: oligomerization and its dependence on ATP binding. *Journal of Cellular Physiology,* 153**,** 353-361.

KIM, S. Y., SHARMA, S., HOSKINS, J. R. & WICKNER, S. (2002). Interaction of the DnaK and DnaJ chaperone system with a native substrate, p1 RepA. *Journal of Biological Chemistry,* 277**,** 44778-44783.

KING, C., EISENBERG, E. & GREENE, L. (1995). Polymerization of 70-kDa heat shock protein by yeast DnaJ in ATP. *Journal of Biological Chemistry,* 270**,** 22535.

KING, C., EISENBERG, E. & GREENE, L. E. (1999). Interaction between Hsc70 and DnaJ homologues: relationship between Hsc70 polymerization and ATPase activity. *Biochemistry,* 38**,** 12452-12459.

KLUCK, C. J., PATZELT, H., GENEVAUX, P., BREHMER, D., RIST, W., SCHNEIDER-MERGENER, J., BUKAU, B. & MAYER, M. P. (2002). Structure-function analysis of HscC, the Escherichia coli member of a novel

subfamily of specialized Hsp70 chaperones. *Journal of Biological Chemistry,* 277**,** 41060-41069.

KRISSINEL, E. & HENRICK, K. (2004). Secondary-structure matching (SSM), a new tool for fast protein structure alignment in three dimensions. *Acta Crystallogr D Biol Crystallogr,* 60**,** 2256-2268.

KRISSINEL, E. & HENRICK, K. (2007). Inference of macromolecular assemblies from crystalline state. *Journal of Molecular Biology,* 372**,** 774-797.

KÜGLER, M., JÄNSCH, L., KRUFT, V., SCHMITZ, U. & BRAUN, H. (1997). Analysis of the chloroplast protein complexes by blue-native polyacrylamide gel electrophoresis (BN-PAGE). *Photosynthesis Research,* 53**,** 35-44.

LAEMMLI, U. (1970). Cleavage of structural proteins during the assembly of the head of bacteriophage T4. *Nature,* 227**,** 680-685.

LANDICK, R., VAUGHN, V., LAU, E. T., VANBOGELEN, R. A., ERICKSON, J. W. & NEIDHARDT, F. C. (1984). Nucleotide sequence of the heat shock regulatory gene of E. coli suggests its protein product may be a transcription factor. *Cell,* 38**,** 175-182.

LANDRY, S. J., JORDAN, R., MCMACKEN, R. & GIERASCH, L. M. (1992). Different conformations for the same polypeptide bound to chaperones DnaK and GroEL. *Nature,* 355**,** 455-457.

LANGER, T., LU, C., ECHOLS, H., FLANAGAN, J., HAYER, M. K. & HARTL, F. U. (1992). Successive action of DnaK, DnaJ and GroEL along the pathway of chaperone-mediated protein folding. *Nature,* 356**,** 683-689.

LASKEY, R. A., HONDA, B. M., MILLS, A. D. & FINCH, J. T. (1978). Nucleosomes are assembled by an acidic protein which binds histones and transfers them to DNA. *Nature,* 275**,** 416-420.

LASKOWSKI, R. A., MACARTHUR, M. W., MOSS, D. S. & THORNTON, J. M. (1993). Procheck - a Program to Check the Stereochemical Quality of Protein Structures. *Journal of Applied Crystallography,* 26**,** 283-291.

LAUFEN, T., MAYER, M. P., BEISEL, C., KLOSTERMEIER, D., MOGK, A., REINSTEIN, J. & BUKAU, B. (1999). Mechanism of regulation of hsp70 chaperones by DnaJ cochaperones. *Proc Natl Acad Sci U S A,* 96**,** 5452-5457.

LENG, C. H., BRODSKY, J. L. & WANG, C. (1998). Isolation and characterization of a DnaJ-like protein in rats: the C-terminal 10-kDa domain of hsc70 is not essential for stimulating the ATP-hydrolytic activity of hsc70 by a DnaJ-like protein. *Protein Science,* 7**,** 1186-1194.

LEVINSON, W., OPPERMANN, H. & JACKSON, J. (1980). Transition series metals and sulfhydryl reagents induce the synthesis of four proteins in eukaryotic cells. *Biochim Biophys Acta,* 606**,** 170-180.

LEVINTHAL, C. ARE THERE PATHWAYS FOR PROTEIN FOLDING?

LEVY, E. J., MCCARTY, J., BUKAU, B. & CHIRICO, W. J. (1995). Conserved ATPase and luciferase refolding activities between bacteria and yeast Hsp70 chaperones and modulators. *FEBS Lett,* 368**,** 435-440.

LI, G. C. & LASZLO, A. (1985). Amino-Acid Analogs While Inducing Heat-Shock Proteins Sensitize Cho Cells to Thermal-Damage. *Journal of Cellular Physiology,* 122**,** 91-97.

LI, G. C. & WERB, Z. (1982). Correlation between Synthesis of Heat-Shock Proteins and Development of Thermotolerance in Chinese-Hamster Fibroblasts. *Proceedings of the National Academy of Sciences of the United States of America-Biological Sciences,* 79**,** 3218-3222.

LI, J., QIAN, X. & SHA, B. (2003). The crystal structure of the yeast Hsp40 Ydj1 complexed with its peptide substrate. *Structure,* 11**,** 1475-1483.

LI, J. & SHA, B. (2005). Structure-based mutagenesis studies of the peptide substrate binding fragment of type I heat-shock protein 40. *Biochemical Journal,* 386**,** 453-460.

LIBEREK, K., MARSZALEK, J., ANG, D., GEORGOPOULOS, C. & ZYLICZ, M. (1991). Escherichia coli DnaJ and GrpE heat shock proteins jointly stimulate ATPase activity of DnaK. *Proceedings of the National Academy of Sciences of the United States of America,* 88**,** 2874.

LIBEREK, K., SKOWYRA, D., ZYLICZ, M., JOHNSON, C. & GEORGOPOULOS, C. (1991). The Escherichia-Coli Dnak Chaperone, the 70-Kda Heat-Shock Protein Eukaryotic Equivalent, Changes Conformation Upon Atp Hydrolysis, Thus Triggering Its Dissociation from a Bound Target Protein. *Journal of Biological Chemistry,* 266**,** 14491-14496.

LINDQUIST, S. & CRAIG, E. (1988). The heat-shock proteins. *Annual Review of Genetics,* 22**,** 631-677.

LITTLECHILD, J. (1991). Protein crystallization: magical or logical: can we establish some general rules? *Journal of Physics D: Applied Physics,* 24**,** 111.

LIU, Q. & HENDRICKSON, W. A. (2007). Insights into Hsp70 chaperone activity from a crystal structure of the yeast Hsp110 Sse1. *Cell,* 131**,** 106-120.

LU, Z. & CYR, D. M. (1998). Protein folding activity of Hsp70 is modified differentially by the Hsp40 co-chaperones Sis1 and Ydj1. *Journal of Biological Chemistry,* 273**,** 27824-27830.

MACARIO, A. J. & CONWAY DE MACARIO, E. (2005). Sick chaperones, cellular stress, and disease. *N Engl J Med,* 353**,** 1489-1501.

MACARIO, A. J., LANGE, M., AHRING, B. K. & CONWAY DE MACARIO, E. (1999). Stress genes and proteins in the archaea. *Microbiol Mol Biol Rev,* 63**,** 923-967, table of contents.

MACARIO, A. J. L. & DE MACARIO, E. C. (2005). Mechanisms of disease - Sick chaperones, cellular stress, and disease. *New England Journal of Medicine,* 353**,** 1489-1501.

MAJESKI, A. E. & DICE, J. F. (2004). Mechanisms of chaperone-mediated autophagy. *Int J Biochem Cell Biol,* 36**,** 2435-2444.

MANDEL, M. & HIGA, A. (1970). Calcium-dependent bacteriophage DNA infection* 1. *Journal of Molecular Biology,* 53**,** 159-162.

MARTINEZ-YAMOUT, M., LEGGE, G. B., ZHANG, O., WRIGHT, P. E. & DYSON, H. J. (2000). Solution structure of the cysteine-rich domain of the

Escherichia coli chaperone protein DnaJ. *Journal of Molecular Biology,* 300**,** 805-818.

MARX, J. L. (1983). Surviving heat shock and other stresses. *Science,* 221**,** 251-253.

MATTHEWS, B. (1968). Solvent content of protein crystals. *Journal of Molecular Biology,* 33**,** 491-497.

MAYER, M. P. & BUKAU, B. (2005). Hsp70 chaperones: cellular functions and molecular mechanism. *Cellular and Molecular Life Sciences,* 62**,** 670-684.

MAYER, M. P., LAUFEN, T., PAAL, K., MCCARTY, J. S. & BUKAU, B. (1999). Investigation of the interaction between DnaK and DnaJ by surface plasmon resonance spectroscopy. *Journal of Molecular Biology,* 289**,** 1131-1144.

MAYER, M. P., RUDIGER, S. & BUKAU, B. (2000). Molecular basis for interactions of the DnaK chaperone with substrates. *Biol Chem,* 381**,** 877-885.

MAYER, M. P., SCHRODER, H., RUDIGER, S., PAAL, K., LAUFEN, T. & BUKAU, B. (2000). Multistep mechanism of substrate binding determines chaperone activity of Hsp70. *Nature Structural Biology,* 7**,** 586-593.

MCCARTY, J. S., BUCHBERGER, A., REINSTEIN, J. & BUKAU, B. (1995). The role of ATP in the functional cycle of the DnaK chaperone system. *Journal of Molecular Biology,* 249**,** 126-137.

MCPHERSON, A. (1999). Crystallization of biological macromolecules. *Cold Springs Harbor Laboratory*.

MEIMARIDOU, E., GOOLJAR, S. & CHAPPLE, J. (2009). From hatching to dispatching: the multiple cellular roles of the Hsp70 molecular chaperone machinery. *Journal of molecular endocrinology,* 42**,** 1.

MENORET, A. (2004). Purification of recombinant and endogenous HSP70s. *Methods,* 32**,** 7-12.

MINAMI, Y., HOHFELD, J., OHTSUKA, K. & HARTL, F. U. (1996). Regulation of the heat-shock protein 70 reaction cycle by the mammalian DnaJ homolog, Hsp40. *Journal of Biological Chemistry,* 271**,** 19617-19624.

MINTON, A. (2000). Implications of macromolecular crowding for protein assembly. *Current Opinion in Structural Biology,* 10**,** 34-39.

MONTGOMERY, D. L., MORIMOTO, R. I. & GIERASCH, L. M. (1999). Mutations in the substrate binding domain of the Escherichia coli 70 kDa molecular chaperone, DnaK, which alter substrate affinity or interdomain coupling. *Journal of Molecular Biology,* 286**,** 915-932.

MOON, I. S., PARK, I. S., SCHENKER, L. T., KENNEDY, M. B., MOON, J.-I. & JIN, I. (2001). Presence of both Constitutive and Inducible Forms of Heat Shock Protein 70 in the Cerebral Cortex and Hippocampal Synapses. *Cerebral Cortex,* 11**,** 238-248.

MORIMOTO, R. (1998). Regulation of the heat shock transcriptional response: cross talk between a family of heat shock factors, molecular chaperones, and negative regulators. *Genes & Development,* 12**,** 3788.

MORIMOTO, R. I. (1993). Cells in stress: transcriptional activation of heat shock genes. *Science,* 259**,** 1409-1410.

MORISHIMA, N. (2005). Control of cell fate by Hsp70: more than an evanescent meeting. *J Biochem,* 137**,** 449-453.

MORO, F., OKAMOTO, K., DONZEAU, M., NEUPERT, W. & BRUNNER, M. (2002). Mitochondrial protein import: molecular basis of the ATP-dependent interaction of MtHsp70 with Tim44. *Journal of Biological Chemistry,* 277**,** 6874-6880.

MORRIS, A., MACARTHUR, M., HUTCHINSON, E. & THORNTON, J. (1992). Stereochemical quality of protein structure coordinates. *Proteins: Structure, Function, and Bioinformatics,* 12**,** 345-364.

MORRISON, D. (1977). Transformation in Escherichia coli: cryogenic preservation of competent cells. *Journal of Bacteriology,* 132**,** 349.

MORSHAUSER, R. C., HU, W., WANG, H., PANG, Y., FLYNN, G. C. & ZUIDERWEG, E. R. (1999). High-resolution solution structure of the 18 kDa substrate-binding domain of the mammalian chaperone protein Hsc70. *Journal of Molecular Biology,* 289**,** 1387-1403.

MOSSER, D., CARON, A., BOURGET, L., DENIS-LAROSE, C. & MASSIE, B. (1997). Role of the human heat shock protein hsp70 in protection against stress-induced apoptosis. *Molecular and Cellular Biology,* 17**,** 5317.

MOTOHASHI, K., TAGUCHI, H., ISHII, N. & YOSHIDA, M. (1994). Isolation of the stable hexameric DnaK. DnaJ complex from Thermus thermophilus. *Journal of Biological Chemistry,* 269**,** 27074.

NAM, S. H. & WALSH, M. K. (2002). Affinity purification and characterization of the Escherichia coli molecular chaperones. *Protein Expr Purif,* 24**,** 282-291.

NARDAI, G., VÉGH, E., PROHÁSZKA, Z. & CSERMELY, P. (2006). Chaperone-related immune dysfunction: an emergent property of distorted chaperone networks. *Trends in Immunology,* 27**,** 74-79.

NEMOTO, T. K., FUKUMA, Y., ITOH, H., TAKAGI, T. & ONO, T. (2006). A disulfide bridge mediated by cysteine 574 is formed in the dimer of the 70-kDa heat shock protein. *Journal of Biochemistry,* 139**,** 677-687.

NICOLL, W. S., BOSHOFF, A., LUDEWIG, M. H., HENNESSY, F., JUNG, M. & BLATCH, G. L. (2006). Approaches to the isolation and characterization of molecular chaperones. *Protein Expr Purif,* 46**,** 1-15.

NOLLEN, E. A., KABAKOV, A. E., BRUNSTING, J. F., KANON, B., HOHFELD, J. & KAMPINGA, H. H. (2001). Modulation of in vivo HSP70 chaperone activity by Hip and Bag-1. *Journal of Biological Chemistry,* 276**,** 4677-4682.

O'BRIEN, M. & MCKAY, D. (1993). Threonine 204 of the chaperone protein Hsc70 influences the structure of the active site, but is not essential for ATP hydrolysis. *Journal of Biological Chemistry,* 268**,** 24323.

O'BRIEN, M. C., FLAHERTY, K. M. & MCKAY, D. B. (1996). Lysine 71 of the chaperone protein Hsc70 Is essential for ATP hydrolysis. *Journal of Biological Chemistry,* 271**,** 15874-15878.

O'BRIEN, M. C. & MCKAY, D. B. (1995). How potassium affects the activity of the molecular chaperone Hsc70. I. Potassium is required for optimal ATPase activity. *Journal of Biological Chemistry,* 270**,** 2247-2250.

OHI, M., LI, Y., CHENG, Y. & WALZ, T. (2004). Negative staining and image classification—powerful tools in modern electron microscopy. *Biological procedures online,* 6**,** 23-34.

O'MALLEY, K., MAURON, A., BARCHAS, J. D. & KEDES, L. (1985). Constitutively expressed rat mRNA encoding a 70-kilodalton heat-shock-like protein. *Molecular and Cellular Biology,* 5**,** 3476-3483.

OTWINOWSKI, Z. & MINOR, W. (1997). Processing of X-ray diffraction data collected in oscillation mode. *Methods in Enzymology***,** 307-325.

PALLEROS, D., RAID, K., SHI, L., WELCH, W. & FINK, A. (1993). ATP-induced protein Hsp70 complex dissociation requires K+ but not ATP hydrolysis.

PALLEROS, D., REID, K., SHI, L. & FINK, A. (1993). DnaK ATPase activity revisited. *FEBS Letters,* 336**,** 124-128.

PALLEROS, D. R., SHI, L., REID, K. L. & FINK, A. L. (1994). hsp70-protein complexes. Complex stability and conformation of bound substrate protein. *Journal of Biological Chemistry,* 269**,** 13107-13114.

PALLEROS, D. R., WELCH, W. J. & FINK, A. L. (1991). Interaction of hsp70 with unfolded proteins: effects of temperature and nucleotides on the kinetics of binding. *Proc Natl Acad Sci U S A,* 88**,** 5719-5723.

PELLECCHIA, M., MONTGOMERY, D., STEVENS, S., VANDER KOOI, C., FENG, H., GIERASCH, L. & ZUIDERWEG, E. (2000). Structural insights into substrate binding by the molecular chaperone DnaK. *Nature Structural & Molecular Biology,* 7**,** 298-303.

PELLECCHIA, M., SZYPERSKI, T., WALL, D., GEORGOPOULOS, C. & WÜTHRICH, K. (1996). NMR Structure of the J-domain and the Gly/Phe-rich Region of theEscherichia coliDnaJ Chaperone. *Journal of Molecular Biology,* 260**,** 236-250.

PERDRIZET, G. A., KANEKO, H., BUCKLEY, T. M., FISHMAN, M. A. & SCHWEIZER, R. T. (1990). Heat shock protects pig kidneys against warm ischemic injury. *Transplant Proc,* 22**,** 460-461.

PERLMUTTER, D. H. (1999). Misfolded proteins in the endoplasmic reticulum. *Lab Invest,* 79**,** 623-638.

PETER WALSH, D. & YIN CHERN LAW, D. (2004). The J-protein family: modulating protein assembly, disassembly and translocation. *Embo Reports,* 5**,** 567-571.

PHILO, J. (2003). Characterizing the aggregation and conformation of protein therapeutics. *American biotechnology laboratory,* 21**,** 22-29.

PLECKAITYTE, M., MISTINIENE, E., MICHAILOVIENE, V. & ZVIRBLIS, G. (2003). Identification and characterization of a Hsp70 (DnaK) chaperone system from Meiothermus ruber. *Molecular Genetics and Genomics,* 269**,** 109-115.

POLIER, S., DRAGOVIC, Z., HARTL, F. U. & BRACHER, A. (2008). Structural basis for the cooperation of Hsp70 and Hsp110 chaperones in protein folding. *Cell,* 133**,** 1068-1079.

QIAN, Y. Q., PATEL, D., HARTL, F. U. & MCCOLL, D. J. (1996). Nuclear magnetic resonance solution structure of the human Hsp40 (HDJ-1) J-domain. *Journal of Molecular Biology,* 260**,** 224-235.

QIU, X., SHAO, Y., MIAO, S. & WANG, L. (2006). The diversity of the DnaJ/Hsp40 family, the crucial partners for Hsp70 chaperones. *Cellular and Molecular Life Sciences,* 63**,** 2560-2570.

QU, B. H. & THOMAS, P. J. (1996). Alteration of the cystic fibrosis transmembrane conductance regulator folding pathway - Effects of the Delta F508 mutation on the thermodynamic stability and folding yield of NBD1. *Journal of Biological Chemistry,* 271**,** 7261-7264.

RADFORD, S. E. (2000). Protein folding: progress made and promises ahead. *Trends in Biochemical Sciences,* 25**,** 611-618.

RADFORD, S. E. & DOBSON, C. M. (1999). From computer simulations to human disease: Emerging themes in protein folding. *Cell,* 97**,** 291-298.

RAMACHANDRAN, G. N., RAMAKRISHNAN, C. & SASISEKHARAN, V. (1963). Stereochemistry of polypeptide chain configurations. *Journal of Molecular Biology,* 7**,** 95-99.

RAYNES, D. A. & GUERRIERO, V. (1998). Inhibition of Hsp70 ATPase activity and protein renaturation by a novel Hsp70-binding protein. *Journal of Biological Chemistry,* 273**,** 32883-32888.

REVINGTON, M., HOLDER, T. M. & ZUIDERWEG, E. R. (2004). NMR study of nucleotide-induced changes in the nucleotide binding domain of Thermus thermophilus Hsp70 chaperone DnaK: implications for the allosteric mechanism. *Journal of Biological Chemistry,* 279**,** 33958-33967.

REVINGTON, M., ZHANG, Y., YIP, G. N., KUROCHKIN, A. V. & ZUIDERWEG, E. R. (2005). NMR investigations of allosteric processes in a two-domain Thermus thermophilus Hsp70 molecular chaperone. *Journal of Molecular Biology,* 349**,** 163-183.

RITOSSA, F. (1963). New puffs induced by temperature shock, DNP and salicylate in salivary chromosomes of Drosophila melanogaster. *Drosophila Information Service,* 37**,** 122-123.

RUDDON, R. & BEDOWS, E. (1997). Assisted protein folding. *Journal of Biological Chemistry,* 272**,** 3125.

RÜDIGER, S., GERMEROTH, L., SCHNEIDER-MERGENER, J., BUKAU, B. (1997). Substrate specificity of the DnaK chaperone determined by screening cellulose-bound peptide libraries. *The EMBO Journal,* 16, 1501 – 1507.

RUDIGER, S., SCHNEIDER-MERGENER, J. & BUKAU, B. (2001). Its substrate specificity characterizes the DnaJ co-chaperone as a scanning factor for the DnaK chaperone. *EMBO Journal,* 20**,** 1042-1050.

RUSSELL, R., KARZAI, A. W., MEHL, A. F. & MCMACKEN, R. (1999). DnaJ dramatically stimulates ATP hydrolysis by DnaK: Insight into targeting of Hsp70 proteins to polypeptide substrates. *Biochemistry,* 38**,** 4165-4176.

SADIS, S. & HIGHTOWER, L. E. (1992). Unfolded proteins stimulate molecular chaperone Hsc70 ATPase by accelerating ADP/ATP exchange. *Biochemistry,* 31**,** 9406-9412.

SAKAKIBARA, Y. (1988). The dnaK gene of Escherichia coli functions in initiation of chromosome replication. *Journal of Bacteriology,* 170**,** 972.

SAMBROOK, J., FRITSCH, E.F. & MANIATIS, T. (1989). Molecular cloning: a laboratory manual, 2 nd edition.*Cold Spring Harbor Laboratory Press*

SARGE, K., MURPHY, S. & MORIMOTO, R. (1993). Activation of heat shock gene transcription by heat shock factor 1 involves oligomerization, acquisition of DNA-binding activity, and nuclear localization and can occur in the absence of stress. *Molecular and Cellular Biology,* 13**,** 1392.

SCHÄGGER, H. & VON JAGOW, G. (1991). Blue native electrophoresis for isolation of membrane protein complexes in enzymatically active form. *Analytical Biochemistry,* 199**,** 223-231.

SCHEICH, C., KUMMEL, D., SOUMAILAKAKIS, D., HEINEMANN, U. & BUSSOW, K. (2007). Vectors for co-expression of an unrestricted number of proteins. *Nucleic Acids Res,* 35**,** e43.

SCHLESINGER, M. (1990). Heat shock proteins. *Journal of Biological Chemistry,* 265**,** 12111-12114.

SCHLOSSMAN, D. M., SCHMID, S. L., BRAELL, W. A. & ROTHMAN, J. E. (1984). An Enzyme That Removes Clathrin Coats - Purification of an Uncoating Atpase. *Journal of Cell Biology,* 99**,** 723-733.

SCHMID, D., BAICI, A., GEHRING, H. & CHRISTEN, P. (1994). Kinetics of molecular chaperone action. *Science,* 263**,** 971.

SCHÖNFELD, H., SCHMIDT, D., SCHRÖDER, H. & BUKAU, B. (1995). The DnaK chaperone system of Escherichia coli: quaternary structures and interactions of the DnaK and GrpE components. *Journal of Biological Chemistry,* 270**,** 2183.

SCHUCK, P. (2000). Size-distribution analysis of macromolecules by sedimentation velocity ultracentrifugation and lamm equation modeling. *Biophysical Journal,* 78**,** 1606-1619.

SCHUERMANN, J. P., JIANG, J., CUELLAR, J., LLORCA, O., WANG, L., GIMENEZ, L. E., JIN, S., TAYLOR, A. B., DEMELER, B., MORANO, K. A., HART, P. J., VALPUESTA, J. M., LAFER, E. M. & SOUSA, R. (2008). Structure of the Hsp110:Hsc70 Nucleotide Exchange Machine. *Molecular Cell,* 31**,** 232-243.

SHA, B., LEE, S. & CYR, D. M. (2000). The crystal structure of the peptide-binding fragment from the yeast Hsp40 protein Sis1. *Structure,* 8**,** 799-807.

SHANER, L. & MORANO, K. (2007). All in the family: atypical Hsp70 chaperones are conserved modulators of Hsp70 activity. *Cell Stress & Chaperones,* 12**,** 1.

SHANER, L., SOUSA, R. & MORANO, K. A. (2006). Characterization of Hsp70 binding and nucleotide exchange by the yeast Hsp110 chaperone Sse1. *Biochemistry,* 45**,** 15075-15084.

SHIDA, M., ARAKAWA, A., ISHII, R., KISHISHITA, S., TAKAGI, T., KUKIMOTO-NIINO, M., SUGANO, S., TANAKA, A., SHIROUZU, M. & YOKOYAMA, S. (2010). Direct inter-subdomain interactions switch between the closed and open forms of the Hsp70 nucleotide-binding domain in the nucleotide-free state. *Acta Crystallographica Section D: Biological Crystallography,* 66**,** 223-232.

SHOMURA, Y., DRAGOVIC, Z., CHANG, H.-C., TZVETKOV, N., YOUNG, J. C., BRODSKY, J. L., GUERRIERO, V., HARTL, F. U. & BRACHER, A. (2005). Regulation of Hsp70 Function by HspBP1: Structural Analysis Reveals an Alternate Mechanism for Hsp70 Nucleotide Exchange. *Molecular Cell,* 17**,** 367-379.

SLEPENKOV, S. & WITT, S. (2002). The unfolding story of the Escherichia coli Hsp70 DnaK: is DnaK a holdase or an unfoldase? *Molecular Microbiology,* 45**,** 1197-1206.

SMITH, D. F., SULLIVAN, W. P., MARION, T. N., ZAITSU, K., MADDEN, B., MCCORMICK, D. J. & TOFT, D. O. (1993). Identification of a 60-Kilodalton Stress-Related Protein, P60, Which Interacts with Hsp90 and Hsp70. *Molecular and Cellular Biology,* 13**,** 869-876.

SMYTH, M. S. & MARTIN, J. H. J. (2000). x Ray crystallography. *Molecular Pathology,* 53:**,** 8-14.

SONDERMANN, H., SCHEUFLER, C., SCHNEIDER, C., HOHFELD, J., HARTL, F. U. & MOAREFI, I. (2001). Structure of a Bag/Hsc70 complex: convergent functional evolution of Hsp70 nucleotide exchange factors. *Science,* 291**,** 1553-1557.

SOUSA, R. & LAFER, E. M. (2006). Keep the traffic moving: mechanism of the Hsp70 motor. *Traffic,* 7**,** 1596-1603.

SRIRAM, M., OSIPIUK, J., FREEMAN, B., MORIMOTO, R. & JOACHIMIAK, A. (1997). Human Hsp70 molecular chaperone binds two calcium ions within the ATPase domain. *Structure,* 5**,** 403-414.

STRUB, M., HOH, F., SANCHEZ, J., STRUB, J., BÖCK, A., AUMELAS, A. & DUMAS, C. (2003). Selenomethionine and selenocysteine double labeling strategy for crystallographic phasing. *Structure,* 11**,** 1359-1367.

STRYER, L., BERG, J. M., TYMOCZKO, J. L. (2002). Biochemistry (5th ed.), *New York: W. H. Freeman*

SUH, W. C., BURKHOLDER, W. F., LU, C. Z., ZHAO, X., GOTTESMAN, M. E. & GROSS, C. A. (1998). Interaction of the Hsp70 molecular chaperone, DnaK, with its cochaperone DnaJ. *Proceedings of the National Academy of Sciences of the United States of America,* 95**,** 15223-15228.

SUH, W. C., LU, C. Z. & GROSS, C. A. (1999). Structural features required for the interaction of the Hsp70 molecular chaperone DnaK with its cochaperone DnaJ. *Journal of Biological Chemistry,* 274**,** 30534-30539.

SUPPINI, J. P., AMOR, M., ALIX, J. H. & LADJIMI, M. M. (2004). Complementation of an Escherichia coli DnaK defect by Hsc70-DnaK chimeric proteins. *J Bacteriol,* 186**,** 6248-6253.

SWAIN, J. F., DINLER, G., SIVENDRAN, R., MONTGOMERY, D. L., STOTZ, M. & GIERASCH, L. M. (2007). Hsp70 chaperone ligands control domain association via an allosteric mechanism mediated by the interdomain linker. *Molecular Cell,* 26**,** 27-39.

SZABO, A., KORSZUN, R., HARTL, F. U. & FLANAGAN, J. (1996). A zinc finger-like domain of the molecular chaperone DnaJ is involved in binding to denatured protein substrates. *EMBO Journal,* 15**,** 408-417.

SZABO, A., LANGER, T., SCHRODER, H., FLANAGAN, J., BUKAU, B. & HARTL, F. U. (1994). The Atp Hydrolysis-Dependent Reaction Cycle of the Escherichia-Coli Hsp70 System - Dnak, Dnaj, and Grpe. *Proceedings of the National Academy of Sciences of the United States of America,* 91**,** 10345-10349.

TAKAYAMA, S., XIE, Z. & REED, J. C. (1999). An evolutionarily conserved family of Hsp70/Hsc70 molecular chaperone regulators. *Journal of Biological Chemistry,* 274**,** 781-786.

TAKENAKA, I., LEUNG, S., MCANDREW, S., BROWN, J. & HIGHTOWER, L. (1995). Hsc70-binding peptides selected from a phage display peptide library that resemble organellar targeting sequences. *Journal of Biological Chemistry,* 270**,** 19839.

TERLECKY, S., CHIANG, H., OLSON, T. & DICE, J. (1992). Protein and peptide binding and stimulation of in vitro lysosomal proteolysis by the 73-kDa heat shock cognate protein. *Journal of Biological Chemistry,* 267**,** 9202.

THOMAS, P., QU, B. & PEDERSEN, P. (1995). Defective protein folding as a basis of human disease. *Trends in Biochemical Sciences,* 20**,** 456-459.

THOMPSON, J., HIGGINS, D. & GIBSON, T. (1994). CLUSTAL W: improving the sensitivity of progressive multiple sequence alignment through sequence weighting, position-specific gap penalties and weight matrix choice. *Nucleic Acids Research,* 22**,** 4673.

TICKLE, I. & DRIESSEN, H. (1996). Molecular replacement using known structural information. *Methods in Molecular Biology (JM Walker, ed.),* 56**,** 173-203.

TILLY, K., MCKITTRICK, N., ZYLICZ, M. & GEORGOPOULOS, C. (1983). The dnaK protein modulates the heat-shock response of Escherichia coli. *Cell,* 34**,** 641-646.

TISSIERES, A., MITCHELL, H. K. & TRACY, U. M. (1974). Protein synthesis in salivary glands of Drosophila melanogaster: Relation to chromosome puffs. *Journal of Molecular Biology,* 85**,** 389-398.

TOLEDO, H., CARLINO, A., VIDAL, V., REDFIELD, B., NETTLETON, M., KOCHAN, J., BROT, N. & WEISSBACH, H. (1993). Dissociation of glucose-regulated protein Grp78 and Grp78-IgE Fc complexes by ATP. *Proceedings of the National Academy of Sciences of the United States of America,* 90**,** 2505.

TRUSCOTT, K. N., VOOS, W., FRAZIER, A. E., LIND, M., LI, Y., GEISSLER, A., DUDEK, J., MÜLLER, H., SICKMANN, A., MEYER, H. E., MEISINGER, C., GUIARD, B., REHLING, P. & PFANNER, N. (2003). A J-protein is an essential subunit of the presequence translocase–associated protein import motor of mitochondria. *The Journal of Cell Biology,* 163**,** 707-713.

TSAI, C. J., KUMAR, S., MA, B. & NUSSINOV, R. (1999). Folding funnels, binding funnels, and protein function. *Protein Science,* 8**,** 1181-1190.

TSAI, M. Y. & WANG, C. (1994). Uncoupling of peptide-stimulated ATPase and clathrin-uncoating activity in deletion mutant of hsc70. *Journal of Biological Chemistry,* 269**,** 5958-5962.

UNGEWICKELL, E., UNGEWICKELL, H. & HOLSTEIN, S. E. (1997). Functional interaction of the auxilin J domain with the nucleotide- and substrate-binding modules of Hsc70. *Journal of Biological Chemistry,* 272**,** 19594-19600.

VAGIN, A. & TEPLYAKOV, A. (1997). MOLREP: an automated program for molecular replacement. *Journal of Applied Crystallography,* 30**,** 1022-1025.

VOGEL, M., BUKAU, B. & MAYER, M. (2006). Allosteric regulation of Hsp70 chaperones by a proline switch. *Molecular Cell,* 21**,** 359-367.

VOGEL, M., MAYER, M. P. & BUKAU, B. (2006). Allosteric regulation of Hsp70 chaperones involves a conserved interdomain linker. *Journal of Biological Chemistry,* 281**,** 38705-38711.

VOS, M. J., HAGEMAN, J., CARRA, S. & KAMPINGA, H. H. (2008). Structural and functional diversities between members of the human HSPB, HSPH, HSPA, and DNAJ chaperone families. *Biochemistry,* 47**,** 7001-7011.

WALL, D., ZYLICZ, M. & GEORGOPOULOS, C. (1994). The NH2-terminal 108 amino acids of the Escherichia coli DnaJ protein stimulate the ATPase activity of DnaK and are sufficient for lambda replication. *Journal of Biological Chemistry,* 269**,** 5446.

WALSH, P., BURSAC, D., LAW, Y. C., CYR, D. & LITHGOW, T. (2004). The J-protein family: modulating protein assembly, disassembly and translocation. *Embo Reports,* 5**,** 567-571.

WANG, C. & LEE, M. (1993). High-level expression of soluble rat hsc70 in Escherichia coli: purification and characterization of the cloned enzyme. *Biochemical Journal,* 294**,** 69.

WANG, H., KUROCHKIN, A., PANG, Y., HU, W., FLYNN, G. & ZUIDERWEG, E. (1998). NMR Solution Structure of the 21 kDa Chaperone Protein DnaK Substrate Binding Domain: A Preview of Chaperone- Protein Interaction†. *Biochemistry,* 37**,** 7929-7940.

WANG, K. Y. & SPECTOR, A. (2001). ATP causes small heat shock proteins to release denatured protein. *European Journal of Biochemistry,* 268**,** 6335-6345.

WANG, T. F., CHANG, J. H. & WANG, C. (1993). Identification of the Peptide Binding Domain of Hsc70 - 18-Kilodalton Fragment Located Immediately after Atpase Domain Is Sufficient for High-Affinity Binding. *Journal of Biological Chemistry,* 268**,** 26049-26051.

WEGELE, H., HASLBECK, M. & BUCHNER, J. (2003). Recombinant expression and purification of Ssa1p (Hsp70) from Saccharomyces cerevisiae using Pichia pastoris. *Journal of Chromatography B,* 786**,** 109-115.

WELCH, W. J. (1993). Heat-Shock Proteins Functioning as Molecular Chaperones - Their Roles in Normal and Stressed Cells. *Philosophical Transactions of the Royal Society of London Series B-Biological Sciences,* 339**,** 327-333.

WELCH, W. J. & FERAMISCO, J. R. (1985). Rapid purification of mammalian 70,000-dalton stress proteins: affinity of the proteins for nucleotides. *Mol Cell Biol,* 5**,** 1229-1237.

WESTHOFF, B., CHAPPLE, J. P., VAN DER SPUY, J., HOHFELD, J. & CHEETHAM, M. E. (2005). HSJ1 is a neuronal shuttling factor for the sorting of chaperone clients to the proteasome. *Current Biology,* 15**,** 1058-1064.

WETLAUFER, D. B. & RISTOW, S. (1973). Acquisition of three-dimensional structure of proteins. *Annu Rev Biochem,* 42**,** 135-158.

WILBANKS, S. M., CHEN, L., TSURUTA, H., HODGSON, K. O. & MCKAY, D. B. (1995). Solution small-angle X-ray scattering study of the molecular chaperone Hsc70 and its subfragments. *Biochemistry,* 34**,** 12095-12106.

WILBANKS, S. M., DELUCA-FLAHERTY, C. & MCKAY, D. B. (1994). Structural basis of the 70-kilodalton heat shock cognate protein ATP hydrolytic activity. I. Kinetic analyses of active site mutants. *Journal of Biological Chemistry,* 269**,** 12893-12898.

WILD, J., ALTMAN, E., YURA, T. & GROSS, C. A. (1992). DnaK and DnaJ heat shock proteins participate in protein export in Escherichia coli. *Genes Dev,* 6**,** 1165-1172.

YANG, W., ZHANG, L., LU, Z. G., TAO, W. & ZHAO, Z. H. (2001). A new method for protein coexpression in Escherichia coli using two incompatible plasmids. *Protein Expression and Purification,* 22**,** 472-478.

YON, J. M. (2001). Protein folding: a perspective for biology, medicine and biotechnology. *Brazilian Journal of Medical and Biological Research,* 34**,** 419-435.

ZAPPACOSTA, F., PESSI, A., BIANCHI, E., VENTURINI, S., SOLLAZZO, M., TRAMONTANO, A., MARINO, G. & PUCCI, P. (1996). Probing the tertiary structure of proteins by limited proteolysis and mass spectrometry: the case of Minibody. *Protein Science,* 5**,** 802-813.

ZHANG, C. & GUY, C. (2006). In vitro evidence ofáHsc70 functioning asáaámolecular chaperone during cold stress. *Plant Physiology and Biochemistry,* 44**,** 844-850.

ZHANG, Y. & ZUIDERWEG, E. (2004). The 70-kDa heat shock protein chaperone nucleotide-binding domain in solution unveiled as a molecular machine that can reorient its functional subdomains. *Proceedings of the National Academy of Sciences of the United States of America,* 101**,** 10272.

ZHU, X., ZHAO, X., BURKHOLDER, W. F., GRAGEROV, A., OGATA, C. M., GOTTESMAN, M. E. & HENDRICKSON, W. A. (1996). Structural analysis of substrate binding by the molecular chaperone DnaK. *Science,* 272**,** 1606-1614.

ZYLICZ, M., ANG, D., LIBEREK, K., YAMAMOTO, T. & GEORGOPOULOS, C. (1988). Initiation of lambda DNA replication reconstituted with purified lambda and Escherichia coli replication proteins. *Biochim Biophys Acta,* 951**,** 344-350.

ZYLICZ, M., JAENICKE, R., GETHING, M. & ELLIS, R. (1993). The Escherichia coli Chaperones Involved in DNA Replication [and Discussion]. *Philosophical Transactions: Biological Sciences*, 271-278.